

in control and knockdown cells by using flow cytometry. Cellular accumulation of BCECF in MRP5-silencing cells increased by $80.75 \pm 1.97\%$ and $97.93\% \pm 7.00\%$ ($p < 0.0001$) for MIA PaCa-2 and PANC-1 cells, respectively. MTT ((3-(4,5-Dimethylthiazol-2-yl)-2,5-Diphenyltetrazolium Bromide) assay was undertaken to determine gemcitabine sensitivity, and half-inhibitory concentration (IC_{50}) was calculated. A significant increase in the sensitivity to gemcitabine was observed in ABCC5-transfected cells as compared with the control-siRNA transfected cells. The mean IC_{50} values in MIA PaCa-2 cells with control-siRNA, ABCC5-siRNA-1 and ABCC5-siRNA-2 were 31.64 ± 0.85 nM, 16.48 ± 1.5 nM and 13.56 ± 1.6 nM, respectively. The IC_{50} values in PANC-1 cells for the control, ABCC5-siRNA-1 and ABCC5-siRNA-2 transfected cells were: 5.84 ± 1.80 μ M, 0.90 ± 0.04 μ M and 1.81 ± 0.28 μ M, respectively. The percentage of apoptosis was measured using the flow cytometer based annexin V and PI staining. Silencing ABCC5 significantly increased gemcitabine-induced apoptotic population in both MIA PaCa-2 cells and PANC-1 cells.

For direct and efficient genome editing, CRISPR (clustered regularly interspaced short palindromic repeats)-CAS9 (CRISPR associated protein 9) system was used to target ABCC5 gene at the DNA level. The PANC-1 cells were transfected with CAS9 protein/ABCC5 guide-RNA ribonucleoprotein complexes through liposome-mediated delivery (Chapter 5). From the mixed population of cells, single cell knock-out clones were selected using the limiting dilution method. The efficiency of ABCC5 gene disruption was then assessed by flow cytometry analysis of cell surface MRP5 immunostaining. MTT assay was undertaken to determine gemcitabine sensitivity, and half-inhibitory concentration (IC_{50}) of gemcitabine was calculated. Knocking out ABCC5 significantly decreased MRP5 surface staining by $88.14 \pm 4.87\%$ ($P < 0.0001$). For functional studies of MRP5, cellular accumulation of BCECF in ABCC5-knock out clones increased by $90.36 \pm 2.24\%$ ($p < 0.0001$) compared with those in wild-type. The 72-hr IC_{50} values for the control, Clone 1, 2 and 3 are 12.25 ± 2.32 μ M, 3.20 ± 0.06 μ M, 4.92 ± 0.55 and 5.43 ± 0.82 μ M, respectively, indicating that knocking out ABCC5 significantly increased the sensitivity of PANC-1 cells to gemcitabine.

Taken together, our results confirm that MRP5 confers resistance to gemcitabine and modulation of ABCC5 gene expression increased the sensitivity of MiaPaca-2 and PANC-1 cells to gemcitabine and modulation of ABCC5 activity may represent a novel strategy to reverse gemcitabine resistance in pancreatic cancer cells. Screening tumour MRP5 expression levels to select patients for treatment with gemcitabine-based regimen

1.8	Apoptosis.....	61
1.8.1	Morphological changes involved.....	62
1.8.2	Apoptosis Vs Necrosis.....	65
1.8.3	Apoptosis mechanisms.....	65
1.8.4	Apoptotic pathways in cancer.....	68
1.9	Summary and hypothesis of the thesis.....	69
1.10	AIMS.....	71
Chapter 2 Methodology.....		72
2.1	Cell Culture.....	72
2.1.1	Materials:.....	72
2.1.2	Method.....	72
2.2	Stealth siRNA Transfection.....	73
2.2.1	Materials Required:.....	73
2.2.2	Procedures: Preparation of siRNA stock.....	73
2.2.3	RNA Extraction Protocol.....	97
2.2.4	RNA Quantitation.....	99
2.2.5	cDNA, Primers and real-time-PCR optimisation.....	76
2.3	Cell Viability Assay.....	76
2.3.1	Materials.....	76
2.3.2	Plating cells into 96-well plates.....	77
2.3.3	Experimental Protocol.....	78
2.4	MRP5 functional studies.....	78
2.4.1	Materials.....	78
2.4.2	Methodology.....	79
2.5	Cell apoptosis.....	79
2.5.1	Materials.....	80
2.5.2	Method.....	80
2.6	Surface Staining of MRP5.....	80
2.6.1	Required reagents.....	81
2.6.2	Buffer preparations.....	82
2.6.3	General procedure.....	82
2.7	CRISPR-CAS9 transfection for ABCC5 knock out in Panc1.....	82
2.7.1	Materials required.....	82
2.7.2	Protocol outline.....	83
2.8	Statistical Analysis.....	88
Chapter 3 Development and validation of a real-time PCR method for quantitation of gene expression related to gemcitabine transport and metabolism.....		89
3.1	Background of real-time PCR.....	90
3.2	Quantitation of gene expression by real-time PCR.....	91
3.2.1	Absolute Quantitation.....	91
3.2.2	Relative Quantitation.....	91
3.2.3	Amplification efficiency.....	92
3.2.4	Standard curve method for relative quantification.....	92

4.5.1	siRNA transfection.....	151
4.5.2	BCECF accumulation	153
4.5.3	MTT Assay	154
4.5.4	Apoptosis	155
Chapter 5 Genome-editing in PANC-1 cells using the CRISPR-Cas9 system.....		157
5.1	Materials and methods.....	159
5.1.1	Chemicals	159
5.1.2	CRISPR-Cas9 transfection into PANC-1 cells	159
5.1.3	Cellular BCECF accumulation assay	160
5.1.4	Limited Dilution Method	160
5.1.5	MRP5 Cell surface staining	161
5.1.6	RNA extraction and cDNA synthesis of the knockout cell population ..	161
5.1.7	Real-time quantitative PCR and relative gene expression	161
5.1.8	BCECF accumulation assay for ABCC5 knockout single cell PANC-1 clones	161
5.1.9	Growth inhibition assay: MTT.....	161
5.2	Results	162
5.2.1	BCECF Accumulation: Mixed population.....	162
5.2.2	mRNA Quantitation	163
5.2.3	MRP5 expression: Cell Surface Staining.....	165
5.2.4	BCECF Accumulation: KO Clones	166
5.2.5	MTT Assay	167
5.3	Discussion	169
Chapter 6 General Discussion.....		172
6.1	Restatement of the aims	172
6.2	Summary of results.....	172
6.3	RNAi	175
6.4	Liposomes & siRNA	178
6.5	CRISPR-Cas9.....	178
6.6	Future Directions	180
6.6.1	Multi-targeting for gemcitabine related genes	183
6.6.2	Limitations of gemcitabine Therapy:	184
6.6.3	Liposomes	185
6.6.4	Specific targeting of Cancer cells	187
6.7	Concluding Remarks	188
References.....		189
Appendix A: Supplementary data for siRNA 3		212
Appendix B: qRT-PCR supplementary data.....		213

List of Figures

Figure 1-1: Structures of deoxycytidine, cytosine arabinoside and gemcitabine.....	31
Figure 1-2: Multidrug resistance via increased efflux of drugs (Ref: [115]).....	40
Figure 2-1: Plate layout for cell seeding*	77
Figure 2-2: Target map of sgRNA 1	84
Figure 2-3: Target map for sgRNA 2.....	84
Figure 3-1: Reaction setup for One-Step qRT-PCR	107
Figure 3-2: Representative amplification curves for the housekeeping gene GAPDH (A) and target gene	109
Figure 3-3: Amplification specificity by real-time PCR. Melting curves and melting peaks of GAPDH (A) and ABCC5 (B) PCR products.....	109
Figure 3-4: Amplification curves for GAPDH (A) and ABCC5 (B) in PANC- 1 cells.	111
Figure 3-5: Amplification specificity by real-time PCR. Melting curves and melting peaks of GAPDH (A) and ABCC5 (B) target gene in PANC-1	111
Figure 3-6: Amplification Curves for RPL13A in MIA PaCa-2 cells	113
Figure 3-7: Amplification specificity by real-time PCR. Melting Curves and melting peaks of RPL13A in MIA PaCa-2 cells	113
Figure 3-8: Amplification curves for RPL13A in PANC-1 cell line	115
Figure 3-9: Amplification specificity by real-time PCR. Melting Curves and melting peaks of RPL13A in PANC-1 cells.....	115
Figure 3-10: Inter-day GAPDH variation in MIA PaCa-2 cells treated with ABCC5-siRNA and scramble RNA sequences. Multiple comparisons between control and different treatment groups were analysed using one-way ANOVA with Dunnett's post-hoc.....	117
Figure 3-11: Inter-day variations for RPL13A in MIA PaCa-2 cells treated with ABCC5-siRNA and scramble RNA sequences. Multiple comparisons between control and different treatment groups were analysed using one-way ANOVA with Dunnett's post-hoc.....	117
Figure 3-12: Inter-day variation for GAPDH in PANC-1 cells treated with ABCC5-siRNA and scramble RNA. Multiple comparisons between control and different treatment groups were analysed using one-way ANOVA with Dunnett's post-hoc. ...	118
Figure 3-13: Inter-day variation for RPL13A in PANC-1 cells treated with ABCC5-siRNA and scramble RNA sequences. Multiple comparisons between control and different treatment groups were analysed using one-way ANOVA with Dunnett's post-hoc.....	118
Figure 4-1: Percentage of ABCC5 knockdown in MIA PaCa-2 cells by 3 different siRNAs sequences (20 pmol each). Data are presented as the mean and SEM from three independent experiments; n=3. Multiple comparisons between control and different treatment groups were analysed using one-way ANOVA with Dunnett's post-hoc. *** $P < 0.0001$	126

- Figure 4-2: Percentage ABCC5 knockdown in MIA PaCa-2 by 3 different sequences (10 pmol each). Data are presented as the mean and SEM from three independent experiments, n=3 (number of repeats). Multiple comparisons between control and different treatment groups were analysed using one-way ANOVA with Dunnett's post-hoc. *** $P < 0.0001$ 127
- Figure 4-3: Off-target effects of ABCC5 siRNA transfection (10 pmol each) in MIA PaCa-2 cells. Data are presented as the mean and SEM from three independent experiments; n=3. Multiple comparisons between control and different treatment groups were analysed using one-way ANOVA with Dunnett's post-hoc. *** $P < 0.0001$, ** $P < 0.01$, *** $P < 0.001$, **** $P < 0.0001$ 128
- Figure 4-4: Comparison of Off-target effects in ABCC5-siRNA transfected MIA PaCa-2 cells. Data are presented as the mean and SEM from three independent experiments; n=3. Multiple comparisons between control and different treatment groups were analysed using one-way ANOVA with Dunnett's post-hoc. *** $P < 0.0001$, * $P < 0.05$, ** $P < 0.01$, *** $P < 0.001$, **** $P < 0.0001$ 129
- Figure 4-5: Percentage of ABCC5 knockdown in PANC-1 cells by 3 different siRNAs sequences (20 pmol each). Data are presented as the mean and SEM from three independent experiments. Multiple comparisons between control and different treatment groups were analysed using one-way ANOVA with Dunnett's post-hoc. **** $P < 0.0001$ 130
- Figure 4-6: Percentage ABCC5 knockdown in PANC-1 cells by 3 different siRNA sequences (10 pmol each), Multiple comparisons between control and different treatment groups were analysed using one-way ANOVA with Dunnett's post-hoc. **** $P < 0.0001$ 131
- Figure 4-7: Comparison of Off-target effects in control and ABCC5-siRNA transfected PANC-1 cells. Data are presented as the mean and SEM from three independent experiments; n=3. Multiple comparisons between control and different treatment groups were analysed using one-way ANOVA with Dunnett's post-hoc, * $P = 0.0158$, ** $P = 0.0067$, *** $P < 0.001$, **** $P < 0.0001$ 132
- Figure 4-8: Off-target effects of ABCC5 siRNA transfection on other ABC transporters and gemcitabine metabolism-related enzymes in PANC-1 cells. Data are presented as the mean and SEM from three independent experiments; n=3. Multiple comparisons between control and different treatment groups were analysed using one-way ANOVA with Dunnett's post-hoc * $P = 0.0158$, ** $P = 0.0067$, *** $P < 0.001$, **** $P < 0.0001$.. 133
- Figure 4-9: Overlay data for MRP5 surface staining in PANC-1 cells. (A) The cell surface expression of MRP5 was assessed by staining the PANC-1 cells with anti-MRP5 primary (Red) and control isotype IgG2a antibody (Green). Plots (B), (C) and (D) show MRP5 surface immunostaining in PANC-1 cells treated with ABCC5-siRNA 1, 2 and 3 (All green) and control siRNA (Red), respectively..... 134
- Figure 4-10: Mean MRP5 cell surface staining in ABCC5 and control siRNA transfected PANC-1 cells. Data are presented as the mean and SEM from three independent experiments; n=3. Multiple comparisons between control and different treatment groups were analysed using one-way ANOVA with Dunnett's post-hoc. **** $P < 0.0001$ 135
- Figure 4-11: BCECF accumulation in MIA PaCa-2 cells 5 min after incubation with BCECF-AM in the presence and absence of curcumin (CUC, 10 μ M). Data are presented as the mean and SEM from three independent experiments; n=3. Student's t-

test was used for comparison between control and CUC treated cells. **** $P < 0.0001$	136
Figure 4-12: BCECF accumulation in PANC-1 cells 5 min after incubation with BCECF in the presence and absence of CUC (10 μ M), ** $P < 0.05$. Data are presented as the mean and SEM from three independent experiments; n=3. Student's t-test was used for comparison between control and different treatment.	136
Figure 4-13: BCECF accumulation in ABCC5 and control siRNA transfected MIA PaCa-2 cells. All data are normalized as a percentage of the mean intensity value determined in control-siRNA transfected cells. Data are presented as the mean and SEM from three independent experiments; n=3. Multiple comparisons between control and different treatment groups were analysed using one-way ANOVA with Dunnett's post-hoc. **** $P < 0.0001$	137
Figure 4-14: BCECF accumulation in ABCC5 siRNA transfected PANC-1 cells. All data are normalized as a percentage of the mean intensity value determined in control-siRNA transfected cells. Data are presented as the mean and SEM of fluorescence percentage from three independent experiments, n=3. Multiple comparisons between control and different treatment groups were analysed using one-way ANOVA with Dunnett's post-hoc. **** $P < 0.0001$	138
Figure 4-15: Comparison of mean gemcitabine IC ₅₀ values (nM) in ABCC5-siRNA and control transfected MIA PaCa-2 cells. Data from three independent experiments are presented as the mean and SEM, n=3. Multiple comparisons between control and different treatment groups were analysed using one-way ANOVA with Dunnett's post-hoc (**** $P < 0.0001$).....	139
Figure 4-16: Comparison of gemcitabine-induced cytotoxicity between ABCC5-siRNA-1 and control siRNA transfected MIA PaCa-2 cells. Data are presented as the mean and SEM from three independent experiments; n=3.	140
Figure 4-17: Comparison of gemcitabine-induced cytotoxicity in ABCC5-siRNA-2 and control-siRNA transfected MIA PaCa-2 cells. Data are presented as the mean and SEM from three independent experiments; n=3	140
Figure 4-18: Comparison of mean gemcitabine IC ₅₀ values in ABCC5 and control-siRNA transfected PANC-1 cells. Data from three independent experiments are presented as the mean and SEM; n=3. Multiple comparisons between control and different treatment groups were analysed using one-way ANOVA with Dunnett's post-hoc. **** $P < 0.0001$	141
Figure 4-19: Comparison of gemcitabine-induced cytotoxicity in ABCC5-siRNA-1 transfected and control PANC-1 cells. Data are presented as the mean and SEM from three independent experiments; n=3	142
Figure 4-20: Comparison of gemcitabine-induced cytotoxicity in ABCC5-siRNA-2 transfected and control PANC-1 cells. Data are presented as the mean and SEM from three independent experiments; n=3	142
Figure 4-21: Apoptosis detection using annexin V staining in siRNAs-transfected MIA PaCa-2 cells.....	145
Figure 4-22: Percentage of gated viable cells of control and ABCC5-siRNA transfected MIA PaCa-2 cells treated with gemcitabine (200, 400 and 800 nM) for 24 hrs. Data are presented as the mean and SEM from three independent experiments, n=3. Multiple comparisons between control and different treatment groups were analysed using two-way ANOVA with Dunnett's multiple comparison test. ** $P < 0.05$ and **** $P < 0.0001$	146

Figure 5-9: Comparison of mean gemcitabine IC ₅₀ values for ABCC5 knockout PANC-1 clones. Data are presented as the mean and SEM from three independent experiments; n=3. Multiple comparisons between control and different treatment groups were analysed using one-way ANOVA with Dunnett's post-hoc. * <i>P</i> <0.05, ** <i>P</i> <0.005	167
Figure 5-10: Comparison of gemcitabine cytotoxicity in ABCC5 knockout clone-1 and control in PANC-1 cells Data are presented as the mean and SEM from three independent experiments; n=3.	168
Figure 5-11: Comparison of gemcitabine cytotoxicity in ABCC5 knockout clone -2 and control in PANC-1 cells. Data are presented as the mean and SEM from three independent experiments; n=3.	168
Figure 5-12: Comparison of gemcitabine cytotoxicity in ABCC5 knockout clone-3 and control in PANC-1 cells. Data are presented as the mean and SEM from three independent experiments; n=3.	168
Figure 0-1: Comparison of gemcitabine induced cytotoxicity in ABCC5-siRNA-3 transfected MIA PaCa-2 cells and control	212
Figure 0-2: Comparison of gemcitabine induced cytotoxicity in ABCC5-siRNA-3 transfected PANC-1 cells and control.....	212
Figure 0-1: Off-target effects - amplification curves of 7 ABC transporters, dCK, CDA, hENT1 and GAPDH in MIA PaCa-2 cells. Refer to the table: 3-5 for details on primer sequences and target genes.....	213
Figure 0-2: Off-target effects – amplification curves of 7 ABC transporters, dCK, CDA, hENT1 and GAPDH in PANC-1.	213
 Appendix A: Supplementary data for siRNA 3	 212

List of Tables

Table 1-1: Registered cases of pancreatic cancer in New Zealand.....	19
Table 1-2: Deaths due to pancreatic cancer	19
Table 1-3: Pancreatic cancer incidences and age.....	21
Table 1-4: Pancreatic cancer incidences and age.....	21
Table 1-5: Pancreatic Cancer Risk Factors (Ref: [10]).....	23
Table 1-6: ABC genes (Ref: [114]).....	41
Table 1-7: Human ABC transporter pseudogenes (Ref: [114]).....	43
Table 1-8: Substrates of ABC transporters (Ref: [115]).....	48
Table 1-9: Inhibitors of ABC transporters (Ref: [115]).....	53
Table 2-1: siRNA mixture composition for transfection	75
Table 2-2: Transfection mix for CRISPR-Cas9	83
Table 2-3 Thermocycler program for DNA extraction	86
Table 2-4 PCR amplification mix	86
Table 2-5 PCR parameters for DNA extraction.....	87
Table 2-6 Reaction conditions for re-annealing reaction.....	88
Table 3-1: Scaling up and down the volume of RLT buffer (cell lysis buffer)	97
Table 3-2: Template primer mix for 1 reaction.....	101
Table 3-3: Reaction mix for cDNA synthesis	101
Table 3-4: Reaction mix for one step Rt-PCR	102
Table 3-5: Reaction conditions for One-Step qRT-PC	103
Table 3-6: Primer sequences for the target genes	104
Table 3-7: Primer sequences of the reference genes.....	105
Table 3-8: reaction mix for One-Step qRT-PCR	105
Table 3-9: Variations of housekeeping gene GAPDH in MIA PaCa-2 cells.....	110
Table 3-10: Variations of housekeeping gene GAPDH in PANC-1 cells	112
Table 3-11: Variations of housekeeping gene RPL13A in MIA PaCa-2 cells treated with ABCC5-siRNA and scramble RNA sequences.	114
Table 3-12: Variations of housekeeping gene RPL13A in PANC-1 cells treated with ABCC5-siRNA and scramble RNA sequences	116
Table 4-1: Mean % apoptosis for scrambled siRNA transfected MIA PaCa-2 cells treated with gemcitabine for 24 hrs. Data are presented as the mean and SEM from three independent experiments, n=3.** $P < 0.05$	143
Table 4-2: Mean % percentage apoptosis for ABCC5- siRNA-1 transfected MIA PaCa-2 cells. Data are presented as the mean and SEM from three independent experiments, n=3. **** $P < 0.0001$	143

Table 4-3: Mean % percentage apoptosis for ABCC5-siRNA-2 transfected MIA PaCa-2 cells. Data are presented as the mean and SEM from three independent experiments, n=3. **** $P < 0.0001$	144
Table 4-4: Mean % apoptosis for scrambled siRNA transfected PANC-1 cells. Data are presented as the mean and SEM from three independent experiments, n=3. * $P < 0.05$, ** $P < 0.005$ and **** $P < 0.0001$	147
Table 4-5: Mean % apoptosis for ABCC5-siRNA-1 transfected PANC-1 cells. Data are presented as the mean and SEM from three independent experiments, n=3. **** $P < 0.0001$	147
Table 4-6: Mean % apoptosis for ABCC5-siRNA-1 transfected PANC-1 cells. Data are presented as the mean and SEM from three independent experiments, n=3. **** $P < 0.0001$	148

1.1 Aetiology of pancreatic cancer

Alteration in cancer incidences may occur due to various reasons; depicted in Weir et al.[7] and could be classified in three distinct classes: (1) alteration in the cancer risk factors or the diagnosis practices, (2) growth of the population, and (3) ageing. While population growth is straightforwardly identified with the variation in an absolute number of cancer cases in a nation and is specific to that country, the two other factors are especially germane to pancreatic cancer. Change in cancer risk could be considered as the most apparent factor: e.g. change in lung cancer frequency that parallels the pandemic of tobacco utilisation. However, not at all like lung cancers which are to a great extent caused by tobacco smoke, the pancreatic tumour is a multifactorial disease [5]. A significant number of its risk factors have been distinguished (see the following segment 1.2 and 1.3). However, they only explain a tiny fraction of total incidences. Since exposures to these risk factors frequently fluctuate in various ways (i.e., reducing the smoking balance by growing commonness of obesity or diabetes), it is improbable to explain pancreatic cancer incidences by change(s) in just single risk factor [5].

1.1.1 Population Aging

Population ageing is one of the significant factors in the elevation of the number of cancer incidences diagnosed in developed nations. This fact is especially valid for pancreatic cancer which is firmly age subordinate [5]. In an ageing nation like Italy, these days close to 10% of all pancreatic cancer cases are analysed before age 60, around 55% between age 60 and 80, and surprisingly 35% in elderly individuals matured 80 years or more. This is a result of the surprising increment in life expectancy that happened in Italy, or in other westernised nations, in the course of the most recent century, bouncing from 35 years in the late 1800s to more than 80 years as of now [5].

For the nations like Italy increase in the pancreatic cancer incidence rate was observed for the ageing population while the incidence was quite stable for the population below 70 [5]. Similar pattern could be seen in New Zealand for pancreatic cancer incidences; number of incidence/rate increases with the aging population (Table 3 and 4).

Age at registration	0–4	5–9	10–14	15–19	20–24	25–29	30–34	35–39	40–44
Total	0	0	0	0	1	1	1	0	5
Male	0	0	0	0	1	0	0	0	2
Female	0	0	0	0	0	1	1	0	3

Table 1-3: Pancreatic cancer incidences and age

Ref: New Zealand Cancer Registry

Age at registration	45–49	50–54	55–59	60–64	65–69	70–74	75–79	80–84	85+
Total	16	22	41	57	71	79	70	75	65
Male	9	9	27	28	39	45	31	37	29
Female	7	13	14	29	32	34	39	38	36

Table 1-4: Pancreatic cancer incidences and age

Ref: New Zealand Cancer Registry

1.1.2 Other risk factors

A statistically important relation was established for many risk factors associated with pancreatic cancer while some were found to be non-significant after the meta-analysis [5]. Interestingly, the association of the non-O blood group is also considered as one of the risk factors and genetic factor associated with pancreatic cancer. Still, further studies are needed to confirm the relationship between non-O blood group and pancreatic cancer. History of pancreatic cancer in the family approximately doubles the risk of pancreatic cancer, and 5– 10% of patients with pancreatic malignancy are suspected to have underlying germline disorders [19]. A non-O blood group, another inherited trademark was found to be consistently connected with a higher risk of pancreatic cancer [5]. Smoking of tobacco is one of the most significant and established lifestyle-related risk factors, is responsible for ~20% of all pancreatic cancer tumours. Even though a typical reason for pancreatitis, substantial liquor consumption is connected just with the modest expanded risk of pancreatic cancer [5]. Numerous elements related to

the metabolic disorder, obesity [5], reduced glucose resilience, and history of diabetes additionally increments the risk, while atopic allergy and utilisation of metformin for diabetes treatment are related to a decreased risk of pancreatic cancer [5]. Other medical conditions, for example, a history of chronic pancreatitis [5] or cholecystectomy [8], infection with *Helicobacter pylori*, hepatitis B [9], or hepatitis C virus likewise intensify the risk of creating pancreatic malignancy. Pancreatic cancer has also been related to the food habits of the individual and consumption of red meat, and processed meat utilisation has been identified as one of the risk factors. While a reduction in the risk is proposed with the consumption of fruits, vegetables and folates [5]. A few meta-investigations affirmed no relationship with the consumption of tea or coffee, with add up to fat, dairy items, dietary acrylamide, or fish consumption. A few of these risk factors are related to relative risk more prominent than two and could be utilised for recognising people who could profit by screening [5]. These incorporate people with a history of pancreatic cancer in the family, with a background marked by unending or innate pancreatitis, or who have another genetic predisposition for developing the sickness [5].

Pancreatic cancer risk has also been associated with the lifestyle, and few environmental factors could also increase the risk. The most widely recognized risk factor for pancreatic adenocarcinoma related to the lifestyle of an individual is tobacco smoking. Past studies have proposed that tobacco smoking doubles the risk of pancreatic cancer as compared to the population which never smoked. In a study, ~25% of pancreatic tumours were found in the cigarette smoking population [10]. Not only smoking is associated with pancreatic cancer, but it is also responsible for a large number of mutations in the pancreatic cancer tumours making it more difficult for treatment [10]. A significant reduction in the risk factor was found with the population which has already quit smoking recently, and the risk of pancreatic cancer is further reduced for the population which left smoking 15-20 years ago. [10]. Longstanding type II diabetes mellitus was also accounted for as one of the risk factors of pancreatic cancer. A population with more than 10 years of type II diabetes has a higher risk of pancreatic cancer as compared to the population which never had type II diabetes [11]. Furthermore, new onset diabetes could also be an indication of pancreatic cancer. Around 1% of patients with newly developed diabetes develop pancreatic cancer tumours inside 3 years of their analysis of diabetes, proposing that new beginning diabetes could be used as an indicator marker for pancreatic cancer. Even though the

percentage is such patients is very less, regular screening of type II diabetes patients for pancreatic cancer is recommended [11]. Body mass index (BMI) is also related to type II diabetes, and some studies have also proposed relation of BMI with pancreatic cancer [10]. Though it has not been completely proven yet, the deliberate loss of weight to achieve proper BMI reduces the risk of type II diabetes mellites and thus reduces the risk of pancreatic cancer too [10]. Other risk factors associated with the pancreatic cancer are high liquor consumption and pancreatitis. Heavy liquor consumption (more than 6 drinks every day) has been related with an expanded danger of pancreatic disease with an OR (odds ratio) of 1.46. Low (1 drink/day) or no liquor utilization does not seem to build risk. Perpetual pancreatitis additionally hoists the risk of pancreatic cancer [10]. A study showed that people with chronic pancreatitis history have a more than 2 fold high risk of pancreatic cancer [10].

Risk Factor	Risk Estimate (95% CI)
Current Cigarette Smoking	OR* = 2.20 (1.71–2.83)
Past Cigarette Smoking	OR=1.64 (1.36–1.97)
1–10 years since quitting	OR=1.12 (0.86–1.44)
15–20 years since quitting	
Diabetes Mellitus	RR* =7.94 (95% CI, 4.70–12.55)
<3 years	OR 1.51 (95% CI=1.16–1.96)
>10 years duration	
BMI* (>35 vs 18.9–24.9)	OR =1.55 (95%CI=1.16 – 2.07)
Heavy Alcohol (> 6 drinks/day)	OR 1.46 (95%CI=1.16–1.83)
Pancreatitis (>2 years)	2.71-fold (95% CI 1.96–3.74)

Table 1-5: Pancreatic Cancer Risk Factors (Ref: [10])

*BMI= Body mass index; OR=odds ratio; RR=relative risk

1.1.3 Signs and Symptoms

Pancreatic cancer is one of the most difficult types of cancer to diagnose and treat and unfortunately, most of the patients are diagnosed at a very later stage of the malady when the malignancy is in its metastatic stage Some of the common symptoms of pancreatic c cancer are unnecessary weight loss, jaundice, epigastric pain and migratory thrombophlebitis (Trousseau's syndrome) [10]. Depression is quite common in

pancreatic cancer patients, but in some cases, the onset of depression was seen before the diagnosis of pancreatic cancer. Indicating that pancreatic cancer tumour is associated with the depression triggering factors, though comprehensive studies are required to make a conclusive decision on this [10]. With the improvements in the sensitivity of imaging technologies, multi-detector processed tomography (MDCT), magnetic resonance imaging (MRI), and endoscopic ultrasound (EUS) are used in the present time for the detection of pancreatic cancer tumour. CT and MRI both can be utilised to stage cancer, and three-dimensional recreation can give itemised data on the tumour structure and its interactions with the adjacent vessels. Pathology is the gold standard for the diagnosis, and at the time of endoscopic ultrasound, issues can be examined. Use of positron emission tomography (PET) imaging has been proposed in a few cases [10, 12].

1.1.4 Pancreatic cancer: Clinical Staging

After pancreatic cancer diagnosis, the second step is vigilant staging, because the regimen depends on the stage. The American Joint Committee on Cancer (AJCC) staging framework, which incorporates the TNM (tumour, lymph node and metastasis) characterization, is the most extensively utilized system to stage pancreatic cancer [13]. Lately, some amendments have been done in this system to underscore the significance of surgery of cancer, and it has been streamlined to increase the survival by stage. AJCC recommended resectability stages incorporate stages I and II, and the subset of Stage III that is characterized as marginal resectable. The un-resectable classifications incorporate the subset of Stage III and IV. Stage III which is locally progressed (unresectable) and Stage IV is metastatic [10]. Such classification of the tumour on the basis of the stages is dependent on the metastatic growth and tumour interaction with the nearby environment. Staging of the tumour is a significant process as it decides the fate of tumour resectability, e.g. tumours in stage IV are metastatic, and their resection is not recommended [10]. Some of the sites where cancer metastasis can be commonly seen are lungs, liver, and peritoneum, and these regions are not precisely evaluated by physical exam. Pelvic nodes and palpable supraclavicular do occur but are infrequent. In this way, the identification of additional local metastases depends vigorously on imaging studies about and the discerning use of laparoscopy. In the absence of metastatic malady, the tumour interaction with the adjacent major vessels characterizes resectability [14]. Some of the vessels which are included in this decision are the superior mesenteric and portal veins, superior mesenteric artery, the celiac axis.

For the patients with no or very less tumour interaction with the vessel are considered for resection while for the patients with higher tumour interaction levels are staged metastatic, i.e. stage III. The stage is further classified into the locally advanced tumour or marginally resectable tumour; depending on the level of tumour interaction with the vessels [10, 14]

One of the major reasons for the late detection of pancreatic cancer is the absence of any visibly detectable symptoms and unavailability of biomarkers for early diagnosis. At the time detection, most of the pancreatic cancer tumours are in their metastatic stage and becomes very invasive resulting in the poor response to therapy. Around half of the patients diagnosed have metastatic disease. Heterogenous nature of PDAC and its plasticity makes pancreatic cancer more resistance to any sort of therapy. Progression of cancer through sequential stages comprises amassing morphological and hereditary modifications. It was also seen in PDAC that alteration in the signalling pathways occurs [1]. Over-activation of numerous signalling pathways associated with progression and proliferation and additionally mutations in tumour suppressor genes are frequently recognised in PDAC, affecting cell multiplication, survival and intrusion. The extensive range of hereditary and metabolic rejuvenation enables PDAC to get by under severe conditions and increments proliferative capacity. Moreover, recent examination of gene expression and activity considered the characterisation of detected mutations into four particular phenotypic subtypes characterised as the squamous, pancreatic progenitor, immunogenic and aberrantly, differentiated endocrine-exocrine (ADEX) [15]. Each of the subtypes represented by various mutational topographies, tumour histopathological structures correspond with the various diagnosis. Moreover, a highly diffused and compact stroma called desmoplasia is formed around a tumour, adding to its resistance and impacting tumour movement and intrusion [16]. All the reasons mentioned above make pancreatic tumour impervious to most of the drug therapies, demanding for more novel ways to enhance PDAC patients' survival. Orthodox cytotoxic treatments, for example, radio and chemotherapy, have been somewhat less-efficient in enhancing patients' odds for survival, offering negligible advantages. Single-agent gemcitabine (which is the gold standard for chemotherapy in pancreatic cancer patients) and its combinations with other drugs were unsuccessful in significantly improving patient's survival. Similarly, results with multidrug regimens (e.g., folinic acid-fluorouracil-irinotecan-oxaliplatin also known as FOLFIRINOX) and targeted treatments were disappointing [1]. In this manner, there is a significant

requirement for improvement of novel, compelling procedures meaning to propel current therapeutic regimens. Improvements in the field of tailored, more customised treatments are of high significance. Numerous preclinical and clinical examinations are being created keeping in mind the end goal to address these focuses; in any case, because the greater part of them are in early stages, it is still too early to reach any conclusion [1].

1.1.5 Treatment

Like most of the cancer pancreatic cancer is also an intricate disease, and as mentioned before the ideal treatment as a matter of first importance relies on accurate staging. Resection is recommended for the stage I/II pancreatic cancer patients followed by adjuvant therapy or Neoadjuvant treatment. However, application of the neo-adjuvant therapy for stage III marginal resectable tumours after surgery is still questionable [10]. Chemotherapy and chemo-radiotherapy are recommended for patients with advanced disease. A more substantial part of these patients, in the end, creates metastatic disease. Systemic treatment is recommended for Stage IV patients with good performance while for those with poor general health supportive therapy is suggested [10]. As pancreatic cancer is usually diagnosed at the later stages, there is a high chance of the relapse even after tumour resection and chemotherapy. There is a 40-60 % chance of relapse in the patients after the surgery, and 2-3% mortality rate was also observed [10]. It could take up to 2-3 months period of time for the patient receiving chemotherapy and chemo-radiotherapy for complete recuperation to a standard quality of life; unfortunately, survival for a longer period is rare. The median survival period for the patients receiving tumour is around 17– 27 months and the survival beyond 5 years of time is roughly 20%. As we now know that pancreatic cancer is a multifactorial disease and thus, a multidisciplinary approach is needed to increase the survival rate in the patients [10].

1.2 Therapeutic management of pancreatic cancer

Adjuvant therapy is the most common regimen for the patients with the early stage of the disease. Most of the times patients are diagnosed with a later stage of the disease and thus show poor prognoses. With no treatment, these patients could hardly survive for 12- 14 weeks [4]. gemcitabine is a standard chemotherapeutic drug, and for patients with the advanced disease, it is used as a first-line treatment drug. Patients treated with gemcitabine show significant progress in the median and one-year survival rates compared with 5-fluorouracil (5 FU) [4]. Gemcitabine in combination with paclitaxel expanded the mean survival from 6.7 to 8.7 months, and when administered with

FOLFIRINOX (folinic acid, 5 FU, irinotecan, and oxaliplatin) treatment, the average survival rate expanded from 6.8 to 11.2 months [4, 17]. A few clinical advances in chemotherapy were accomplished by high quality, large-scale, prospective and randomized clinical trials. Adjuvant therapy with gemcitabine or fluorouracil has indicated promising impacts to enhance general survival [18-20]. In 2007, Oettle et al. [21] revealed that adjuvant therapy using gemcitabine enhanced the survival up to 5 years. In 2010, Neoptolemos et al. [20] published adjuvant use of fluorouracil in addition to folinic acid had comparable outcomes with gemcitabine. In 2013, adjuvant use of gemcitabine was accounted for to enhance the 5-year overall survival. In 2016, Uesaka et al. [22] uncovered that adjuvant use of oral fluorouracil (S-1) accomplished 44.1% of 5-year overall survival.

Recently, Neoptolemos et al. [23] reported an enhanced median survival rate for the patients receiving adjuvant therapy in combination of gemcitabine with capecitabine. In 2011, Conroy et al. [24] reported in their study that patients receiving FOLFIRINOX based adjuvant therapy showed better survival rates as compared to the gemcitabine. In 2016, Wang-Gillam et al. [25] revealed nanoliposomal irinotecan in combination with fluorouracil and folinic acid altogether increased the survival rate in metastatic pancreatic cancer population who already got gemcitabine-based treatment. Theoretically, neoadjuvant treatment has several benefits over adjuvant treatment including better drug absorption, assessment of response, improved resectability rate and increased margin-negative resection rate [26]. In any case, the impacts of neoadjuvant treatment in pancreatic malignancy have not been affirmed. In 2015, Ferrone et al. [27] reported that neoadjuvant FOLFIRINOX for the patients with borderline resectable pancreatic malignancy resulted in the reduction of tumour size and lower morbidity [18, 27].

1.3 Therapy for Metastatic Cancer

The morbidity rate is quite high for the patients in the metastatic stage of pancreatic cancer and chemotherapy remains the principle choice for such patients. Radiation with chemotherapy is another alternative for unresectable, metastatic disease [28]. Regardless, the impacts accomplished by both treatments mentioned above mildly enhance the survival rate and lowered cancer-related symptoms. Additionally, combination chemotherapy, which is related with marginally better results, is restricted just to patients with a decent performance status (PS). Thus, depending on the PS, PDAC patients might be subjected to mix or single-agent treatment. Multidrug regimens

could potentially enhance the patient's anti-tumour response, but there is a risk of higher toxicity and more adverse effects on the subject's health [29]. Though most of the therapeutic regimens have some intricacies, e.g. reduction in blood cell counts, vomiting and diarrhoea, nausea, mouth ulcers, constipation, poor appetite, nervous system changes, hair loss, and infertility. Some of the side effects, like blood clotting and weight loss, are one of the reasons for less efficacy of these treatments, forcing their early termination. Since 1997, gemcitabine has been acknowledged as a source of perspective first-line treatment drug for patients with a decent execution status. Its advantage over 5-FU has been accounted in various individual studies. In a comparative phase III study (126 patients) between single-agent gemcitabine and 5-FU, a clinical benefit response was observed by 23.8% of gemcitabine-treated patients compared with 4.8% of 5-FU-treated patients [1]. The mean survival time for the patients receiving gemcitabine and 5-FU based treatment was 5.6 and 4.4 months while the one-year survival rate for gemcitabine was 18% and for 5-FU was 2% [1]. gemcitabine was additionally seen to improve patients' disease-related symptoms. Another stage II/III trials likewise revealed a positive or fractional positive response to gemcitabine, in the range of 5.4% to 12% [30, 31] and overall median survival time in the range 5 to 7.2 months [25]. One-year survival of 18% and the median survival time of 6.2 months were accounted for in the successive study [32]. Apart from grade 3 and 4 myelosuppression that was seen in around 30% of patients [32], lower systemic toxicity was ascribed to gemcitabine regimen.

Lately, CO-101, a lipid-drug conjugate of gemcitabine has been developed to independently enter the human cancer cells without human equilibrative nucleoside transporter 1 (hENT1). CO-101 was developed in view of overcoming the drug resistance, but no significant improvements were seen [33]. A modified version of gemcitabine (Acelarin) is right now under scrutiny in a stage III trial, with the expectation to delay the tumour resistance [1]. The addition of a phosphoramidite motif to gemcitabine was expected to decrease resistance by PDAC cells after gemcitabine treatment. The information obtained so far showed an increase in the intracellular concentration of gemcitabine [1]. Thus, for patients with stage III pancreatic cancer, gemcitabine has more clinical benefits and higher survival rate over 5-FU. For gemcitabine monotherapy, the recommended dose in patients with stage III disease is 1000 mg/m² over 30 minutes, weekly for 3 weeks every 28 [34].

1.3.1 Pancreatic cancer: One of the most resistant cancer

Pancreatic cancer is one of the most treatment-resistant cancer to chemotherapy. To increase gemcitabine efficacy, many combinational trials with other drugs have been suggested, e.g. capecitabine, cisplatin, 5-FU and oxaliplatin [35]. Some of these combination studies yielded good survival rates, but considering the toxic effects and multidrug resistance, none of these combinations was more compelling than gemcitabine monotherapy. The overall survival rate even after the drug combination stays the same. There could be a few reasons for such resistance, and impaired drug delivery pathways could be one of them [36]. It is also hypothesised that inside pancreatic tumours there are solid tumour masses which have insufficient vasculature with intense desmoplastic reaction [37]. Thus, it is challenging for any drug to breach the fortress (stroma area) and reach the solid tumours. Chemotherapy can also initiate a drug resistance response (acquired resistance) in pancreatic cancer [35].

1.3.2 Recurrent Disease

For patients encountering relapse of the disease following resection, a confirmatory biopsy is recommended. If not received before chemo-radiation could be used for patients with the locally advanced disease. Patients with metastatic disease the treatment choices are impacted by the period of time from the culmination of adjuvant therapy to the detection of metastases [38]. In all instances of recurrent disease, a clinical trial is a preferred alternative, and best supportive care is recommended [34]. Most of the studies focusing on chemoresistance in advanced pancreatic malignancy centres around gemcitabine, as the information on the activity of other drugs remains preliminary. The cause behind the susceptibility of pancreatic cancer to gemcitabine than other chemotherapeutic agents is still not well understood [4]. Nevertheless, of this sensitivity, most of the patients receiving gemcitabine-based chemotherapy develop resistance to the drug, which implies that the investigation of the causes responsible for gemcitabine chemoresistance is critical. A few cellular factors, e.g. human equilibrative nucleoside transporter 1 (hENT1), enzymes like deoxycytidine kinase (dCK) or cytidine deaminase (CDA) are under scrutiny for gemcitabine resistance [4]. To better understand the gemcitabine resistance in pancreatic cancer it is imperative first to understand the mechanism of gemcitabine working.

1.4 Gemcitabine pharmacology

Gemcitabine (2, 2-difluorodeoxycytidine, dFdC) is a deoxycytidine analogue (Fig. 1) with activity against human leukaemia and solid murine tumours. Even though the structurally and functionally related deoxycytidine analogue 1- β -D-arabinofuranosylecytosine (Ara-C) is just active against leukaemia, gemcitabine has been observed to be active against a few solid tumours, for example, non-small cell lung cancer (NSCLC), small cell lung cancer (SCLC), ovarian and pancreatic cancers [39]. Though the activation steps of Ara-C and gemcitabine are fundamentally the same, gemcitabine has a more complex mechanism with more cellular targets. Changes in these cell targets may cause an adverse effect on the sensitivity of gemcitabine, although resistance could be multifactorial [39]. Currently, gemcitabine is primarily used as the first-line treatment for most of the pancreatic cancer types and development of resistance against gemcitabine has been observed over time. Such resistance in case of pancreatic cancer is multifaceted and may be both acquired and innate [4]. The mechanism of gemcitabine metabolism, action and resistance are described further in detail.

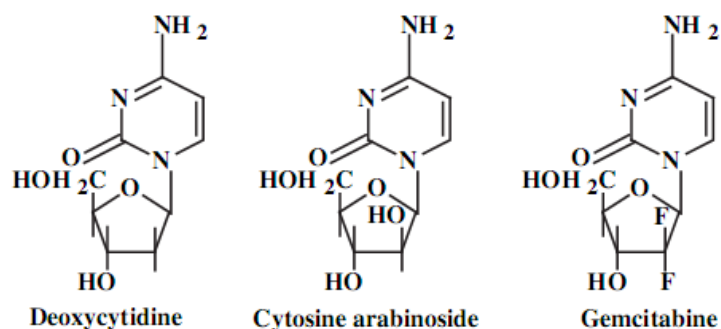


Figure 1-1: Structures of deoxycytidine, cytosine arabinoside and gemcitabine

(Ref: [40])

1.4.1 Transport/uptake of gemcitabine

Gemcitabine, a nucleoside analogue, is hydrophilic in nature and requires an active uptake through the cell membranes. For the passage of nucleoside analogues in or out of cells, specialised transport systems are involved. Seven discrete carriers for the transport of nucleosides are present, sodium-dependent type (concentrative nucleoside transporter - CNT) or of the sodium-independent type (equilibrative nucleoside transporter - ENT) [41]. Further, ENT is classified into two major subtypes; the equilibrative-sensitive (es) and equilibrative inhibitor (ei) resistant transporters [41-44]. Two equilibrative nucleoside transporters (ENTs; ENT1 (SLC29A1) and ENT2 (SLC29A2) and three concentrative nucleoside transporters (CNTs) CNT1 (SLC28A1), CNT2 (SLC28A2), and CNT3 (SLC28A3) are the major nucleoside transporters responsible for the transport of gemcitabine across cell membrane [34, 45, 46]. Studies [46] have reported that cell deficient with the nucleoside transporters are very resistant to gemcitabine therapy. Human cell lines kinetic studies reported that gemcitabine's intracellular uptake is mediated mainly by ENT1 and, to a lesser degree, by CNT1 and CNT3. Studies done by Spratlin J. et al. [47] showed that pancreatic cancer patients with some or detectable expression of ENT1 have a better survival rate compared to those with no or very low ENT1 expression. Therefore, ENT1 mRNA/protein level in tumour tissues could be used as a predictive marker for gemcitabine-based chemotherapy in pancreatic cancer patients, though conclusive studies are needed in this area [45, 46].

1.4.2 Cellular metabolism and mechanism of action

After uptake into the cells via specialised transporters, gemcitabine is activated by phosphorylation intracellularly by deoxycytidine kinase (dCK). gemcitabine after the

phosphorylation produces 2',2'-difluoro-2'-deoxycytidine monophosphate (dFdCMP); rate-limiting step [39], which is then, converted into its active diphosphate and triphosphate metabolites (dFdCDP and dFdCTP). gemcitabine had a K_m value of 4.6 μM for dCK while for deoxycytidine it has K_m value of 1.51 μM , this makes gemcitabine a good substrate for dCK [48]. Also, dCK affinity for gemcitabine is higher than that for Ara-C ($K_m=3.6$ and 8.81 μM [39], respectively) and the V_{max}/K_m ratio is more favourable [39, 46, 49]. Active metabolites of gemcitabine (dFdCTP) get inserted into the DNA strand during DNA synthesis resulting inhibition of synthesis that's mainly how gemcitabine exerts its cytotoxic effect. gemcitabine exhibits 'self-potentialiation' in which dFdCDP potentially prevents the execution of ribonucleotide reductase (RR) [49]. Thymidine kinase 2 (TK2), a mitochondrial enzyme was also found to phosphorylate gemcitabine. Its substrate specificity is however only 5–10% of that for deoxycytidine [46, 50] but still can play a significant role in the gemcitabine sensitivity. TK2 phosphorylates dCyd (deoxycytidine) far more efficiently than gemcitabine while dCK phosphorylates dCyd and gemcitabine both. Thus, an increase in the dCK/TK2 activity could lead to a better dFdCTP/dCTP ratio, eventually greater toxicity. Thus, for increased gemcitabine toxicity a low TK2 activity is required. Though up till now direct evidence of gemcitabine phosphorylation by TK2 is lagging in the intact cells. Further research is required to verify specific mitochondrial peculiarities induced by gemcitabine to confirm the role of TK2 in either gemcitabine toxicity or antitumor activity. Deficiency of the dCK enzyme has been identified as one of the most frequent causes of gemcitabine resistance [39, 46, 51].

1.4.3 Ribonucleotide Reductase (RR)

Several metabolites of gemcitabine can inhibit various enzymes, leading to self-potentialiation of gemcitabine action. The inhibition of RR by dFdCDP is one of the most critical self-potentiating mechanisms. dFdCDP is also one of such significant metabolites of gemcitabine inhibiting the RR enzyme. RR is responsible for the production of dNTP (deoxyribonucleotide triphosphate) pool that is further used for DNA synthesis. By inhibiting RR, dFdCDP reduces the competitive dCTP pool which is a potent inhibitor of dCK enzyme leading to more efficient phosphorylation of gemcitabine. In studies it was found that RRM1 or subunit 1 of RR enzyme is associated with gemcitabine resistance, signifying that RRM1 could be a significant determinant for antitumor activity of gemcitabine [46].

1.4.4 Gemcitabine De-activation

Gemcitabine has multi molecular target inside the cell and therefore has many factors involved in the deactivation, e.g. absence of proper transporters, inactivation or low activity of dCK enzyme and transport of drugs outside the cell by active ABC transporters. Cytidine deaminase (CDA) is one such enzyme involved in the detoxification of gemcitabine by salvaging pyrimidines. 90% of gemcitabine is inactivated by conversion into 2-deoxy-2, 2 difluorouridine (dFdU) by CDA. Although an in vitro study demonstrated CDA confers resistance to gemcitabine, it was found that patients with deficient or very low CDA activity showed an increased systemic gemcitabine exposure and thus high toxicities in a prospective pharmacogenomic study [52], suggesting CDA may not be an appropriate tumour-specific target to reversing gemcitabine resistance. Gemcitabine has a 50% lower affinity for CDA enzyme than does deoxycytidine (K_m : 95.7 and 46.7 μM , respectively) [45, 48]. Deamination of dFdCMP to 2,2-difluorodeoxyuridine monophosphate (dFdUMP) by dCMP deaminase and consequently to dFdU is also one of the inactivation pathways of gemcitabine. Gemcitabine and dFdU both are not substrates for pyrimidine nucleoside phosphorylases. Thus, they are excreted out of the cell by ABC (ATP binding cassette) transporters. This detoxification of gemcitabine leads to the shorter overall survival of the pancreatic carcinoma patient [46].

1.4.5 Transporters and metabolic enzymes

As mentioned before that gemcitabine is hydrophilic and thus, it depends on various transporters for its entry into the cells and exercises its cytotoxic effect. Prior studies by Mackey et al. [53] recognised key transporters engaged in the uptake of gemcitabine and showed the requirement for their movement for gemcitabine sensitivity [53, 54]. Mackey et al. [55] found that the human equilibrative transporters 1 and 2 (hENT1 and hENT2) could intercede transport of gemcitabine (K_m of 160 μM and 740 μM , respectively), the human concentrative nucleoside transporter 1 (hCNT1) had the best intrinsic transport activity (V_{max} : K_m of 0.24 $\text{pmol}/\mu\text{M}/\text{min}$) [53]. Thus, both transporters hENT1 and hCNT1 play a very significant role in the drug efficacy and output of the treatment [56]. Both immunohistochemical and transcriptional hENT1 expression has been associated with the survival of the patients receiving gemcitabine therapy [56-58]. Even though the roles of these transporters are well characterised in pancreatic cancer, but still the reason behind low drug efficacy remains vague. Some

studies have suggested the roles of enzymes which are involved in salvaging the effect of the drug.

After crossing the cell membrane, gemcitabine is further metabolised and phosphorylated into its active di (dFdC-DP) and triphosphate (dFdC-TP) form by the deoxycytidine kinase (dCK) enzyme. These activated moieties (dFdCTP) of gemcitabine, instigates masked chain termination restricting further DNA polymerase activity [56].

Thus, conversion of gemcitabine into its active moieties is a “rate-limiting step” [39], and deficiency in dCK expression could result in a higher level of gemcitabine resistance in the pancreatic cancer cells [59]. Overexpression of dCK was found to enhance the gemcitabine efficacy significantly in pancreatic cancer cell lines. Clinically, low immunohistochemical expression of dCK corresponded with decreased overall survival [56]. HuR is an RNA binding protein, and its low expression is linked with the higher mortality rate in the pancreatic cancer patient because of its capacity to manage dCK levels [56, 60].

As explained previously, gemcitabine inactivation is carried out by cytidine deaminase (CDA), by removal of NH₂ group from the pyrimidine, enabling the uracil metabolite to be effluxed from the cell. CDA induced gemcitabine inhibition causes a reduction in dFdCTP catabolism, henceforth driving the self-potential of gemcitabine action [56]. A few studies have also reported a dramatic increase in the chemosensitivity up to 54-folds of cancer cell lines with the inhibition of CDA [56, 61]. However, CDA in pancreatic cancer has been unfavourable because CDA gene polymorphisms are associated with gemcitabine toxicity (e.g., haematological toxicity, high-grade neutropenia) rather than anticancer efficacy [56, 62]. Though further studies are vital, specific modification in the CDA expression level in tumours could be encouraging but challenging in improving gemcitabine sensitivity.

1.5 Potential molecular targets

Other factors which could be considered in enhancing the gemcitabine cytotoxicity incorporates factors influencing DNA synthesis and repair especially ribonucleotide reductase subunits 1 and 2 (RRM1 and RRM2). RRM1 and RRM2 are restrained by dFdCDP and dFdCTP from repairing faulty DNA. The transcriptional upregulation of the bigger subunit, RRM1, has been seen to increase the acquired resistance in

pancreatic cancer cell lines [56, 63]. Steadily, low expression of RRM1 in tumours corresponds with upgraded gemcitabine response particularly in recurrent cases [63, 64]. Thus, this RRM1 seems to have a variable relationship with the overall survival and no relationship with disease-free survival [64, 65]. In this manner, the RRM1 expression looks more acquired than innate.

For RRM2, a few studies have demonstrated elevated protein expression in pancreatic cancer cell lines [56]. Knockdown of RRM2 using RNAi reduced gemcitabine resistance and intrusiveness in cells, while it suppressed tumour development, improved apoptosis, and repressed metastasis in xenograft models [56]. Besides, Ohhashi et al. [59] discovered a decrease in cell growth with the hindrance of RRM1 and RRM2 even without gemcitabine treatment [56]. Thus for overall survival and median survival low level of RRM2 expression is favourable in the patients receiving gemcitabine treatment [66].

There is an immediate need to understand the various molecular process involved in the drug resistance of pancreatic cancer and come up with an effective regimen for pancreatic cancer. Characterisation of gene overexpression may lead to the development of new screening systems and markers and additionally new gene therapy procedures [35]. Pancreatic cancer shows various mutations, and thus most of the genes are not specific making the tailored therapies less efficient. Thus, detailed profiling of all the genes involved in the drug resistance and the genes which are overexpressed is very necessary to increase the overall survival rate in the pancreatic cancer patients. Such gene profiling could help us in narrowing down the gene target range, and specific genes related to drug resistance could be targeted augmenting the efficiency of the existing chemo-and radiation therapy for pancreatic cancer. Pancreatic cancer showed both intrinsic (de novo) and acquired (therapy-induced) chemo-resistant behaviours. The gemcitabine-based regime is the most commonly used for pancreatic cancer with improved clinical outcomes. However, the overall survival rate is still very low. One of the major reasons for the failure or less efficiency of chemotherapy is either the innate or acquired drug resistance. Up until now, a few mechanisms have been proposed to understand such resistance, e.g. impaired drug delivery pathways, escaping apoptosis, overexpression of ABC transporters and angiogenesis. Thus a comprehensive study of the mechanisms involved in drug resistance is required to increase the drug efficacy in pancreatic cancer [35]. Earlier studies have proposed various mechanisms of drug

resistance in pancreatic cancer, including abnormal gene expression, mutations, deregulation of critical signalling pathways [35].

1.5.1 Abnormal Gene expression

One of the major factors related to gemcitabine resistance in pancreatic cancer is genetic and/or epigenetic variations. Multidrug resistance (MDR) as the name suggests is a mechanism responsible for resistance to numerous therapeutic drugs and prompts ineffectualness in the chemotherapeutic treatment of pancreatic cancer. The MDR phenotype is frequently ascribed to the overexpression of certain drug efflux pumps. Overexpression of these drug efflux pumps causes less accumulation of drugs into the target cells leading to increased drug resistance. Members from the ATP binding cassette (ABC) transporter superfamily have been found to be actively involved in the drug efflux and MDR in a variety of cancers. One of the proposed mechanism for ABC transporters is that they act as hydrophobic vacuum cleaners by effluxing xenobiotics from the cells by utilising energy from ATP hydrolysis [35].

Currently, in humans, 49 ABC transporters genes have been recognised and classified into seven subfamilies. Specifically, members of ABCB/Pgp, ABCC, and ABCG subfamilies have been reported to be significantly involved in multidrug resistance in tumour cell lines. P-glycoprotein (P-gp), member of ABC-B family is one of the best characterised ABC transporters; physical structures of many other ABC transporters (especially MRP and BCRP) are based on P-gp's structure [35]. In many cancer types, higher P-glycoprotein levels have been reported, and these higher levels have been found to be associated with MDR [67]. Members of ABCC family e.g. MRP1 (ABCC1), MRP3 (ABCC3), MRP4 (ABCC4), and MRP5 (ABCC5), have been found to overexpressed in pancreatic tumour [67] and are suspected to confer MDR in pancreatic cell lines *in-vitro* against a few chemotherapeutic drugs including gemcitabine [68] and 5-FU [35]. Due to the significant involvement of ABC transporters in MDR, it is believed that their inhibition could lead to more efficient results in the chemotherapy. Thus, over the time many inhibitors have been developed for ABC transporters, and their combinations with the drug have been tried to increase the drug-efficacy.

The intracellular uptake of gemcitabine (Refer to section 1.4.1 of this chapter for more details) is subject to nucleoside transporters, for example, human equilibrative nucleoside transporter-1 (hENT1) [35]. *In vitro* studies have demonstrated that

reduction in hENT1 levels reduces the intracellular uptake of gemcitabine thus declining the efficacy of the drug [54]. Changes in the activity of enzymes involved in gemcitabine metabolism can also negatively influence gemcitabine potency [39]. For instance, deoxycytidine kinase (DCK), CDA and ribonucleoside reductases M1 and M2 have been appeared to relate with gemcitabine resistance [35, 69]. Considering the previous knowledge of MDR mechanism in pancreatic cancer, numerous investigations have been done to create powerful treatments targeting abnormally expressed genes, signalling pathways, and tumour microenvironment, which contributes to the drug resistance in pancreatic cancer. In addition to standard chemotherapy, scanning for new molecular targets involved in drug resistance may overcome MDR and increase the efficiency of treatment in comparison with the single-agent regimen for a pancreatic tumour [35].

1.5.2 Targets for reversing gemcitabine resistance

As we know, members of the ABCC family are actively involved in effluxing nucleoside-based drug analogues out of the cells, and their overexpression in pancreatic cancer cells make them primary suspects for MDR. Especially, MDR proteins (MRP1, MRP3, MRP4, MRP5 and P-glycoprotein) were found to be overexpressed in pancreatic cancer cells. Thus, blocking MDR proteins could play a huge role in reducing drug resistance in pancreatic cancer [35]. ABC transporters of ABCC family play a very crucial role in gemcitabine efflux. MRP4 and MRP5 have also been localised in the duct cells, acinar cells, and pancreatic cells [67]. Studies [70-73] have also reported that MRP5 confers resistance to gemcitabine and its moieties. Studies [74] have also reported variations in the MRP5 levels in the tumour grading correlated with the mRNA expression. gemcitabine alone or in combination with other chemotherapeutic drugs can cause several-fold induction in mRNA expression of the influx and efflux proteins including ENT1 and MRP5, which are involved in gemcitabine uptake and efflux, respectively. Studies [75, 76] have also reported several folds of induction in MRP5 and hENT1 levels after the execution of gemcitabine. MRP5 and hENT1 are involved in the efflux of and uptake of gemcitabine and its moieties respectively. Two individuals from the multidrug resistance protein (MRP) family, MRP4, and MRP5 have been indicated to transport cAMP and cGMP [77-79]. In the studies [80] it was found that MRP4 and MRP5 overexpressing cells show higher cGMP and cAMP efflux in an ATP-dependent manner. MRP5 is a low-affinity cyclic nucleotide transporter that acts as an efflux pump [80]. MRP5 from the MRP family is confined in the plasma membrane and work

as a transporter that pair ATP hydrolysis to the efflux of organic anions [81, 82]. MRP5 was shown to transport the monophosphorylated type of nucleoside analogue drugs [83-85].

In a few studies [67, 74, 86-94] upregulation of ABC transporters has been reported pancreatic cancer cells. Specifically, MRP3, MRP4, and MRP5 proteins were found to be up-regulated in human pancreatic tissue and pancreatic carcinoma [74]. Also, few studies have reported a higher mRNA level of ABC5 in the pancreatic cancer cells as compared to normal pancreatic tissue [67]. On the other hand, the role of individual MRP isoforms to chemoresistance of pancreatic tissue or pancreatic carcinomas towards specific drug is not clear yet. Such innate or acquired chemoresistance of an organ or cell sort can be because of induced expression and functional localisation of ABC transporter proteins. For example, the expression level of a few MRP isoforms has been shown to be affected by drugs or to contrast from typical conditions under pathophysiologic conditions [95-97]. Gemcitabine is a deoxycytidine analogue that vies for DNA incorporation [98]. Nucleoside analogues are an essential class of drugs utilised as a part of the treatment of tumour and viral diseases. A few studies have demonstrated that a change in uptake transporters can intervene in resistance against these drugs and metabolising enzymes [99, 100]. As we know now that gemcitabine is prodrug and its active metabolites are dFdCDP and dFdCTP, and studies have demonstrated that nucleotide analogues and cyclic nucleotides are substrates for MRP4 and MRP5 [80, 101, 102]. Overexpression of one of these pumps may bring about resistance against anticancer and antiviral drugs [71, 78, 80, 85, 94, 103]. The MRP5 A-2G AA genotype also showed a significant association with overall survival in pancreatic cancer patients [93].

1.6 ABC Transporters and MDR

MDR is an intricate process that can happen because of a few biochemical mechanisms that are still not wholly comprehended [104]: **i)** altered membrane transport either by decreased drug uptake or by increased drug efflux (Fig 3.0) [105]; **ii)** perturbed expression of target enzymes or altered target enzymes [106]; **iii)** altered drug activation or degradation [107]; **iv)** enhanced DNA repair [108]; **v)** failure to undergo apoptosis [109]. Some of these mechanisms may coincide, rendering the objective cell obstinate to treatment with drugs targeting a single target. The most commonly involved and contemplated mechanism of MDR is altered cell membrane transport [110]. This sort of resistance is because of a lower drug intake of the cell or increased efflux of the

chemotherapeutic drug, because of the over-expression of various transporter proteins that act as extrusion pumps. Several families of efflux pumps, which can utilise a variety of energy sources are present in mammals and microorganisms [111-113].

The membrane transport proteins are categorised in four different subtypes: ion channels; co-transporters; aquaporins; and ATP-dependent pumps[114]. Genes from each of the four classes are ancient, i.e. they can be found in most prokaryotes and almost all eukaryotes. The eukaryotic cell transporters are involved in the movement of amino acids, ions, sugars and various xenobiotics in the cell and many cell organelles except nuclear membranes [114]. Membrane transport proteins could be passive or active. When the substrates are transported down the concentration gradient, they are called as passive transporters (aka uniporters or facilitative transporters) [114].

Like ATP pumps, cotransporters intervene coupled reactions, i.e. they are involved in the coupling of energetically unfavourable reaction to energetically favourable reaction. When the movement of transported and co-transported molecules is unidirectional across the cell membrane the transporter is known as symporter; when vice versa it is called an antiporter (or exchanger) [114]. If the intracellular net charge post transport is negative than the procedure is named electronegative; if the net charge post transport is positive than the procedure electropositive. If the subsequent intracellular net charge stays unaltered, the procedure is named electroneutral [114].

Ion channels are pore-forming membrane proteins that assist in building and keeping up slight voltage gradient across the cell membrane. Thus, ion-channels are involved in the regulation of the cell's electric potential by permitting the ion flow down their electrochemical gradient. In general, ion-channels are found in the closed state and have a very high efficiency of transport for cationic and anionic substrates. More than 400 genes are known for ion channel subunits. Ion channel transporters move ions at a slower rate than channel proteins [114]. Aquaporins represent a unique class of transporter proteins, which mediate bi-directional water transport. In humans to date 13 putatively functional AQP genes have been reported (<http://www.genenames.org/>).

ABC transporters are the ATP dependent transmembrane efflux proteins which are involved in the import/export of various substrates in and out of the cells against their electrochemical gradient. These transporters are further divided as exporters and importers based on their transport direction. Importers are responsible for the substrate uptake into the cells while the exporters are involved in the efflux [114].

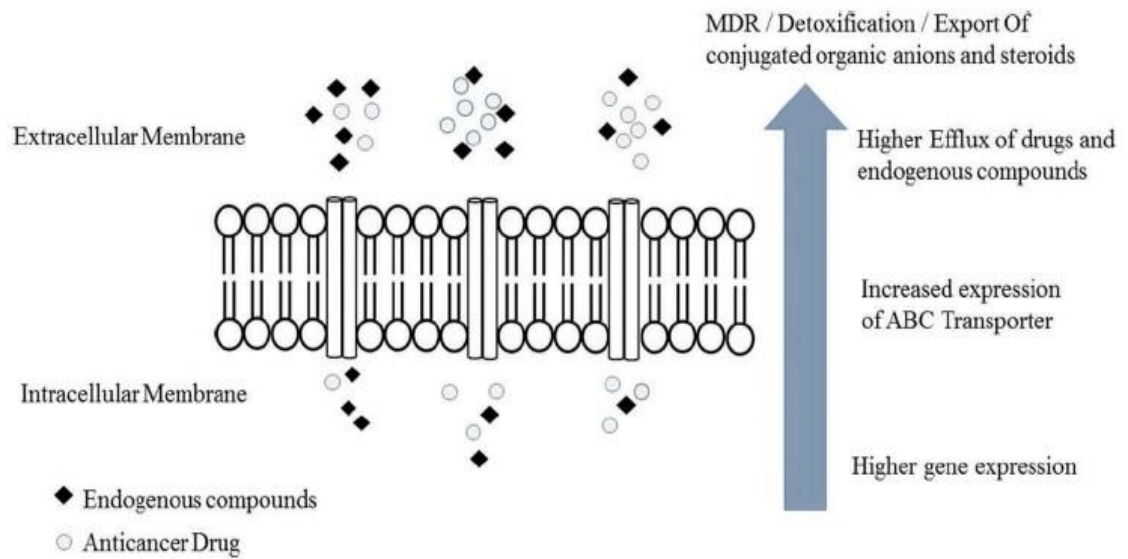


Figure 1-2: Multidrug resistance via increased efflux of drugs (Ref: [115])

1.6.1 Details of the ABC proteins

There are four domains in the core unit of ABC transporters. These four domains comprise two nucleotide binding domains (NBDs) and two transmembrane domains (TMDs). The NBD is composed of highly conserved domains; the Walker A and Walker B sequences (the ABC signature motif), the H loop and the Q loop and the TMDs have several hydrophobic α -helices. The two NBDs bind together and provide the site for ATP hydrolysis (subsequently giving the energy for transport), while the TMDs are responsible for substrate recognition and translocation of the substrates across the cell membrane. Some of the ABC proteins were found to be 'half-transporters,' i.e. the two subunits bind as homodimers or a heterodimer [114]. The human genome has 49 ABC genes known so far, orchestrated in seven subfamilies, assigned A to G (Table 1-6).

Subfamily name	Aliases	Number of genes	Number of pseudogenes
ABCA	ABC1	12	5
ABCB	MDR	11	4
ABCC	MRP	13	2
ABCD	ALD	4	4
ABCE	OABP	1	2
ABCF	GGN20	3	2
ABCG	BCRP	5	2
Total		49	21

Table 1-6: ABC genes (Ref: [114])

Subfamily A of the ABC family (ABCA)

So far 12 genes are known for subfamily A, and most of them are involved in the lipid transport in different organs and cell types. Some of the ABCA proteins weigh more than 2,100 amino acids in length and are amongst some of the largest ABC transporters. The biggest ABCA protein known so far is ABCA13 and has 5,058 residues, making it. Mutations in specific ABCA genes have been to be associated with the genetic disorders, such as Tangier disease T1, familial high-density lipoprotein (HDL) deficiency, age-related macular degeneration and retinitis pigmentosa [114, 115].

Subfamily B of the ABC family (ABCB)

This sub-family in humans has 11 genes and has four full transporters and 7 half transporters. Some of the members of this family have been found to be associated with the MDR in many cancer types, and that's why this family is also known as the "MDR family". Mutations in ABCB genes have been found to be associated with genetic disorders, but still, a conclusive study is needed to affirm their role. ABCB mutations have been linked with ankylosing spondylitis, diabetes type 2, coeliac disease, lethal neonatal syndrome, X-linked sideroblastic anaemia with ataxia, and several cholestatic liver diseases [114].

Subfamily C of the ABC family (ABCC)

This family contains 13 genes including the cystic fibrosis gene (CFTR, aka ABCC7). Most of the members of this family are known to be involved in MDR. Some of the other functions of the members of this family are - ion-channel and toxin excretion. Mutations in the ABCC genes have been associated with multidrug resistance, autosomal recessive diseases such as cystic fibrosis, and hyperinsulinemic hypoglycaemia. Many studies have suggested the involvement of members of this family in pancreatic cancer drug resistance explained further in this thesis [114].

Subfamily D of the ABC family (ABCD)

This family has 4 genes in humans known so far and is also known as ALD transporters. These four genes code for half-transporters and are responsible for coding 49 distinct proteins by alternative splicing. Mutations in ABCD genes were found to be associated with ALD and Zellweger disorder [114].

Subfamily E of the ABC family (ABCE)

ABCE1 is a single member of this family, and it is an organic anion-binding protein. ABCE1 has 1 NBD but lack TMDs, making it far-fetched that this protein capacities as a transporter. Due to 15 alternatively spliced transcripts, the ABCE1 gene encodes five distinct proteins and functions to promote interferon activity [114].

Subfamily F of the ABC family (ABCF)

Alongside ABCE1, ABCF individuals likewise have ATP-binding domains, however, no TMD and thus no transporter activity. ABCF genes encode 26 distinct proteins via alternate splicing. ABCF genes were found to be upregulated by tumour necrosis factor- α . Thus, individuals of this family are suspected to play a part in the inflammatory process. No disease has been related, up until this point, with either the ABCE or ABCF genes [114].

Subfamily G of the ABC family (ABCG)

This subfamily involves no less than five genes that encode 'reverse half-transporters', implying that they form the second half of a heterodimer. Mutations in ABCG genes have been involved in sterol accumulation issues and atherosclerosis. Because of alternative splicing, 18 distinct subunit proteins have been recognised as a product of the five ABCG genes [114].

Parental gene	Pseudogene	Chromosomal location	Accession number
ABCA3	ABCA17P	16p13.3	DQ266102
ABCA10	ABCA10P	4p16.3	AK024359
Abca14*	ABCA14P1	16p12.2	
Abca15*	ABCA15P1	16p12.2	DR731461
	ABCA15P2	16p12.1	
ABCB4	ABCB4P	4q32.1	
ABCB10	ABCB10P1	15q11.2	
	ABCB10P2	15q13.1	
	ABCB10P3	15q13.1	
ABCC6	ABCC6P1	16p12.3	DB11925
	ABCC6P2	16p13.11	
ABCD1	ABCD1P1	2p11.1	AY344117
	ABCD1P2	10p11.1	
	ABCD1P3	16p11.2	
	ABCD1P4	22q11.1	
ABCE1	ABCE1P1	1q31.2	
	ABCE1P2	7p15.3	
ABCF2	ABCF2P1	3p11.2	
	ABCF2P2	7q11.2	
ABCG2	ABCG2P1	14q24.3	
	ABCG2P2	15q23	

Table 1-7: Human ABC transporter pseudogenes (Ref: [114])

*Abca14, Abca15 and Abca16 are mouse genes, with no human orthologues. The mouse genome contains 52 ABC genes, whereas the human genome carries 49 ABC genes.

1.6.2 ABC transporters and their roles in tumour resistance and progression

Most of the chemotherapeutic drugs are infused intravenously in the body and thus have complex pharmacokinetics and pharmacogenomics when it comes to their metabolism, e.g. uptake and efflux into the cells. ABC transporters play a crucial part in the drug metabolism as their expression can affect the drug kinetics of the executed chemotherapeutic agent.

ABC transporters are involved in the active efflux of the drug moieties out of the cells, i.e. they efflux the drug metabolites against the concentration gradient using ATP as the energy source. Such active efflux dramatically reduces drug efficacy and makes chemotherapy treatment very difficult. Many studies [116] have reported up-regulation of the ABC transporters in the cancer cells making the cancer type more resistant to the chemotherapeutic drugs. These ABC transporters exhibit a wide spectrum of drug substrates, e.g. P-gp substrates include doxorubicin, docetaxel and etoposide (refer to table 8). Some tumour cells with higher levels of Pgp automatically becomes resistant to the range of Pgp substrates. Such type of MDR could be innate or acquired, and Interestingly it occurs not by acquired mutations but by increased ABCB1 expression via monoallelic promoter capture [117]. Thus, initial screening of expression levels of various drug transporters could be a good start for the selection of chemotherapeutic agents. A study [116] has also proposed the role of Pgp in cell differentiation and metastasis.

Not all cancer types exhibit resistance mediated by Pgp various other ABC transporters, e.g. MRPs and BCRP are also involved in the exertion of MDR. MRP family comprises 13 members with a size range from 1325 to 1545 amino acids, which is encoded by the ABCC gene family [116, 118]. MRP1/ABCC1, considered as the second significant efflux pump, is one of the MRP individuals and its ability for drug efflux counteracts successful treatment of a range of anticancer drugs, for example, methotrexate and vincristine [118]. Overexpression of MRP1 has been found in numerous sorts of tumours where it assumes a critical part in tumour resistance, conferring a severe relapse in patients. Some clinical examination even demonstrated the overexpression of MRP1 and treatment for MRP1 appear to be more compelling than target P-gp [116]. MRP4 and MRP5's significance in the efflux of nucleoside-based analogues and their over-expression in the pancreatic cancer cells has already been stated before. Thus, a more comprehensive study in profiling ABC transporters are needed to design better

chemotherapeutic treatment which could lead to an increase in the overall survival of the patients.

1.6.3 ABC transporters: Subdivision

Importers

ABC transporters are further subdivided into importers and exporters, based on the direction of substrate movement. Both importers and exporters have two transmembrane domains (TMDs) and two cytoplasmic nucleotide-binding domains (NBDs), powered by the hydrolysis of ATP. The TMDs and NBDs together form the translocator [119]. ABC importers, which on structural and mechanistic grounds are subdivided into type I, II, and III importers (Fig. 5) [120]. The mechanism of transport of type I and II ABC importers include the binding and release of the substrate from an extra-cytoplasmic substrate-binding protein (SBP) and alternating access of the substrate-binding pocket inside the translocator domain [119]. Type III importers, also named energy-coupling factor (ECF) transporters, capture ligands through a so-called S-components, which are small integral membrane proteins that accomplice with a transmembrane coupling protein and two NBDs to shape a full transporter. The mechanism of transport of kind III importers could involve substrate translocation by toppling of the S-component rather than alternating access of the translocator domain [119].

ABC Exporters

ABC exporters are responsible for the extrusion of substances from the cis- to the trans-side of the lipid bilayer, the site of ATP consumption is usually referred as the Cis side in the transport [119]. ABC transporters are comprised of four core domains, two transmembrane domains and two nucleotide binding domains (NBDs). Transmembrane domains (TMDs) have six transmembrane helices [exception - macrolide transporter MacB] [121] and are phylogenetically diverse. Thus, TMDs are involved in the substrate recognition and translocation from ci to the trans side. NBDs provide the site for ATP binding and thus provide energy for the efflux [122]. Apart from these 4 core domains, a large variety of cytoplasmic, extracellular, and transmembrane-spanning domains have been defined for ABC exporters, which play diverse roles in the regulation of the core transporter and recognition of other protein-binding partners. Some of the examples of such extra domain are the R-domain of CFTR [123], the TMD0-domain of TAP1/2 [124], and the periplasmic domain of MacB need to recognise the periplasmic membrane fusion protein MacA [125].

ABC Transporters	Substrates	References
ABCB1	<p>Analgesics: asimadoline, fentanyl, morphine, pentazocine</p> <p>Antiarrhythmics: amiodarone, digoxin, lidocaine, propafenone, quinidine, verapamil</p> <p>Antibiotics: cefoperazone, ceftriaxone, clarithromycin, doxycycline, erythromycin, gramicidin A, gramicidin D, grepafloxacin, itraconazole, ketoconazole, levofloxacin, rifampicin, sparfloxacin, tetracycline, valinomycin</p> <p>Anticancer drugs: 5-fluorouracil, actinomycin D, bisantrene, chlorambucil, colchicine, cisplatin, cytarabine, daunorubicin, docetaxel, doxorubicin, epirubicin, etoposide, gefitinib, hydroxyurea, irinotecan (CPT-11), methotrexate, mitomycin C, mitoxantrone, paclitaxel, tamoxifen, teniposide, topotecan, vinblastine, vincristine</p> <p>Antihistamines: cimetidine, fexofenadine, ranitidine, terfenadine</p> <p>Antilipidemic: lovastatin, simvastatin</p> <p>Calcium channel blockers: azidopine, bepridil, diltiazem, felodipine, nifedipine, nisoldipine, nitrendipine, tiapamil, verapamil</p> <p>Fluorescent dyes: calcein AM (calcein acetoxymethylester), Hoechst 33342, rhodamine 123</p> <p>HIV-protease inhibitors: amprenavir, indinavir, lopinavir, nelfinavir, saquinavir, ritonavir</p> <p>Immunosuppressive agents: cyclosporin A, cyclosporin H, FK506, sirolimus, tacrolimus, valsopodar (PSC-833)</p> <p>Natural products: curcuminoids, flavonoids</p> <p>Neuroleptics: chlorpromazine, phenothiazine</p> <p>Others: BCECF-AM, bepridil, calcein-AM, diltiazem, endosulfan, leupeptin, methyl parathion, paraquat, pepstatin A, trifluoperazine, trans-flupentixol</p>	[126-129]
ABCC1	Antibiotics: Anthracyclines	[127-131]

	Anticancer drugs: mitoxantrone, vinca alkaloids, imatinib, epipodophyllotoxins, camptothecins, colchicine and methotrexate	
	HIV-protease inhibitors: saquinavir	
	Heavy metal oxyanions: Arsenite, Trivalent antimony	
ABCC2	Antibiotics: ampicillin, azithromycin, cefodizime, ceftriaxone, grepafloxacin, irinotecan	[126-128, 130-135]
	Anticancer drugs: cisplatin, doxorubicin, epirubicin, etoposide, irinotecan, mitoxantrone, methotrexate, SN-38, vinblastine, vincristine, oxaliplatin	
	Antihypertensives: olmesartan, temocapril	
	HIV drugs: adefovir, cidofovir, indinavir, lopinavir, nelfinavir, ritonavir, saquinavir	
	Others: ethinylestradiol-3-O-glucuronide, genistein-7-glucoside, p-Aminohippurate, phloridzin, quercetin 4'- β -glucoside, vinca alkaloids	
ABCC3	Methotrexate, epipodophyllotoxins, teniposide	[126, 131, 134, 136]
ABCC4	Thiopurines, PMEA, methotrexate, AZT, camptothecins	[126, 131, 134, 136]
ABCC5	Thiopurines, methotrexate, cisplatin, gemcitabine, PMEA and AZT	[126, 131, 134, 136]
ABCC6	Anthracyclines, cisplatin and epipodophyllotoxins	[126, 131, 134, 136]
ABCC10	Vinca alkaloids and taxanes	[127, 128, 134, 136]
ABCC11	Thiopurines, steroid sulfates, 5-FU	[127, 128, 134, 136]
ABCG2	Antibiotics: ciprofloxacin, norfloxacin, ofloxacin Anticancer drugs: daunorubicin, doxorubicin, epirubicin, etoposide, gefitinib, imatinib, irinotecan, mitoxantrone,	[126-128, 135, 136]

methotrexate, SN-38, teniposide, topotecan,

Antivirals: delavirdine, lopinavir, lamivudine, nelfinavir,
zidovudine

Antihypertensives: reserpine

Calcium channel blockers: nifedipine

Lipid-lowering drugs: cerivastatin, pravastatin, rosuvastatin

Others: azidothymidine, chrysin, cyclosporin A, lamivudine,
ortataxel, quercetin

Table 1-8: Substrates of ABC transporters (Ref: [115])

1.6.4 Mechanism of Action of MDR Exporter

Step 1: Ligand-TMDs a high-affinity open NBD dimer conformation

ABC transporters exhibit a high affinity for the ligand in a nucleotide-free state. A conformational change could be seen in the structure of NBDs after ligand-binding to TMDs [137-143], transduced through ICLs of the TMDs, which interdigitate with NBDs. The close vicinity of the ICLs with the Q-circle and Walker A motifs recommends that the coupling of the ligand could straightforwardly impact the affinity of the NBDs for ATP [143]. As recommended by fundamental investigations of some crystals of HlyB and LolD with surprising conformities of the Walker A motif, which would block binding of ATP [144, 145], albeit with a component this is in no way, shape or form clear. Proof for an increment in a proclivity for ATP in the vicinity of ligand has been hard to gauge and is to a great extent indirect.

Step 2: Conformational change in the TMDs for ligand translocation

Structural data demonstrate two molecules of ATP at the NBD dimer interface, inferring that they act in a single step. Development of the NBD dimer closed around the ATP has been figured to produce a lot of free energies [146]. A few particular estimations propose that this available energy is utilised to reconfigure the TMDs [138, 139, 141, 142]. The degree of this conformational change is vast and can be imagined at a low determination for P-glycoprotein [147]. This may include breaking associations between TM helices and arrangement of new contacts with diverse accomplices. Of course, this adjustment can change both the position and natural inclination of the ligand binding site.

Step 3: ATP hydrolysis starts disintegration of the closed NBD dimer

The transient nature of isolated NBD dimers incited by ATP is followed by the ATP hydrolysis [146], and substrate-assisted catalysis proposed for HlyD [148]. This hydrolysis destabilises the closed NBD dimer [143]. For some ABC transporters like P-glycoprotein, hydrolysis of both ATPs is essential for the consummation of the transport cycle [143, 149] and the ATPs are hydrolysed simultaneously [150-153]. The two ATP binding pockets of P-glycoprotein (Pgp) have been demonstrated to be biochemically different. However yet it is not clear whether this is a reason for non-simultaneous hydrolysis or the aftereffect of it [150]. In other ABC transporters, for example, in MRP1 and CFTR, hydrolysis of only one ATP may be adequate to drive the protein through the conformational cycle [154, 155]. The post-hydrolytic state can be shifted into steady conformity once phosphate has left. This type of the protein, which may imitate the ADP-Pi state, has compliance distinct from the ATP-bound and nucleotide-free forms [147, 156] and may be coupled to transport from distinctive drug binding pockets in Pgp [157, 158].

Step 4: Pi then ADP is released to finish the transport cycle and re-establish protein to a high-affinity state for ligand

Following hydrolysis, the phosphate is released from the protein. The rapid release of phosphate, which allows the protein to be trapped with ADP and vanadate, relates well to the reinstatement of high-affinity vinblastine binding to P-glycoprotein, representing that the conformational change associated with the phosphate release is also coupled to the ligand binding sites [159]. The affinity of the ABC transporters for ADP is low, and ADP is not capable of stabilising the dimeric interaction of isolated NBDs [160].

1.6.5 ABCC5 (MRP5)

Particularly individuals from the ABCB family including MDR1 P-glycoprotein and individuals from the ABCC family have been demonstrated to be responsible for mediating multidrug resistance [161-164]. The human ATP-binding cassette transporter family C (ABCC) comprises of 12 individuals, 9 of which involve the gathering of multidrug resistance proteins (MRP1–MRP9; ABCC1–ABCC6 and ABCC10–ABCC12) [162-164]. MRPs are essential membrane proteins mediating the ATP-dependent export of natural anions out of cells. In this way, the members of MRP1–MRP6 are the best-characterized paralogs with respect to their substrate range. MRP1, MRP2, MRP3 and MRP6 transport lipophilic mixes conjugated with glutathione, glucuronate or sulfate [162-164]. Substrates for MRP4 and MRP5 incorporate cyclic

nucleotides and nucleotide analogues [71, 78, 165, 166]. Furthermore, MRP4 has been recognized as a co-transporter for reduced glutathione with bile salts and as a transporter for prostaglandins and the steroid dehydroepiandrosterone-3-sulfate (DHEAS) [71]. Nevertheless endogenous mixes, MRP members have the capacity to export a mixture of natural anions of toxicological significance and are significant in conferring resistance to cytotoxic and antiviral drugs [167]. A few studies reported the interpretation of ABC transporters in the human pancreas, pancreatitis, and pancreatic carcinoma [74, 86-92]. Specifically, MRP3, MRP4, and MRP5 proteins were found to be expressed in human pancreatic tissue and pancreatic carcinoma [74]. On the other hand, the role of individual MRP isoforms to chemoresistance of pancreatic tissue or pancreatic carcinomas towards specific drug is not clear yet. Such natural or gained chemoresistance of an organ or cell sort can be because of induced expression and functional localization of ABC transporter proteins. For example, the expression level of a few MRP isoforms has been shown to be affected by drugs or to contrast from typical conditions under pathophysiologic conditions [95-97]. Gemcitabine is a deoxycytidine analogue that vies for DNA incorporation [98]. Nucleoside analogues are an essential class of drugs utilized as a part of the treatment of tumours and viral diseases. A few studies have demonstrated that resistance against these drugs can be intervened by a change in uptake transporters and metabolizing enzymes [99, 100]. However, recent studies propose that efflux pumps are significant modulators of resistance against nucleoside-based analogues. Accordingly, it has been demonstrated that nucleotide analogues and cyclic nucleotides are substrates for MRP4 and MRP5 [80, 101, 102]. Overexpression of one of these pumps may bring about resistance against anticancer and antiviral drugs [71, 78, 80, 85].

It has been demonstrated that nucleotide analogues and cyclic nucleotides are substrates for MRP5 and MRP4 and, mainly, gemcitabine was accounted for to be a common substrate for the MRP5 efflux pump. One study demonstrated a noteworthy relationship between the expression level of MRP5 and gemcitabine affectability in a non-small cell lung cancer cell line [168]. Another study showed that HEK293 cells overexpressing the human MRP5 protein are twice as resistant to gemcitabine, juxtaposed with vector control cells. Nevertheless, a past study has demonstrated that MRP5 mRNA level was substantially higher in pancreatic carcinoma tissue versus normal pancreatic tissue, recommending that overexpression of MRP5 could add to drug resistance in pancreatic cancer [103].

MRP5 Localization

MRP5 protein has been recognised in the epithelial cells of the urethra, smooth muscle cells and endothelial cells in the heart, in the basal membrane of syncytiotrophoblasts, and in and around foetal vessels of the placenta. In the human brain, MRP5 was localised in astrocytes and pyramidal neurons and in the blood-brain barrier, where it was found in the luminal (i.e., apical) membrane of brain capillary endothelial cells [169].

MRP5 Substrates

The broad substrate specificity of MRP5 for organic anions contains the anionic dye fluorescein diacetate [169], the cyclic nucleotides cGMP and cAMP [170], various nucleoside monophosphate analogues, and some glutathione S-conjugates [73]. The finding that MRP5 capacities as a cyclic nucleotide export pump [170] were consequently affirmed in studies with intact cells [72]. The ATP-dependent cyclic nucleotide transport by MRP5 was restrained by several phosphodiesterase inhibitors, some of which are structurally closely related with cGMP and perhaps able to improve intracellular cyclic nucleotide concentration by obstructing their degradation and their export [170]. In this manner, MRP5, together with MRP4, may critically add to the regulation of the tissue levels of cAMP and cGMP. Be that as it may, the affinity of MRP5 to cAMP and cGMP and the relative contribution of phosphodiesterases to the control of tissue levels of cyclic nucleotides appear to differ contingent upon the cellular systems [169].

Inhibitors of Multidrug Resistance Proteins of the ABCC Subfamily

Inhibition of transport intervened by members from the MRP subfamily has been based initially concerning the structural analogues of the prototypic substrate LTC₄ and its cysteinylglycine derivative LTD₄ [170, 171]. Potent LTD₄ receptor antagonist has been created for the treatment of asthma, and the quinoline derivative MK571 represents an early example of the development of these drugs [169]. MK571 has been initially used as a potent competitive inhibitor of ATP-dependent LTC₄ transport [171] and as a contender for direct photoaffinity labelling of MRP1 with [3H] LTC₄ [169, 170]. MK571 has often been viewed as a potent and useful competitive inhibitor of MRP1-mediated transport; notwithstanding, it is additionally a competitive inhibitor of other MRP subfamily individuals that transport LTC₄. Also, we observed inhibition of the hepatic uptake transporter OATP1B3 by MK571 with a K_i value of 0.6 mM [169]. Therefore, MK571 and additionally a few other LTD₄ receptor antagonists are

structural analogues of cysteinyl leukotrienes with a preferential high-affinity binding to LTD4 receptors rather than selective inhibitors of MRP-mediated transport [169]. Cyclosporin A is a decent yet nonselective inhibitor of MRP1 and MRP2, notwithstanding its more potent inhibition of MDR1 P-glycoprotein, of the ATP-dependent bile salt export pump, and uptake transporters OATP1B1 and OATP1B3 [15].

The most advanced compounds among the published MRP inhibitors are a few cyclohexyl-linked tricyclic isoxazoles that have been developed as potent and specific inhibitors of the MRP1-mediated ATP-dependent transport in membrane vesicles, in intact cells, and in vivo in mice [172, 173]. It is quite essential to note that these tricyclic isoxazoles, as studied in detail with LY475776, depend on their activity on the presence of millimolar concentrations of GSH, as present in living cells. Among MRP homologs the tricyclic isoxazole LY475776 is by all accounts highly specific for MRP1 [169, 173]. Specific inhibitors directed against MRP4 might be of considerable therapeutic interest to meddle with the cellular release of pro-inflammatory mediators such as prostaglandins and leukotrienes, or with the release of nucleotides in platelet function [169].

However, potent, selective, as well as cell-specific inhibition of MRP4, has not yet been published. Useful inhibitors of MRP4 incorporate a few nonsteroidal anti-inflammatory agents, for example, indomethacin and sulindac sulfide in the presence of GSH, phosphodiesterase inhibitors, for example, dipyridamole, trequinsin, and sildenafil, and LTD4 receptor antagonists, for example, MK571 and montelukast. Useful inhibition of MRP4 in studies about with inside-out membrane vesicles is likewise accomplished by cholytaurine (taurocholate) together with 5 mM GSH [169, 174]. Specific inhibition of MRP5 has not been accomplished yet. A few phosphodiesterase inhibitors, for example, trequinsin, dipyridamole, zaprinast, and sildenafil indicate inhibitory potential [170], yet the potency fluctuates relying upon the cell system and is by all accounts less than initially portrayed [169, 170]. Feeble and nonselective inhibitors incorporate probenecid and benzbromarone [170]. Established CFTR inhibitors, for example, the arylaminobenzoates diphenylamine-2-carboxylate and 5-nitro-2-(3-phenylpropylamino)benzoate (NPPB) are generally strong inhibitors of MRP5 [175]. Interestingly, these compounds also inhibit MRP8 (ABC11) [169]. MRP7 confers resistance to docetaxel, nucleotide analogues, and epothilone B, recommending that these compounds or their metabolites interface with MRP7 [171, 176].

ABC Transporters	Inhibitors	References
ABCB1	Verapamil, cyclosporine-A, GF120918, PSC833 (Valspodar), LY335979, XR9576, OC144-093	[135, 136, 177]
ABCC1	Ibrutinib, 3ATA, LTC ₄ , MK571, S-decylglutathione, sulfinpyrazone, benzbromarone, probenecid	[135, 136, 177, 178]
ABCC2	GSH-conjugated catechol metabolite, LTC ₄ , fluorescein, methotrexate, cyclosporine-A, benzbromarone, sulfinpyrazone, probenecid, PSC 833, PAK-104P, thioridazine, MK571, curcumin, myricetin	[135, 136, 177, 178]
ABCC3	Benzbromarone, indomethacin, probenecid, sulfinpyrazone	[135, 136, 177]
ABCC4	3ATA	[136]
ABCC5	Sulfinpyrazone, trequensin, sildenafil, curcumin	[135, 136, 177]
ABCC10	Nilotinib, Erlitinib, imatinib	[136]
ABCG2	GF120918, fumitremorgin C (FTC), Ko134, tyrosine kinase inhibitors	[135, 136, 177]

Table 1-9: Inhibitors of ABC transporters (Ref: [115])

MRP 5 Structure and Mechanism

MRp5 molecular model based on the substrate releasing confirmation is expressed in many tissues; at the highest amount in skeletal muscle, at intermediate levels in kidney, testis, heart and cerebrum, however scarcely recognisable in the lung and liver [179-181]. The protein is localised in smooth muscle cells of the corpus cavernosum, ureter, and bladder, and mucosa in ureter and urethra [182], in mind, and hairlike endothelial cells in the cerebrum, yet predominantly present in pyramidal neurons and astrocytes [183], and in the placenta [184]. This membrane protein is also present in human erythrocytes and is responsible for high-affinity transport of cGMP [78].

Immunoprecipitation of MRP5 causes a marked reduction in cGMP high-affinity transport across human erythrocyte membranes [185], and the transporter segregates in a stereospecific way between cGMP analogues [186, 187].

To explain the atomic construction modelling of MRP5, [187] have developed a 3D sub-atomic model of MRP5 by homology with the X-ray crystal structure of Sav1866 [188]. Homology between two proteins is determined by sequence similarity of the functional parts of two proteins having a common progenitor, which shows the presence of similar structures, e.g. homologous protein fold. Notwithstanding, the amino acid composition in the binding site region may vary between protein homologues, and two homologues may bind different drugs. MRP5 is in the MRP5 group of the ABC-transporter superfamily, containing four main domains in sequential order: transmembrane space (TMD) 1, nucleotide tying area (NBD) 1, TMD2 and NBD2, subsequently [187]. The TMDs each contain six TMHs (transmembrane helices). The TMD0 segment of MRP1 is not present in MRP5, which gives MRP5 a P-glycoprotein-like core structure [81]. As per the functional-phylogenetic classification system for transmembrane solute transporters [44], the ABC transporters are in category 3 (primary active transporters), subclass A (diphosphate bond hydrolysis-driven transporters) and family 1 (ABC superfamily) [187].

Sav1866 is a homo-dimeric prokaryotic efflux permease, which includes 12 TMHs. The crystallised structure is caught in outward-confronting ATP-bound compliance [188]. The fundamental relationship in the middle of Sav1866 and P-glycoprotein has been affirmed [189, 190], and among the ABCC transporters, MRP5 is most like P-glycoprotein [81], showing that the Sav1866 X-ray crystal structure can be utilised as a layout for developing an MRP5 display by homology. MRP5 and P-glycoprotein are in subfamilies 3.A.208 and 3.A.201, respectively [191] and are not distant given phylogeny; with P-glycoprotein in family DPL, and MRP5 in family OAD) [192]. Phylogenetic investigations of ABC transporters have shown that eukaryotic ABCB transporters (including P-glycoprotein), ABCC transporters (counting MRP5), and bacterial ABC transporters have common ancestors, and also have similar domain organisations [193]. The transport cycle of ATPases takes after an arrangement of steps where the free energy contained inside of the ATP particle is coupled to the translocation events. Initially, the substrate is perceived from the intracellular side; then the ATPase is stimulated, and the substrate is translocated across the membrane. Eventually, the substrate is released into the extracellular space. The proposed MRP5

model is in an outward confirmation, apparently expressive to a substrate releasing conformation. The MRP5 model was assessed by the docking of cGMP and contrasting the outcomes and site-directed mutagenesis data [187].

The MRP5 model

The energy minimized MRP5 model is indicated in Fig. 1. The two TMDs form a central cavity that is open to the extracellular side and closed to the intracellular side. In this conformation, the cavity lining residues were contributed by TMHs 1e3, 5e9, 11 and 12. TMH5 of TMD1 was stuffed against TMH8 of TMD2 and TMH2 of TMD1 was pressed against TMH11 of TMD2. The TMDs were turned in respect to the NBDs, and towards the extracellular side the TMHs swerved into two symmetrical parts, one section comprising of TMHs 1 and 2 of TMD1 and TMHs 9e12 of TMD2, and one section comprising of TMHs 7 and 8 of TMD2 and TMHs 3e6 of TMD1 (Fig. 1). The loop interfacing NBD1 and TMD2 of MRP5 was α -helical from residue 790 to 835 and extended conformation from residue 836 to 848. Fig. 2 reveals the EPS surface of the MRP5 model (panel A) furthermore a close up of the putative substrate transport cavity (panel B) [187]. The EPS of the membrane region of the model had a dipole moment, being more positive towards the intracellular side. However, the NBD parts most inaccessible from the membrane had areas with negative EPS (Fig. 2, panel A). As demonstrated in panel B, the EPS of the translocation area was typically positive. When seen from the extracellular side, the substrate transport chamber is oval form, with a size of approx. 7 to 20 Å (Fig. 2, panel B), and shut towards the intracellular side. The two NBDs, including the nucleotide binding sites formed by the motifs Walker A, Walker B, Q-loop and switch area, were firmly packed at the intracellular side of the membrane [187]. The two nucleotide binding sites were in immediate contact at the joint interface between the NBDs. The auxiliary structure of the regions of each NBD forming the contact area between the two NBDs was generally in an extended conformation. The interactions between the TMDs were mostly hydrophobic while the interactions between the NBDs were rather hydrophilic [187]

1.7 siRNA

In the past few years area of molecular biology has been transformed quite thoroughly and significant advances have been made in the field of small non-coding RNAs. These small non-coding RNAs are involved in the regulation of genes and genomes; regulation occurs at many different levels, e.g. translation, genome function and RNA processing [240]. Most of the regulations involved in the gene expression or its control

are inhibitory, and thus they are incorporated under a common heading of RNA silencing. Small RNAs gets attached to the effector protein complex directly and act as a specificity factor; guiding the siRNA-effector protein complex to the target nucleic acid. The binding of the target nucleic acid to the siRNA-effector protein complex occurs via base-pairing interactions [240]. So far, a few classes of small RNAs have appeared, but based on their origin, structure, biological roles and association with the effector protein they have been broadly classified under three main categories - short interfering RNAs (siRNAs), microRNAs (miRNAs), and piwi-interacting RNAs (piRNAs) [240]. siRNAs and miRNAs are characterised by the double-stranded structure of their precursor and are generally found in both phylogenetic and physiological terms [240]. piRNA executes their functions in the germline and derives from a precursor which is still not wholly comprehended but seem to be single-stranded. The significant difference in piRNAs and si/mi RNAs is that they bind to the different subsets of the effector proteins; si/mi RNAs associate with the Ago clade of Argonaute proteins and piRNAs with Piwi clade proteins [240].

In 1993 Ambros and co-workers [350] were the first to discover miRNA from *Caenorhabditis elegans* as an endogenous regulator. Fire, Mello and colleagues [351] five years later reported exogenous double-stranded RNA (dsRNA) silences gene explicitly via the process of RNA interference aka RNAi. In the year 1999 RNAi in plants was observed to be performed by a 20-25 nt RNAs which matched the sequence of the silencing trigger [243]. Soon after that, the direct conversion of dsRNAs into 21-23 nt siRNAs was recognised; siRNAs, guardian of genome integrity against foreign or invasive nucleic acid, e.g. transposons, viruses and transgenes [242]. Single-stranded forms of siRNAs execute the silencing effect or RNAi via effector assemblies known as RNA-induced silencing complexes (RISCs) [352]. The target gene is recognised by the small RNA component; it identifies the target gene thru Watson-Crick base pairing [240]. Thus, siRNA silencing is willingly reprogrammable and therefore whenever the genome faces new threats due to the foreign invaders, it can neutralise the threat itself by integrating them into the siRNA mediated silencing process and neutralise or degrade the threat and maintain the genome integrity [240]. The presence of RNAi in human cells gave us the opportunity of using this procedure for gene therapy. Cancer is a disease of the gene, and the assemblage of genetic and epigenetic abnormalities typifying cancer cells present new and precise targets for cancer treatment [269] [353]. The concept of personalised cancer therapy (i.e. analysing genetic defects of an

individual cancer patient by quantitatively determining over and under-expression of both gene & protein) is becoming possible now because of the growing understanding of proteomic, genetic and pharmacogenetic tools. RNAi is a posttranscriptional control process in which the introduction of long dsRNA leads to suppression of target mRNA with complementary sequences [269].

1.7.1 siRNA: Mechanism of action

siRNA/RNAi executes its effects by the introduction of dsRNA into the cell; this dsRNA is cleaved into the small fragments (21-23 nucleotide long) by the endonuclease Dicer. Dicer is a member of the RNase III family and is a dsRNA-specific ribonuclease and cleaves the dsRNA in an ATP dependent manner [194, 195]. These small fragments of cleaved RNA are known as siRNA which further form an assembly with the proteins and create an RNA-induced silencing complex (RISC) [195, 196]. ATP triggers RISC, and its activation causes unwinding of the dsRNA. RISC is comprised of Argonaute protein (Ago-2) which are potent to remove or cleave the passenger strand of the un-winded siRNA duplex. This single-stranded guide RNA together with RISC guides this complex to the target mRNA [195-197]. Target is recognised by the complementary base pairing to the siRNA antisense strand. After integration of the complex to the target, sequence-specific degradation of mRNA's complementary strand occurs via Ago-2 protein's endonucleolytic activity resulting in transient gene silencing [196]. Thus, three sets of macromolecules- dicer, Ago-2 protein and 21-23 nucleotide siRNA are recognised as the signature components of RNA silencing [195].

1.7.2 Dicer proteins

Dicer is one of the critical components of siRNA mediated silencing, as double-stranded nature of the siRNA precursor is apparent, and we all know that RNase III has dsRNA specific nucleases characteristics [196, 197]. Thus, the enzymes with domains of RNase III were quickly recognised as key contenders. Organisms like mammals and nematodes have shown the use of just single Dicer, which is responsible for the biogenesis of siRNA while some organisms have demonstrated the use of multiple Dicer proteins [194]. Genetic, biochemical and structural studies have drawn a model in which the RNase III and PAZ domains performs the crucial parts in executing siRNAs especially from the ends of dsRNA molecules [198, 199]. Argonaute proteins share the PAZ domains and bind to the RNA ends, particularly to the duplex ends with short (2 nucleotide (nt)) 3' overhangs. The substrate dsRNA then spreads about two helical turns along the protein surface before it reaches a single processing centre while the other end

is involved with the Dicer PAZ domain [194, 197]. The centre stays in a forked structure of an intramolecular dimer including the RNase III domains [194, 197]. Each strand is cleaved by one of the two RNase III active sites resulting in the staggered duplex scission to create new ends with 2 nt 3' overhangs [197]. This reaction results in a fifty-monophosphate leftover on the products ends [194, 197].

1.7.3 Argonaute Protein

Argonaute superfamily is further sub-divided into three subgroups: piRNAs binding proteins also known as the Piwi clade, the Ago clade - miRNAs and siRNAs binding proteins, and a third clade which has been reported only in nematodes so far [194, 200]. Argonaute proteins are necessary for the execution of all gene regulatory process which involves 20-30 nt RNAs as these proteins are the significant and defining components of the RISC [194]. As described earlier the double-stranded product of Dicer is inserted into the RISC assembly pathway causing duplex un-winding, resulting in the stable attachment of the two strands to the Ago effector protein [194]. This stably associated strand is called the guide strand which is responsible for the recognition of the target nucleotide [194]. The non-attached strand is named as the passenger strand and is disposed-off. As stated before, the guide strand acknowledges the target via Watson-Crick base pairing [194, 201]. The characteristic property for recognition of Argonaute proteins is the presence of the PAZ domain (shared with Dicer), the PIWI domain that is exclusive to the Argonaute superfamily, and the N and Mid domains [194]. A significant leap forward was the finding that the PIWI domain embraces an RNase H-like overlay that at times can catalyse endonucleolytic cleavage of a base-paired target [201-203]. This underlying cut speaks to the necessary initial phase in a subset of siRNA silencing that continues through RNA destabilisation. The protein structures have been less useful up to this point in clarifying non-endonucleolytic methods of silencing, which isn't astonishing given the generous list of different components that are important in those cases [194]. In humans, four of the eight proteins are from the Ago clade and connect with siRNAs [196, 197], yet little distinction has been accounted up to this point in the populace of small RNAs that they bind, so the level of functional specialisation in humans stays indistinct [194].

1.7.4 RISC Assembly and siRNA Strand Selection

RISC has been characterised biochemically in humans and has three proteins—Dicer, TRBP (transactivation response element RNA-binding protein), and Ago-2— these proteins bind with each other even without the dsRNA trigger [204, 205]. This ‘trimer’

is also known as the RISC-loading complex and can bind dsRNA, chopping it into a siRNA, loading the siRNA into Ago-2, and disposing of the passenger strand to create functional RISC [206]. Supplementary proteins connect with Ago complexes from human cells [201, 207, 208]. However, they are not significant for RISC loading or target cleavage. Selection of strand is independent of the presence of a related mRNA target, as pre-formed RISC is customised to cut, a heterologous target can do as such when the target is included later [194]. In vitro and in vivo data uncovered that strand choice is managed by the relative thermodynamic dependable stabilities of the two duplex ends [197]. This thermodynamic stability is ranked for the selection of strands, i.e. the strand with the highest stability gets inserted in the RISC [194, 209]. The siRNAs with same base pairing stabilities will have their either strands inserted in the RISC complex with the almost same frequency. In a typical siRNA interference, the inserted stand of RISC will guide the complex to the target nucleotide resulting in the degradation of the target [194, 209]. PIWI domain of the Ago protein is responsible for the initiation of degradation of the target. This "slicer" activity is quite precise: the phosphodiester linkage between the target nucleotides that are matched with siRNA residues 10 and 11 (including from the 5' end) are sliced to create products with 5'-monophosphate and 3'-hydroxyl end [197]. When this underlying cut is made, the cell's exonucleases assault the fragments to finish the degradative procedure [210]. The recently created 3' end of the RISC product is additionally a substrate for oligouridylation, which can advance exonucleolytic targeting [211]. After the cleavage target separates from the siRNA, liberating RISC to cleave supplementary targets. Sometimes, highly purified types of RISC fail to cleave their targets with multiple turnovers [212, 213], proposing that other factors influence product release, which is probably going to be driven by ATP hydrolysis [197]. Mismatches at or close to the centre of the siRNA/target duplex stifle endonucleolytic cleavage; moreover, some siRNA programmed Ago proteins need endonuclease activity even with paired targets [197].

In the present era, various bioinformatic tools are available to design the siRNA targeting a specific gene. However, it has been observed that the silencing effects are not very specific due to the involvement of many biological reactions and the complex mechanism of siRNA [197, 204, 214, 215]. These non-specific effects or "Off-target" effects are sometimes due to the presence of dsRNA molecules or due to transfection and experimental manipulation of the cells [197, 215]. Off-target effects are identified

with the siRNA itself and most frequently partial complementarity of the sense or antisense strands to an unintended target [215]. These effects sometimes are concentration dependent. Effector periods of posttranscriptional siRNA silencing are thought to ensue fundamentally in the cytoplasm. siRNA binding initiates the localisation of Ago proteins into subcellular foci called P-bodies [216] that have higher mRNA degradation factors. Though P body localisation does not give off an impression of being entirely required for RNAi [217], and the nuclear environment is additionally agreeable to RNAi [218].

1.7.5 Factors affecting RNAi:

RNAi in cultured mammalian cells is turning into a standard research technique to study the qualities of individual genes [219]. RNAi proficiency can be impacted by numerous calculates in the mammalian cells, a percentage of the central points are depicted here [220]. **First** and foremost, and the most crucial component is the decision of the target site. The best target site should be at 100 nt downstream of the translation initiation site. At the same time, the most vulnerable site on mRNA is obscure.

Furthermore, the auxiliary structures & mRNA- binding proteins likewise impact the accessibility to siRNA. Still, a systematic study needs to be done in this area [221]. **The second component** is the choice of transfection strategy and furthermore the transfection conditions, for example, cell density, transfection reagents and the incubation time of transfection. Time of transfection varies for the different cell types and the targeted gene. Despite the strong knockdown abilities of siRNA, transfection system has its weak points, e.g. transient silencing effects and difficulties in transfection depending on cell types [219]. Efficacy of RNAi is restricted by the amount of the oligomer that successfully enters into the target cells [221]. In the clinical background, this is primarily subjected to the strategy of siRNA delivery. A perfect delivery vehicle must have the capacity to specifically and differentially target tumours versus normal tissue, homogeneously circulate through the tumour mass and enter the tumour cells after systemic administration [222]. Non-viral polymeric delivery systems, specifically those with biodegradable parts, have vastly improved safety profiles than their viral counterparts. To promote endocytosis the non-viral vehicles for siRNA delivery are combined with negatively charged nucleic acids with the negatively charged glycocalyx on external cell membranes [223-225]. There are three noteworthy types of non-viral delivery vehicle systems; engineered polymers, regular/biodegradable polymers and lipids [226, 227]. It was found that transfection of siRNA using lipophilic agents such

as liposomes, Oligofectamine™ & TransIt-TKOTM increase the transfection efficiency. As siRNA only targets the mRNA and not the proteins, protein turnover rate should also be accounted for in the effectiveness of transfection; the **third factor**. Experiments were carried out in which the fluorescent siRNAs were used, to determine their fate in cells. Weak fluorescence signals were observed after 48 hours of incubation. Depicting the decrease in the siRNA population inside the cells due to dilution, which shows that siRNA mediated cell silencing last for 3-5 cell doubling times. Thus, Multiple transfections are necessary in case the protein is unusually stable, or the cell needs to be grown for an extended period. **Fourth** and the last factor is the concentration of siRNA, if two or more genes are being knocked down simultaneously then there is a possibility that two siRNA may compete with each other using the limited available RNAi machinery [222]. Exquisite sequence specificity of RNAi enables specific knockdown of mutated genes.

1.8 Apoptosis

For a long time, it was believed that cell death occurs only via the external chemically induced factors. But the development of cell biology in the last decade has shown some astonishing facts about cell death, and now we know that cell death also occurs via a suicidal process that is controlled by the cell itself [228]. This type of programmed cell death is known as “apoptosis”. Kerr et al. [229] were first to use the term apoptosis in 1972 to describe a morphologically different form of death. Detailed analysis of apoptosis was first done in nematodes *Caenorhabditis elegans* [230], this was the foundation of our knowledge of apoptosis [231]. The studies in nematodes showed that 1090 cells were generated in the organism for the formation of the adult worm. 131 out of 1090 cells undergo apoptosis at a specific time course during the developmental process of the organism. This apoptosis or programmed cell death is an essential part of the organism’s developmental process and shows a notifiable precision of the method [231]. Thus, apoptosis has been widely accepted as a process of programmed cell death involving genetical determinants for the elimination of cells. Though, this eliminates the possibility of other types of programmed cell death which may occur in nature or are yet to be discovered [228]. There are several reasons which could lead to apoptosis in cells (discussed further in this chapter), but few common factors which could be driving apoptosis are – homeostasis for maintaining cell numbers in tissues, it could also be part of the organism’s defence mechanisms where the mutated or damaged cells of the organisms are discarded [229]. Apoptosis could also be exploited by its manual

induction, e.g. introduction of xenobiotics in organisms' toxic to cells used in the cancer chemotherapy. These drugs result in DNA damage of the cell leading to apoptosis via a specific molecular pathway (discussed further in this chapter).

1.8.1 Morphological changes involved

Programmed cell death causes significant morphological changes in the cell, such as reduction in cell volume and pyknosis, which are visible under a light microscope [229]. Reduction in the cell volume increase the cytoplasmic density and causing the cell organelles to pack more tightly [231]. One of the most characteristic features of apoptosis is pyknosis, i.e. condensation of the cell's chromatin. Blebbing of the cellular membrane can be seen during apoptosis followed by karyorrhexis and cell gets fragmented into the apoptotic bodies during a process called "budding" [231]. These fragmented apoptotic bodies are comprised of cell organelles with or without nuclear membrane and are subjected to phagocytosis by the macrophages, neoplastic cells or parenchymal cells [231, 232]. Up till now, no inflammatory reaction has been reported to be associated with apoptotic cells as the cellular contents are not discharged into the interstitial tissue, rapid phagocytosis prevents secondary necrosis and lastly engulfing cells do not generate any anti-inflammatory cytokines [228, 233]. Thus, various efforts and researches have been made to better understand and detect the process of apoptosis. One of the most common approaches for cell apoptosis detection is via labelling phosphatidylserine (PS) using fluorescent antibodies. But to understand the process of apoptosis detection, it is imperative to understand the mechanism of apoptosis.

A cell in its lifetime is frequently exposed to various death, and survival triggers and information about the molecular mechanisms controlling these triggers is limited [228]. Some of the most common apoptosis triggers are – chemotherapeutic agents, DNA damage and the absence of growth factors [228]. These triggers may induce a series of events leading to cell apoptosis, but the time involved may vary for each event. This time is also known as the "trigger phase" and can be defined as the lag time between exposure to the trigger and first morphological sign of apoptosis [228]. The trigger phase may vary from cell to cell, type of trigger and the underlying mechanism and the growth conditions of the cell [228].

Nonetheless the type of cells involved or the type of trigger, all mechanisms seem to have a common factor, i.e. activation of proteolytic machinery [228]. This machinery

requires interleukin converting enzyme (ICE) and caspases [234]. This early apoptosis phase seems to have a few genes involves, e.g. bcl2 gene family, this family is considered as a protector against apoptosis by opposing the effect of bax gene family. Studies have shown that both genes products forms wither hetero or homodimers and the relative quantity of either product determine the cell's fate [228]. The beginning of the apoptotic phase is characterised by the activation of proteolytic enzymes, e.g. caspases which result in the denaturation of cellular proteins such as nuclear matrix, poly-ADP ribose polymerase and the cytoskeleton [228]. This beginning phase of apoptosis is also known as "execution phase", and it also involves the display of PS on the cell's outer membrane [228]. A molecular mechanism involving the display of PS is still not completely understood.

In the previous studies [228] an uneven distribution of the various phospholipids was observed for the inner and outer leaflets of the plasma membrane. This observation was mainly seen in the distribution of choline-containing phospholipids, phosphatidylcholine and sphingomyelin which could be found primarily on the outer side of the plasma membrane while phosphatidylethanolamine and PS (negatively charged phospholipid) could be seen on the inner side of the plasma membrane, i.e. cytosol facing side [235]. This observation regarding the uneven distribution of phospholipids was first seen in the erythrocytes, but later it was also found in nucleated cell types also.

Flippases are the membrane proteins that help in the translocation of lipid molecules from inner to the outer leaflet of the plasma membrane. These flippases are suspected to be involved in the uneven distribution of the phospholipids in viable cells, and Connor et al. [236] also demonstrated that this process is Mg^{2+} /ATP- dependent. This translocase activity is ubiquitous and is majorly responsible for the asymmetric distribution of the PS in non-nucleated and nucleated cell types. Apart from flippases bovine enzyme was also recently demonstrated to show the translocase activity. The bovine enzyme is a member of the sub-family of P-type adenosine triphosphate [237] and the multidrug-resistance protein encoded by the *mdr2* gene [238]. However, more studies are needed in this area to prove the involvement of the bovine enzyme in the translocation activity.

Flippase's translocation of PS from inner to the outer leaflet of the cell membrane was first demonstrated for platelets and erythrocytes. Such translocation of PS from inner to

outer membrane is very significant in these cell types as it helps in catalysing coagulation by activated platelets and elimination through the reticuloendothelial system of senescent erythrocytes [228]. Fadok and co-workers [239, 240] later on demonstrated that leukocytes in the apoptotic phase expose PS on the outer leaflet of the plasma membrane. This PS on the outer leaflet of the cell act as a tag or signal for the macrophages to recognise the apoptotic cell for phagocytosis. Till date precise molecular mechanism nothing such PS exposure is undefined, but this finding led researchers to think that if we can find a molecule (fluorescently labelled) which can bind to the PS on the outer leaflet of the cell membrane than we can conveniently distinguish the apoptotic cells from rest of the cell population. These investigations were more eased by the finding that annexin V binds to the PS in the presence of calcium [228]. Bohn and colleagues [241] were first to report and isolate annexin V and called it placental protein 4 (PP4) while Reutellingsperger et al. [233] isolated it from the umbilical cord and named it vascular-anticoagulant- α due to its anticoagulant property. It was named annexin V due to its homology with the annexin protein family. Annexin V protein was found to be expressed successfully in the bacterial systems which opened gates for further investigation in the field of recombinant proteins. Various studies were carried out to find out the biochemical and physiological properties of annexin V. However, its property of binding to the phospholipid is the most exploited property of annexin V so far. Conjugation of annexin V with FITC or biotin has eased studies related to PS exposure and has served as a primary tool in apoptosis determination. In the studies it was found that integrity of PS on the outer leaflet of the plasma membrane is quite stable, i.e. it appears at the early stage of the apoptosis and lasts till the cell is disintegrated into the apoptotic bodies. As stated, before that molecular mechanism underlying apoptosis is still not completely comprehended, but the involvement of caspases in the apoptosis process is well recognised. In the recent studies [232] it was found that inhibitors of caspases could prevent PS externalisation. Same observations were also made by Castedo et al. [242] which demonstrated disruption of the mitochondrial transmembrane potential ($\Delta\psi_m$) prior translocation of PS to the outer leaflet of the membrane. Further Susin et al. [243] showed that disruption of ($\Delta\psi_m$) primes the release of the apoptosis-inducing factors. Caspase inhibitor Z-VAD could block this apoptosis-inducing factor [228]. It could be assumed that PS externalisation is the downstream result of caspase activations and could be an early phenomenon of the “execution phase”. Along these lines, we can state that loss of membrane asymmetry is the essential phase of apoptosis, started at the time

following the caspase proteolytic course however conceivably going before nuclear condensation and breakdown of intracellular cytoskeletal and nuclear matrix constituents [232].

1.8.2 Apoptosis Vs Necrosis

Necrosis is another process involved in cell death and to distinguish it morphologically from the apoptosis could be a bit difficult. Both process apoptosis and necrosis can happen independently and simultaneously in nature [231]. Necrosis is a toxic and energy independent process capable of influencing a single or group of cells. There are two major factors which influence the necrosis process – (i) energy supply interference of the cell and (ii) cell membrane damage [231]. Few of the necrotic morphological characteristics are – involvement of an increase in cell volume formation of cytoplasmic blebs and vacuoles, ribosomal disintegration, swollen or damaged mitochondrion and lysosomes, distended endoplasmic reticulum and eventually cell membrane disintegration[231]. This is one of the major differences among apoptosis and necrosis, i.e. cell membrane disintegration releases the cell contents in the adjoining tissue leading to the generation of an inflammatory signal which is absent in apoptosis [231]. Pyknosis and karyorrhexis could happen in necrosis too and could be part of various cytomorphological alteration happening during the process of necrosis. Though both apoptosis and necrosis involve cell death, they are quite different from each other but involve an overlap [231]. Previous studies have shown that apoptosis and necrosis are morphological reflections of a shared biochemical network called as the “apoptosis-necrosis continuum” [244], e.g. common factors involved in the conversion of a continuing apoptosis process into a necrotic process include caspases availability and intracellular ATP. Death of cell depends on the cell death signal, tissue developmental stage and type of tissue and physiologic milieu [244].

1.8.3 Apoptosis mechanisms

Apoptosis is an energy-dependent process and involves several processes happening simultaneously. Two mechanisms of apoptosis have been proposed so far – the extrinsic pathway and the intrinsic or mitochondrial pathway. But later in the studies, it was found that both pathways are inter-related, and reactions or molecules involved in one pathway can affect the other pathway [245]. Apart from the pathways mentioned above the involvement of a third pathway is also suspected. This third pathway involves T-cell mediated cytotoxicity and perforin-granzyme-dependent killing of the cells. Though, it is also suggested that all these pathways eventually act through the same mechanism

which is also called as execution pathway [231]. Execution pathway begins with the denaturation of DNA by caspase-3 which ultimately leads to the degradation of nuclear proteins and the complete cytoskeletal, production of apoptotic bodies and finally phagocytosis of the cells [231].

Extrinsic pathway

This apoptotic pathway encompasses transmembrane receptor-mediated interactions, e.g. death receptors (members of the tumour necrosis factor (TNF) receptor gene family). Like death receptors, TNF receptor family has an analogous cysteine-rich extracellular domain and a cytoplasmic domain of approximately 80 amino acids known as “death domain” [246]. Death domain plays a very significant role in transmitting the death signal from the surface of the cell to the intracellular signalling pathways. The best-characterised ligands and the corresponding death receptors till date are – TNF- α /TNFR1, Apo2L/DR5, FasL/FasR, Apo2L/DR3 and Apo2L/DR4 [231]. FasL/FasR and TNF- α /TNFR1 are the best models which characterise the extrinsic pathway. These models include receptor clustering and binding to the homologues trimeric ligands [231]. This binding results in the activation of the cytoplasmic adapter proteins show corresponding death domains that associate with the receptors. This leads to the formation of the death-inducing signalling complex (DISC) which eventually activates caspase-8, and the execution phase of the apoptosis is initiated [231].

Perforin/granzyme pathway

Cytotoxicity intervened by the T-cells is another form of type IV hypersensitivity where the antigen-carrying cells are killed by the CD8⁺ cells [231]. This is also known as CTL-induced apoptosis, and FasL/FasR is the best model which can explain such interaction so far. In CTL induced apoptosis cytotoxic T-lymphocytes (CTLs) can kill the target cells via the extrinsic pathway [231]. Though, it was also seen that the cytotoxic effects on the tumour or virus-infected cells could also be exerted by a new pathway which includes secretion of the transmembrane pore-forming molecule perforin followed by the exophytic release of cytoplasmic granules via a pore into the target cell/s [247]. For the execution of this mechanism granzymes, A and B are very crucial. Studies have shown that granzyme B could exploit the mitochondrial pathway for amplification of death signal via induction of cytochrome c release [248, 249]. It was also seen that granzyme b is capable of direct activation of caspase-3 and thus upstream signalling pathways can be bypassed leading straight to activation of the execution phase of apoptosis. On the other hand, granzyme A can initiate caspase-

independent activity leading to CTL-induced apoptosis; granzyme A activates DNA cutting through DNase NM23-H1 (tumour repressor gene product) [250]. This DNase plays a very crucial role in immune monitoring to stop cancer from happening by the initiation of the apoptosis in rogue cells.

Intrinsic pathway

This pathway involves a vivid range of non-receptor mediated stimuli that creates intracellular acting directly on the targets and are the mitochondrial origin. These stimuli responsible for the intrinsic pathway could be positive or negative [231]. Negative signals have involvement of specific growth factors, cytokines and hormones that may lead to failure of death programmes eventually leading to apoptosis. While positive stimuli include radiation, hypoxia, hyperthermia, radiation, free radicals and infections (viral). Whether positive or negative these stimuli lead in the alteration of the inner mitochondrial membrane which causes mitochondrial permeability transition (MPT) pore to open. Eventually leading to loss transmembrane potential and release of two main groups of pro-apoptotic proteins. The first group is comprised of cytochrome c, Smac/DIABLO and the serine protease HtrA2/Omi [231]. These proteins are responsible for the initiation of caspase-dependent mitochondrial pathway forming an “apoptosome” [231, 251].

The second group of proteins involves – AIF (apoptosis inducing factors), CAD and endonuclease G. These proteins were found to be released from the mitochondria while apoptosis is happening. Thus, these proteins are induced quite late and are there when the cell has already prepared for the apoptosis. AIF is responsible for the DNA degradation into approximately 50-300 kb size pieces and the condensation of chromatin [252]. The endonuclease is involved in the cleavage of nuclear chromatin to form oligonucleosomal DNA fragments [253]. CAD is responsible for more pronounced condensation and is also involved in DNA fragmentation. These mitochondrial events during the apoptosis are controlled by the members of the Bcl-2 family of proteins and tumour suppressor p53 protein is shown to be significantly involved in the regulation of BCL-2 family; still, the underlying mechanism is not well understood [231].

Execution pathway

As we now know that both intrinsic and extrinsic pathways converge into the execution pathway and that’s why the execution pathway is considered to be the last pathway of apoptosis. Execution pathway involves the activation of execution caspases (caspase 3,

6 and 7) followed by induction of cytoplasmic endonucleases and proteases [231]. Which eventually leads to the degradation of nuclear material and nuclear and cytoskeletal proteins. Apart from these execution caspases are also involved in the degradation of cytokeratins, PARP, the plasma membrane cytoskeletal protein alpha fodrin and the nuclear protein NuMA. These simultaneous events lead to the morphological and biochemical changes which are characteristic of apoptotic cells [231].

This brings us to the last component of the apoptosis, which is the phagocytosis of the apoptotic cell. Translocation of PS from inner to the outer leaflet of the plasma membrane occurs on the surface of apoptotic cells signalling for phagocytosis [231]. Though the mechanism behind this translocation is still not completely comprehended, it has been associated with the loss of aminophospholipid translocase activity and non-specific flip-flop of phospholipids of different classes. Few studies have also suggested the involvement of Fas, caspase-8 and caspase-3 in the PS externalisation [254, 255]. Thus, PS on the outer leaflet initiates a phagocytosis response which is non-inflammatory, facilitating disposal of apoptotic cells.

1.8.4 Apoptotic pathways in cancer

Tumour necrosis factor receptors: Fas and TRAIL

Initiation of apoptosis was reported by the activation of the tumour necrosis factor receptor of the death receptor family. TNF-R1, DR3, DR6, TNF-R1, TRAIL-R1/2 and Fas are some of the tumour necrosis factors involved [232].

Bcl-2 family

This family is significantly involved in apoptosis and contains essential regulators of the apoptosis. This family was found to be overexpressed in many cancer types. Studies have shown that their overexpression is responsible for many chemotherapeutic drugs leading to resistance while their reduced expression may promote apoptotic response to the chemotherapeutic agents and radiation therapy [232].

Apaf-1 and cytochrome c

Caspase-9 is one of the most significant factors for the initiation of mitochondrial apoptosis. When cells are exposed to external apoptotic stimuli, e.g. chemotherapeutic drugs or radiations which could interfere with the DNA repair or affect DNA synthesis, pro-apoptotic BH3-only proteins get activated causing oligomerisation of P53 effector Bax/Bak [232]. Followed by the mitochondrial outer membrane permeabilisation

leading to the release of factors from the inner membrane space causing promoting apoptosis. Bcl-2 family could hijack this process leading to cell survival [232].

NF- κ B

This class of protein is involved in many bio-regulatory processes like – cell proliferation, stress response, apoptosis, tumorigenesis and cellular differentiation. The significance of NF- κ B in the process of apoptosis is well known [256]. In brief activation of NF- κ B happens when the degradation of I κ B protein occurs. This degradation leads to the entry of NF- κ B into the cell nucleus where it sabotages apoptosis by its transcriptional regulation activity of specific genes [232].

p53

For the mitochondrial-mediated apoptosis, this (p53) nuclear transcription factor plays a very crucial role by controlling the apoptotic signal of the intrinsic pathway. It is one of the most significant apoptosis promoting and tumour inhibition factor. Thus, many antineoplastic drugs or drug metabolites target the p53-related signalling pathway. p53 mainly exerts its effects by the stimulation of various positive regulators of apoptosis, e.g. DR-5 and Bax [232].

MicroRNAs (miRNAs)

These RNAs plays a crucial role in the regulation of 30% gene expression and thus are of grave importance. Some members of the miRNA family are actively involved in the apoptotic pathways, e.g. tumour suppressor miR-15a-miR16-1, let-7 and miR-29 [232]. As we have previously stated that the Bcl-2 family has the potential to jeopardise apoptosis, miR15-a and miR-16-1 could target Bcl-2 and promote cell apoptosis. Previous studies have also suggested that overexpression of miR-15a-miR-16-1 in vitro reduced Bcl-2 levels and induced apoptosis [232].

1.9 Summary and hypothesis of the thesis

Several processes are responsible for drug resistance in pancreatic cancer cells; one of the important processes is the increased drug efflux [257] which leads to decreased drug accumulation in cancer cells. Proteins belonging to the ATP-binding cassette (ABC) family of transporters efficiently mediates the drug efflux [258-261]. Several members of the multidrug resistance protein family (MRPs), MDR1 P-glycoprotein, and the breast cancer resistance protein (BCRP) have been demonstrated to confer chemoresistance or multidrug resistance. These (MRP) transporters belong to the ABCC (MRP1-MRP9; gene symbol: ABCC1–ABCC6 and ABCC10–ABCC12), a family of

the ABC transporters, [67, 94]. MRPs are integral membrane proteins mediating the ATP-dependent export of organic anions out of cells. Localizations in duct cells, acinar cells, and pancreatic cancer cells were observed for MRP4 and MRP5. The MRP5 mRNA level was significantly higher in pancreatic carcinoma tissue compared to normal pancreatic tissue. MRP5 has also been demonstrated to confer resistance against gemcitabine phosphorylated metabolites [85, 94, 168, 262, 263]. The MRP5 A-2G AA genotype also showed a significant association with overall survival in pancreatic cancer patients [93]. Many remedies have been suggested to overcome this resistance, e.g. by use of suicide genes or chemical/natural inhibitors. One such strategy to overcome drug efflux is “silencing the MRP genes” using small interfering RNAs (siRNA) [263] or via genome editing (CRISPR-CAS9 gene knock out).

It is evident that when ABC transporter protein MRP5 (ABCC5) overexpressed in the plasma membrane of pancreatic cancer cells; remove gemcitabine from the cells and decrease the amount of gemcitabine intracellularly resulting in decreased cell death [67, 93, 94, 168]; silencing of these genes could decrease the drug efflux [168]. Therefore, we hypothesised that increased expression of a specific ABC transporter protein MRP5 confers gemcitabine resistance in pancreatic cancer cells and gene silencing using siRNA or genome editing could reduce the drug efflux and therefore increase the gemcitabine efficacy. ABC transporters protect body cells from xenobiotic compounds, but their overexpression in cancer cells makes chemotherapy practically impossible. Thus, the potential importance of inhibition of MRPs in drug resistance is, therefore, high. Development of safe and effective inhibitors of ABC transporters could be a measure to overcome drug resistance and could accelerate the effect of chemotherapy. Gaining better insight into the role of ABC transporters in cancer cell resistance to chemotherapy might lead to new and better anti-cancer strategies.

1.10 AIMS

This project proposes to investigate the role of MRP5 in gemcitabine resistance in pancreatic cancer cells. The specific aims include:

- To develop and validate a robust qPCR assay to evaluate the mRNA expression level of gemcitabine-related transporter and enzymes.
- Transient knockdown of MRP5 using siRNA and its effects on MRP5 expression, model substrate accumulation and gemcitabine cytotoxicity.
- Genome editing using the CRISPR-CAS9 system and its effects on MRP5 expression, model substrate accumulation and gemcitabine cytotoxicity.

Chapter 2 Methodology

2.1 Cell Culture

Pancreatic Cancer cell lines MIA Paca-2 & Panc-1 were used in this project for in-vitro analysis. These cell lines were cultured using complete RPMI (Roswell Park Memorial Institute (RPMI) 1640 medium) medium supplemented with 10% (v/v) Fetal Bovine Serum (FBS), L- Glutamine (2 mM) (Life technologies, NZ), Penicillin (100 units/mL) and Streptomycin (100 µg/mL)) (Life technologies, NZ) in a moistened atmosphere of 5% CO₂ at 37°C. All cell culture was carried out in aseptic conditions by using a biosafety hood (ESCO, Bio-Strategy®). Once the cell culture was 80-90% confluent, cells were split and sub-cultured.

2.1.1 Materials

- RPMI Medium (CRM) - Life technologies, NZ
- Foetal Bovine Serum (FBS) Medica Pacifica, Auckland, NZ
- Dulbecco's Phosphate Buffered Saline (PBS) - Life technologies
- TrypLE™ Express, no phenol red - Life technologies, NZ
- Freezing Media (usually 10% dimethylsulfoxide, (DMSO +CRM))
- Corning® Cryogenic Vials - Corning
- Corning® Cell culture flasks: T75/T25 - Corning

2.1.2 Method

Revival of cell stock:

The frozen cell stock was quickly thawed at 37°C in the water bath and transferred to the class II tissue culture hood. The cells were then mixed with complete RPMI medium (CRM) and spun at 500 × g, 4°C for 5 mins to pellet the cells. The supernatant was aspirated, and the cell pellet was re-suspended in the complete RPMI medium in the cell culture flasks. The cells were grown (~2-3 days) until confluency of ~80 – 90% was achieved.

Maintenance of cell culture

Once the desired cell confluency was achieved the cells were split by washing with pre-warm PBS briefly followed by trypsinization for 5 mins. The trypsinization was stopped by adding the equal volume of the medium (1:1) and spun for 5mins, 4°C at 500 × g. The supernatant media was discarded, and cells were re-suspended again in complete medium.

The cell viability was determined using the Trypan blue exclusion method. A 10 μ l cell suspension was mixed with 10 μ l of 0.4% Trypan blue (1:1). After this 10 μ l of the cell-dye mix was loaded on the Neubauer's chamber for counting; unstained (live) and stained (dead) cells were counted. Cells were seeded in the new T75 flask with a cell density of 3-4 x 10⁵ cells/T75 flask for both cell lines (MIA Paca-2 and Panc-1) with 6-7 ml of complete RPMI medium. Cells were grown to achieve the confluency of ~80-90% (approximately 3 days). The confluent cell flask was again subjected to splitting, or the cells were used different applications or experiments, e.g. drug cytotoxicity, Apoptosis, transfection, preparing more frozen cell stocks etc. Cell culture over the passage number of 20 was discarded.

Cell Freezing

Before preparing the frozen cell stock, cells were checked for bacterial, yeast, or fungal contamination under a microscope. Cells were trypsinized (above protocol) and spun in a sterile centrifuge tube at 500 \times g for 3-5 min. The supernatant was removed, and cells were subjected to the counting (mentioned above). Cells were re-suspended in the sterile freezing medium with a density of 4-5 x 10⁵ cells/ml. 1 ml of this cell suspension was transferred to each cryo-vial and were put in -20°C for 1 hour. After 1 hour the vials were removed and put in -80°C overnight. Later on, these cryo-vials were transferred to a liquid nitrogen tank for long time preservation.

2.2 Stealth siRNA Transfection

2.2.1 Materials Required

- Cells maintained in RPMI media supplemented with 10% FBS
- Stealth siRNAs for ABCC5- Invitrogen (Assay ID HSS115284, HSS173353, HSS173354)
- Scrambled siRNA - Invitrogen
- Lipofectamine™ RNAiMAX Reagent (Cat. No- 1690160)
- Opti-MEM® I Reduced Serum Medium - GIBCO
- 12-well plates - Eppendorf (Area 391.1 mm²)

2.2.2 Procedures: Preparation of siRNA stock

The supplied siRNAs (20 nmol) was re-suspended in 1 ml of sterile RNase-free water to make a 20 μ M (main stock). This stock was further aliquoted and stored in -20°C. Once thawed, the tube was kept on ice until use. RNA oligonucleotides are susceptible to

degradation by exogenous ribonucleases introduced during handling. As a precaution, RNA oligonucleotides were handled with gloved hands. RNase-free reagents, pipette tips, and tubes were used. Upon receipt, dried RNA oligonucleotides were stored in a non-frost-free freezer at -20°C , at this temperature they are stable for 6 months (according to manufacturer's instructions).

Forward Transfection

Forward transfection was the method of choice to transfect Stealth™ RNAi into mammalian cells in a 12 -well format. For forward transfection cells were plated in CRM one day before and on the next day, the transfection mix was added to the cells. The transfection was carried out by optimising the cell seeding number in a way that 50-60 % confluency was achieved after 24 hours. To each well RNAi duplex - Lipofectamine™ RNAiMAX complex was added on the next day of plating and mixed gently by rocking the plate back and forth. The cells were then incubated for 48 hours and later extracted to check the knockdown efficiency and off-target effects.

For each well to be transfected RNAi duplex-Lipofectamine™ RNAiMAX complexes were prepared as follows:

- a) For 1 transfection reaction 10 pmol RNAi duplex was diluted in 100 μl Opti-MEM® I Medium without serum in an Eppendorf tube (tube 1) and was mixed gently by pipetting up and down.
- b) 2.0 μl of Lipofectamine™ RNAiMAX reagent was mixed with 100 μl of Opti-MEM® I Reduced Serum Medium in an Eppendorf tube (tube 2) and was mixed gently before use
- c) Tube 1 and 2 were mixed and gently pipetted for homogenization. This mixture was incubated for 10-20 minutes at room temperature and then added to 12 well plate.

Culture Plate	Rel. Surf. Area/well (mm ²)	Vol. of Plating medium/well (ml)	Cells / well	Opti-MEM® I/well (μl)	RNAi duplex (pmol)/well	Lipofectamine™ RNAiMAX (μl)/well	Total Volume/well (ml)
12- well	391.1 mm ²	1.0 ml	120 x 10 ⁴	200	10	2.0	1.2 ml

Table 2-1: siRNA mixture composition for transfection

Stealth siRNA (ABCC5): Target locations***siRNA-1***

Primer length: 25

Forward sequence (5' to 3'): CGUGAAGAUUCCAAGUUCAGGAGAA

Reverse sequence (5' to 3'): UUCUCCUGAACUUGGAAUCUUCACG

Chromosome Location Chr. 3: 183919934 - 184018010 on Build GRCh38

siRNA-2

Primer length: 25

Forward sequence (5' to 3'): GAAGCCCAUCCGGACUACUCCAAA

Reverse sequence (5' to 3'): UUUGGAAGUAGUCCGGAUGGGCUUC

Chromosome Location Chr. 3: 183919934 - 184018010 on Build GRCh38

siRNA-3

Primer length: 25

Forward sequence (5' to 3'): CCUCCAUGCAUUCUCAGCUCAGAAU

Reverse sequence (5' to 3'): AUUCUGAGCUGAGAAUGCAUGGAGG

Chromosome Location Chr. 3: 183919934 - 184018010 on Build GRCh38

2.2.3 **RNA Extraction** – Refer to Chapter 3 section 3.6.1

2.2.4 **RNA Quantitation** – Refer to chapter 3 section 3.6.2

2.2.5 **cDNA, Primers and real-time-PCR optimisation-** Refer to chapter 3 section 3.6.3 for the details regarding this section

2.3 Cell Viability Assay

MTT assay was used to screen the gemcitabine cell cytotoxicity effects eventually leading to cell death. A large range of tetrazolium compounds is available to detect viable cells, e.g. MTT, MTS, XTT, and WST-1. MTT (3-(4,5-dimethylthiazol-2-yl)-2,5-diphenyltetrazolium bromide) is the most widely used compound because it is positively charged and easily penetrates viable eukaryotic cells [264]. Other compounds are negatively charged and do not readily penetrate cells [264]. The tetrazolium reduction assay measures some aspect of general metabolism or an enzymatic activity as a marker of viable cells. The assay requires incubation of MTT with gemcitabine-treated cancer cells to convert MTT into purple coloured formazan products that can be detected with a plate reader [264]. Incubating cells with MTT will generate a signal which is proportional to the number of viable cells present, under standard condition. Cells rapidly lose the ability to convert substrate into products with an increase in cell mortality which is the basis of this cell viability assay [264].

2.3.1 Materials

- Phosphate-buffered saline (PBS), sterile
- Dimethylsulfoxide (DMSO) – ThermoFisher Scientific
- Gemcitabine – Sigma (Cat No- G6423-50MG)
- 3-(4,5-dimethylthiazol-2-yl)-2,5-diphenyltetrazolium bromide (MTT) – SIGMA
- Hemocytometer – BOECO, Germany
- Sterile 96-well plates – CORNING (Merck)
- Multichannel pipette (50-200 μ l)
- Cell reservoirs – CORNING (Merck)
- Sterile pipette tips – fisher scientific
- Sterile tubes (0.6 and 1.5 mL) – CORNING (Merck)
- Sterile filter (pore size: 0.25-0.4 μ m) - ThermoFisher Scientific
- Thermo Scientific™ Plate reader (Multiskan™ FC Microplate Photometer)

Storage and Handling

MTT and PBS were stored at 4°C protected from light. At this temperature, MTT powder can stay stable for 12 months. DMSO was stored at room temperature protected from light.

Culturing Cells

The culture conditions used to grow the cells can affect the results and were taken into consideration when analyzing the data. The age of the cultures, number of passages and details of the growth medium can all be important factors, Refer to section 2.1 for the details.

2.3.2 Plating cells into 96-well plates

In general, the cells (MIA Paca-2 and Panc-1) were seeded at the densities of 5,000 cells/well.

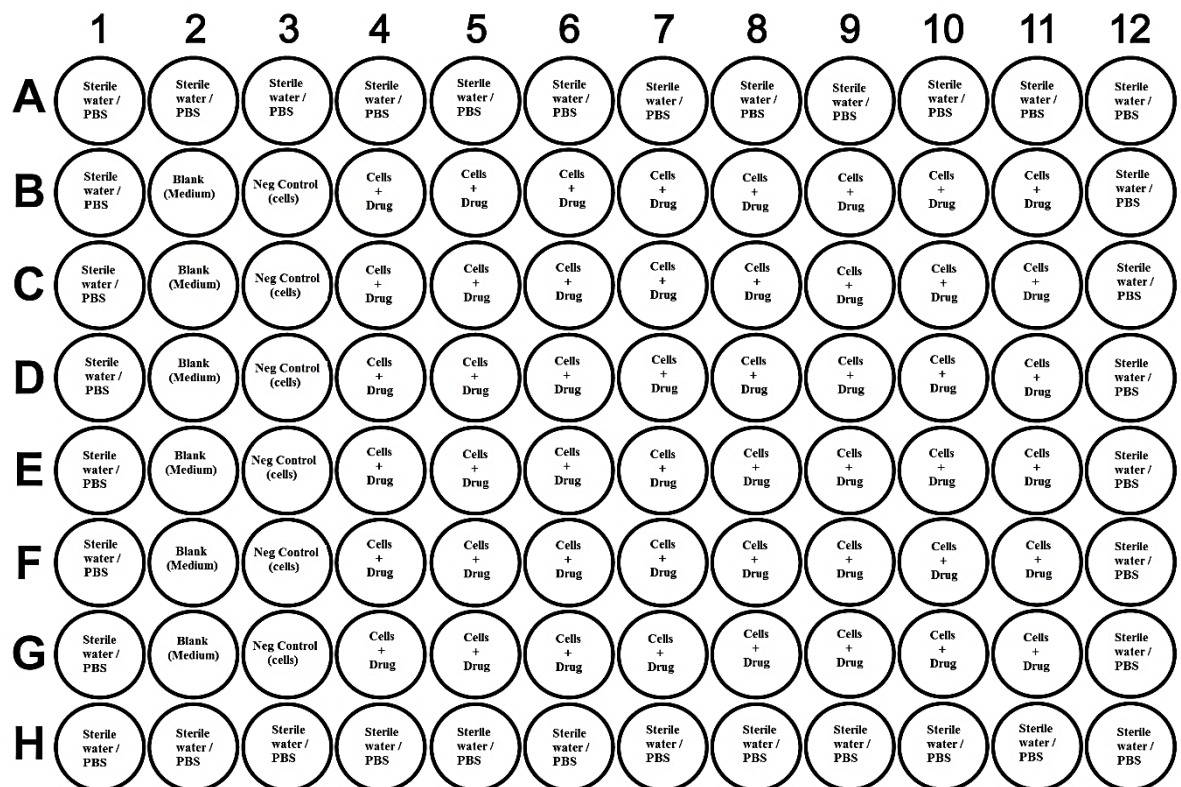


Figure 2-1: Plate layout for cell seeding*

* Blank = CRM, Negative (Neg) control = Cells + no drugs

Volume of sterile H₂O / PBS = 300µl

Volume of Blank = 100µl

Volume of medium for seeding cells = 100µl

2.3.3 Experimental Protocol

Cells were seeded in a 96 well plate with a seeding density of 5000 cells/well and were incubated for 24 hours to allow cells to attach to the well surface. Later, cells were treated with gemcitabine at the various concentration (the highest concentration used was based on preliminary studies or literature data and the rest drug solutions were prepared by serial 1 in 2 dilutions in the consecutive wells) for 72 hours. Cells without drug treatment were used as control (negative). After 72 hours of treatment the entire medium from each well was replaced with 100 μ L of fresh phenol-red free culture medium. A 12 mM MTT stock solution was prepared by adding 1 mL of sterile PBS to 5 mg of MTT, mixed by vortexing or sonication until dissolved. Followed by filtration to dissolve the particulate material. To each well 10 μ L of the 12 mM, MTT stock solution was added. Blank + MTT was used as a control for MTT solution. After the addition of MTT, the 96 well plates were incubated for 4 hours at 37°C. After labelling the cells with MTT, as described above, all but 25 μ L of the medium from the wells was removed, and 150 μ L of DMSO was added to each well and mixed thoroughly (room temperature) using an orbital plate shaker. The plate was again incubated at 37°C for 10 minutes. Just before the absorbance reading, the plate was subjected to mild shaking (in the plate reader). Absorbance was read at 540 nm and 680 nm (reference wavelength). Cell viability was calculated using absorbance values at 540nm and 680nm on a microplate reader.

2.4 MRP5 functional studies

2',7'-Bis(2-carboxyethyl)-5(6)-carboxyfluorescein (BCECF) is an MRP5 specific substrate and can be used to determine the MRP5 activity [265, 266]. An MRP inhibitor curcumin (CUC) was used as a positive control to validate the MRP5 function [265].

2.4.1 Materials

- BCECF - Sigma
- PBS
- TrypLE™ Express, no phenol red - Life technologies, NZ DMSO
- CUC (curcumin) - SIGMA
- MoFlow™ XDP flow cytometer - Beckman Coulter

BCECF–AM Stock Preparation

BCECF–AM Sigma, Product No. – B8806, Packing – 1 mg/ml

Mol. Weight – 808.69 gms/mol, Molarity of Packed product – 1.2 mM (**Stock I**)

The stock I was aliquoted further and preserved in -20°C

Stock II of BCECF-AM (working stock)

Desired molarity - 250µM

Hence, 2.0µl of 1.2 mM BCECF + 8.0 µl of DMSO = 10 µl of 250 µM BCECF

For Uptake Studies: 1.0 µl of stock II was used in 999 µl of the cell suspension to get a final concentration of 0.25µM

2.4.2 Methodology

Cells (MIA Paca-2 and Panc-1) were washed with PBS and trypsinized (section 1.1.2). Later, the cells were washed again with fetal bovine serum (FBS)-free, phenol red-free DMEM medium and were re-suspended in the same medium with a density of about $0.5 - 1 \times 10^6$ cells/ml. The accumulation of BCECF was performed by incubating 1 ml of cells with CUC (final conc. 10µM) or the vehicle (0.1% DMSO; negative control) at 37°C for 15 min, followed by addition of 0.25µM of BCECF-AM (0.1% DMSO). After incubation for another 5 min, the accumulation was stopped by adding 3 ml of ice-cold PBS and centrifugation at $500 \times g$ for 5 min. The cells were then washed with ice-cold PBS again and reconstitute in 0.5 mL ice-cold 1% paraformaldehyde in PBS and placed into ice immediately. The intracellular level of BCECF was measured by using the MoFlow™ XDP flow cytometer (Beckman Coulter, NZ) equipped with a standard laser for excitation at 488 nm and a bandpass filter at 525 nm to detect fluorescence.

2.5 Cell apoptosis

For the determination of apoptosis, the Alexa Fluor® 488 annexin V/Dead Cell Apoptosis Kit was used. The kit contains recombinant annexin V conjugated to a fluorophore the Alexa Fluor® 488 dye. In addition, the kit includes a ready-to-use solution of the red-fluorescent propidium iodide (PI) nucleic acid binding dye and Annexin V binding buffer. After staining a cell population with Alexa Fluor® 488 annexin V and PI in the provided binding buffer, apoptotic cells show green fluorescence, dead cells show red and green fluorescence, and live cells show little or no fluorescence. These populations were detected using a MoFlow™ XDP flow cytometer with the 488 nm line of an argon-ion laser for excitation and the 525 nm for emission

2.5.1 Materials

- Alexa Fluor[®] 488 annexin V/Dead Cell Apoptosis Kit – invitrogen[™]
- RPMI medium
- PBS
- Trypsin
- 6 well plate
- Deionized water/Milli Q water
- Gemcitabine (apoptosis-inducing agent) – sigma (Cat No- G6423-50MG)
- MoFlow[™] XDP flow cytometer

2.5.2 Method

- A. Preparation of 1X annexin binding buffer: for approximately 10 assays 1 ml 5X annexin binding buffer (supplied with the kit) was added to 4 ml deionized water.
- B. Preparation of PI working stock: to prepare 100 µg/ml working solution of PI 45 µl 1X annexin-binding buffer was added to 5 µl of PI stock (supplied) solution.

The procedure for apoptosis detection is as follows:

Cells (MIA Paca-2 and Panc-1) were plated with a density of 1×10^6 cells / ml/well in CRM (section 1.1.2). After 24 hours of seeding, cells were treated with different concentrations of gemcitabine. After 24-48 hours of incubation with gemcitabine cells were harvested (section 1.1.2). Harvested cells were washed again with PBS and re-centrifuged for 5 mins at $500 \times g$. The supernatant was discarded, and the cells were re-suspended in 100µl of 1X Annexin V-binding buffer (refer to part “A” of this section). Alexa Fluro[®]488 annexin V (4.0 µl) and 1 µl 100 µg/ml PI (refer to part “B” of this section) working solution was added to each 100 µl of cell suspension from step 4. Cells were now incubated for 15mins at the room temperature. After the incubation, 400 µl 1X annexin binding buffer was added to the cells and mixed gently by pipetting. Samples were put on ice immediately. The stained cells were analysed using MoFlow[™] XDP flow cytometer.

2.6 Surface Staining of MRP5

MRP5 expression was also confirmed by the surface staining of the protein. Indirect surface staining was the method of choice. This type of staining procedure involves two incubation steps, firstly with a primary antibody and then with a compatible secondary

antibody. The secondary antibody has the fluorescent dye (Alexa Fluor®, FITC, PE, Cy5®, etc.) conjugated.

2.6.1 Required reagents

- Anti-MRP5 monoclonal (1°) antibody (Thermo Fisher, M5II-54, Host: Rat)
- Mouse IgG as isotype control - Thermo Fisher
- Goat Anti-rat IgG H&L (Alexa Fluor® 488, Product # A-11006)
- BSA - Sigma
- Saponin – Sigma (Cat. No – BCBV8000)
- Sodium Azide (NaN₃) - Sigma
- PBS

2.6.2 Buffer preparations

Buffer A: PBS + 0.1% NaN₃ + 0.1% saponin + 1% FBS (pH 7.4 - 7.6, stored at 4°C)

Blocking Buffer: PBS + 5% BSA

Buffer for 1° and 2° antibody dilution – 2% BSA

2.6.3 General procedure

Cells were harvested, washed with PBS and checked for the cell viability. Cells were re-suspended in the buffer 'A', the number of cells for re-suspension: $1-5 \times 10^6$ cells/ml. The above cell suspension was incubated at room temperature for 10 mins. After the incubation, cells were subjected to blocking.

Blocking: cell suspension from step 2 was centrifuged for 5 mins at $400 \times g$ to obtain a cell pellet, and the supernatant was discarded. This cell pellet was re-suspended in the blocking buffer for 15 mins at room temperature. The cells were washed with buffer 'A' after blocking. Washing was carried out by centrifugation of the cells at $400 \times g$ for 5 mins. After washing the cells were re-suspended in the buffer 'A' and aliquoted in 100µl volume to 1.5 ml centrifuge or Eppendorf tubes. To the 100µl cell suspension 1° (1:20) and isotype controls were added (different samples) and incubated at room temperature for 60 mins in the dark. Cell samples from step 6 were washed in ice-cold buffer 'A' (x3) and re-suspended in again in buffer 'A'. To the above cell samples 2° antibody (10 µg/mL) was added and incubated at room temperature for 60 mins in the dark. After 2° antibody incubation the cells were washed with buffer 'A' (x3) and re-suspended again in the buffer 'A'. Cells from step 9 were subjected to flow cytometry analysis.

2.7 CRISPR-CAS9 transfection for ABCC5 knock out in Panc1

2.7.1 Materials required

- gRNA (0.2–3 mg/mL) – invitrogen™ (Cat. No – 1908508)
- Cas9 nuclease (1mg/mL) – invitrogen™ (Cat. No – 00517508)
- Opti-MEM™ I Reduced Serum Medium
- 1.5 ml tubes - Eppendorf

2.7.2 Protocol outline

This protocol was optimised using the gRNA for GeneArt™ Platinum Cas9 Nuclease (Cat.nos. B25640, B25641). GeneArt™ Platinum™ Cas9 Nuclease was stored at -20°C as per the manufacturer's instruction for increased shelf life and to avoid degradation. Eluted gRNAs were immediately stored at -20°C until use. For prolonged storage (>1 month), gRNA can be stored at -80°C. Cells were plated with the initial cell number of 0.5×10^5 cells/ well so that they were up to 70% confluent at the time of transfection. On the next day after seeding, Cas9 nuclease/gRNA/transfection reagent complex was prepared as shown in the table: 2-3 and was added to the cells. Followed by the incubation of 72 hours.

Scaling up or down transfections

Cultu re vessel	Multiplic ation factor ^[1]	Starting cell number ^[2]	Vol. growth mediu m	Tube 1 ^[3]			Tube 2			Cas9 nuclease/gR NA/ transfection reagent complex
				Vol. Opti- MEM ™ I mediu m	Cas9 nuclea se	gRN A (µg)	Cas9 Plus™ Reage nt	Vol. Opti- MEM ™ I mediu m	CRISPRM AX™ Reagent	
12- well	2.00	0.84– 2.4 × 10 ⁵	1	50 µL	1.00	0.25	2 µL	50 µL	3 µL	100 µL

Table 2-2: Transfection mix for CRISPR-Cas9

Cell seeding number is based on the cell growth rate. Cell seeding number was optimised to 0.5×10^5 for PANC1 cells. In Tube 1, the ratio of Cas9 nuclease to gRNA used was 4:1 (µg:µg), while the ratio of Cas9 nuclease to Cas9 Plus™ Reagent was 1:2 (µg:µL).

Design details of gRNA

sgRNA 1

Target DNA Sequence: ACCGTGAAGATTCCAAGTTC

PAM Sequence: AGG

Target locus Chr.3: 184014276 - 184014298 on GRCh38

Strand: Reverse

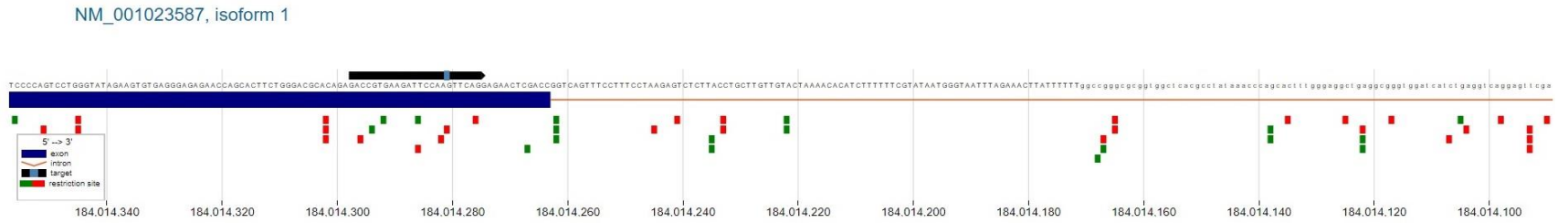


Figure 2-2: Target map of sgRNA 1

sgRNA 2

Target DNA Sequence: TCAGAGCACTCAAGCCATGA, PAM Sequence: TGG

Target locus Chr.3: 183989248 - 183989270 on GRCh38, Strand: Forward

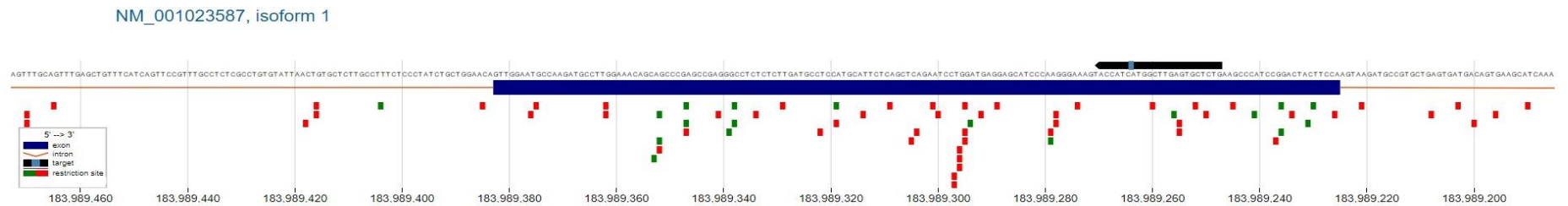


Figure 2-3: Target map for sgRNA 2

2.7.3 The genomic cleavage detection assay

After transfection and clone isolation cleavage assay was performed to detect locus-specific cleavage of genomic DNA using the GeneArt™ Genomic Cleavage Detection Kit (Cat. no. A24372).

Primer design

Genomic DNA at the locus being investigated must be PCR amplified prior to detection. Recommended guidelines were used to ensure optimal amplification and subsequent detection. For best results, primers with $T_m > 55^\circ\text{C}$ were used. Primers were designed for 18–22 bp in length and 45–60% GC content. For efficient amplification, primers were designed to yield amplicon lengths between 400 and 500 bp. Primers were so designed that the potential cleavage site was not in the centre of the amplicon and the detection reaction will yield two distinct product bands.

Harvesting cells

Single cell isolated clone-1 (from sgRNA-2) cells were trypsinised (section 2.1.2) and centrifuged at $200 \times g$ for 5 minutes at 4°C . At least 50,000 and no more than 2×10^6 cells were used in 50 μL Cell Lysis Buffer. Lysate from less than 50,000 cells will be insufficient for PCR amplification and greater than 2×10^6 cells will inhibit the PCR reaction. The volume of lysis buffer can be adjusted based on cell number. After trypsinisation, supernatant was carefully removed and the pellet was used for further lysis reaction (or could be stored at -80°C).

Cell lysis and DNA extraction

50 μL of Cell Lysis Buffer was mixed with 2 μL Protein Degradar in a microcentrifuge tube. This 50 μL of Cell Lysis Buffer/Protein Degradar mix was added to each cell pellet and resuspend the pellet. All the resuspended cell pellets were then transferred to a PCR tube. Following program was used to run the reaction in thermal cycler:

Temp	Time
68°C	15 min
95°C	10 min
4°C	Hold*

Table 2-3 Thermocycler program for DNA extraction

*Following completion, PCR amplification was carried out immediately (or samples could be stored at -20°C).

PCR amplification

Cell lysates were briefly vortexed followed by addition of the following components to a PCR tube:

Component	Sample	Control
Cell lysate	2 μL	—
10 μM F/R primer mix	1 μL	—
Control Template & Primers	—	1 μL
AmpliTaq Gold® 360 Master Mix	25 μL	25 μL
Water	22 μL	24 μL
Total	50 μL	50 μL

Table 2-4 PCR amplification mix

PCR parameters

Following are the PCR reaction parameters:

Stage	Temp	Time	Cycles
Enzyme activation	95°C	10 min	1 X
Denature	95°C	30 sec	40X
Anneal	57°C (T _m)	30 sec	
Extend	72°C	30 sec	
Final extension	72°C	7 min	1X
Hold	4°C	Hold	1 X

Table 2-5 PCR parameters for DNA extraction

The annealing temperature can be adjusted based on the primers used. The extension time could also be adjusted based on the size of amplicon (60 seconds for each kb).

Verification of PCR product

For verification 3 µL of PCR product with 10 µL water was loaded on a 2% agarose gel. If a single band of the correct size is present, with an intensity similar to 50 ng of 400 bp band in the mass ladder, proceed to the denaturing and re-annealing step, or store the PCR product at –20°C for later use. A single band of the expected size is crucial for obtaining accurate cleavage detection. PCR conditions could be optimised; including primers, annealing temperature, and amount of lysate volume until you obtain good quality PCR products.

Cleavage assay: Denaturing and re-annealing reaction

This step serves to randomly anneal the PCR fragments with and without indels to form heterogeneous DNA duplexes. For the reaction 1–3 µl of PCR product was combined with 1 µl 10X Detection Reaction Buffer in a PCR tube and the volume of was brought to 9 µl with Water. The tube was then centrifuged briefly to remove bubbles.

Re-annealing reaction

The tubes from denaturation reaction were subjected to thermal cycler with a heated-lid for re-annealing reaction:

Stage	Temp	Time	Temp/time
1	95°C	5 min	—
2	95°C–85°C	—	–2°C/sec
3	85°C–25°C	—	–0.1°C/sec
4	4°C	—	Hold

Table 2-6 Reaction conditions for re-annealing reaction

Enzyme digestion

Heteroduplex DNA containing the insertion, deletion, or mismatched DNA (indel) is cleaved by the Detection Enzyme confirming the cleavage. 1 µl Detection Enzyme was added to all test samples and mixed well. Followed by the addition of 1 µl of water to all negative control samples. After addition of the detection enzyme samples were incubated at 37°C for 1 hour. Post 1 hour of incubation samples were vortexed briefly, spun down and placed at 4°C (for less than 2 hours).

Gel analysis

All the samples were immediately loaded (entire 10 µl) on a 2% agarose gel. 1 kb DNA ladder was used as the sizing standard in parallel. The gel was used using a UV transilluminator.

2.8 Statistical Analysis

The data are presented as mean values with standard errors (mean ± SEM). All results were from at least 3 independent experiments unless otherwise stated. Linear and non-linear regression analyses will be undertaken as appropriate using Prism 6 software (GraphPad, San Diego, CA, USA). Multiple comparisons between control and different treatment groups will be analysed using one-way analysis of variance (ANOVA) with Dunnett's post-hoc. Student's t-test, two-way ANOVA with post-hoc tests were applied as appropriate. A *p*-value <0.05 was considered significant.

Chapter 3 Development and validation of a real-time PCR method for the quantitation of gene expression related to gemcitabine transport and metabolism

The dawn of PCR and quantitative-real time reverse-transcription PCR (qRT-PCR) transformed things revolutionary in the field of gene expression/molecular biology. Early in the days, PCR technique was only able to generate clones or amplification, but the real-time PCR has made a collection of data possible in the real-time, i.e. data can be produced as the PCR process progress [267]. Thus qRT-PCR combines the amplification and the detection in the single step; achieved through various fluorescent chemistries that correlate PCR product concentration to fluorescent intensity. With the progression of the reaction during real time, when the target amplification is first detected, the reaction is characterised by that point [267]. This point of detection is known as the cycle threshold, and the threshold value is depicted as C_p . The threshold value is referred to the time when fluorescence intensity is higher than the background fluorescence. Thus, low C_p values indicate the higher quantity of target DNA in the sample or starting material. Hence, higher gene activity will yield lower C_p values and vice-versa [267].

There are many advantages of using the qRT-PCR over the other traditional methods to quantify the gene expression. It can generate quantitative data in real time with a precise dynamic range of 7 to 8 log orders of magnitude and post-amplification manipulations are not required. qRT-PCR can detect a single copy of a specific transcript which increases their sensitivity dramatically. qRT-PCRs are 1000-fold more sensitive than dot blot hybridisation and 10,000-100,000-fold more sensitive than RNase protection assays [267]. Apart from this qRT-PCRs can efficiently detect a difference in the gene expression level among samples with a low coefficient of variation than probe hybridisation and endpoint assays such as band densitometry [267]. qRT-PCR can also differentiate between the RNAs (mRNAs) with very similar sequences, and the amount of starting material/sample (RNA) required for the qRT-PCR is decidedly less than other methods of gene expression analysis, and with the proper equipment and condition can be very high throughput [267]. There are a few disadvantages to the qRT-PCR technique, e.g. the required equipment and reagents/kits are expensive. As we now know that qRt-PCR is extremely sensitive and thus needs a sound experimental design. In-depth understanding of normalisation techniques (discussed further in this chapter) is vital for exact results. The general steps of the qRT-PCR are depicted in figure 2.

3.1 Background of real-time PCR

Real-time PCR is further subdivided into four noteworthy stages: the linear ground phase, early exponential phase, log-linear (also known as exponential) phase, and plateau phase [268]. Amid the linear ground stage (typically the initial 10– 15 cycles), PCR is merely starting, and fluorescence at each cycle has not yet transcended background. Baseline fluorescence is figured as of now. At the early exponential stage, the measure of fluorescence has achieved an edge where it is substantially higher (for the most part 10 times the SD of the pattern) than background levels. The cycle at which this happens is known as C_p (as mentioned above) crossing point in LightCycler® literature (Roche Applied Science, Indianapolis, IN, USA) (2,10). C_p is illustrative of the beginning of amplification in the template and is utilised to calculate the results of the experiment [269]. Through the log-linear phase, PCR achieves its optimum amplification period with the PCR product doubling after each cycle in ideal reaction conditions. The plateau stage is eventually reached when reaction components exhaust, and the fluorescence intensity is non-valuable for calculations.

The calculations regarding the activity of any target or housekeeping gene are dependent on the efficacy of the reaction and the crossing point (C_p value) of each sample in the reaction. The calculations are made according to the general PCR equations [270]:

$$N_T = N_{T_0} \times E_T^{C_p T}$$

$$N_R = N_{R_0} \times E_R^{C_p R}$$

Where N_T stands for Number of targets, N_R for Reference molecules at detection threshold C_p , N_{T_0} for Initial number of target, N_{R_0} for Reference molecules, $C_p T$ for Cycle number at target, $C_p R$ for Reference detection threshold (crossing point), E_T for Efficiency of the target, and E_R for Reference amplification

At a certain fluorescence detection level the amplicon numbers of target and housekeeping genes are improbable to be identical due to differences in probe annealing, channel sensitivity, quantum yields/extinction coefficient of dye batches, and FRET efficacy [270]:

$N_T _ N_R \Rightarrow N_T/N_R \neq 1$, but constant for each sample and the calibrator.

To calculate the calibrator normalised relative ratio the relative amount of target/reference of each sample $[NT(S)/NR(S)]$ is divided through the ratio of target/reference of the calibrator $[NT(C)/NR(C)]$ (T : Target, R: Reference, S: Unknown sample, C: Calibrator, K: Constant)

3.2 Quantitation of gene expression by real-time PCR

3.2.1 Absolute Quantitation

To generate a standard curve, this type of quantitation uses known concentration standards which are serially diluted. Through the standard curve, a linear relationship is established between the C_p and the initial amount of total RNA/cDNA which allows the determination of the concentration of unknowns by their C_p values [269]. This strategy assumes all standards and samples/unknowns have approximately equal amplification efficacy [271]. Also, the concentration of serial dilutions ought to include the levels in the experimental samples and remain inside the range of precisely quantifiable and recognisable levels, particular to both the real-time PCR machine and assay.

The PCR standard could be single-stranded DNA (ssDNA), double-stranded DNA (dsDNA), or cRNA bearing the target sequence. Amplification efficiency calculation utilising a standard curve isn't precisely the changing efficiency [272] and may miscalculate efficiencies [268]. Since PCR results are C_p dependent and could be determined early in the exponential phase, alterations in the amplification values barely affect the C_p values. In any case, after 26 cycles, a 5% variance in amplification proficiency can bring about a 2-fold difference of PCR product concentration. DNA standard has been appeared to have a more significant quantification range and more noteworthy sensitivity, reproducibility, and stability than RNA standards [273]. Though, a DNA standard cannot be utilised for a one-step qRT-PCR because of the absence of control for the reverse transcription efficiency [267, 274].

3.2.2 Relative Quantitation

This type of quantitation involves measurement of the changes in comparison to an external reference gene or an external standard aka calibrator [275]. The results are expressed as target/reference ratio, and a number of methods are available to calculate the mean normalised gene expression (discussed further in this chapter).

3.2.3 Amplification efficiency

If the amplification efficiency of the reaction is 100% or 2, then it can be assumed that within the exponential phase of the reaction PCR product concentration is doubling during every cycle. Normalization eliminates all the variables influencing the final result, e.g. variations in sample amount or different hybridisation probe annealing. Therefore the accuracy of the relative quantitation depends highly on the PCR efficiency of the target and reference gene [270].

$N = N_0 \times E^{C_p}$: According to this basic PCR equation, the generated copy number (N) at a particular cycle is a function of the initial copy number (N_0), the PCR efficiency (E) and the cycle number (C_p). Thus, the crossing point (C_p) in a reaction is the cycle at which the amplification enters or begins its exponential/log phase and is also measured as the point that is proportional to the initial concentration [270]. The PCR kinetics is defined by its efficiency, primers for both (target and reference gene) have individual PCR efficiencies and are accounted for overall quantification. Light cycler relative quantification software also performs an efficiency-corrected calculation which allows maximum reproducibility and controls for factors influencing quantification [270].

Amplification efficiency being 2 is very rare, and in most cases, it varies due to the various factors like – high GC content. Thus, if the calculation of the result is by the equation $N = N_0 \times 2^{C_p}$ and has not used the real PCR efficiency, then there is a high probability of getting a significant error with each cycle.

3.2.4 Standard curve method for relative quantification

Using the standard curve amount of each sample is determined and then expressed with respect to a single calibrator sample. The calibrator is designated as 1-fold, with all experimentally derived quantities reported as an n-fold difference relative to the calibrator [267]. As sample quantity is isolated by the calibrator amount, standard curve units are excluded. Thus, only the relative dilution factors of the standards are needed for the quantification. Usually, this method of quantification is used when the amplification efficiencies of the reference and target gene are not the same [276]. It is additionally the least complicated technique for measurement since it requires no planning of exogenous standards, no quantification of calibrator samples, and does not depend on complex arithmetic. Nonetheless, this technique does not incorporate an

endogenous control (more often a housekeeping gene). Thus results need to be normalised.

3.2.5 Comparative Cp ($2^{-\Delta\Delta C_p}$) method

This technique is a mathematical model that computes variations in gene expression as a relative fold difference between the sample and an internal control/reference gene. While this strategy incorporates a correction for non-ideal amplification efficiencies, i.e., not 2 [275], the amplification kinetics of the target gene and reference/housekeeping gene must be almost equivalent because different efficiencies will produce errors when utilising this method [276]. Thus, a validation assay could be performed where serial dilutions are tested for the reference and target gene and the outcomes plotted with the log input concentration for every dilution on the x-axis and difference in Cp (target-reference) for every dilution on the y-axis. The comparative Cp method could be used if the slope of the line is less than 0.1 [275]. The PCR product size ought to be kept little (under 150 bp) and the reaction thoroughly optimised [277]. Since the comparative Cp strategy does not require a standard curve, it is helpful while examining a vast number of samples since all response wells are loaded with sample reactions rather than standards.

3.2.6 Absolute or Relative Quantitation: Pros and Cons

Absolute quantitation is thought to be more work escalated than relative quantitation as a result of the need to make reliable standards for quantitation and incorporate these standards in each PCR [273]. Nonetheless, when performing relative quantitation, the information (Cp) utilised for correlation are arbitrary values and pertinent to the samples run within the same PCR. For a comparison of samples between two different PCRs, it is essential to incorporate a reference control in each plate. In situations where data compared are tested on various days or in different research centres, absolute quantitation might be favoured as outcomes depend on a constant. In terms of fold change data, absolute and relative quantitation strategies create practically comparable results [278].

3.2.7 Controls

There are a few controls that assure the integrity of each step of the real-time PCR. With a negative control DNA contamination in the sample could be accounted. Though, when dealing with various samples, a substitute strategy to keep the identification of genomic DNA is to design the target PCR product to traverse an exon/exon boundary. The

difference in the efficacy of the reverse transcriptase and the amount of RNA included in the reaction can be accounted utilising an endogenous control. Endogenous controls are further discussed in the following part of this chapter under “Normalization”. PCR master mix volume has also been reported as one of the factors for the difference in the reaction efficacy even with the same amount of starting template [276]. A passive reference dye (for example, ROX) is frequently incorporated into the master mix to calculate differences in the PCR master mix volumes and additionally non-PCR-related changes in fluorescence signal. An exogenous control can be used for problems with PCR master mix itself [279].

3.2.8 Normalisation

For a sample to sample, variation normalisation method is used for the gene expression data. The starting material may vary in terms of cell number, RNA integrity or quantity, tissue mass or experimental treatment. Under ideal conditions, mRNA levels can be standardised to cell number, however, when utilising entire tissue sample, this sort of standardisation is implausible [280]. Thus, real-time PCR results are generally normalised against a control gene or aka housekeeping gene that may likewise fill in as a positive control for the reaction. The ideal control gene’s expression is theoretical constant, i.e. it should not change with experimental conditions, different tissue/cell type or sample treatment. Since there are few genes which fulfil this paradigm, for each experimental condition it is essential to validate the expression stability of a control gene for the prerequisites of an experiment before its utilisation for normalisation [281].

3.2.9 Housekeeping genes (mRNA)

Because of the high sensitivity and dynamic range of real-time PCR over conventional quantitation methods, many housekeeping genes, for example, GAPDH and β -actin have been appeared to be influenced by various treatments, biological processes, and even different tissues or cell types [282]. Thus, when utilising a housekeeping gene for standardisation, it is essential to validate its stability with one's samples. In my experiments initially two different housekeeping genes; GAPDH and RPL13A were proposed for the normalisation. We carried out some preliminary tests using two different pancreatic cancer cell lines keeping the reaction conditions constant. We found out that expression of GAPDH was very stable for both two cell lines in the presence and absence of siRNA treatments.

3.3 Applications of qRT-PCR

qRT-PCR is a popular molecular biology technique with a wide range of applications. It is most commonly used in gene quantitation studies and for microarray validation. Lately, scientists have been using it to study various genetic pathways by performing gene expression analysis [283]. One of the most popular applications of this technique is in developmental biology where it is used to study the roles of various genes and their expression levels.

Modulation of gene expression using RNAi technique also incorporates the use of qRT-PCR. miRNA functions in RNA silencing and post-transcriptional regulation of gene expression and have wide applications in oncology, metabolic diseases, and autoimmune diseases. qRT-PCR has been used for high-performance miRNA profiling and validation, i.e. identification of differentially expressed miRNA is carried out using qPCR, and its activity is confirmed for a target gene [284]. Apart from miRNA profiling qRT-PCR is also used for miRNA quantitation where a specific miRNA quantitation is carried out [284]. One of the important application of qRT-PCR is pre-miRNA analysis, i.e. detection of primary miRNAs in human, mouse and rat species [284]. Non-coding transcripts are a significant part of the genome and play an important role in splicing. qRt-PCR has been used for the reliable detection of and quantitation of non-coding human, mouse, or rat transcripts longer than 200 nucleotides [285].

3.3.1 Genetic Variation Analysis Using Real-Time PCR

One of the major branches of pharmacology is pharmacogenetics where the study of different genes is carried out which influence drug transport and metabolism. Such a study is very important for drug efficacy especially for the disease like cancer [286]. Most of the cancers have various mutations which could affect the drug activity during chemotherapy leading to MDR thus profiling of drug metabolism enzymes using qRT-PCR is very significant. Detection of genetic polymorphism and pharmacogenetics marker is also one of the major applications of the qRT-PCR technique. Another major application of qRT-PCR in genetics is the study and detection of rare mutations which also includes SNP genotyping [286].

3.3.2 Clinical applications

There has been a significant increase in the use of real-time PCR for clinical applications, e.g. clinical microbiology, oncology and gene therapy. Nowadays it has become the standard method for disease detection, e.g. detection of microbial genomes,

deletions, mutations, trisomies and free nucleic acids [287]. Specific factors have to be taken into account when working with clinical samples, which do not apply to assays optimised for fundamental molecular research. Of vital importance is a standardisation of the test across different laboratories. Also, appropriate positive and negative controls need to be included in all assays.

3.4 The need for One-Step PCR and One-Step Versus Two-Step Real-Time PCR

As we know now that qRT-PCR first produces complementary DNA (cDNA) with the help of reverse transcription reaction (using RNA as a template) and this cDNA is further subjected for amplification via PCR; monitored in real time. Thus, mRNA quantification via qRT-PCR can be executed as either a one-step reaction, where the whole process of reverse-transcription for cDNA formation and PCR amplification is performed in a single tube or as a two-step process, where cDNA creation and PCR amplification happen in different tubes. There are a few upsides and downsides related to every technique. One-step qRT-PCR is thought to limit experimental variations because both enzymatic reactions occur in a single tube. Be that as it may, this strategy utilises an RNA template, which is inclined to quick degradation if not handled properly. Thus, one step PCR reaction may not be suitable in those cases where the same sample is repeatedly used over the period for analysis. One step reaction is also reported to be less sensitive than two-step procedures [288].

Two-step qRT-PCR isolates the reverse transcription reaction from the real-time PCR thus allowing many different real-time PCR assays of the same cDNA on dilutions. As the reverse transcription reaction is infamous for its profoundly variable reaction efficacy [289], utilising dilutions from a similar cDNA guarantee that reactions from ensuing assays have the same amount of cDNA template as compared to the previous tests. A two-step protocol might be favoured when utilising a DNA binding dye, (for example, SYBR Green I) since it is easier to get rid-off primer dimers through the manipulations of melting temperatures (T_ms) [290]. No process is error free two-step procedure has few disadvantages – tedious, consumes more time, more chances of human errors and high chances of DNA contamination. We started with the traditional two-step PCR process, but due to the large sample size and time required for completion of reactions, we switched on to one step PCR reaction. Not only it drastically reduced the chances of error but also increased work efficiency. The procedure related to both methods is described in detail in the “method” section of this chapter.

3.5 Specific Aims

To assure that an observed gene silencing effect on protein level or gene function is specific to siRNA sequence(s) transfected, the mRNA level of ABCC5 is desired to be measured as its encoded protein (MRP5) has a relatively long half-life. This chapter aims to 1) to develop an efficient, precise and accurate qRT-PCR method to quantitate the expression of multiple genes associated with gemcitabine transport and metabolism in human pancreatic cancer cell lines; 2) to validate the expression stability of housekeeping genes for the specific requirements of siRNA experiments.

3.6 Methods-

3.6.1 RNA Extraction Protocol

Materials and Method

RNA extraction was carried using the RNeasy® Mini Kit from Qiagen (Catalogue No. – 74106)

Equipment and Reagents

- Sterile, RNase-free pipet tips
- Microcentrifuge - Eppendorf
- 70% ethanol - ThermoFisher Scientific
- Trypsin and PBS

Method

The transfected cells (see section 2.2.2) from 12 well plate (minimum cell no. 1×10^5) were used for RNA extraction (not more than 1×10^7 cells). The cells were washed with PBS, trypsinized and collected as a pellet (section 1.1.2) in RNase free polystyrene or Eppendorf tube. The cell pellet was subjected for cell lysis using the cell lysis buffer (RLT buffer) supplied with the RNeasy® Mini kit. The volume of the RLT buffer can be adjusted as per the cell number.

Number of pelleted cells	Volume of Buffer RLT (μ l)
$<5 \times 10^6$	350
$5 \times 10^6 - 1 \times 10^7$	600

Table 3-1: Scaling up and down the volume of RLT buffer (cell lysis buffer)

The cell lysate was homogenized by vortexing for 1 min followed by addition of 1 volume of 70% ethanol. The homogenized cell lysate was gently mixed with ethanol by pipetting up and down a few times. This cell lysate mixture (600-700 μ l) from step 3, including any precipitate was transferred to a RNeasy Mini spin column (supplied with the kit) placed in a 2 ml collection tube. RNeasy Mini spin column was centrifuged for 15 secs at $\geq 8000 \times g$ and the flow through was discarded.

To RNeasy Mini spin column from above step 700 μ l Buffer RW1 was added and centrifuged again for 15 secs at $\geq 8000 \times g$. Flow-through was discarded. To the same RNeasy Mini spin column 500 μ l Buffer RPE was added and centrifuged for 15 secs at $\geq 8000 \times g$. Again flow-through was discarded (this step was repeated twice). The RNeasy spin column was then placed in a new 1.5 ml collection tube. Around 30–50 μ l RNase-free water was added directly to the spin column membrane. Again, centrifugation was carried out for 1 min at $\geq 8000 \times g$ to elute the RNA. The RNA yield or RNA quantitation was carried using Qubit 2.0 (refer 2.2.4). The RNA elution step can be repeated if the expected RNA yield is $>30 \mu\text{g}$.

3.6.2 RNA Quantitation

Materials

- Qubit 2.0 - ThermoFisher Scientific
- Qubit® RNA BR Reagent and Buffer - ThermoFisher Scientific
- Qubit® assay tubes - ThermoFisher Scientific
- Pipettes

Assay parameters

Temperature

Temperature fluctuations can influence the accuracy of the assay. Thus, to minimize temperature fluctuations, the Qubit® RNA BR Reagent and Buffer were stored at room temperature.

Incubation time

The incubation time suggested by the manufacturer is around 2 minutes after mixing the DNA/RNA sample or the standards. This allows the Qubit® assay to reach optimal fluorescence.

Calibrating the Qubit® Fluorometer

Before performing the quantitation of samples, Qubit 2.0 was calibrated. Calibration was performed using the standards supplied with the kit (Standard I and II). The fluorescence signal in the tubes containing standards and samples are stable for no longer than 3 hours, and therefore standards were freshly prepared and used ASAP. The integrity and concentration of these standards are critical for the optimal performance of the Qubit® RNA BR Assay. Thus, RNase-free gloves, pipette tips, and tubes were used all the times.

Method: Preparing samples and standards

The required number of 0.5-mL tubes for standards and samples were set-up and labelled. The Qubit® working solution was prepared by diluting the Qubit® RNA BR Reagent 1:200 in Qubit® RNA BR Buffer. Clean plastic tubes were used each time for preparing the Qubit® working solution. The final volume in each tube was 200 µl, and for each standard tube, 190 µl of Qubit® working solution was used. For each sample tube, 199 µl of the working solution was used. 10 µl of each Qubit® standard was added to the appropriate tube, then mixed by vortexing 2–3 seconds. While 1 ul of the sample

was added to each sample tube for quantitation; mixed by vortexing 2–3 seconds. The final volume in each tube should be 200 μ l. After incubating all tubes at the room temperature first standards were run on Qubit2.0 followed by sample reading. The Qubit® 2.0 Fluorometer gives values for the Qubit® RNA BR Assay in μ g/ml. This reading can be used to generate the stock concentration (done by instrument automatically). After getting the stock concentration, the units can be changed to ng/ μ l (for the stock). This unit conversion comes very handy while calculating the volume of the sample for qRT-PCR.

3.6.3 Two Step Rt PCR

Materials –

1. Transcriptor cDNA synthesis kit – Roche life science, New Zealand
2. Template RNA
3. Primers – IDT (details in appendix)
4. Roche Light Cycler® 2.0 – Roche Diagnostics, New Zealand

Method: cDNA synthesis protocol

For total RNA extraction from cancer lines and siRNA transfected cell lines, RNeasy Protect Mini Kit (Qiagen) was used. The extracted total RNA was stored at -80°C to prevent the denaturation. RNA quantitation was performed using Qubit® 2.0 fluorometer. Knockdown of the target gene was achieved by using three different siRNA. Then qPCR was used to evaluate the knock-down effects. Two-step procedure (mRNA extraction & cDNA formation) was initially used with SYBR green dye on Roche Light Cycler 2.0 (Roche Applied Science). For cDNA synthesis Transcriptor cDNA synthesis kit (Roche Diagnostics) was used. Relative gene expression quantification was calculated according to the comparative threshold cycle method ($2^{-\Delta\Delta\text{Cp}}$) using GAPDH as a reference gene.

All the frozen reagents were thawed and briefly centrifuged before starting the procedure. All the reagents were kept on ice before setting up the reaction. In a sterile, nuclease-free, thin-walled PCR tube on ice, the template-primer mixture for one 20 μ l reaction was prepared by adding the components in the following order.

Component	Vol.	Final Conc.
Total RNA		900 ng
Sequence-Specific Primers		0.5 μ M
Water (PCR Grade)		To make total vol. 13 μ l
Total Volume	13 μ l	

Table 3-2: Template primer mix for 1 reaction

Component	Vol.	Final Conc.
Transcriptor reverse-transcriptase reaction Buffer, 5X conc. (vial 2)	4 μ l	1x (8mM MgCl ₂)
Protector RNase Inhibitor, 40 U/ μ l (vial 3)	0.5 μ l	20 U
dNTP Mix 10mM each (vial 4)	2 μ l	1 mM each
Transcriptor- Reverse transcriptase 20 U/ μ l (vial 1)	0.5 μ l	10 U
Final Volume (including table 3-1)	20 μ l	

Table 3-3: Reaction mix for cDNA synthesis

All the reaction reagents were mixed by gentle pipetting followed by centrifugation to collect the sample at the bottom of the tubes. Later the tubes were placed in a thermal block cycler with a heated lid. The RT (reverse transcription) reaction was incubated for 60 mins at 50°C. Inactivation of the transcriptor reverse transcriptase was achieved by heating to 85°C for 5 mins. The reaction was stopped by placing the tube on ice (at this point the reaction tube may be stored at +2 to +8°C for 1-2 hrs or at -15 to -25°C for

longer periods). For PCR the cDNA was added to the PCR reaction mix without purification. The final MgCl₂ Conc. in the reverse transcription reaction was 8 mM.

3.6.4 PCR on the Roche Light Cycler 2.0

PCR amplification and analysis were done using a Roche Light Cycler 2.0 (Roche Applied Science) with software version 1.1. All reactions were performed with the Light Cycler FastStart DNA Master SYBR green I (Roche Applied Science) by using a 20µl volume in each reaction capillary [291]. For quantification of the MRP5 mRNA, 2 µl cDNA was added before capillaries were capped, centrifuged, and placed in the Light Cycler sample carousel. Negative controls consisting of no-template (water) reaction mixtures were run with all reactions. Data were normalised to the expression reference gene- GAPDH. Table 1 shows the list of forward and reverse sequences reference & target genes which will be used in this project. All the reagents were thawed at room temperature (RT) and briefly centrifuged before use. All the reagents were kept on ice while setting up the reaction.

Component	Vol.	Final Conc.
Light Cycler® Fast Start DNA Master SYBR Green I reaction mix (10x)	2µl	1x
Forward Primer	1µl	0.5µM
Reverse Primer	1µl	0.5µM
MgCl ₂ (25mM)	2.4µl	4mM (1mM are contributed by the Light Cycler® master mix)
Water PCR grade	11.6µl	
Total	18µl	

Table 3-4: Reaction mix for one step Rt-PCR

Denaturation			
Temp (°C)		95°C	
Hold (seconds)		600	
dT/dt (°C/s)		20	
Acq. Mode		None	
Amplification: 45 Cycles			
Temp (°C)	95	58	72
Hold (seconds)	10	30	30
dT/dt (°C/s)	20	20	20
Acq. Mode	None	None	Single
Melting Curve			
Temp (°C)	95	65	95
Hold (seconds)	1	15	0
dT/dt (°C/s)	20	20	0.05
Acq. Mode	None	None	Continuous
Cooling			
Temp (°C)		40	
Hold (seconds)		30	
dT/dt (°C/s)		20	
Acq. Mode		None	

Table 3-5: Reaction conditions for One-Step qRT-PC

qRT-PCR Primers

Genes of Interest	Forward (5'-3')	Reverse (5'-3')	Prod. size
ABCB1 [292]	GCCTGGCAGCTGGAAGACAAATAC	ATGGCCAAAATCACAAGGGTTAGC	252
ABCC1 [292]	AGTGGAACCCCTCTCTGTTTAAG	CCTGATACGTCTTGGTCTTCATC	551
ABCC2 [292]	AATCAGAGTCAAAGCCAAGATGCC	TAGCTTCAGTAGGAATGATTCAGGAGCAC	155
ABCC3 [292]	TCCTTTGCCAACTTTCTCTGCAACTAT	CTGGATCATTGTCTGTCAGATCCGT	153
ABCC4 [292]	TGATGAGCCGTATGTTTTGC	CTTCGGAACGGACTTGACAT	244
ABCC5 [292]	AGAGGTGACCTTTGAGAACGCA	CTCCAGATAACTCCACCAGACGG	172
ABCC11[292]	CCACGGCCCTGCACAACAAG	GGAATTGCCAAAAGCCACGAACA	535
ABCG2 [292]	CCGCGACAGTTTCCAATGACCT	GCCGAAGAGCTGCTGAGAACTGTA	380
hENT1 [293]	GCTGGGTCTGACCGTTGTAT	CTGTACAGGGTGCATGATGG	131
CDA [294]	GTTGCCTTGTTCCCTTGTA	TCTTGCTGCACTTCGGTATG	172
dCK [294]	CGATCTGTGTATAGTGACAG	GTTGGTTTTTCAGTGTCTATG	291

Table 3-6: Primer sequences for the target genes

<u>Reference/Housekeeping Genes</u>			
RPL13A	CATCGTGGCTAAACAGGT		
[295]	ACTG	GCACGACCTTGAGGGCAGCC	320
GAPDH	GCACCGTCAAGGCTGAG		
[296]	AAC	GCCTTCTCCATGGTGGTGAA	151

3.6.5 One Step

Table 3-7: Primer sequences of the reference genes

qRT-PCR

Materials

- LightCycler® EvoScript RNA SYBR® Green I Master- Roche life science, NZ
- LightCycler® 480 Instrument II – Roche Diagnostics, NZ
- 96 well plate
- RNA templates
- Primers - IDT

Reagent	Volume	Final Conc.
For 1 Reaction [μ l]		
Water PCR Grade	10	-
Master, 5x conc.	4	1x
Primer Mix, 20x	1	1x
Total Volume	15	

Table 3-8: reaction mix for One-Step qRT-PCR

For each reaction, 5 μ l of RNA was used (900 ng in total)

One Step PCR reaction Setup

Program Name	RT						
Cycles	1	Analysis Mode	None				
Target (°C)	Acquisition Mode	Hold (hh:mm:ss)	Ramp Rate (°C/s)	Acquisitions (per °C)	Sec Target (°C)	Step size (°C)	Step Delay (cycles)
60	None	00:15:00	4.40		0	0	0
Program Name	Initial denaturation						
Cycles	1	Analysis Mode	None				
Target (°C)	Acquisition Mode	Hold (hh:mm:ss)	Ramp Rate (°C/s)	Acquisitions (per °C)	Sec Target (°C)	Step size (°C)	Step Delay (cycles)
95	None	00:10:00	4.40		0	0	0
Program Name	amplification						
Cycles	45	Analysis Mode	Quantification				
Target (°C)	Acquisition Mode	Hold (hh:mm:ss)	Ramp Rate (°C/s)	Acquisitions (per °C)	Sec Target (°C)	Step size (°C)	Step Delay (cycles)

95	None	00:00:10	4.40		0	0	0
58	None	00:00:30	2.20		0	0	0
72	Single	00:00:30	4.40		0	0	0
Program Name	melting						
Cycles	1	Analysis Mode	Melting Curves				
Target (°C)	Acquisition Mode	Hold (hh:mm:ss)	Ramp Rate (°C/s)	Acquisitions (per °C)	Sec Target (°C)	Step size (°C)	Step Delay (cycles)
95	Continuous		0.10	6	0	0	0
65	None	00:00:15	2.20		0	0	0
Program Name	cooling						
Cycles	1	Analysis Mode	None				
Target (°C)	Acquisition Mode	Hold (hh:mm:ss)	Ramp Rate (°C/s)	Acquisitions (per °C)	Sec Target (°C)	Step size (°C)	Step Delay (cycles)
40	None	00:00:30	2.20		0	0	0

Figure 3-1: Reaction setup for One-Step qRT-PCR

3.6.6 Data analysis

Intra-day variation in the housekeeping gene expression was calculated using the formula = Standard deviation of the Cp values / Mean Cp. The standard deviation and mean Cp were calculated using the Cp values of house-keeping gene replicates of the same day. The inter-day variation was calculated using the mean intra-day variation of reference gene for at least three separate sets of experiments carried out on different days. To calculate the gene knock-down Livak's method of relative gene expression was used. The Cp values of target genes (both in negative control and siRNA treated samples) were normalised to the same reference gene yielding the ΔCp values for the target (ΔCpT) and control (ΔCpN). These ΔCp values were then used to calculate the fold change ($\Delta\Delta\text{Cp}$) in the gene activity value using the formula $\Delta\Delta\text{Cp} = \Delta\text{CpT} - \Delta\text{CpN}$. Relative quantitation of gene expression was calculated using the formula: $2^{-(\Delta\Delta\text{Cp})}$. The percentage of knockdown was calculated using the formula: $(1 - 2^{\Delta\Delta\text{Cp}}) \times 100$.

3.7 Results

3.7.1 Amplification and Melting curves for MIA PaCa-2 GAPDH

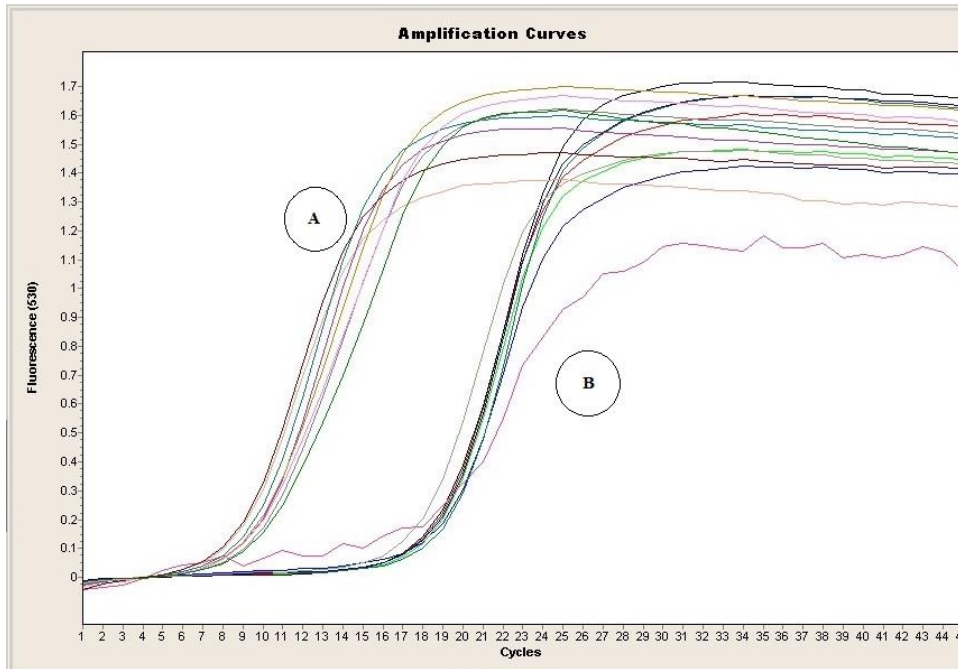


Figure 3-2: Representative amplification curves for the housekeeping gene GAPDH (A) and target gene ABCC5 (B). Refer to table 3-8 for mean Cp values

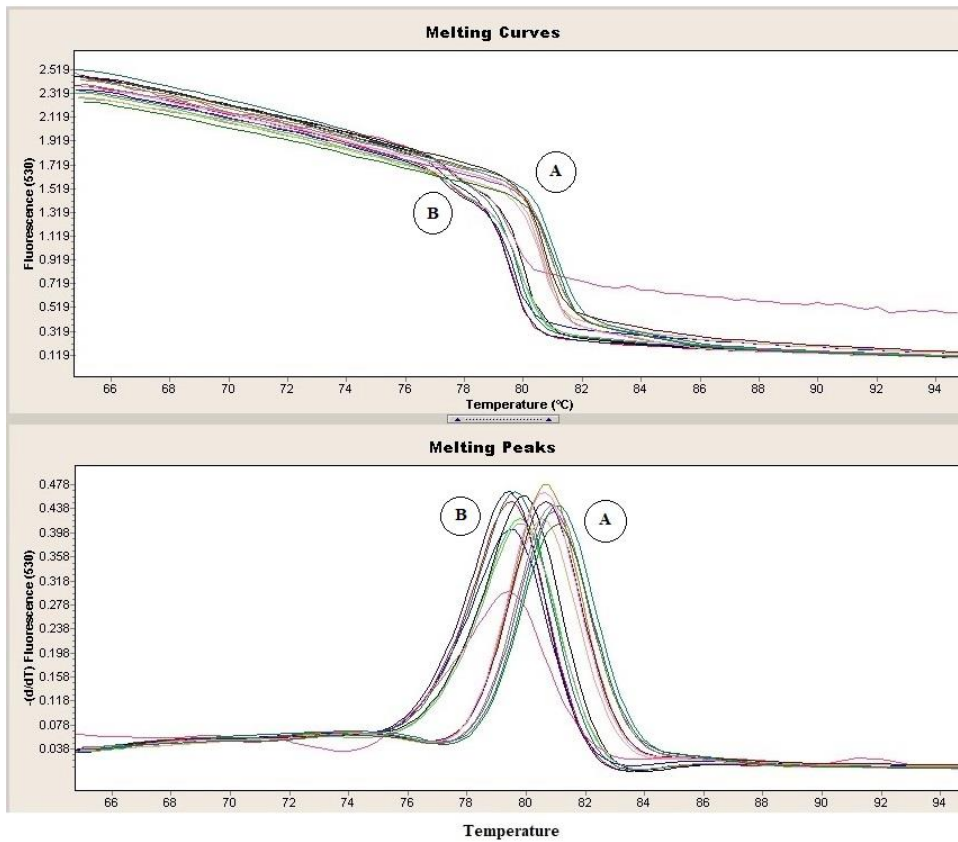


Figure 3-3: Amplification specificity by real-time PCR. Melting curves and melting peaks of GAPDH (A) and ABCC5 (B) PCR products

3.7.2 Variations of housekeeping gene GAPDH

Cell line: MIA PaCa-2

	Intra-Day Variation		Inter-Day Variation
Day 1	Mean Cp	% CV	
GAPDH Si1	8.26	2.75	
GAPDH Si2	8.97	1.13	
GAPDH Si3	8.50	2.07	
GAPDH Control	8.82	0.80	
Day 2	Mean Cp	% CV	
GAPDH Si1	8.86	1.54	≤ 5%
GAPDH Si2	9.0	4.31	
GAPDH Si3	9.06	0.73	
GAPDH Control	9.52	2.7	
Day 3	Mean Cp	% CV	
GAPDH Si1	8.52	2.94	
GAPDH Si2	8.56	3.33	
GAPDH Si3	8.67	1.73	
GAPDH Control	8.86	2.89	

Table 3-9: Variations of housekeeping gene GAPDH in MIA PaCa-2 cells

The individual experiments were carried out in duplicate for each day and were repeated over three different days. The same lot of kit reagents were used every single time, and initial RNA concentration was kept constant for all the experiments. Si1, Si2 and Si3 represent the three different small interference (Si) RNA sequences used for the transfection on the same cell line, and GAPDH control is the negative control, i.e. scrambled siRNA transfected cells. Variation values $\leq 5\%$ are significant.

3.7.3 Amplification curves for PANC-1 GAPDH

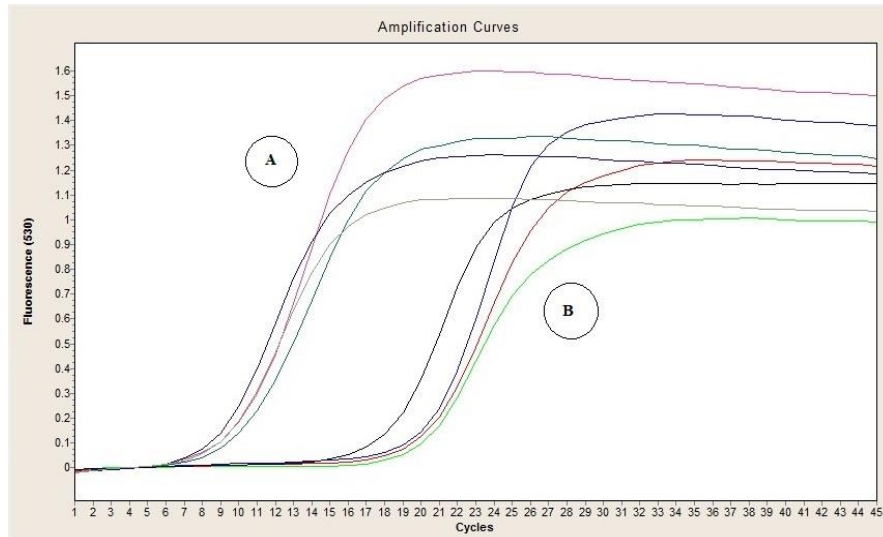


Figure 3-4: Amplification curves for GAPDH (A) and ABCC5 (B) in PANC- 1 cells.

Refer to table 3-9 for mean Cp values

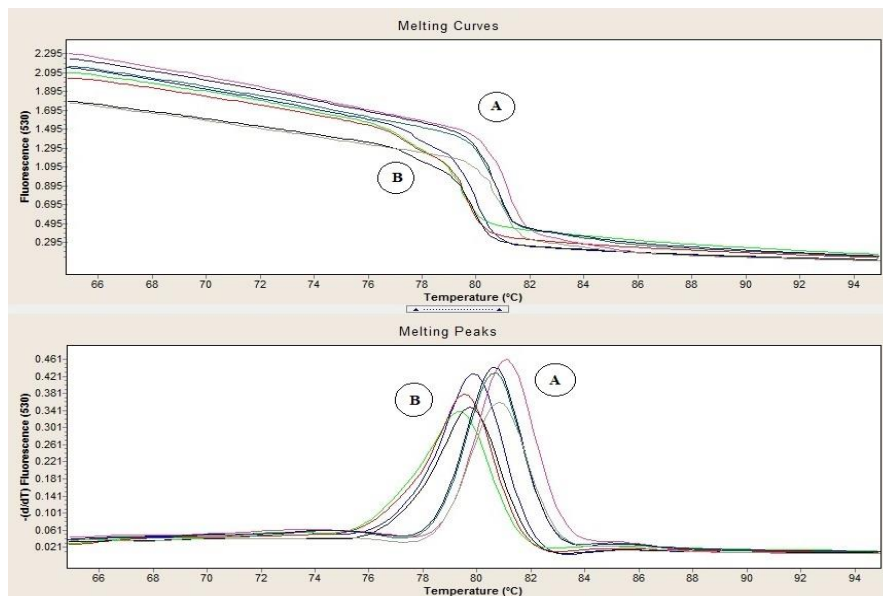


Figure 3-5: Amplification specificity by real-time PCR. Melting curves and melting peaks of GAPDH (A) and ABCC5 (B) target gene in PANC-1

Cell line: PANC-1

	Intraday Variation	Inter-day Variation
Day 1		
	Mean Cp	% CV
GAPDH Si1	9.56	2.92
GAPDH Si2	9.59	3.86
GAPDH Si3	9.49	0.79
GAPDH Control	10.27	0.68
Day 2		
	Mean Cp	% CV
GAPDH Si1	9.94	1.10 ≤ 5%
GAPDH Si2	9.72	1.03
GAPDH Si3	9.66	0.74
GAPDH Control	9.88	0.46
Day 3		
	Mean Cp	% CV
GAPDH Si1	9.56	4.14
GAPDH Si2	9.86	2.71
GAPDH Si3	9.81	0.71
GAPDH Control	9.35	0.80

Table 3-10: Variations of housekeeping gene GAPDH in PANC-1 cells

The individual experiments were carried out in duplicate for each day and were repeated over three different days. The same lot of kit reagents were used every single time, and initial RNA concentration was kept constant for all the experiments. Si1, Si2 and Si3 represent the three different small interference (Si) RNA sequences used for the

transfection on the same cell line, and GAPDH control is the negative control, i.e. scrambled siRNA transfected cells. Variation values $\leq 5\%$ are significant.

Housekeeping gene: RPL13A

MIA PaCa-2

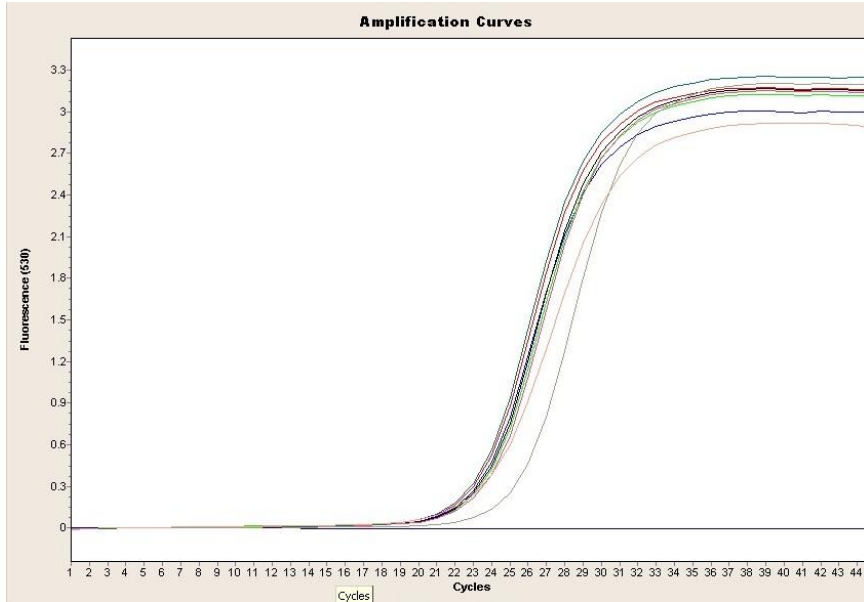


Figure 3-6: Amplification Curves for RPL13A in MIA PaCa-2 cells

Refer to the table: 3-10 for mean Cp values

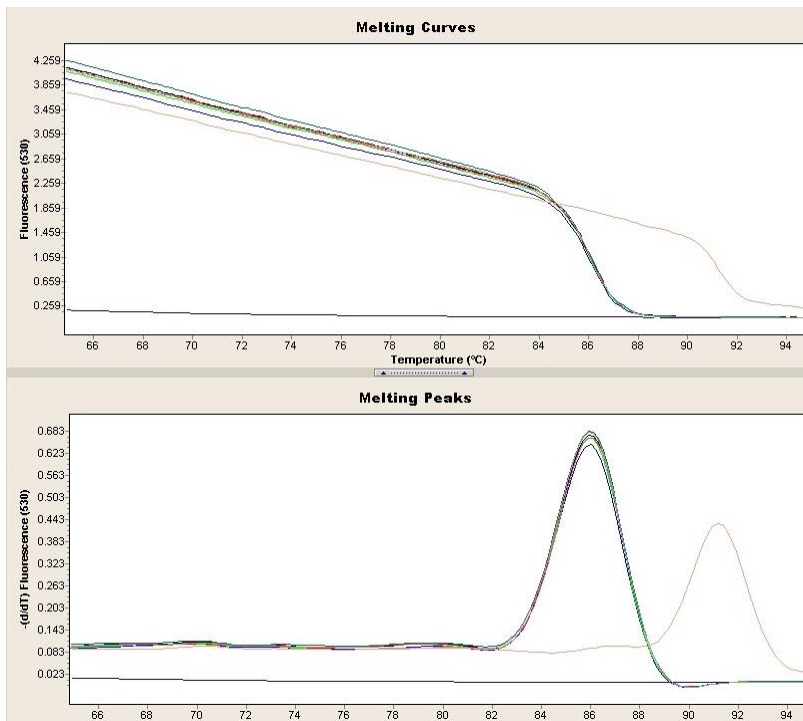


Figure 3-7: Amplification specificity by real-time PCR. Melting Curves and melting peaks of RPL13A in MIA PaCa-2 cells

Inter-day Variation: RPL13A

Day 1	Mean Cp	CV	
RPL13A Si1	19.02	3.89	
RPL13A Si2	20.31	2.36	
RPL13A Si3	20.05	0.55	
RPL13A Neg	19.95	3.35	
Day 2			
	Mean Cp	CV	
RPL13A Si1	20.84	5.78	
RPL13A Si2	19.95	1.63	
RPL13A Si3	19.54	1.74	
RPL13A Neg	19.28	3.60	≤ 5%
Day 3			
	Mean Cp	CV	
RPL13A Si1	19.46	1.80	
RPL13A Si2	19.54	0.47	
RPL13A Si3	18.97	5.80	
RPL13A Neg	18.79	2.71	

Table 3-11: Variations of housekeeping gene RPL13A in MIA PaCa-2 cells treated with ABCC5-siRNA and scramble RNA sequences.

The individual experiments were carried out in duplicate for each day and were repeated over three different days. The same lot of kit reagents were used every single time, and initial RNA concentration was kept constant for all the experiments. Si1, Si2 and Si3 represent the three different small interference (Si) RNA sequences used for the transfection on the same cell line, and GAPDH control is the negative control, i.e. scrambled siRNA transfected cells. Variation values $\leq 5\%$ are significant.

RPL13A: PANC-1

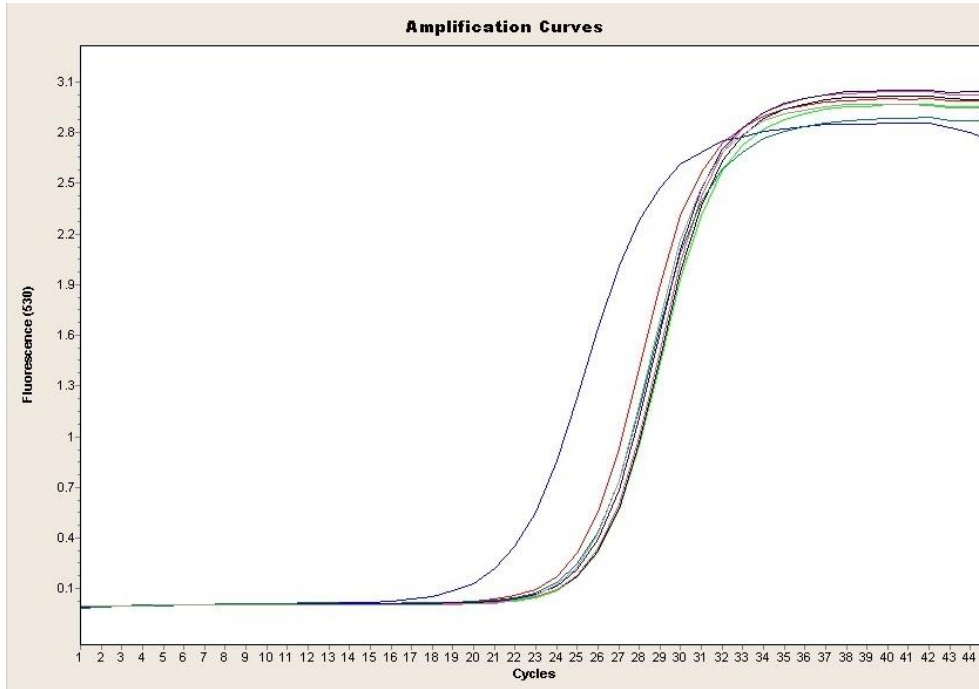


Figure 3-8: Amplification curves for RPL13A in PANC-1 cell line

Refer to the table: 3-11 for mean Cp values

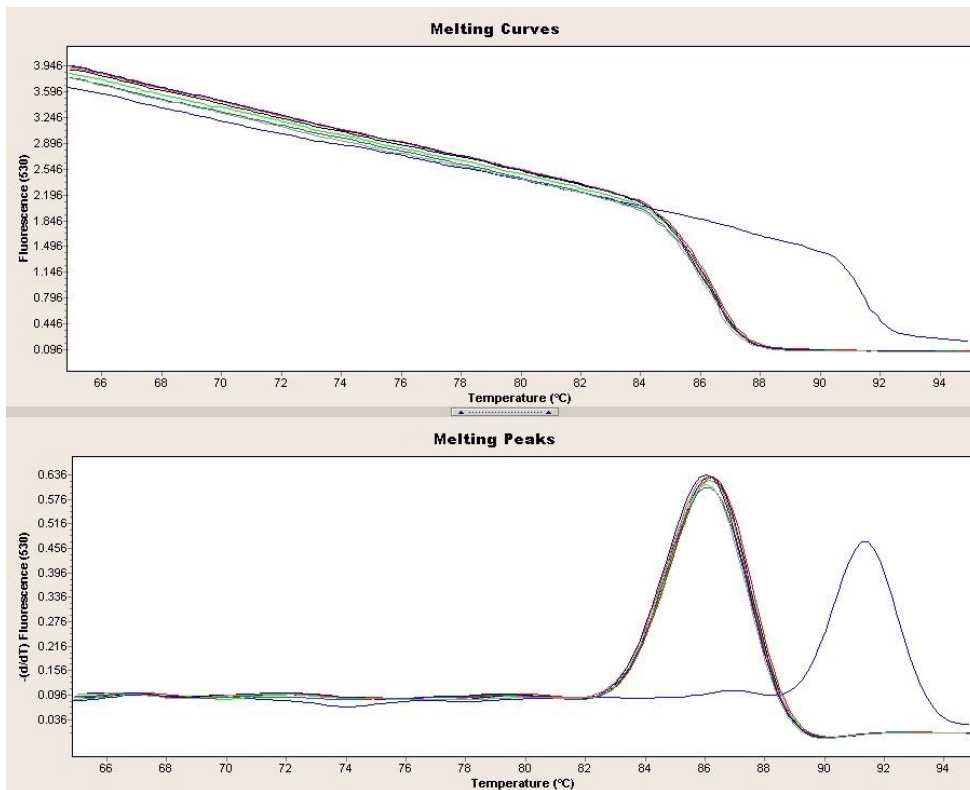


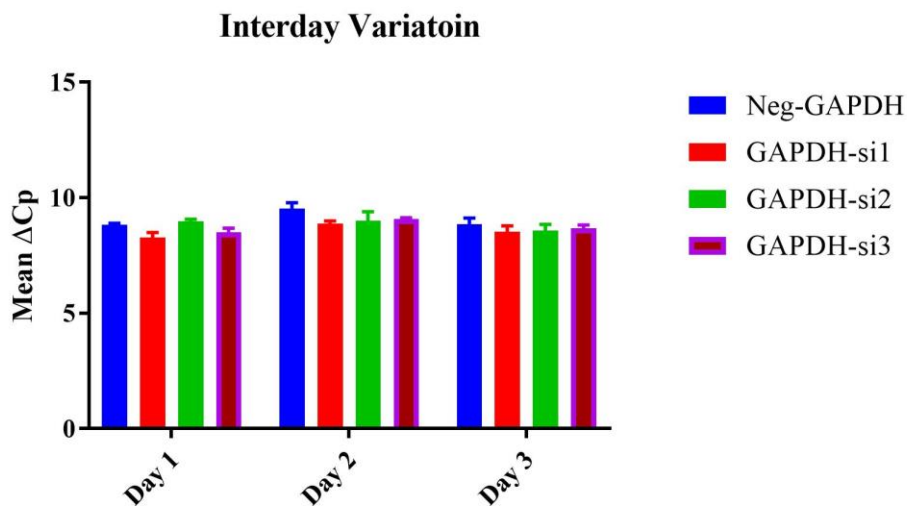
Figure 3-9: Amplification specificity by real-time PCR. Melting Curves and melting peaks of RPL13A in PANC-1 cells

RPL13A Variation: PANC-1

Day 1	Mean	CV	
RPL13A Si1	26.29	1.94	
RPL13A Si2	23.87	0.47	
RPL13A Si3	17.99	1.08	
RPL13A Neg	17.90	3.77	
Day 2	Mean	CV	
RPL13A Si1	27.20	1.41	
RPL13A Si2	21.12	4.83	≤ 5%
RPL13A Si3	18.97	3.25	
RPL13A Neg	19.33	2.47	
Day 3	Mean	CV	
RPL13A Si1	26.98	0.50	
RPL13A Si2	21.95	12.50	
RPL13A Si3	19.70	0.83	
RPL13A Neg	18.20	3.73	

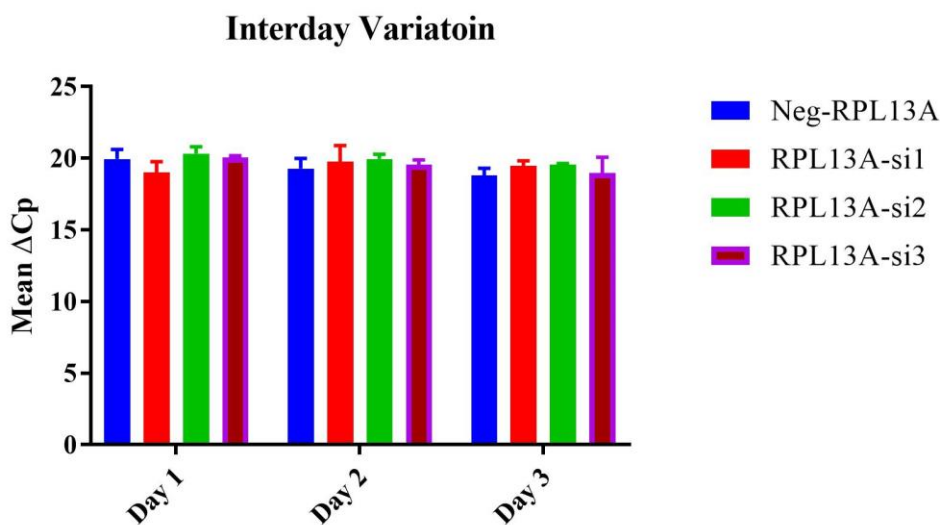
Table 3-12: Variations of housekeeping gene RPL13A in PANC-1 cells treated with ABCC5-siRNA and scramble RNA sequences

The individual experiments were carried out in duplicate for each day and were repeated over three different days. The same lot of kit reagents were used every single time, and initial RNA concentration was kept constant for all the experiments. Si1, Si2 and Si3 represent the three different small interference (Si) RNA sequences used for the transfection on the same cell line, and GAPDH control is the negative control, i.e. scrambled siRNA transfected cells. Variation values $\leq 5\%$ are significant.



Cell line: MIA PaCa-2

Figure 3-10: Inter-day GAPDH variation in MIA PaCa-2 cells treated with ABCC5-siRNA and scramble RNA sequences. Multiple comparisons between control and different treatment groups were analysed using one-way ANOVA with Dunnett's post-hoc.



Cell line: MIA PaCa-2

Figure 3-11: Inter-day variations for RPL13A in MIA PaCa-2 cells treated with ABCC5-siRNA and scramble RNA sequences. Multiple comparisons between control and different treatment groups were analysed using one-way ANOVA with Dunnett's post-hoc.

Figures 3-11 and 3-12 show stable expression of GAPDH and RPL13A over different days with minimum variation in the activity. Low ΔC_p values of GAPDH in MIA PaCa-2 cells indicates higher GAPDH expression as compared to RPL13A.

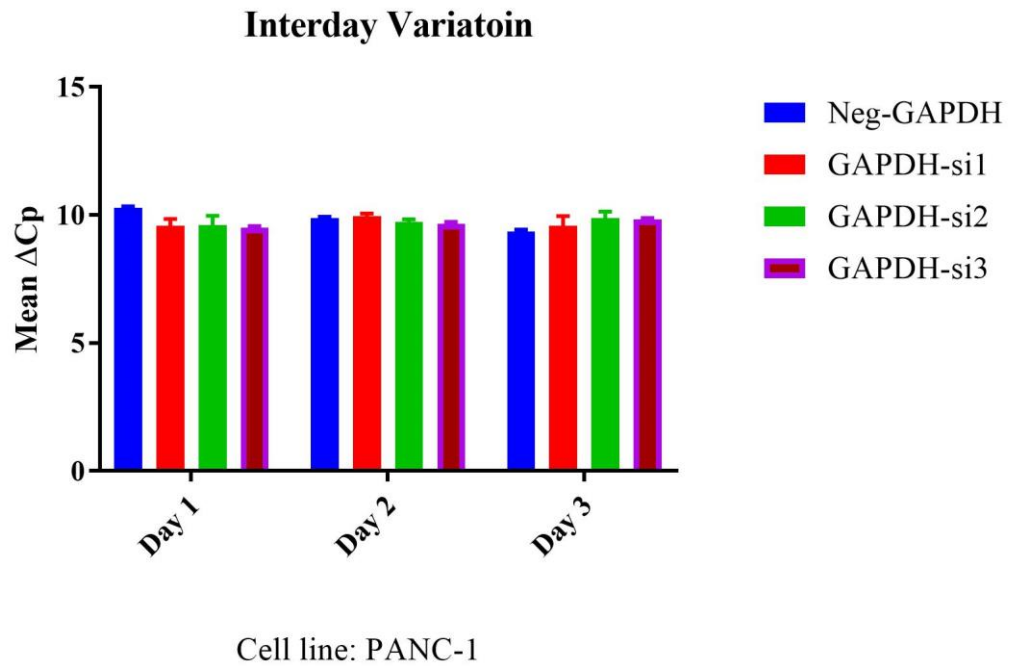


Figure 3-12: Inter-day variation for GAPDH in PANC-1 cells treated with ABCC5-siRNA and scramble RNA. Multiple comparisons between control and different treatment groups were analysed using one-way ANOVA with Dunnett's post-hoc.

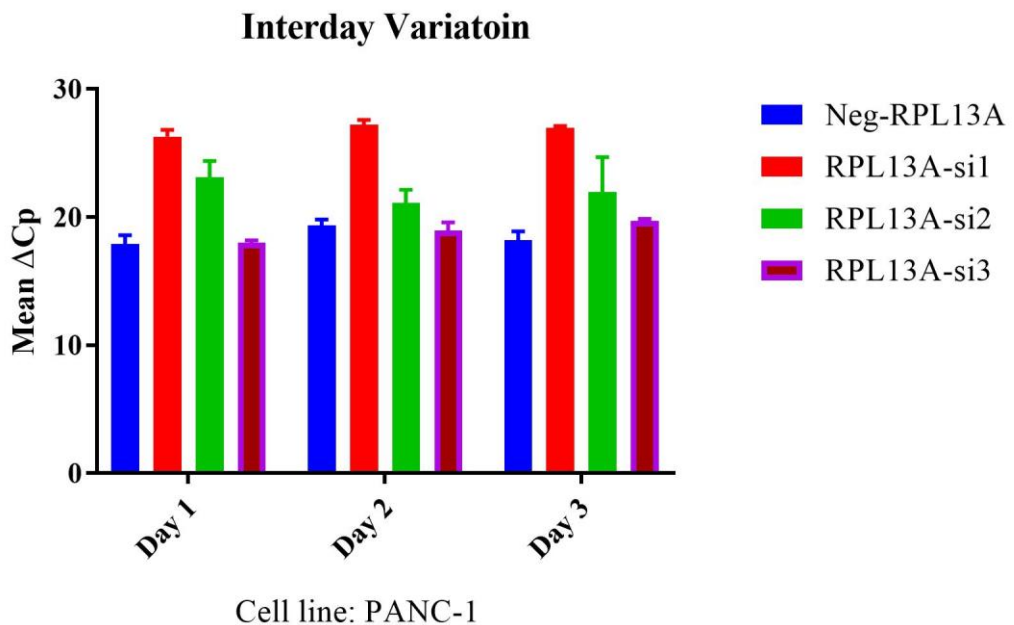


Figure 3-13: Inter-day variation for RPL13A in PANC-1 cells treated with ABCC5-siRNA and scramble RNA sequences. Multiple comparisons between control and different treatment groups were analysed using one-way ANOVA with Dunnett's post-hoc.

Like MIA PaCa-2 cells PANC-1 also showed high GAPDH expression than RPL13A. Thus, for future experiments, only GAPDH was used as a reference gene due to its high and stable expression in both pancreatic cancer cell lines.

3.8 Discussion

In principle, PCR is quite precise and expectable, yet, minor discrepancies in reaction components such as master mix, primer/sample concentration, thermal cycling conditions, and mispriming events in the initial stages of the reaction can prompt huge changes in the total measure of amplified products [279, 297]. Thus, due to the various stages involved; that may cause an experimental error and affect the end results of this high sensitivity RT-PCR reaction it is imperative to evaluate the factors that may cause variation. Such evaluations of variations help in producing more accurate data. Regardless of the method of choice, i.e. one step or two step PCR there are some factors which can cause variation, e.g. cDNA synthesis can significantly affect the overall data quality of the RT-PCR (two-step PCR). Reaction components like dithiothreitol (DTT) and reverse transcriptase enzyme could also have effects on the reaction kinetics, especially in the one-step PCR [298, 299]. Usually to avoid such variation use of DTT is not recommended [300]. The oligonucleotides employed for RT-priming influence overall cDNA levels. Going by the hierarchy of effectiveness gene-specific primers yield the best results followed by oligo(dT) and in the end, random hexamer primers which are least efficient [299].

Concentration and structure of the RNA template and reverse transcriptase enzyme could also play a significant role in the variation during cDNA synthesis. Factors like presence of protein complexes on the target RNA and different abilities of various reverse transcriptase enzyme to read over RNA secondary structure may interfere with the reaction by instigating dissociation, skipping over looped regions and enzyme pausing [298]. This could be solved by raising the reaction temperature over 47°C [301]. As specified in the normalization segment (3.2.8), different cell lines and the samples within the same line (treated/non-treated), could have variation in the housekeeping gene activity. Thus, it is essential to test the compatibility of the housekeeping gene(s) employed in the reaction. We used GAPDH as it showed relatively stable expression in the cell lines used and normalised results were consistent with the protein functional studies (refer chapter 4). Further, GAPDH had low Cp values which indicate higher/abundant gene expression and thus made GAPDH a perfect fit for the housekeeping gene for our experiments. Things like assay design, primer design, primer stability and specificity and the product size are few of the significant factors which may have an impact on the amplification efficacy and could significantly affect overall results. One of the primary reasons for the variation is human

error; a minimum of 1% of relative error is possible even for the most precise pipetting. Running a standard curve for each run could facilitate eliminating/minimizing human errors. The experimental variations could be avoided by using the same batch of reagents like master mixes, buffers, enzymes and pipets [267].

Setting up of RT-PCR involves various stages and reagents which increase the chances of variation. Thus, it is imperative to measure the intraassay and interassay variations to avoid any misinterpretation of the data. Use of C_p values for variation calculation is still under scrutiny as they are logarithmic values and could raise chances of misinterpretation of actual variability. Another suggested approach for variation calculation is using linear values (e.g. copy number) to get the relatively exact measurements of coefficients of variation. To quantify the amount of variation in a single assay when the same template is run multiple times on the same plate with the same reagents; “Intra-sample” variation is calculated. To quantify the amount of variation; all the samples were executed in the triplicate and the variation among samples was calculated using the mean ΔC_p and standard deviation values (as described in the section 3.6.6) [267]. This type of variation could be caused by both primers and templates. It is generally predicted that lower initial template/primer concentration may generate a high variation. Reproducibility of results in PCR is influenced by distribution statistics and stochastic effects (Poisson’s Law; [277]). Inter-assay variation is calculated to see the difference between results of the same sample when running on either identical or different days (i.e. two completely different sets of experiments). This calculation may often be performed using data from either a calibrator or standard sample because these are usually included on all plates. We used both interday and intraday calculation techniques to measure the variation in our results. Comparative C_p ($2^{-\Delta\Delta C_p}$) method was used to calculate the knock-down and off-target effects of siRNA on the ABCC5 gene. The methodology and results of the siRNA transfection in pancreatic cancer cells are discussed in detail in the next chapter (chapter 4) of this thesis.

Chapter 4 Modulation of ABCC5 using siRNA in MIA Paca-2 and PANC-1 cell lines

Modulation of gene activity is one of the most popular methods to increase drug efficacy *in vitro*. Many techniques are available currently for modulation of gene activity, RNAi in cultured mammalian cells is turning into a standard research technique to study qualities of individual genes. RNAi proficiency can be impacted by numerous calculates in the mammalian cells, e.g. selection of the target site. The best target site should be at 100 nt downstream of the translation begin site. Furthermore, the auxiliary structures & mRNA- binding proteins likewise impact the accessibility to siRNA. Choice of transfection strategy and transfection conditions, for example, cell density, transfection reagents and the transfection time also have a significant impact on efficiency. For our experiments, the initial cell number was optimised considering the cell doubling number and the amount of siRNA. Time of transfection varies for the different cell types and for the targeted genes. Despite the potent knockdown abilities of siRNA, transfection system has its frail points, e.g. transient silencing effects and difficulties in transfection depending on cell types. Efficacy of RNAi is restricted by the amount of the oligomer that successfully enters the tumour cells. Thus, competent delivery of siRNA is very necessary for the efficient knockdown of the target gene. Non-viral polymeric delivery systems, specifically those with biodegradable parts, have vastly improved safety profiles than their viral counterparts. There are three noteworthy classes of non-viral delivery vehicle systems; engineered polymers, regular/biodegradable polymers and lipids. It was found that transfection of siRNA using lipophilic agents such as liposomes, OligofectamineTM & TransIt-TKOTM increase the transfection efficiency. Considering the above points, we designed our experiments using three different siRNA sequences initially, and lipofectamineTM was used for the delivery of siRNA into the pancreatic cancer cell lines *in vitro*. After optimising the transfection conditions and achieving a good knock-down percentage of the target gene (ABCC5), further experiments were carried out for drug cytotoxicity, functional study of the protein and off-target effects of the siRNA. As siRNA only targets the mRNA and not the proteins, protein turnover rate should also be accounted in the effectiveness of transfection.

4.1 MRP5 Functional studies

Flow cytometry screening is a fast, straightforward and cost-effective tool that can be used for various assays. Substrate accumulation and efflux, apoptosis, cell cycle analysis and cell sorting are few of the examples of multiple assays. Flow cytometers stream cells from a suspension, one at a time simultaneously through a laser and an electronic identifier (refer chapter 4 for a more detailed mechanism) [302, 303]. Flow cytometers can be furnished with different lasers and fluorescence channels to evaluate cell size, intracellular complexity and fluorescence at multiple emission wavelengths at a rate of hundreds to thousands of cells/second [303]. The capability to quantify fluorescence in single cells is utilised to track the intracellular accumulation of ABC transporter test substrates. The principle behind the assay is if the cells are fed with a compound which is a specific substrate of the ABC transporter of choice than its accumulation in the cells is inversely proportional to the activity of that ABC transporter, i.e. higher the activity of the transporter lower is the substrate accumulation in the cells. This low accumulation can be recorded via the fluorescence level of the cell. The utilisation of a test substrate to characterise the inhibition of the ABC transporters alludes as an 'indirect setup' [304-306].

In accumulation assay substrate is allowed to accumulate in the cells of interest and the reaction is stopped once the steady state is achieved (for substrate accumulation). Followed by multiple washing of the cells to get rid of the extracellular substrate before the flow cytometer analysis. Thus, in theory, if there is successful inhibition of ABC transporter in the cells than the influx/efflux equilibrium will get shifted, and a higher steady-state concentration is achieved. In our experiments, we used this principal to check the transient knockdown of the ABCC5 gene activity and thus the functional activity of the MRP5 protein. The logic was ABCC5 siRNA transfected cells should have a low MRP5 protein and thus higher accumulation of BCECF (2',7'-Bis(2-carboxyethyl)-5(6)-carboxyfluorescein) in the cells as compared to the control.

4.2 Drug cytotoxicity assay: MTT

MTT (3-[4,5-dimethylthiazol-2-yl]-2,5 diphenyl tetrazolium bromide) assay was first described 30 years ago by Mosmann [307], is used for the measurement of cell viability and thus one of the most popular applications of this assay is the determination of drug cytotoxicity [308, 309]. MTT assay is based on the principle that most of the live cells have constant mitochondrial activity and thus increase or decrease in the number of

viable cells is linearly related to mitochondrial activity [308]. All viable cells metabolise tetrazolium salt (MTT) into purple formazon crystals by mitochondrial succinic dehydrogenases reflecting the mitochondrial activity. Succinate dehydrogenase enzyme is part of complex II at the inner mitochondrial membrane and of Krebs cycle [308, 309]. The assay is considered to reflect both the number of cells and the activity status of the mitochondria. These formazon crystals are water-insoluble and can be further solubilised into DMSO for homogenous measurement using an optical plate reader. Thus, decrease or increase in the viable cell numbers can be measured by measuring the optical density reflecting the formazon concentration in the solution. Primary cell lines and established cell lines are both suitable for the MTT assay [309]. For the dividing cell lines (or cell lines) drug cytotoxicity is measured by a decrease in the number of drug-treated cells as compared to the control (non-drug treated), reflecting the growth inhibition. The drug sensitivity is usually represented as the concentration of the drug required to achieve the 50% of cell growth inhibition as compared to the control [308, 310]. This concentration of the drug is known as a 50% inhibitory concentration or the IC_{50} value of the drug. For the primary or non-dividing cells, the drug sensitivity is measured as an enhanced cell kill of treated cells as compared with the control or non-treated cells [308]. This concentration of the drug in the primary cells is known as “50% lethal concentration” or IC_{50} values of the drug [308, 310]. We used IC_{50} value for representing the drug sensitivity in our experiments for the cell lines – MIA PaCa-2 and PANC-1. Previous literature has a reported gemcitabine’s IC_{50} value in the range of 20nM - 5 μ M and, 800nM – 50 μ M for MIA PaCa-2 and PANC-1 respectively. We carried out our experiments in the same concentration range initially to find out the IC_{50} value.

4.3 Materials and Methods:

4.3.1 Materials

The details of all the consumables required are mentioned in detail in chapter 2 of this thesis; Refer to the section 2.2.2 of chapter 2.

4.3.2 siRNA Transfection

Forward transfection was the method of choice to transfect Stealth™ RNAi into mammalian cells in a 12 -well format. For forward transfections, cells were plated in CRM one day before the transfection and on the next day transfection mix was added to the cells. The transfection was carried out in the following manner-

- The plating cell number was optimised in a way that 50-60 % confluency was achieved after 24 hours.
- To each well RNAi duplex - Lipofectamine™ RNAi MAX complex was added and mixed gently by rocking the plate back and forth.
- The cells were then incubated for 48 hours and later extracted to check the knockdown efficiency and off-target effects.

For more details on the optimisation of transfection procedure, Refer to section 2.2.2 of chapter 2

4.3.3 Primers, Rt-PCR and Relative gene expression calculations

Refer to chapter 3 for the detailed discussion of this section

4.3.4 Cell surface staining

Intracellular cell surface staining was carried out to determine the MRP5 surface expression. Indirect detection using the fluorescent secondary antibody was the method of choice. The technique is called indirect detection due to the involvement of secondary antibody. When using the secondary antibody, there are chances of generating background signals due to the non-specific binding of the secondary antibody with endogenous immunoglobulins on the cells or with immunoglobulins in the antibody diluent. The non-specificity of MRP5 staining was also calculated and normalised with host-species matched IgG2a isotype control. Secondary antibodies were conjugated with Alexa Fluor 488. Refer to chapter 2 section 2.6.3 for more detailed methodology. The data were mean fluorescence intensity (MFI) as a % of control siRNA-treated and were calculated using the equation below:

$$\left[\frac{\text{MFI (ABCC5 siRNA)} - \text{MFI (Isotype control)}}{\text{MFI (control siRNA)} - \text{MFI (Isotype control)}} \right] \times 100 = \text{MFI as \% of control}$$

Flow cytometry histograms were analysed using the Kaluza software and represent the fluorescence distribution of 10,000 cell events.

4.3.5 MRP5 Functional assay

Cell-permeable 2',7'-Bis(2-carboxyethyl)-5(6)-carboxy fluorescein- acetoxymethyl ester (BCECF-AM) is an uncharged, non-fluorescent molecule. Cellular non-specific esterases cleave the lipophilic blocking groups of BCECF-AM resulting in a charged

fluorescent form of the molecule. In comparison to the parent BCECF-AM ester, this charged molecule (BCECF) has a very low rate of membrane permeability. This is utilised for the studies including pH measurement in various cell types and various cellular assays such as multidrug resistance, indirect measurement of membrane protein expression, adhesion, viability and cytotoxicity.

BCECF is a specific MRP5 substrate and can be used to determine the MRP5 activity. MRP inhibitors such as curcumin (Cuc) or MK571 can be used to inhibit the efflux (positive control). Knockdown and control cells were trypsinised and then washed with fetal bovine serum-free and phenol red-free DMEM and resuspended in this medium with a cell density of about $0.5-1 \times 10^6$ cells/ml [311]. The accumulation assay was performed by incubating the 1 ml of cells with 0.1% DMSO or a well-defined MRP5 inhibitor curcumin (10 μ M, 0.1% DMSO) at 37°C for 15 min, followed by addition of BCECF (Final concentration of 0.25 μ M, 0.1% DMSO). After incubation for another 5 min, the efflux of BCECF was stopped by adding 3 ml of ice-cold PBS [311]. The cells were washed with ice-cold PBS once and then reconstituted in 0.5 mL of ice-cold PBS containing 1% paraformaldehyde and then placed into ice immediately. The intracellular level of BCECF can be analysed using the MoFlow™ XDP flow cytometer equipped with a standard laser for excitation at 488 nm and a bandpass filter at 525 nm to detect fluorescence [311]. Refer to section 2.4.2 of chapter 2

4.3.6 Cell Viability Assay

Cell viability was performed by treating the control and knockdown cells for 72 hours with gemcitabine followed by the addition of MTT. The formazon crystals were later dissolved in DMSO, and the optical density was recorded using the Thermo Scientific™ Multiskan™ FC Microplate Photometer. Refer to section 2.3.3 of chapter 2 for more details on the procedure.

4.3.7 Apoptosis assay

Annexin V is unable to bind to the viable cells as it is impermeable to the phospholipid bilayer and cannot bind to the PS which is still on the inner leaflet of the plasma membrane. However, as we now know that when cells undergo apoptosis, PS is translocated from internal to the external leaflet of the plasma membrane and thus, it is available for binding to annexin V [228]. But for the dead cells also the PS is available for binding due to loss plasma membrane integrity and therefore to distinguish between the apoptotic and dead cells a membrane impermeable DNA stain, e.g. propidium iodide

(PI) could be used simultaneously while staining. Use of fluorescent annexin V and PI facilitates investigations of the cell apoptosis population while using flow cytometry [240]. Refer to chapter 2 section 2.5.2 for the detailed methodology of apoptosis assay.

4.4 Results:

4.4.1 Optimisation of siRNA concentration for knockdown

MIA Paca-2

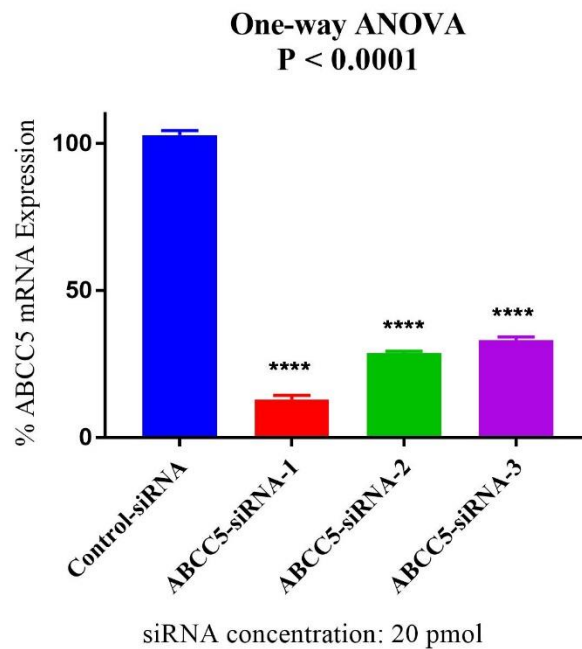


Figure 4-1: Percentage of ABCC5 knockdown in MIA PaCa-2 cells by 3 different siRNAs sequences (20 pmol each). Data are presented as the mean and SEM from three independent experiments; n=3. Multiple comparisons between control and different treatment groups were analysed using one-way ANOVA with Dunnett's post-hoc. *** $P < 0.0001$

Figure 4-1 Shows mean percentage knockdown for 3 different sequences of siRNA at 20 pmols for 48 hours. Significant reduction in the ABCC5 activity was seen for all ABCC5-siRNAs as compared to the control ($p < 0.0001$). Compared with control, the ABCC5 mRNA level was decreased by $87.03 \pm 1.37 \%$, $71.35 \pm 0.75 \%$ and $66.95 \pm 1.14 \%$ in ABCC5-siRNA1, 2 and 3 transfected MIA PaCa-2 cells, respectively.

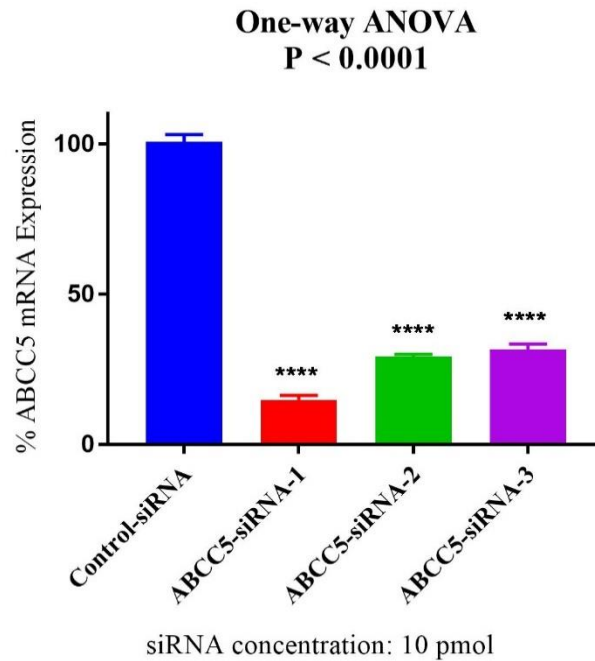


Figure 4-2: Percentage ABCC5 knockdown in MIA PaCa-2 by 3 different sequences (10 pmol each). Data are presented as the mean and SEM from three independent experiments, n=3 (number of repeats). Multiple comparisons between control and different treatment groups were analysed using one-way ANOVA with Dunnett's post-hoc. **** $P < 0.0001$

siRNA transfection was carried out for two different doses of 20 and 10 pmols to find out the low effective dose. Both concentrations resulted in the significant ($p < 0.0001$) decrease in the ABCC5 mRNA expression 48 hours after transfection. We decided to continue with a dose of 10 pmol. ABCC5-siRNA-1 was the most efficient as compared to the other two sequences as it yielded the highest knockdown percentage of 85.18 ± 1.50 %. ABCC5-siRNA-2 and 3 gave mean knockdown percentages of 70.73 ± 0.75 % and 68.31 ± 1.74 % respectively.

Off-target effects in MIA PaCa-2

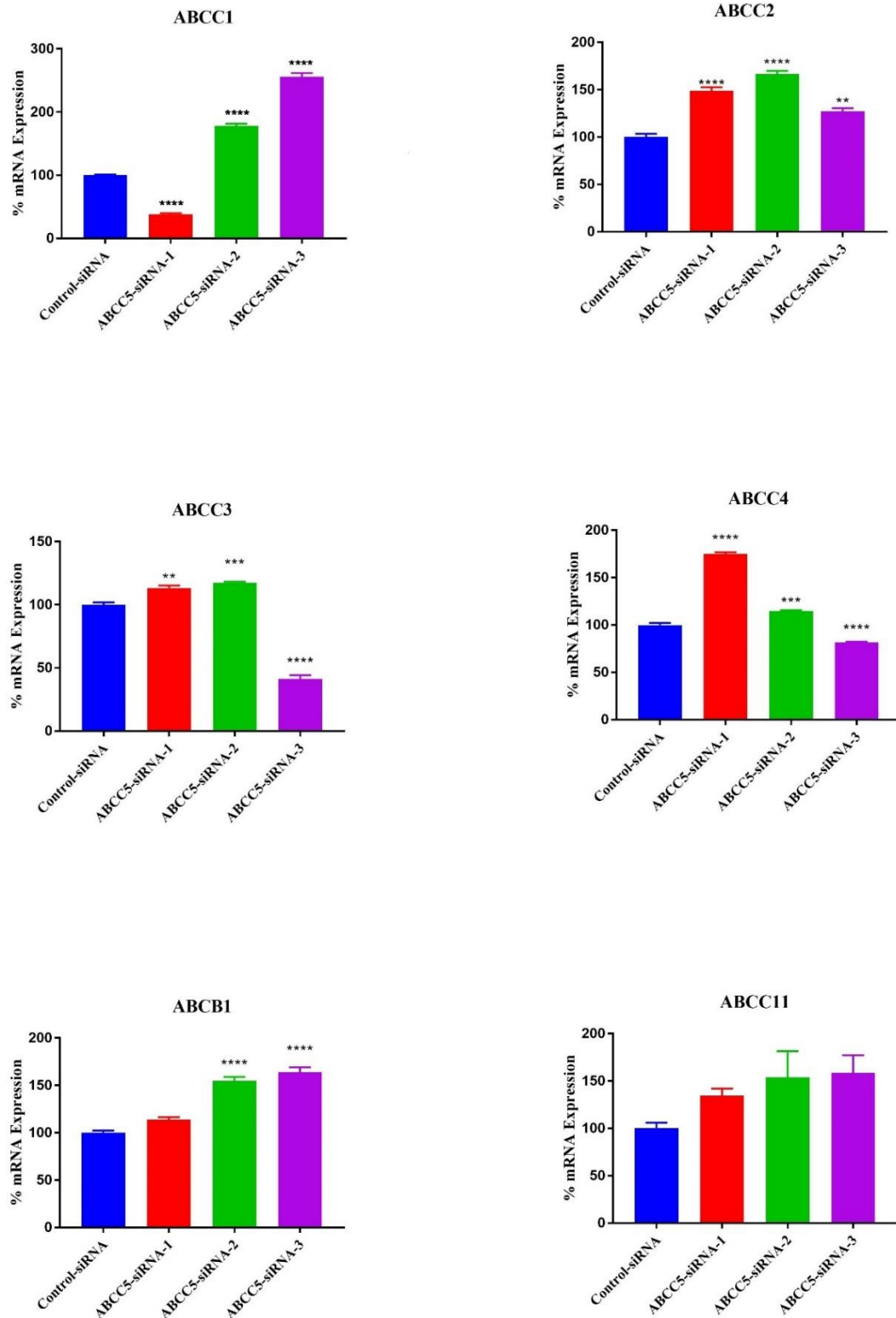


Figure 4-3: Off-target effects of ABCC5 siRNA transfection (10 pmol each) in MIA PaCa-2 cells. Data are presented as the mean and SEM from three independent experiments; $n=3$. Multiple comparisons between control and different treatment groups were analysed using one-way ANOVA with Dunnett's post-hoc. *** $P < 0.0001$, ** $P < 0.01$, *** $P < 0.001$, **** $P < 0.0001$.

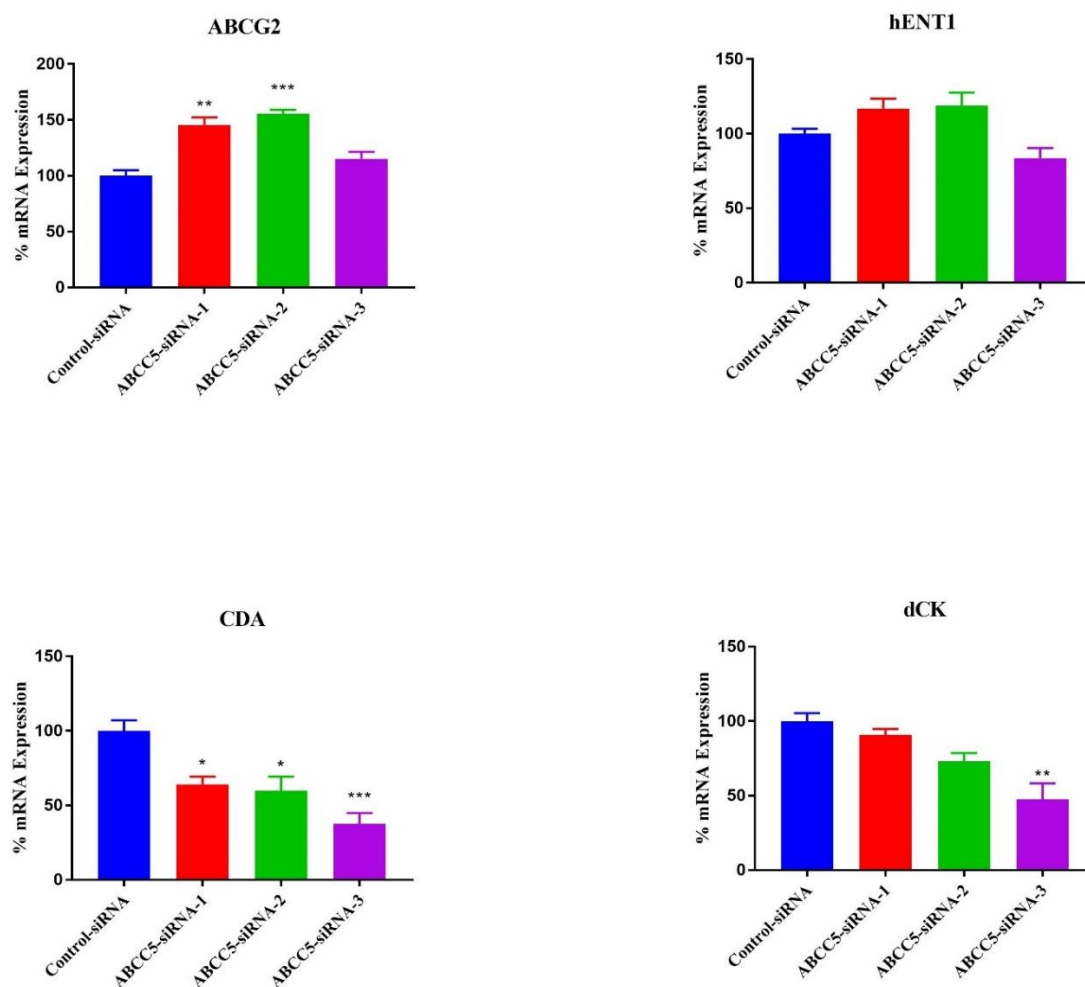


Figure 4-4: Comparison of Off-target effects in ABCC5-siRNA transfected MIA PaCa-2 cells. Data are presented as the mean and SEM from three independent experiments; n=3. Multiple comparisons between control and different treatment groups were analysed using one-way ANOVA with Dunnett's post-hoc. *** $P < 0.0001$, * $P < 0.05$, ** $P < 0.01$, *** $P < 0.001$, **** $P < 0.0001$

We tested off-target effects of ABCC5-siRNA transfection on other transporters and the enzymes (dCK and CDA) involved in gemcitabine metabolism (refer chapter 1 section 1.4 for a detailed discussion of the drug metabolism). Though siRNA sequences were efficient in knocking down the target gene (transient) they do have some off-target effects. As we can see from the above results, most of the ABC transporters genes were upregulated after the transfection. Off-target effects were highest for the siRNA-3 as compared with the other two sequences, even after reducing the siRNA concentration to the lowest effective dose. Thus, we decided to continue with, only sequence 1 and 2 for further experiments. For all siRNA sequences, a parallel knockdown effect was observed for the enzymes dCK and CDA after transfection. A slight upregulation of the hENT1 gene (responsible for gemcitabine uptake) was seen after the transfection, but its percentage of upregulation was quite low to take into the account. Thus, we can say

from the results that MIA PaCa-2 cells could be transfected using liposome delivery vehicle efficiently, but the off-target effects are significant post-transfection.

PANC-1

Optimisation of siRNA concentrations for knockdown

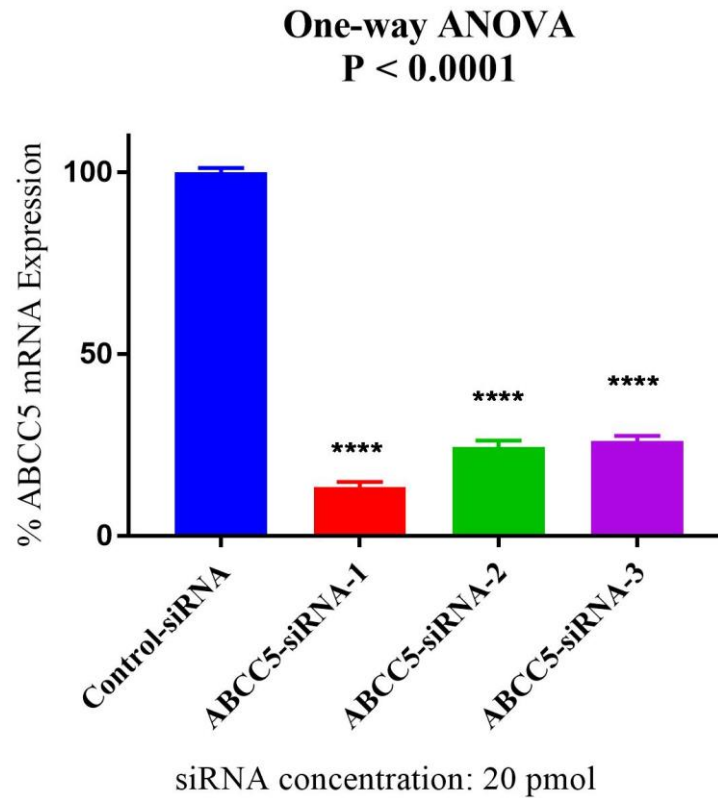


Figure 4-5: Percentage of ABCC5 knockdown in PANC-1 cells by 3 different siRNAs sequences (20 pmol each). Data are presented as the mean and SEM from three independent experiments. Multiple comparisons between control and different treatment groups were analysed using one-way ANOVA with Dunnett's post-hoc. **** $P < 0.0001$

Significant (**** $p < 0.0001$) reduction in the ABCC5 activity was seen for all ABCC5-siRNAs as compared to the control when transfection was carried out for 48 hours. Mean ABCC5 knockdown for siRNA-1, 2 and 3 were 86.58 ± 1.50 %, 75.53 ± 1.79 % and 73.81 ± 1.35 % respectively. Multiple comparisons between control and different treatment groups were analysed using one-way ANOVA with Dunnett's post-hoc.

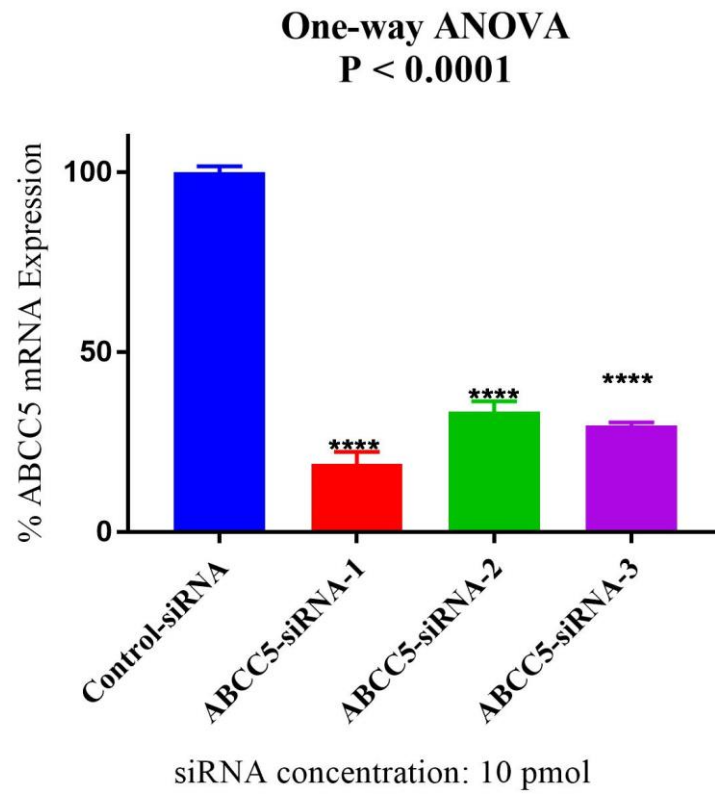


Figure 4-6: Percentage ABCC5 knockdown in PANC-1 cells by 3 different siRNA sequences (10 pmol each), Multiple comparisons between control and different treatment groups were analysed using one-way ANOVA with Dunnett's post-hoc. **** $P < 0.0001$

Mean ABCC5 knockdown in PANC-1 cells treated with siRNA-1, 2 and 3 at 10 pmols each were 80.94 ± 3.26 %, 66.47 ± 2.83 % and 70.46 ± 0.94 % respectively.

Off-target effects in PANC – 1

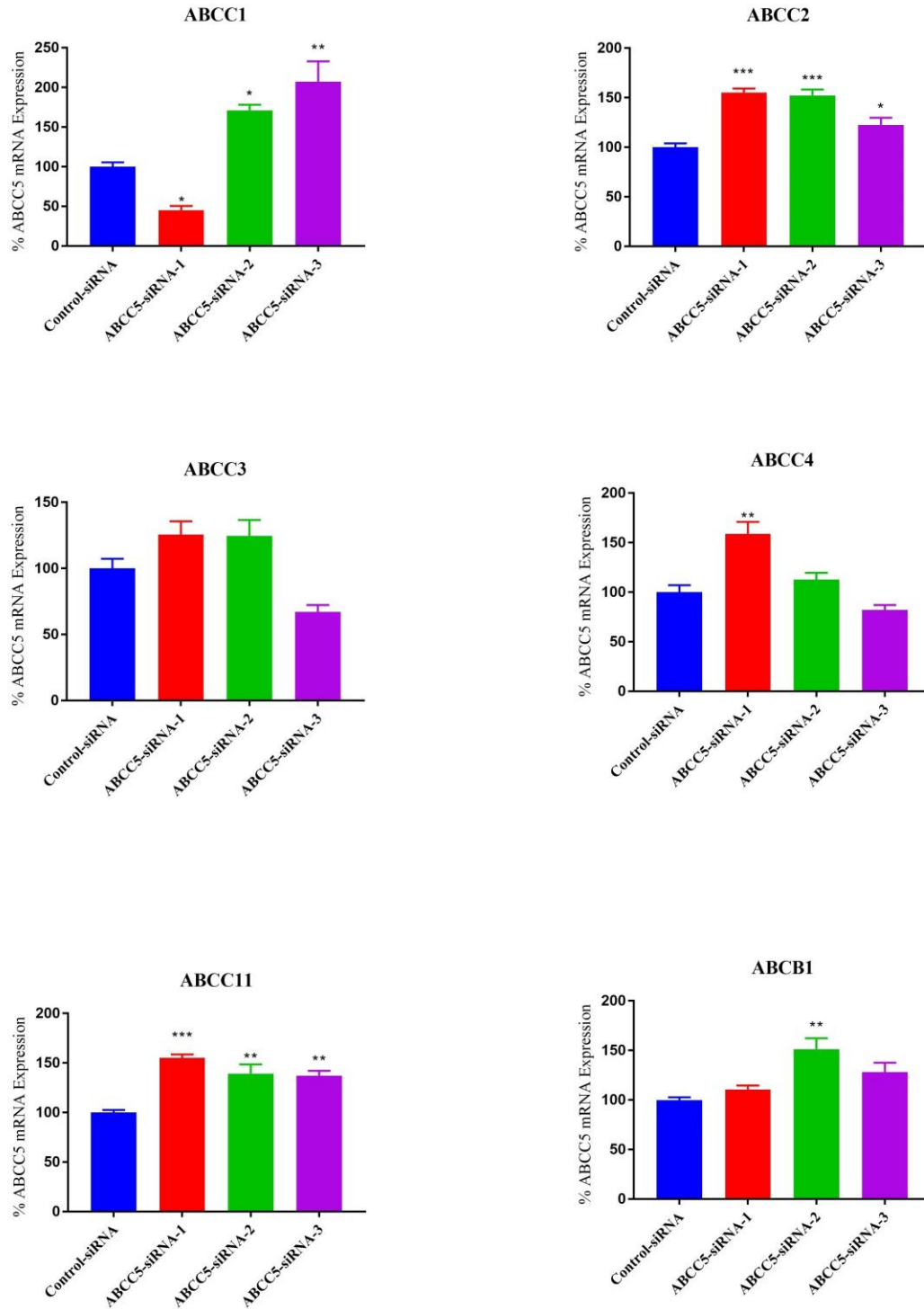


Figure 4-7: Comparison of Off-target effects in control and ABCC5-siRNA transfected PANC-1 cells. Data are presented as the mean and SEM from three independent experiments; n=3. Multiple comparisons between control and different treatment groups were analysed using one-way ANOVA with Dunnett's post-hoc, * $P=0.0158$, ** $P=0.0067$, *** $P<0.001$, **** $P<0.0001$

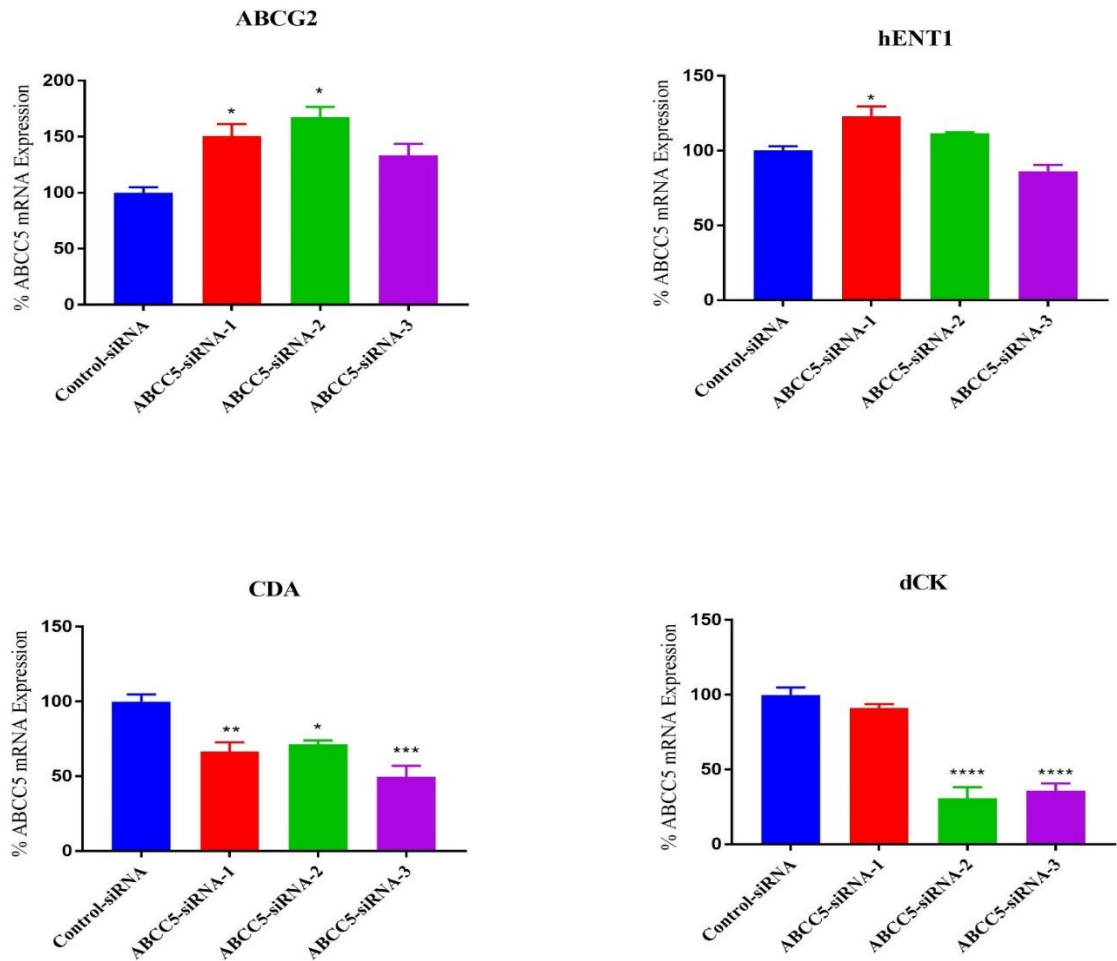


Figure 4-8: Off-target effects of ABCC5 siRNA transfection on other ABC transporters and gemcitabine metabolism-related enzymes in PANC-1 cells. Data are presented as the mean and SEM from three independent experiments; $n=3$. Multiple comparisons between control and different treatment groups were analysed using one-way ANOVA with Dunnett's post-hoc * $P= 0.0158$, ** $P= 0.0067$, *** $P<0.001$, **** $P<0.0001$

Similar to the MIA PaCa-2 cells off-target effects can be seen in the PANC-1 cells too. A general trend in the up-regulation of other transporter genes was observed while the knockdown effect was recognised for the dCK and CDA enzymes. In PANC-1 cells knockdown effect on dCK enzymes were quite significant for siRNA sequence 2 and 3. Such difference in the off-target effects could be explained by the use of different cell types. Off-target effects for hENT1 (up-regulation) transporter followed the general trend except for the siRNA sequence three, where a slight knockdown in the gene activity can be seen. Three biological replicates were used to assess silencing of the intended targets by real-time PCR, and the primers were obtained from IDT (Refer to chapter 3 section 3.6.4 for primer details). Real-time PCR was performed in a total volume of 20 μ l, using the Evo script® I PCR Master Mix from Roche as described in the manufacturer's protocol (Refer to section 3.6.5 for details). Roche's Light

Cycler®480 was used for the qRT-PCR related experiments. Relative mRNA levels were calculated as $2^{\Delta\Delta Ct}$ values (Refer to Chapter 3 section 3.6.6 for more details). Multiple comparisons between control and different treatment groups were analysed using one-way ANOVA with Dunnett's post-hoc.

4.4.2 Surface staining of ABCC5 knockdown cells

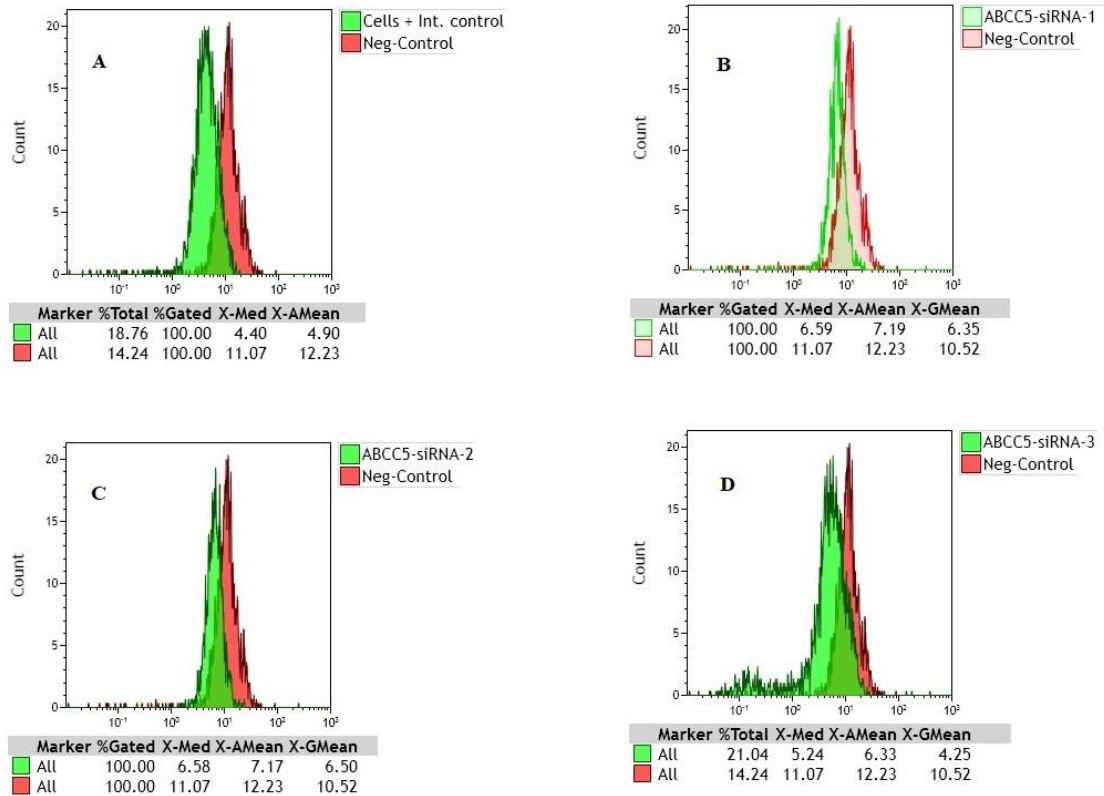


Figure 4-9: Overlay data for MRP5 surface staining in PANC-1 cells. (A) The cell surface expression of MRP5 was assessed by staining the PANC-1 cells with anti-MRP5 primary (Red) and control isotype IgG2a antibody (Green). Plots (B), (C) and (D) show MRP5 surface immunostaining in PANC-1 cells treated with ABCC5-siRNA 1, 2 and 3 (All green) and control siRNA (Red), respectively.

The ABCC5 gene silencing was further confirmed at the protein level in PANC-1 cells treated with 3 different siRNA sequences in Figure 4-11 which show the fluorescence readings recorded by using the flow cytometer. The geometric means of the fluorescence values were collected and the graph (Figure: 4-12) was plotted after normalisation with the internal control.

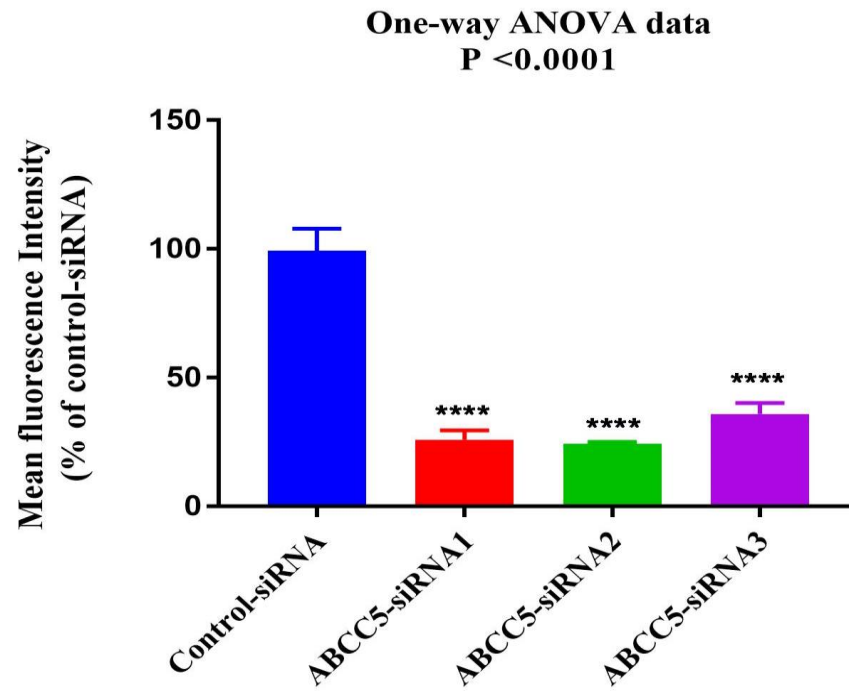


Figure 4-10: Mean MRP5 cell surface staining in ABCC5 and control siRNA transfected PANC-1 cells. Data are presented as the mean and SEM from three independent experiments; n=3. Multiple comparisons between control and different treatment groups were analysed using one-way ANOVA with Dunnett's post-hoc. **** $P < 0.0001$

The surface staining of MRP5 is a direct confirmation of the successful knockdown of ABCC5 at the protein level. Figure 4-12 shows a significant decrease in the surface expression of MRP5 protein in the ABCC5 knockdown cells as compared to the control. The mean MRP5 fluorescence intensity in PANC-1 cells treated with ABCC5-siRNA1, 2 and 3 was only $24.74 \pm 1.88 \%$, $25.20 \pm 3.19 \%$ and $30.01 \pm 3.02 \%$ of the control value, respectively.

4.4.3 MRP5 Functional assay

Preliminary BCECF results

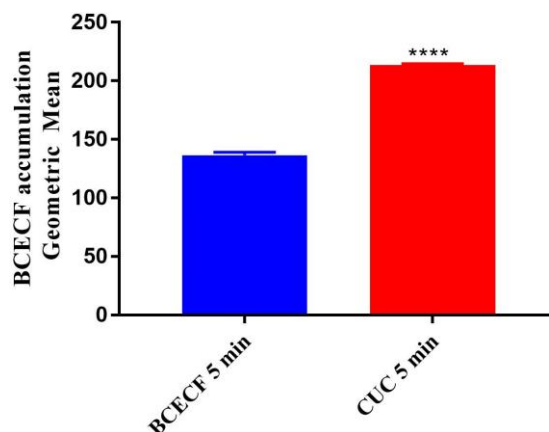


Figure 4-11: BCECF accumulation in MIA PaCa-2 cells 5 min after incubation with BCECF-AM in the presence and absence of curcumin (CUC, 10 μ M). Data are presented as the mean and SEM from three independent experiments; n=3. Student's t-test was used for comparison between control and CUC treated cells. **** $P < 0.0001$

CUC (curcumin) has been demonstrated to inhibit MRP5 activity [265] thus it was used as the positive control.

Preliminary BCECF results for PANC -1

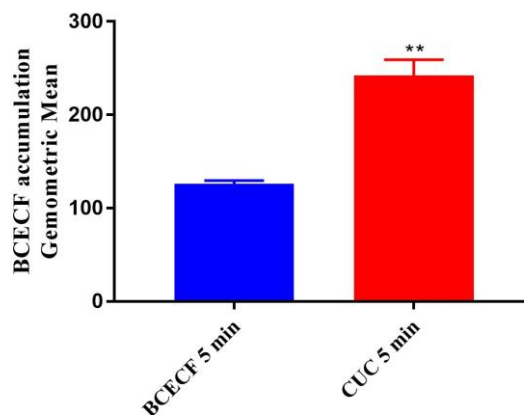


Figure 4-12: BCECF accumulation in PANC-1 cells 5 min after incubation with BCECF in the presence and absence of CUC (10 μ M), ** $P < 0.05$. Data are presented as the mean and SEM from three independent experiments; n=3. Student's t-test was used for comparison between control and different treatment.

Our preliminary data show that a steady state was reached after five minutes of time. curcumin analogue was used as the positive control as it has been shown to inhibit MRP5 [265] in Mia PaCa-2 and PANC-1 cells. The mean cellular fluorescence intensity (BCECF accumulation) in MIA PaCa-2 cells was 136.56 ± 2.39 and 213.65 ± 1.02 , respectively, in the absence and presence of CUC. While the mean fluorescence intensity was increased by two-fold (126.113 ± 3.47 vs 242.22 ± 16.84) by CUC in

PANC-1 cells. Taken together, this suggests functional expression of MRP5 in Mia PaCa-2 and PANC-1 cells

siRNA knockdown results for MIA PaCa-2

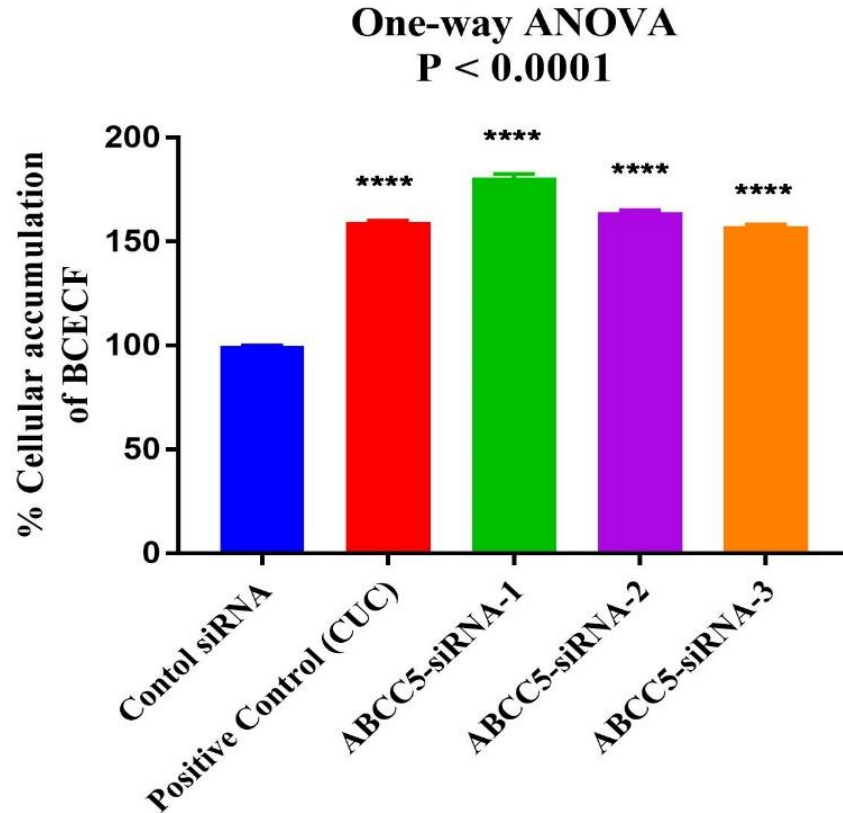


Figure 4-13: BCECF accumulation in ABCC5 and control siRNA transfected MIA PaCa-2 cells. All data are normalized as a percentage of the mean intensity value determined in control-siRNA transfected cells. Data are presented as the mean and SEM from three independent experiments; n=3. Multiple comparisons between control and different treatment groups were analysed using one-way ANOVA with Dunnett's post-hoc. **** $P < 0.0001$

Figure 4-15 shows that BCECF cellular accumulation was significantly higher in MIA PaCa-2 cells pre-treated with CUC, ABCC5-siRNA1, 2 and 3, with the normalized values of 159.39 % \pm 0.60%, 180.75 % \pm 1.97 %, 164.12 % \pm 1.01 % and 157.46 % \pm 0.80 %, respectively, compared with control.

siRNA knockdown results for PANC – 1

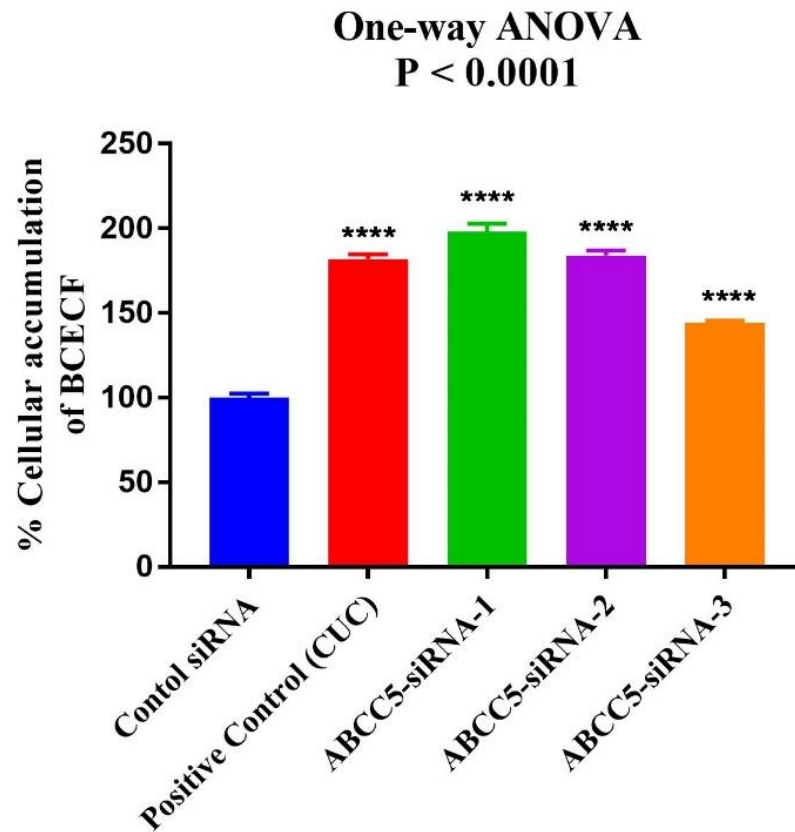


Figure 4-14: BCECF accumulation in ABCC5 siRNA transfected PANC-1 cells. All data are normalized as a percentage of the mean intensity value determined in control-siRNA transfected cells. Data are presented as the mean and SEM of fluorescence percentage from three independent experiments, n=3. Multiple comparisons between control and different treatment groups were analysed using one-way ANOVA with Dunnett's post-hoc. **** $P < 0.0001$

After ABCC5 knockdown the percentage accumulation of BCECF for three siRNA sequences was significantly higher than the control (Figure 4-16) which indicates low MRP5 levels and confirmation of successful gene knockdown on the protein level. Silencing MRP5 led to an increase of cellular accumulation of BCECF by $44 \pm 2.0 \%$ to $97.93 \pm 7.0 \%$ ($P < 0.001$).

4.4.4 Cell Viability assay: MTT

MIA PaCa-2

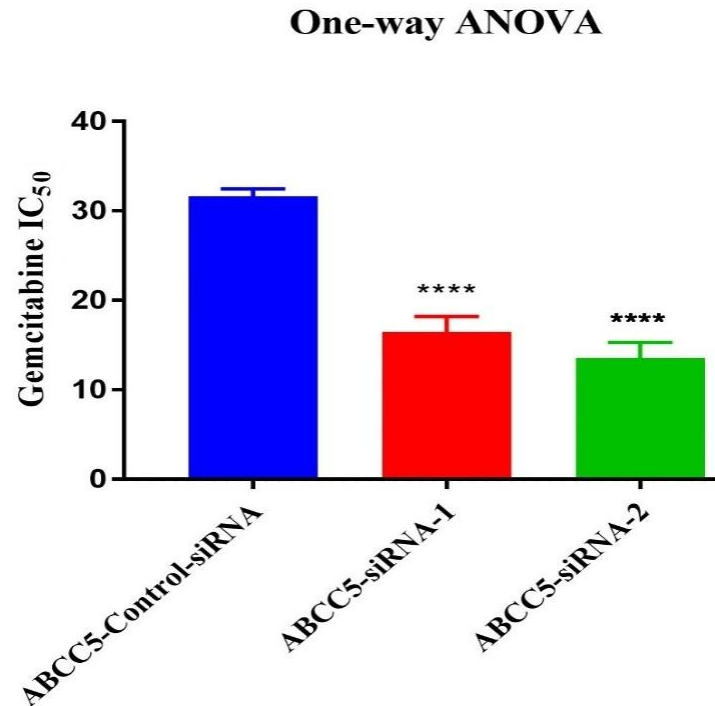


Figure 4-15: Comparison of mean gemcitabine IC₅₀ values (nM) in ABCC5-siRNA and control transfected MIA PaCa-2 cells. Data from three independent experiments are presented as the mean and SEM, n=3. Multiple comparisons between control and different treatment groups were analysed using one-way ANOVA with Dunnett's post-hoc (*****P*<0.0001).

Figure 4-17 shows the effects of MRP5 silencing on the sensitivity to gemcitabine in MIA PaCa-2 cells. A significant (*****P*<0.0001) increase in the gemcitabine sensitivity was seen for the ABCC5 knockdown cells as compared to the control. The mean IC₅₀ values for Control-siRNA, ABCC5-siRNA-1 and ABCC5-siRNA-2 were 31.64 ± 0.85 nM, 16.48 ± 1.5 nM and 13.56 ± 1.6 nM, respectively.

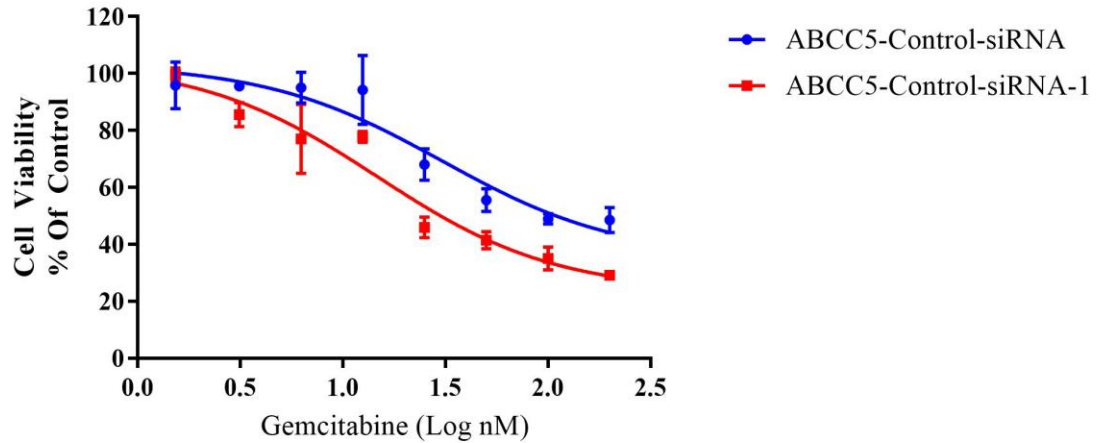


Figure 4-16: Comparison of gemcitabine-induced cytotoxicity between ABCC5-siRNA-1 and control siRNA transfected MIA PaCa-2 cells. Data are presented as the mean and SEM from three independent experiments; n=3.

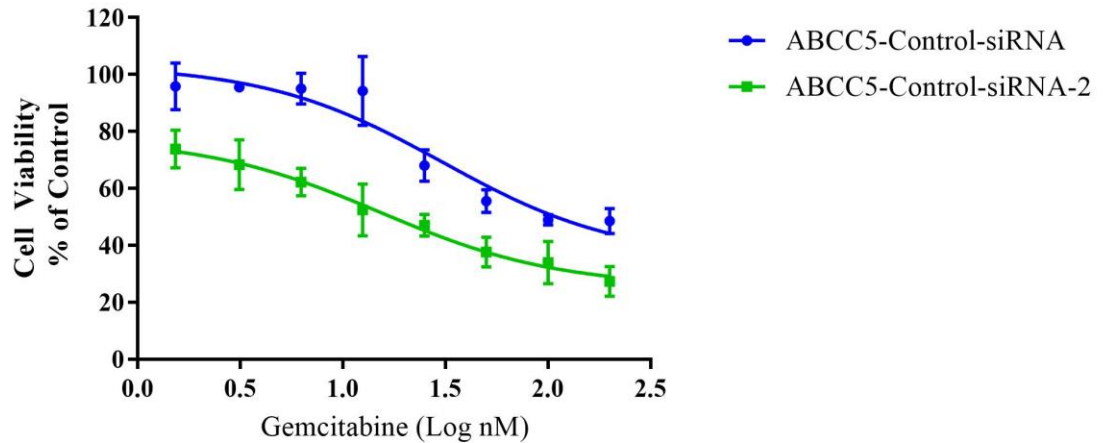


Figure 4-17: Comparison of gemcitabine-induced cytotoxicity in ABCC5-siRNA-2 and control-siRNA transfected MIA PaCa-2 cells. Data are presented as the mean and SEM from three independent experiments; n=3

Figures 4-18 and 4-19 show silencing MRP5 increased gemcitabine sensitivity in MIA PaCa-2 cells transfected with two different ABCC5-siRNAs. ABCC5 knockdown cells not only show a significant increase in gemcitabine sensitivity but a curve shift analysis shows a synergistic effect.

PANC-1

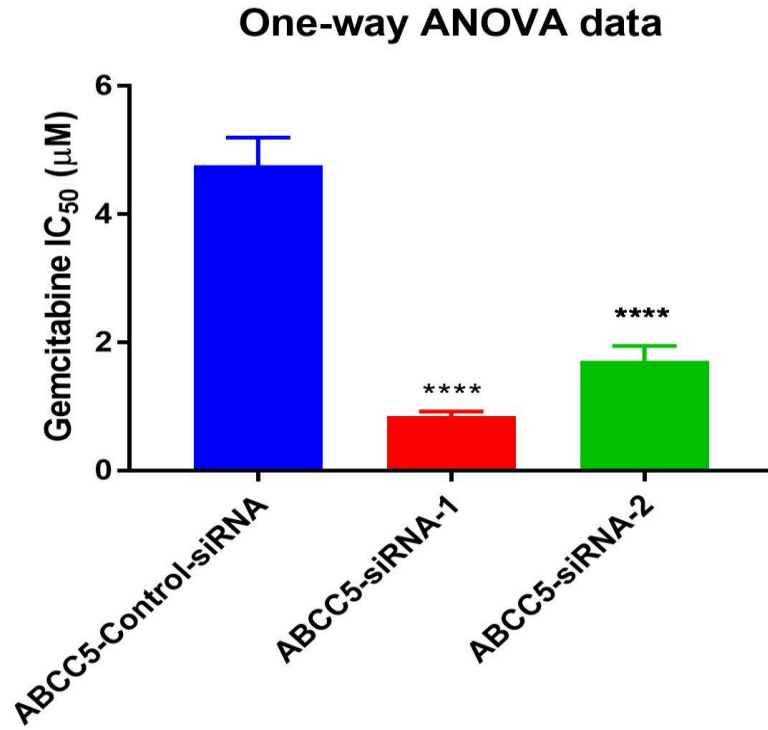


Figure 4-18: Comparison of mean gemcitabine IC₅₀ values in ABCC5 and control-siRNA transfected PANC-1 cells. Data from three independent experiments are presented as the mean and SEM; n=3. Multiple comparisons between control and different treatment groups were analysed using one-way ANOVA with Dunnett's post-hoc. **** $P < 0.0001$

Figure 4-20 shows IC₅₀ values against gemcitabine were 3- to 6-fold higher in PANC-1 cells transfected with control siRNA compared with those transfected with ABCC5-siRNAs. The IC₅₀ values for the control, ABCC5-siRNA-1 and ABCC5-siRNA-2 transfected cells were $5.84 \pm 1.8 \mu\text{M}$, $0.90 \pm 0.04 \mu\text{M}$ and $1.81 \pm 0.28 \mu\text{M}$, respectively.

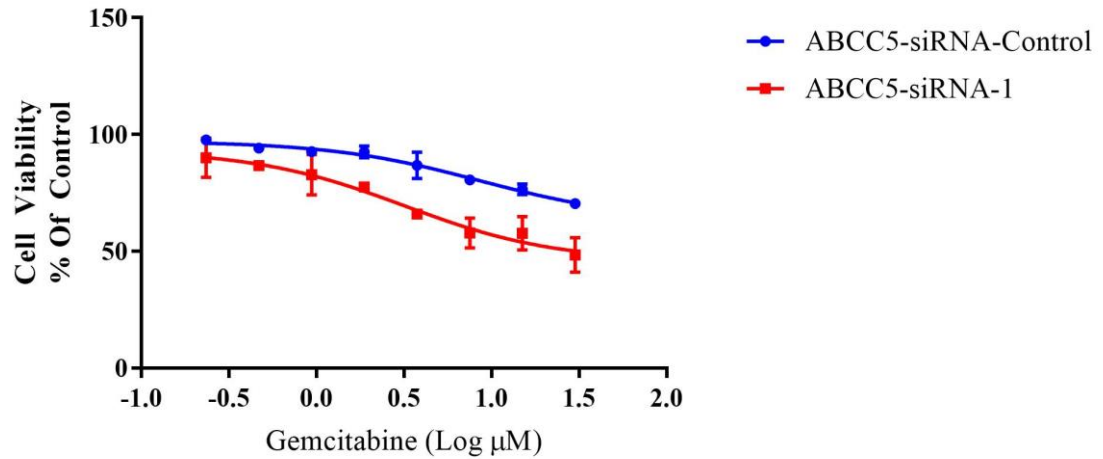


Figure 4-19: Comparison of gemcitabine-induced cytotoxicity in ABCC5-siRNA-1 transfected and control PANC-1 cells. Data are presented as the mean and SEM from three independent experiments; n=3

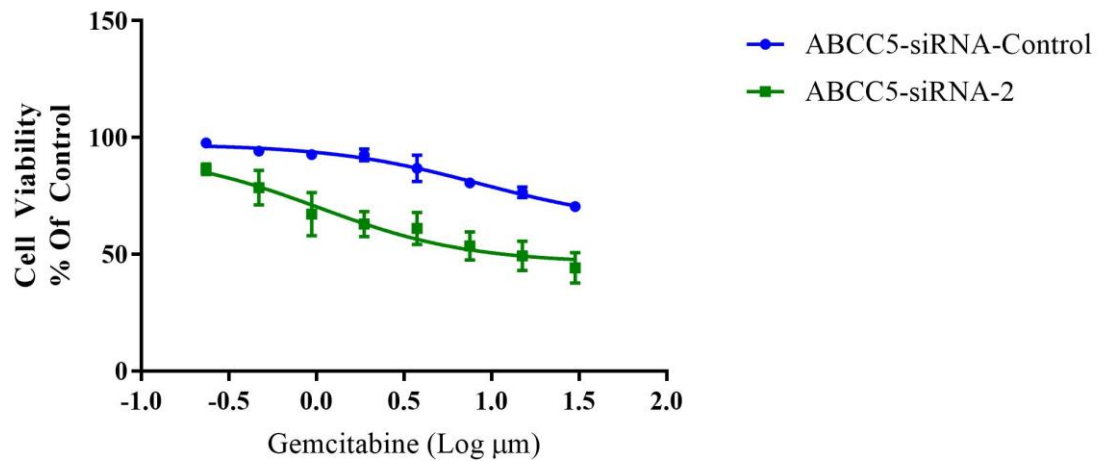


Figure 4-20: Comparison of gemcitabine-induced cytotoxicity in ABCC5-siRNA-2 transfected and control PANC-1 cells. Data are presented as the mean and SEM from three independent experiments; n=3

Both MIA PaCa-2 and PANC-1 cells showed an increase in the gemcitabine sensitivity for the ABCC5 knockdown cells suggesting the crucial role of MRP5 in drug resistance.

4.4.5 Effects of ABCC5 silencing on gemcitabine-induced apoptosis

Apoptosis assay of ABCC5 transfected MIA PaCa-2 cells

MIA PaCa-2: ABCC5-Control-siRNA

Drug concentration	Viable Cells (%)	Apoptosis (%)
No treatment	98.11 ± 1.08	1.24 ± 0.12
800 nM	76.94 ± 1.01	19.24 ± 0.15**
400 nM	73.45 ± 3.22	25.38 ± 3.28**
200 nM	72.7 ± 2.31	25.71 ± 2.50**

Table 4-1: Mean % apoptosis for scrambled siRNA transfected MIA PaCa-2 cells treated with gemcitabine for 24 hrs. Data are presented as the mean and SEM from three independent experiments, n=3. ** $P < 0.05$

MIA PaCa-2: ABCC5-siRNA-1

Drug concentration	Viable Cells (%)	Apoptosis (%)
No treatment	97.65 ± 1.25	0.55 ± 0.15
800 nM	21.16 ± 4.18	72.55 ± 1.05*****
400 nM	24.37 ± 4.17	76.22 ± 1.49*****
200 nM	16.64 ± 3.34	78.26 ± 1.69*****

Table 4-2: Mean % percentage apoptosis for ABCC5- siRNA-1 transfected MIA PaCa-2 cells. Data are presented as the mean and SEM from three independent experiments, n=3. ***** $P < 0.0001$

MIA PaCa-2: ABCC5-siRNA-2

Drug concentration	Viable Cells (%)	Apoptosis (%)
No treatment	94.86 ± 3.80	3.14 ± 0.39
800 nM	27.07 ± 1.05	71.10 ± 10.91****
400 nM	14.85 ± 0.15	83.85 ± 0.41****
200 nM	10.57 ± 0.9	87.14 ± 0.81 ****

Table 4-3: Mean % percentage apoptosis for ABCC5-siRNA-2 transfected MIA PaCa-2 cells. Data are presented as the mean and SEM from three independent experiments, n=3. **** $P < 0.0001$

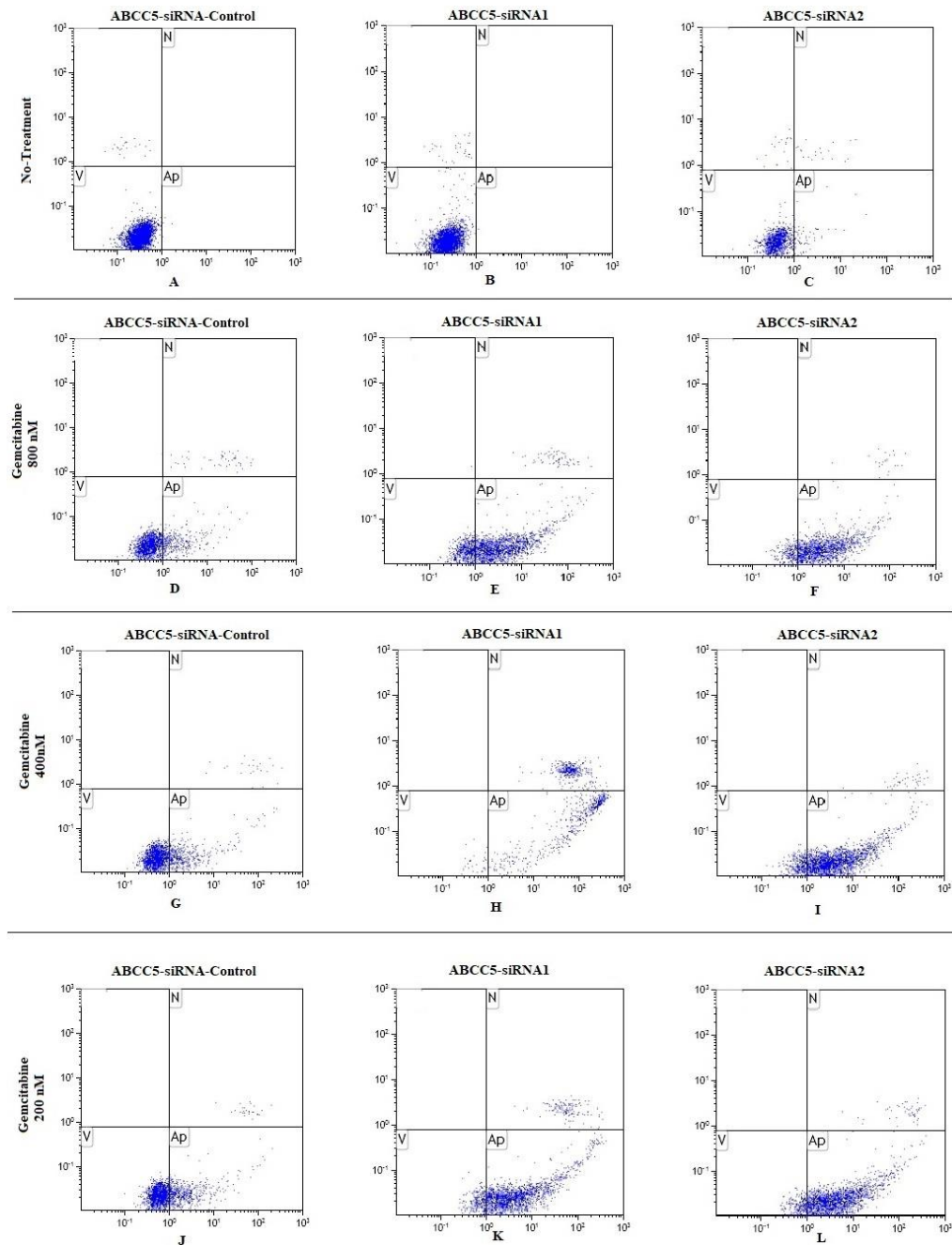


Figure 4-21: Apoptosis detection using annexin V staining in siRNAs-transfected MIA PaCa-2 cells. All cell populations were treated with Annexin V and PI. Viable cells (V), apoptotic (A) and necrotic populations can be seen in the left lower, right lower and right upper quadrants of each image of the Figure 4-21. Images A-C show control and ABCC5 siRNA transfected cells population without any drug treatment. while images D-F, G-I and J-L represent 3 genecitabine concentrations 800nM, 400nM and 200nM for MiaPaCa-2 cells transfected with control-siRNA and ABCC5 siRNA-1 and 2, respectively.

Apoptosis assay- MIA PaCa-2 cells: Two-way Anova

Two-way ANOVA

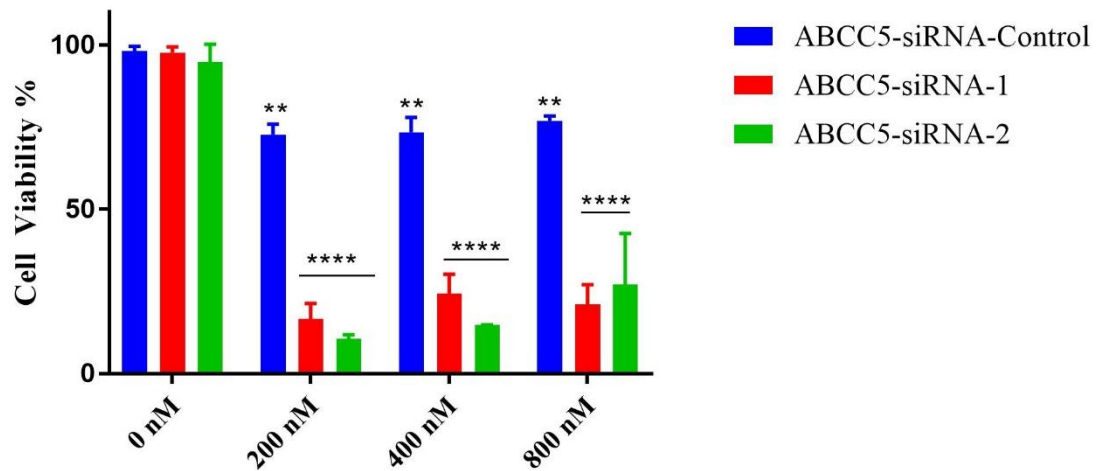


Figure 4-22: Percentage of gated viable cells of control and ABCC5-siRNA transfected MIA PaCa-2 cells treated with gemcitabine (200, 400 and 800 nM) for 24 hrs. Data are presented as the mean and SEM from three independent experiments, n=3. Multiple comparisons between control and different treatment groups were analysed using two-way ANOVA with Dunnett's multiple comparison test. ** $P < 0.05$ and **** $P < 0.0001$.

Transfection of ABCC-5 or control siRNA has no apparent effects on % gated viable cells. The percentage of viable cells was significantly reduced after gemcitabine treatment for ABCC-5 siRNAs transfected cells MIA PaCa-2 compared with control. Refer to table 4-1, 4-2 and 4-3 for mean viability percentages.

Two-way ANOVA

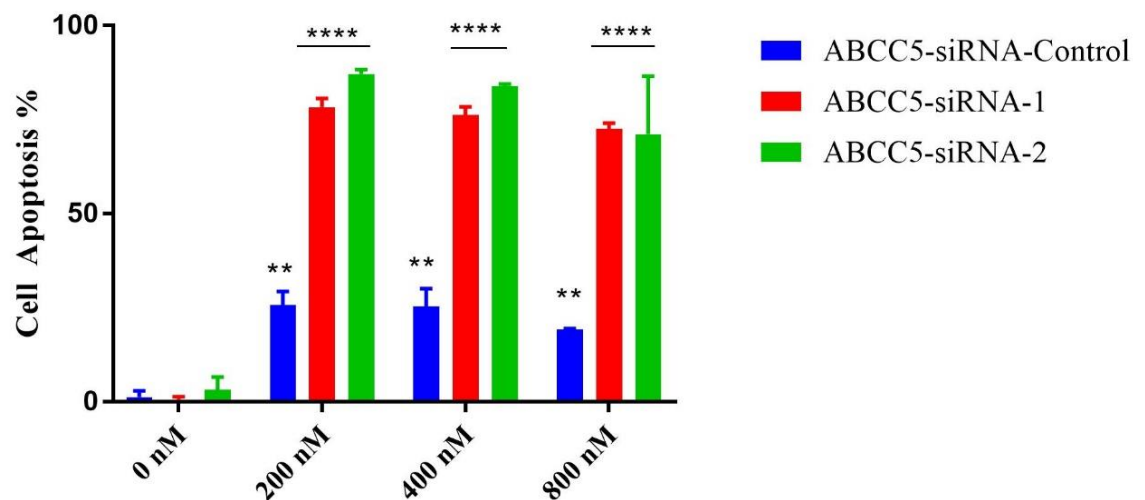


Figure 4-23: Mean percentage of gated apoptotic cells of control and ABCC5-siRNA transfected MIA PaCa-2 cells treated with gemcitabine (200, 400 and 800 nM) for 24 hrs. Data are presented as the mean

and SEM from three independent experiments, n=3. Multiple comparisons between control and different treatment groups were analysed using two-way ANOVA with Dunnett's multiple comparison test. ** $P < 0.05$ and **** $P < 0.0001$

Figure 4-23 shows a significant increase of gemcitabine-induced apoptotic effects on ABCC-5 siRNA transfected cells compared with control. All 3-different concentration showed a dramatic increase in the cell apoptosis after 24 hours of gemcitabine treatment as compared to the control. Refer to table 4-1, 4-2 and 4-3 for mean apoptosis percentages.

Apoptosis assay data for ABCC5 transfected PANC-1 cells

PANC-1: ABCC5-Control-siRNA

Drug concentration	Viable Cells (%)	Apoptosis (%)
No treatment	95.97 ± 1.78	3.85 ± 0.7
800 nM	74.38 ± 3.02	22.94 ± 0.51****
400 nM	81.77 ± 1.42	17.26 ± 0.97***
200 nM	88.6 ± 0.65	10.13 ± 0.19*

Table 4-4: Mean % apoptosis for scrambled siRNA transfected PANC-1 cells. Data are presented as the mean and SEM from three independent experiments, n=3. * $P < 0.05$, *** $P < 0.005$ and **** $P < 0.0001$

PANC-1: ABCC5-siRNA-1

Drug concentration	Viable Cells (%)	Apoptosis (%)
No treatment	96.36 ± 2.63	2.30 ± 0.63
800 nM	53.31 ± 1.20	43.38 ± 1.48 ****
400 nM	70.21 ± 3.30	25.355 ± 2.79 ****
200 nM	81.57 ± 0.99	17.585 ± 0.68****

Table 4-5: Mean % apoptosis for ABCC5-siRNA-1 transfected PANC-1 cells. Data are presented as the mean and SEM from three independent experiments, n=3. **** $P < 0.0001$

PANC-1: ABCC5-siRNA-2

Drug concentration	Viable Cells (%)	Apoptosis (%)
No treatment	97.17 ± 1.15	1.85 ± 0.68
800 nM	54.16 ± 0.24	39.07 ± 1.61 ****
400 nM	70.83 ± 2.99	23.30 ± 2.30****
200 nM	81.77 ± 1.27	17.37 ± 0.92 ****

Table 4-6: Mean % apoptosis for ABCC5-siRNA-1 transfected PANC-1 cells. Data are presented as the mean and SEM from three independent experiments, n=3. **** $P < 0.0001$

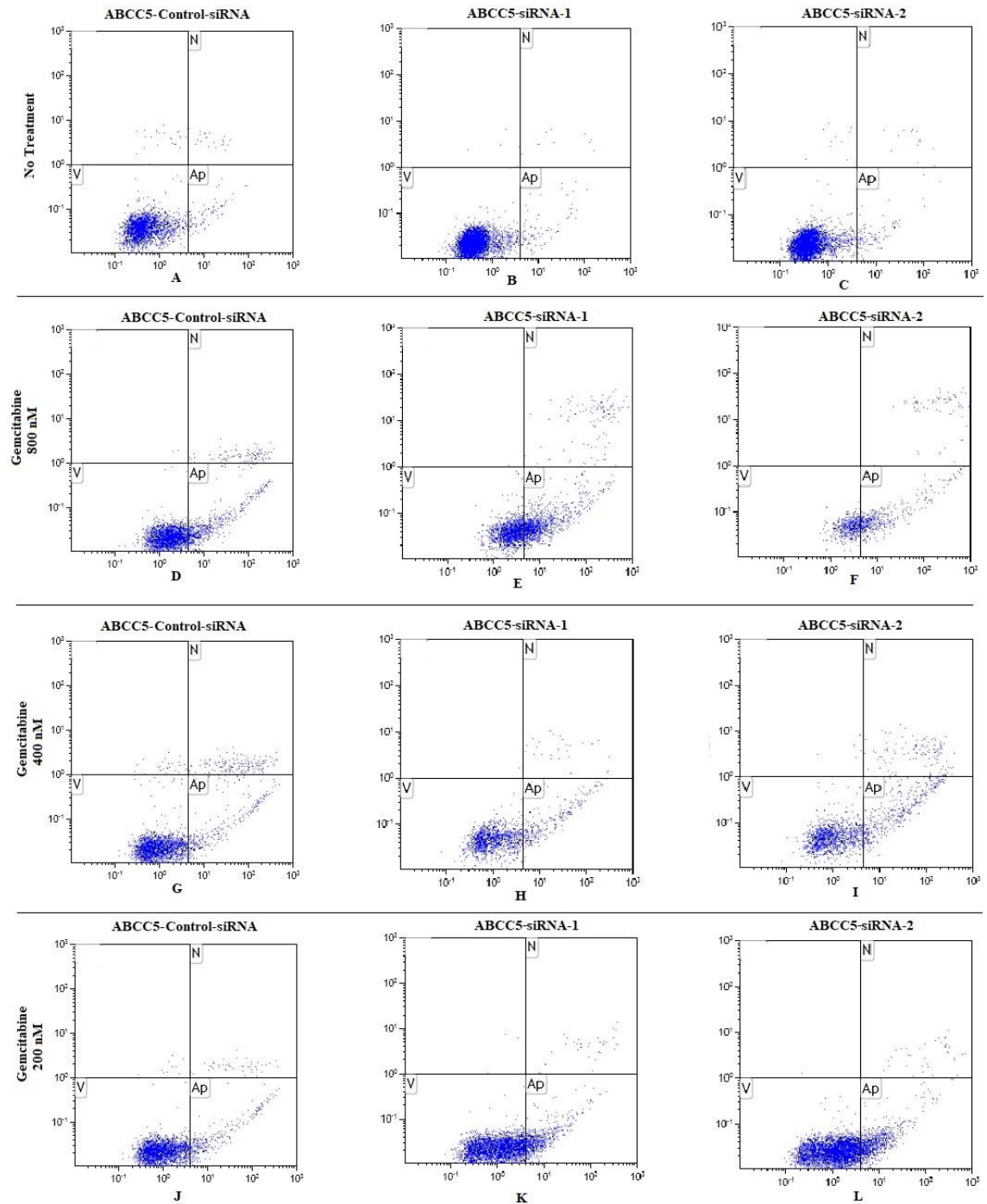


Figure 4-24: Annexin V staining for apoptosis detection in siRNAs-transfected PANC-1 cells

The gated viable cells (V), apoptotic (A) and necrotic (N) populations can be seen in the corresponding quadrants of each image of Figure 4-24. Images D-F, G-I and J-L represent 3 gemcitabine treatment at concentrations of 800nM, 400nM and 200nM in control-siRNA and ABCC5 siRNA-1 and 2 transfected PANC-1 cells, respectively.

Apoptosis assay PANC-1 cells: Two-way Anova

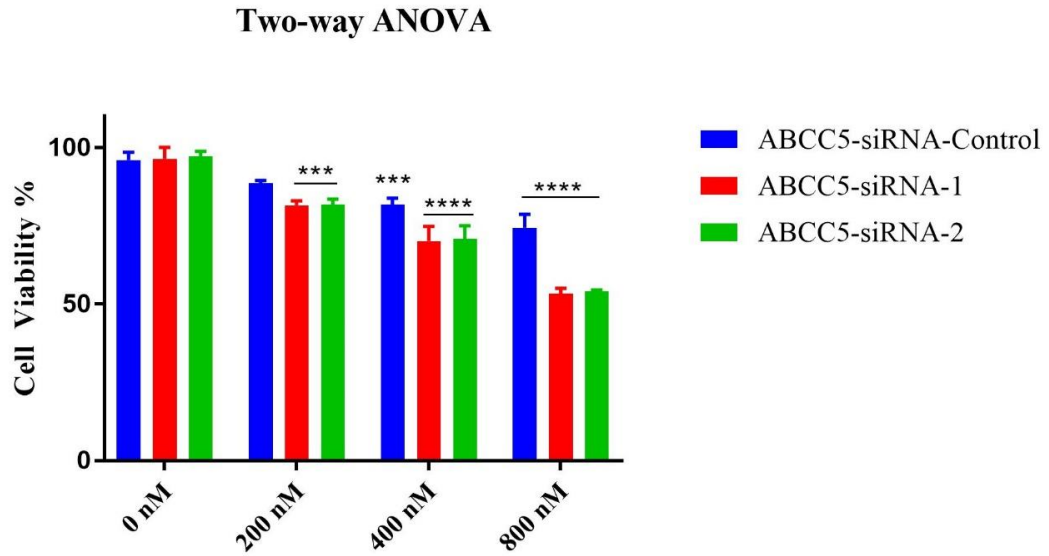


Figure 4-25: Mean percentage of gated viable cells of control and ABCC-5 siRNA transfected PANC-1 cells. Multiple comparisons between control and different treatment groups were analysed using two-way ANOVA with Dunnett's multiple comparison test. *** $P < 0.005$ and **** $P < 0.0001$.

Similarly, PANC-1 cell viability was reduced for gemcitabine-treated cells. A dose-dependent decrease in the cell viability was observed and was significant in the ABCC5-transfected cells as compared to the control. Refer to table 4-4, 4-5 and 4-6 for mean viability data.

Two-way ANOVA

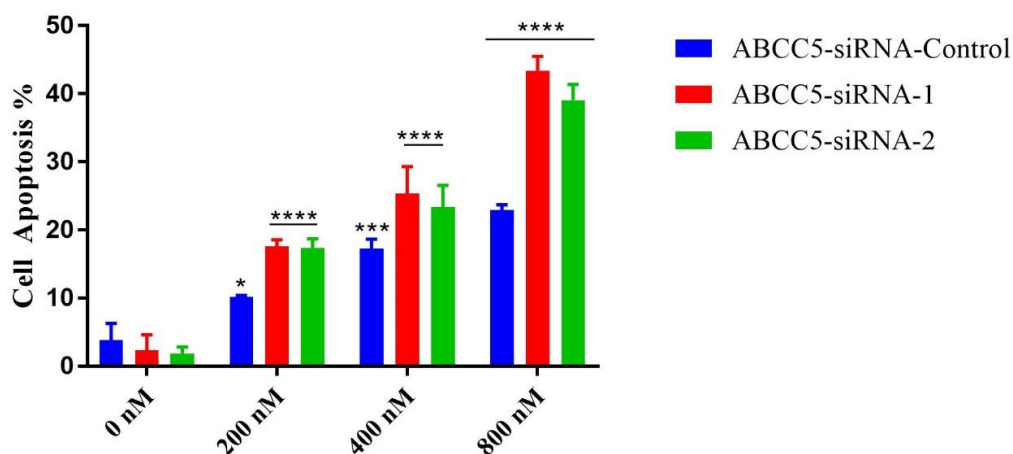


Figure 4-26: Mean percentage of gated apoptotic cells of control and ABCC-5 siRNA transfected PANC-1 cells treated with gemcitabine (200, 400 and 800 nM) for 48 hrs. Multiple comparisons between control and different treatment groups were analysed using two-way ANOVA with Dunnett's multiple comparison test. * $P = 0.028$, *** $P < 0.005$ and **** $P < 0.0001$

Mean apoptosis percentage was significantly higher in the ABCC5-siRNA-transfected cells as compared to the control. Refer to tables 4-4, 4-5 and 4-6 for mean apoptosis percentages.

4.5 Discussion

4.5.1 siRNA transfection

Like every other method, RNAi is not perfect and has its complications. Empirically RNAi was observed to function in several organisms, but some of them are RNAi negative, e.g. *Saccharomyces cerevisiae*, *Trypanosoma cruzi* and *Leishmania major* [194]. As they lack necessary components like Dicer and RISC thus, RNAi cannot be executed in them. The most important concern raised during the RNAi study was the specificity of approach [312, 313]. Earlier RNAi was believed to be very specific and accurate. But studies [214, 314-316] over the past few years have shown significant off-target effects with the use of RNAi. Though siRNA could still direct the RNAi to the target site, there is a lack of complete sequence similarity [317] thus, Agrawal et al. [209] have raised concerns about the specificity of gene repression in RNAi. Consolidated, the above examinations of RNAi off-target effects yielded mixed results. Perhaps, therefore, RNAi doesn't unequivocally control for off-target effects on a routine basis [215]. Lack of specificity subsequently results in knockdown of unknown or unintended genes which has considerable negative implications for functional genomics. For finding the uncertainties related to RNAi, off-target effects must be

assessed for each gene expressed by the organism under study, by considering multiple possible factors affecting off-target silencing [194]. Such comprehensive studies are tedious, expensive and cumbersome to conduct experimentally [215].

As our study focused on enhancing the gemcitabine cytotoxicity by knocking down ABCC5 activity, we evaluated off-target effects of the genes related to the drug transport and metabolism (especially ABC transporters and enzymes of gemcitabine mechanism). As mentioned before, off-target effects influence functional genomics, and thus it becomes tough to predict the exact nature of the results. Studies [215, 318] have also accounted for the role of siRNA concentration in the off-target effects. It was shown that optimising the siRNA concentration to a low effective dose where it silences the target gene potently can significantly reduce the off-target effects that undergo substantial changes in expression [318]. The off-targets effects induced by one of three siRNAs (ABCC5-siRNA-3) were still considerably high even after dose optimisation. Thus, this siRNA (ABCC5-siRNA-3) was excluded from the studies. The off-target effects included both transcripts that were complementary to the seed region of the siRNA and transcripts that lacked seed complementarity [320]. Factors which affect the siRNA efficiency are the length of siRNA, the length of dsRNA, the length of siRNA-target sequence mismatch, the position of a mismatch inside the siRNA sequence, the situation of dsRNA inside the target and the transfection methods [214, 321].

However, even after optimisation of siRNA dose and sequences, several ABC transporters genes (i.e., ABCC2, -4 and ABCG2) were shown to be up-regulated in two abovementioned ABCC5-silencing pancreatic cancer cells, which would have played some roles in the detoxification of gemcitabine moieties. ABCC1 appears to be down-regulated by siRNA-1 but upregulated by siRNA-2 in both cell lines tested. However, the increased gemcitabine sensitivity in these cells rules out, if not all, the possibility that these ABC transporters directly confer resistance to gemcitabine. More studies are needed in this area to see if up-regulation of other transporters has any effects on the gemcitabine sensitivity.

Apart from the transporter genes, slight downregulation (20 – 30%) in the CDA mRNA level were detected in both cell lines treated by both siRNA sequences, while the dCK level was decreased only in PANC-1 cells treated by ABCC-5 siRNA-2 sequence. dCK plays a major part in the gemcitabine metabolism (activation pathway) by phosphorylation, its downregulation could have affected the gemcitabine efficacy

leading to low sensitivity. CDA enzyme is involved in gemcitabine de-toxification and its downregulation could contribute to increased gemcitabine cytotoxicity. However, the contribution of such slight CDA downregulation remains unknown. In summary, we did observe that ABCC5 knockdown plays an essential role in gemcitabine cytotoxicity, the contribution of off-target effects (especially CDA downregulation) cannot be completely ruled out the situation of dsRNA inside the target [215, 319]. BCECF accumulation

One of the significant problems with accumulation assay is variability, but this can be eliminated or reduced to a minimal level using single time-point [306]. Apart from the variability, there are few other factors involved in the accumulation assay which could affect the results or reading, e.g. concentration of the substrate, health of the cells and flow cytometry gating strategies. Substrate (BCECF) concentration is critical as it might affect the number of viable cells and thus influencing the results. Necrotic or dead cells tend to show a variation in the fluorescence reading due to the ineffective or lack of esterase enzyme; needed for conversion of BCECF-ester to BCECF which is fluorescent. Cell membrane gets compromised in the apoptotic or early apoptotic phase and thus the results from these cell population cannot be validated as the protein of interest (MRP5) is a membrane transporter. Therefore, the health of the cells should be checked carefully before the experiment, and necrotic or apoptotic cells should be excluded. Another concern with the use of flow cytometer is cell aggregation; this could give false positive data. Things like elongated trypsinisation time or putting cells in the suspension for an extended period before the experiment could increase the cell aggregation, i.e. cells stick together to form doublets or triplets. These cell aggregates during the fluorescence reading are counted as single cells leading to higher fluorescence values yielding false positive results. Apart from careful experimental practices flow cytometer gating techniques could be used to exclude such cell aggregates of the data. For example, after forward and side-scatter gating of the cell population, height to area gating or log height- log area gating could be applied to get rid-off the doublets. For a valid comparison of the data and to limit the variability parameters of gating were kept constant for all samples. Cell passage number is one of the primary reasons for variation; cells in different growth phase may have different levels of ABC expression. To avoid such variation, we limit our cell passage number to 20.

4.5.2 MTT Assay

MTT assay is one of the most popular assays used for testing cell viability. But one of the disadvantages associated with this assay is the probability of active succinate dehydrogenase in the dead cells. Succinate dehydrogenase is needed for the conversion of MTT into purple formazan crystals which is a characteristic property of viable cells. The activity of this enzyme in the dead cells could give us some percentage of false negative or positive results. Before measuring the fluorescence we changed the complete RPMI medium (contains phenol red and 10% FBS) to serum-free DMEM medium. Both phenol red and serum could absorb light in the same wavelength as MTT and could generate a background signal reducing the dynamic range of the assay. Thus, the use of phenol red-free medium without serum is recommended while performing photometry. MIA PaCa-2 and PANC-1 cells have a doubling time of 40 and 52 hours respectively. Thus, the initial cell seeding number of both cells were different, i.e. 5000 and 8000 cells/well for MIA PaCa-2 and PANC-1 respectively. Cell number optimisation is one of the crucial steps to avoid false positive/negative results. Cell lines with a less cell doubling time could grow rapidly leading to the exhaustion of the medium nutrients and eventually leading to cell death. Only freshly prepared MTT was used in the experiment to avoid crystallisation and MTT degradation, as it is both light and temperature sensitivity. One of the most crucial steps of MTT preparation is filter sterilisation of the solution with a 0.22 µm filter, this avoids any un-dissolved MTT crystals and reduce the probability of variation in the MTT data. Comparison of IC₅₀ values among the cell lines also suggest the fact that PANC-1 cells (~ 6 µM) are more resistant to gemcitabine as compared to MIA PaCa-2 (~ 30 nM), which is consistent with previous reports [320]. The probable reason for such high resistance could be the presence of a different apoptosis pathway(s) in PANC-1 cells and thus leading to more resistance.

Our data mainly shows significantly lower IC₅₀ values for the knockdown cell lines as compared to the control leading to the conclusion that MRP5 plays a crucial role in gemcitabine's chemosensitivity. As mentioned before, the off-target effects of siRNA transfection on gemcitabine metabolism, to a less extent, could contribute to the differences in IC₅₀ values. Nevertheless, given the marginal off-target effects (20 to 30% decrease in CDA mRNA), it is reasonable to suggest that MRP5 is the major factor which contributed to cellular gemcitabine disposition and thus its therapeutic effects.

4.5.3 Apoptosis

Programmed cell death (PCD) is an integral part of the developmental process and may help in maintaining the equilibrium between cell, death and survival [232, 321]. Apoptosis is also significant when it comes to the survival and drug resistance in the cancer cells. Drugs like gemcitabine, capecitabine and 5-FU have shown to induce apoptosis in cancer cells (even though they have different mechanisms), eventually leading to cell mortality. There are many molecular factors and various mechanisms involved in the process of apoptosis. Previously, accumulating evidence has also shown that cancer cells are resistant towards the drug-induced apoptosis through multiple mechanisms involving drug efflux and DNA repairs.

Gemcitabine is a pro-drug, and its metabolites have various targets in the cells. Gemcitabine is activated by phosphorylation intracellularly by deoxycytidine kinase (dCK). Gemcitabine after phosphorylation produces dFdCMP; rate-limiting step, which is then, converted into its active diphosphate and triphosphate metabolites (dFdCDP and dFdCTP). Active metabolites of gemcitabine (dFdCTP) get inserted into the DNA strand during DNA synthesis resulting inhibition of synthesis that's mainly how gemcitabine exerts its cytotoxic effect. Also, gemcitabine has a unique mechanism of action known as 'self-potential', in which dFdCDP potentially inhibits the ribonucleotide reductase (RR). RR enzyme is responsible for the production of dNTP pools which are further used for DNA synthesis. Thus, gemcitabine is a potent external stimulus to induce apoptosis providing sufficient intracellular concentration of active moieties can be achieved. We hypothesised that gemcitabine's detoxification by MRP5 protein has a major role in limiting its pro-apoptotic efficacy. Our results show that silencing MRP5 in MIA PaCa-2 and PANC-1 cells led to the higher apoptotic population as compared to the control. But as we know that gemcitabine has multiple targets and thus a complex mechanism, we included dCK and CDA enzymes in the studies of our off-target gene. For the PANC-1 cell line, we found that siRNA transfection, in general, had some knocking-down effect on the CDA and dCK enzymes. The off-target effects for the dCK enzymes may not be significant as a low dCK level would have decreased apoptotic rate in ABCC5-siRNA transfected cells.

On the contrary, marginal but significant off-target knockdown effects were seen for the CDA mRNA levels in both cell lines tested. Thus, to predict the exact mechanism for the increase in the apoptosis percentage for the ABCC5 silencing cells becomes difficult, however, given the ABCC5 knockdown is by ~85% in both cell lines, it is

reasonable to suggest that MRP5 activity is one of the most significant factors for gemcitabine-induced apoptosis. hENT1 plays a very significant role in the uptake of gemcitabine, and that's why we included it in our off-target studies. The hENT1 expression was marginally high for the ABCC5 transfected cells as compared to the control in both cell lines. This marginally high hENT1 expression is not statistically significant to play a major role in affecting the apoptosis. Our off-target data also shows overexpression of most of the transporters after ABCC5-siRNA transfection. But a significantly higher percentage of apoptosis in MRP5 knockdown cells indicates that other ABC transporters have no significant relation with gemcitabine de-toxification. Another interesting factor which was observed during our studies was the optimisation of drug incubation time for the knock-down cells. It was observed that apoptosis induction was quite early for MIA Paca-2 cells as compared to PANC-1. We found that 48 hours gemcitabine treatment in MIA PaCa-2 cells significantly increased the number of dead cells which are lost in the washing step of apoptosis leaving very few viable cell numbers in the apoptosis assay. Thus, the gemcitabine incubation time was reduced to 24 hours, and a significantly high apoptosis population was seen in the knockdown cells as compared to the control in the MIA Paca-2 cell line. On the contrary, no significant difference was seen in the PANC-1 cells when incubated for 24 hours and thus the drug incubation time was increased to 48 hours for PANC-1 cells. This suggests the fact that even though gemcitabine mechanism is same for both cell lines, PANC-1 cells may have multiple mechanisms to induce resistance to apoptosis, in other words, PANC-1 cells are more resistant to the gemcitabine than MIA PaCa-2 cells.

Chapter 5 Genome-editing in PANC-1 cells using the CRISPR-Cas9 system

It is evident from the previous chapter that MRP5 plays a crucial role in drug resistance and the use of siRNA for gene knockdown increases drug sensitivity. Though siRNA transfection and the technique are very straightforward, the use of siRNA has some major drawbacks, e.g. the gene knockdown effect is transient, and siRNA could cause some significant off-target effects. Thus, to overcome these problems we decided to create a knockout cell line using a gene editing tool with minimum off-target effects. Over the past few years, gene editing has made some revolutionary developments. A few gene editing techniques are currently in practice, e.g. zinc-finger nucleases (ZFN), transcription activator-like effector nucleases (TALENs) and most recently developed RNA-guided CRISPR (Clustered Regularly Interspaced Short Palindromic Repeats)-Cas (CRISPR-associated proteins) nuclease system [322]. ZFN and TALENs have a similar mechanism of action; both can create a double-stranded break (DSBs) in the DNA at a specific site by tethering endonuclease catalytic domains to integrated DNA-binding proteins [322]. On the other hand, the CRISPR-Cas system uses a guide RNA (gRNA) to target the specific site on the DNA and create a double-stranded break. Thus, the CRISPR-Cas system is more accessible to design, precise and suitable for a variety of cell types [322].

CRISPR-Cas system was first discovered in bacteria and archaea as a part of their adaptive immune system [323]. It was observed that this adaptive immune system could identify and neutralise mobile genetic elements like viruses and plasmid DNA in a specific manner [323]. CRISPR-Cas system is a family of proteins, and on the basis of endonuclease protein (Cas) and guide RNA it is further sub-divided into Class 1 (Types I, III and IV) and Class 2 (Types II, V and VI) [323, 324]. Generally, Class 2 sub-family is used for the gene editing purposes because of its simple design. Class 2 has just a single multi-domain protein, e.g. Type II Cas nuclease (Cas9) integrated with heterogeneously expressing gRNA. Guide-RNA or sgRNA is a chimera of CRISPR RNA (crRNA) and transactivation RNA (tracrRNA). The dual-tracrRNA:crRNA together are designated as sgRNA [323, 324]. CRISPR RNA is complementary to the target sequence, and tracrRNA provides a scaffolding structure which holds and stabilises the sgRNA (5' end)-CAS protein (3' end) complex [324]. sgRNAs are usually 20-22 base pair long, and after recognising the protospacer adjacent motif (PAM), sgRNA binds to the target sequence by Watson-Crick base-pairing [323, 324]. After binding of the sgRNA to the

target sequence, CAS protein creates a double-stranded nick 3-4 nucleotide upstream of the PAM site[324]. For our experiments, we used endonuclease Cas9 protein to create dsDNA nicks. The cas9 protein comprises two nuclease domains RuvC and HNH. Non-complementary DNA strands are cleaved by RuvC domain while HNH domain is responsible for the cleavage of complementary strands of DNA [324].

These double-stranded breaks are repaired by the DNA repair machinery via non-homologous end joining (NHEJ) or the homologous directed repair (HDR)[323-325]. NHEJ is an error-prone process and could randomly join the breaks in the DNA chain creating either insertion or deletion (indels) at the site[322-325]. These indels at the target site disrupt the gene activity by causing frameshift mutation or by insertion of premature stop codons within the open reading frames (ORFs) of the target sequence [324, 325]. More precise genetic editing can be done by using the HDR pathway with a homologous DNA template, which could be used to correct genetic changes and induce intended mutations [324, 325]. For our experiments, we used the NHEJ pathway as we wanted to knock out the target gene. We transfected PANC-1 cells with a lipofectamineTM coated complex of ABCC5-sgRNA and CAS9 protein to create indels at the target site causing frame mutation (via NHEJ) and thus knockout of ABCC5 activity.

CRISPR-Cas9 system has several advantages over the other gene editing tools, e.g. CRISPR-Cas9 needs sgRNA for DNA targeting, sgRNA synthesis is both relatively easy and cost-efficient[325]. Many bioinformatics tools are available for free to design the sgRNA. One of the significant advantages of this method is multiple genes targeting at the same time by using different sgRNA simultaneously [323, 325, 326]. Unlike siRNA, the CRISPR-Cas9 system is independent of the use of any cell machinery, e.g. RNAi needs RISC for its function which could affect multiple gene targeting[323-325]. A few Cas9 protein variants are also available commercially which could be used for different purposes, e.g. epigenome targeting by catalytically de-activated Cas9 (dCas9)[325]. Another advantage of the CRISPR-Cas9 system over RNAi is that it works on a DNA level; editing the gene [325]. Thus, gene knockout effects are permanent with a probability of less off-target effects. CRISPR-Cas system is reported to have less cytotoxicity and high targeting efficacy compared with ZFNs and TALENs. The specificity of the targeted sequence can be easily altered in CRISPR-Cas system by changing the sgRNA but in ZFNs and TALENs protein engineering is required every single time for the new target [322-325].

72 hours after the transfection of the ABCC5-sgRNA-2-Cas9 complex, single cell ABCC5 knockout clones were isolated by using a limited dilution method [322]. These single cell clones (from sgrNa-2) were then sub-cultured for 3-4 weeks to get enough cell population for MRP5 functional testing. MRP5 functional testing was carried out using the BCECF accumulation assay, and MRP5 surface expression was quantified using the cell surface staining method. We also confirmed the ABCC5 mRNA levels using the qRT-PCR technique. Drug cytotoxicity assay was carried using the MTT method. For MTT assay the cells were seeded in 96 wells plate followed by the drug treatment after 24 hours of seeding. Drug treatment was carried out for 72 hours followed by the addition of MTT. The decrease or increase in the viable cell numbers can be measured by measuring the optical density reflecting the formazon concentration in the solution Thus, the main aims of this chapter are as follows –

- To create an ABCC5 knockout PANC-1 cell line using the CRISPR-Cas9 system
- Isolate and validate ABCC5 knockout single cell PANC-1 population
- To measure the cellular accumulation of BCECF in ABCC5 knockout PANC1 cells.
- Quantification of MRP5 level in knockout and control (only Cas9 transfected) PANC-1 cells
- Compare the IC₅₀ value of gemcitabine for non-knockout (control) and ABCC5 knockout PANC-1 cells

5.1 Materials and methods

5.1.1 Chemicals

Refer to chapter 2 section 2.7 for the detailed description of the reagents, kits and the apparatuses.

5.1.2 CRISPR-Cas9 transfection into PANC-1 cells

The CRISPR-Cas9 transfection was carried out using CRISPRMAX™ Reagent forward transfection method. Initially, two different sgRNAs were used for the transfection of PANC-1 cells. The recommended sgRNA, Cas9 and CRISPRMAX™ Reagent concentrations were used for the transfection, for more details on the transfection method, Refer to chapter 2 section 2.7.2. Time of transfection was 72 hours as recommended in the manufacturer's protocol (Refer chapter 2 section 2.7).

In the forward transfection cells are plated a day before transfection, and the cell number is optimised to achieve 50-60% confluency of cells after 24 hours. After 24 hours of the cell seeding sgRNA-Cas9 complex was prepared in serum and antibiotic free Opti-MEMTM Reduced Serum medium with Cas9 plus reagent separately in tube-1. CRISPRMAXTM reagent was diluted in Opti-MEMTM Reduced Serum medium in a tube-2. Later, both tubes were mixed and incubated at the room temperature for 10 mins followed by the addition of this mixture to the cells. Refer to chapter 2 section 2.7.2 for more details. The cells were incubated for 72 hr at 37°C in 5% CO₂ with 95% humidified air. After 72 hrs incubation cells were used for the different experimental assays.

5.1.3 Cellular BCECF accumulation assay

After the transfection, BCECF accumulation assay was carried out to compare the difference in accumulation between control (only Cas9 transfected) and transfected cell lines. As we now know that BCECF is a substrate of MRP5 and its higher accumulation represents low MRP5 activity. Thus, higher BCECF accumulation in the assay can indirectly confirm the presence of a knockout cell population in the transfected PANC-1 cells. The percentage difference of BCECF accumulation could also be an indirect indicator of the knockout efficacy. The concept is- even though there is a mixed population of knockout and non-knockout cells after the transfection, but, if the transfected cells show remarkably high BCECF accumulation than there could be a high percentage of the knockout cell population in the transfected pool of cells. As described in chapter 2 section 2.6.2 BCECF accumulation was performed using only 5 minutes time course and CUC was used as the positive control. Experiments were repeated three times independently.

5.1.4 Limited Dilution Method

After confirmation of the presence of a knockout cell population in the transfected pool of cells. Limited dilution method was carried out to isolate the single cell ABCC5-knockout PANC-1 clones. The CRISPR-Cas9 transfected cells (for sgRNA-2) were trypsinised and suspended in the complete growth medium (Refer to chapter 2 section 2.1.1 and 2.12 for medium composition and cell culture technique). The cells were then counted on Neubauer's chamber under a microscope and were seeded in a 96 well plate. The starting seeding number of the cells was 100 cells/well followed by the serial 1:2 dilution of the cell population. After 24 hours of seeding, cells were observed under the microscope to confirm the dilution. It took ~2 weeks of time for single cell population

to achieve 80% confluency in a 96 wells plate before transferring to a 25cm² flask for propagation.

5.1.5 MRP5 Cell surface staining

MRP5 surface expression in PANC-1 cells was carried out using an indirect protein labelling method. This method includes the use of two antibodies – primary Anti-MRP5 monoclonal antibody (Thermofisher, M5II-54, Host: Rat) and a secondary Goat Anti-rat IgG H&L (Alexa Fluor® 488, Product # A-11006) antibody. Mouse IgG was used as an isotype control for validation of the data. The isotype control was conjugated with Alexa Fluor 488 secondary antibody. As the MRP5 antibody was targeting the internal epitome of the protein saponin was used to increase the cell permeability. Saponin in low concentrations is not toxic for cells. To further prevent the internalisation of the membrane protein MRP5, sodium-azide was included in the cell treatment before labelling of primary antibody. Refer to chapter 2 section 2.6 for details on reagents and methodology. For the assay PANC-1 control (only Cas9 transfected) and ABCC5 knockout cells were trypsinised, counted and collected in an Eppendorf tube at a density of 1×10^6 per ml. The cells were then permeabilised and blocked as described in section 2.6.3 of chapter 2. The experiment was repeated twice independently.

5.1.6 RNA extraction of the knockout cell population

Refer to chapter 2 section 2.2.3 for details on materials and the methodology used

5.1.7 Real-time quantitative PCR and relative gene expression

Refer to chapter 3 section 3.6.5 for assay optimisation and the materials used.

5.1.8 BCECF accumulation assay for ABCC5 knockout single cell PANC-1 clones

The same procedure as described in section 2.4.2 of chapter 2 was followed for the time course of 5 mins. Both control (only Cas9 transfected) and knockout cell population were subjected for the accumulation assay with CUC as the positive control.

5.1.9 Growth inhibition assay: MTT

Gemcitabine cytotoxicity for the control (only Cas9 transfected) and ABCC5 knockout PANC-1 cells was determined using MTT (3-(4,5-Dimethylthiazol-2-yl)-2,5-Diphenyltetrazolium Bromide) assay. As mentioned before, the MTT assay quantifies a number of viable cells after gemcitabine treatment. Cells were seeded in 96 wells plate at a seeding density of 8000cells/well followed by gemcitabine addition after 24 hours.

After 72 hours of drug treatment, MTT assay was carried out as described in section 2.3.3 of chapter 2. All the experiments were repeated individually 3 times.

5.2 Results

5.2.1 BCECF Accumulation: Mixed population

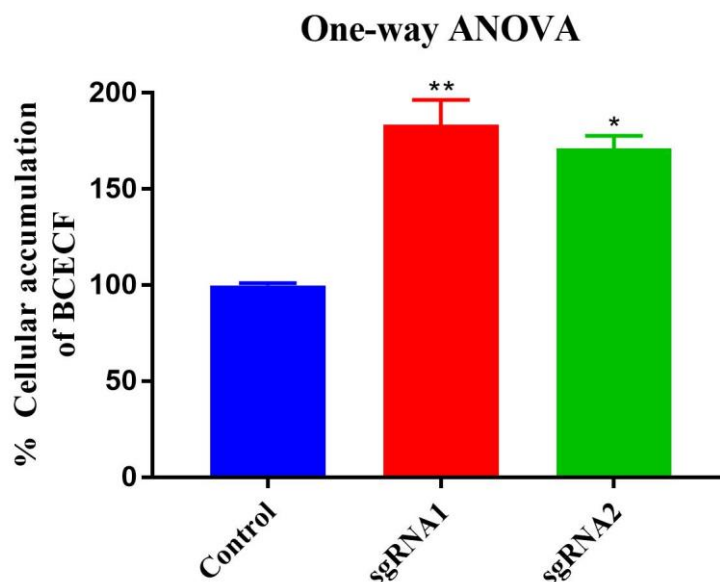


Figure 5-1: Percentage increase in BCECF accumulation for CRISPR-Cas9 transfected PANC-1 cells for both guide RNAs (sgRNA1 and sgRNA2). Data are presented as the mean and SEM from three independent experiments; n=3. Multiple comparisons between control and different treatment groups were analysed using one-way ANOVA with Dunnett's post-hoc. * $P = 0.010$ and ** $P = 0.0056$.

Figure 5-1 shows the mean percentage BCECF accumulation for transfected and control (only Cas9 transfected) PANC-1 cells before isolation of single cell clone population. We used two different guide RNAs (sgRNA1 and sg RNA2) for the ABCC5 knockout. As we can see from the above figure that mean BCECF accumulation for transfected is significantly higher than the control population. This higher BCECF accumulation not only shows successful knockout of the ABCC5 gene in the transfected population but indirectly represents a high transfection efficiency. The mean % BCECF accumulation for CUC, sgRNA1 and sgRNA2 populations are – 129.85 ± 7.74 , 183.57 ± 10.5 and 171.07 ± 5.46 respectively. BCECF accumulation was increased by 1.4 and 1.3 folds for sgRNA1 and sgRNA2 respectively.

5.2.2 mRNA Quantitation

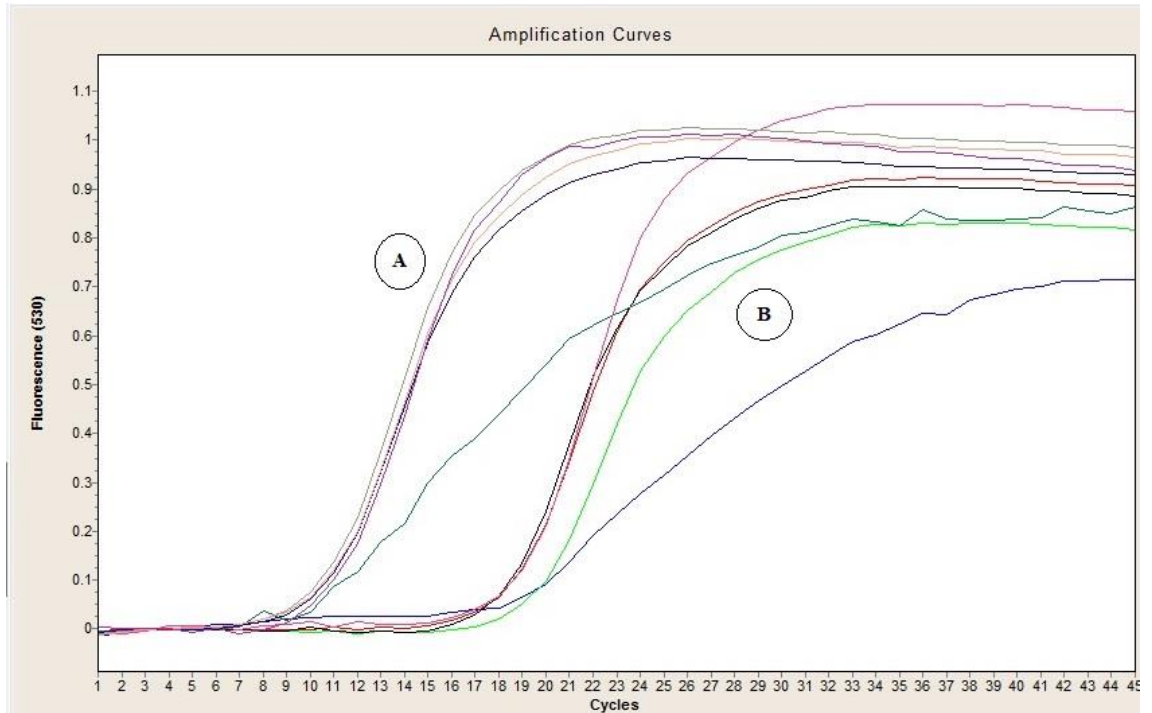


Figure 5-2: Amplification curves of target gene ABCC5 (B) and GAPDH (A) in single cell CRISPR-knock out clones of PANC-1

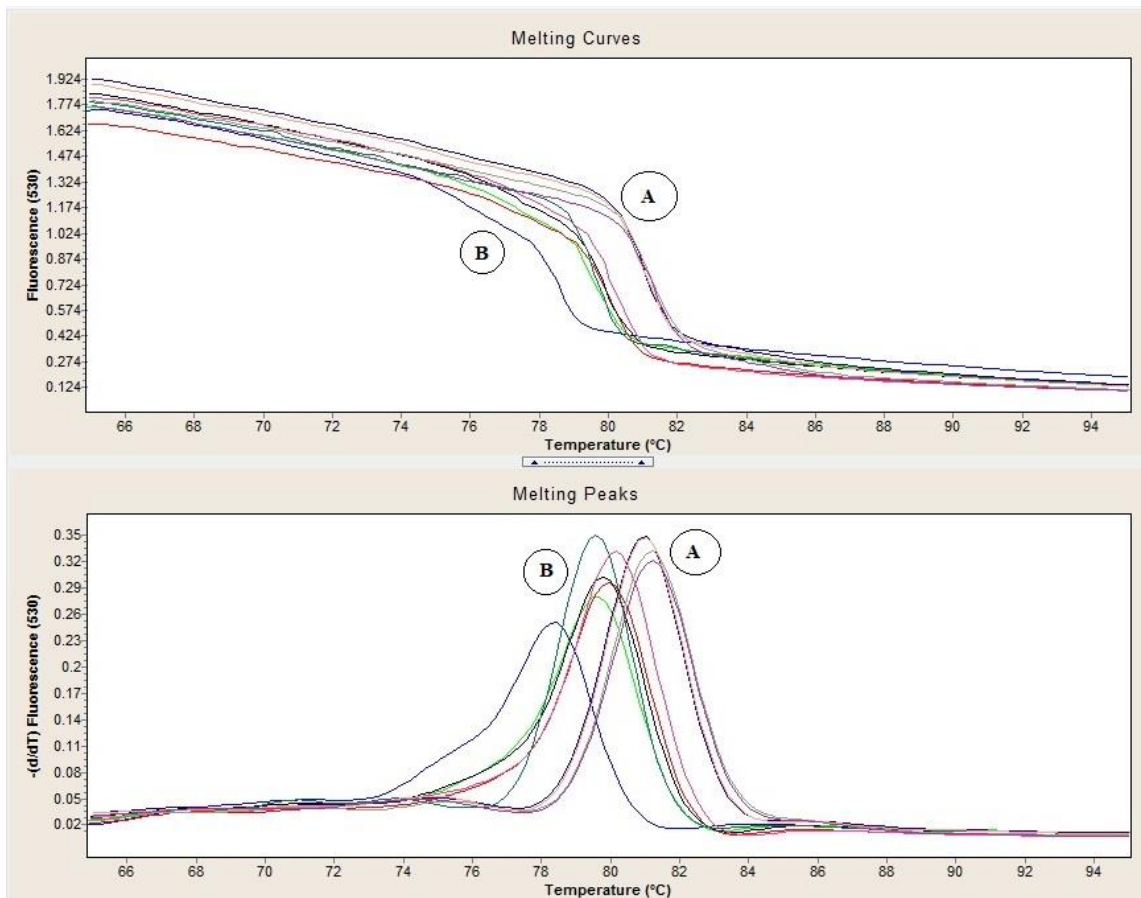


Figure 5-3: Amplification specificity by real-time PCR. Melting curves and melting peaks of ABCC5 (B) and GAPDH (A) in single cell CRISPR-knockout clones of PANC-1

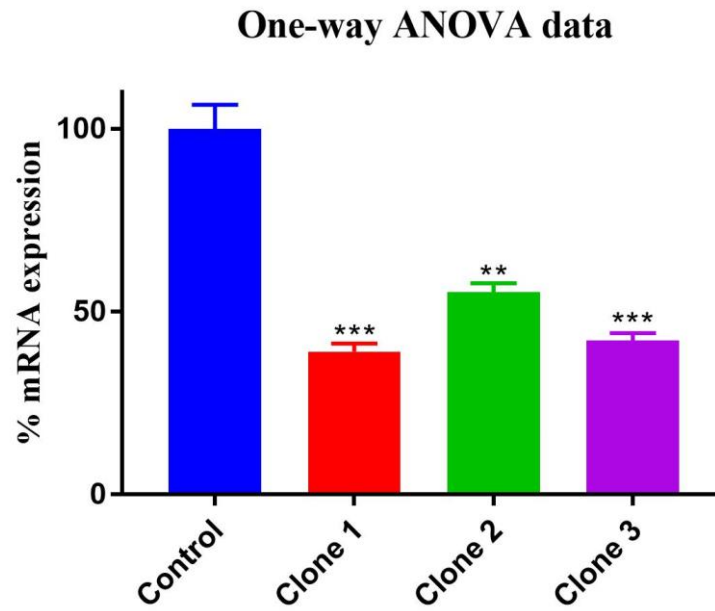


Figure 5-4: Shows mean % ABCC5 mRNA expression in single cell ABCC5 knockout clones of PANC-1.

For Clone 1, 2 and 3, (from sgRNA-2) the mean percentage of ABCC5 mRNA level – 48.33 ± 1.79 %, 56.27 ± 1.34 % and 48.46 ± 1.63 % of the control (only Cas9 transfected), respectively. Data are presented as the mean and SEM from three independent experiments; $n=3$. Multiple comparisons between control and different treatment groups were analysed using one-way ANOVA with Dunnett's post-hoc. $**P < 0.05$ and $***P < 0.005$.

5.2.3 MRP5 expression: Cell Surface Staining

Overlay Data: Surface staining

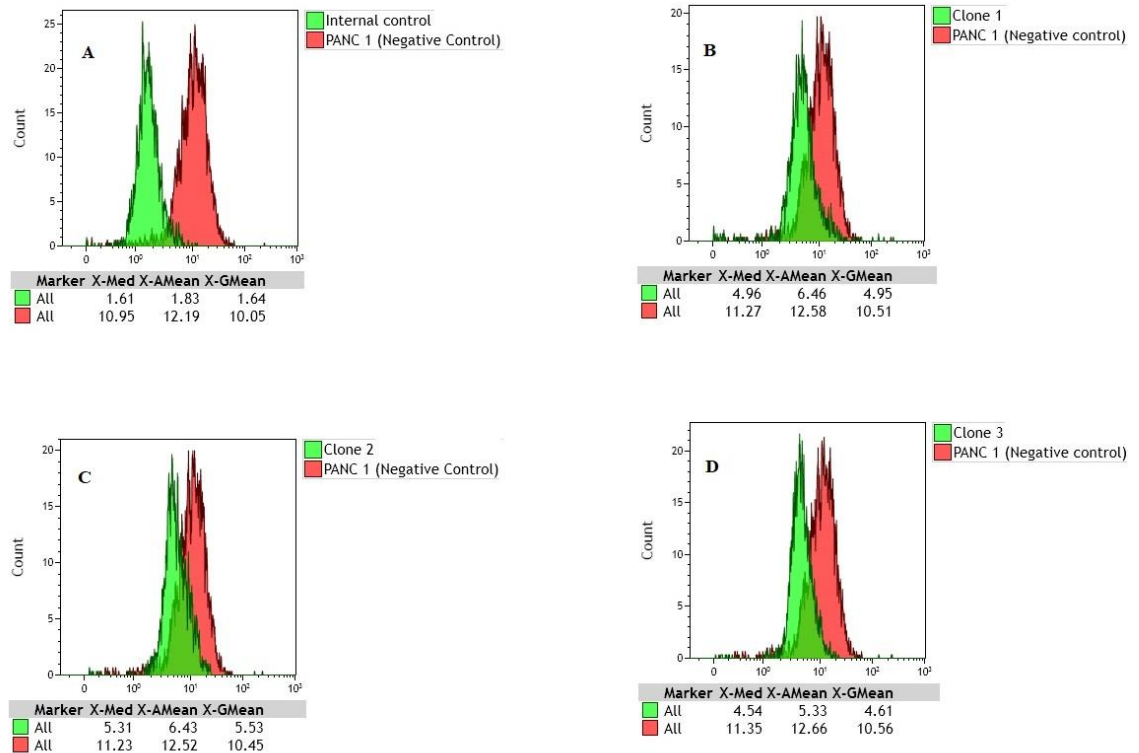


Figure 5-5: Overlay data for MRP5 surface staining in PANC-1 cells. (A) The cell surface expression of MRP5 was assessed by staining the PANC-1 cells with anti-MRP5 primary (Red) and control isotype IgG2a antibody (Green). Plots (B), (C) and (D) show MRP5 surface immunostaining in PANC-1 ABCC5 knockout clones 1, 2 and 3 (All green) and control (only Cas9 transfected) (Red), respectively

One-way ANOVA data

$P < 0.0001$

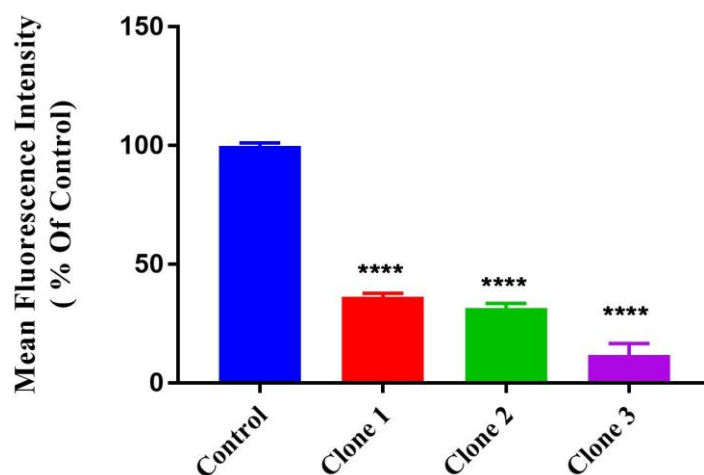


Figure 5-6: Mean MRP5 expression in ABCC5 knockout clones of PANC-1 cells. Multiple comparisons between control (only Cas9 transfected) and different treatment groups were analysed using one-way ANOVA with Dunnett's post-hoc, $n=3$. **** $P < 0.0001$

Reduction in the MRP5 levels is a direct confirmation of the successful knockout of ABCC5 activity on the protein level. A significant decrease in the MRP5 levels was seen for the PANC-1 knockout clones as compared to the control (only Cas9 transfected PANC-1 cells). The mean MRP5 fluorescence intensities for ABCC5 knockout Clone1, 2 and 3 (from sgRNA-2) as compared to control (Only Cas9 transfected Panc-1 cells) were $36.27 \pm 1.22 \%$, $31.52 \pm 1.66 \%$ and $11.86 \pm 4.87 \%$ respectively.

5.2.4 BCECF Accumulation: KO Clones

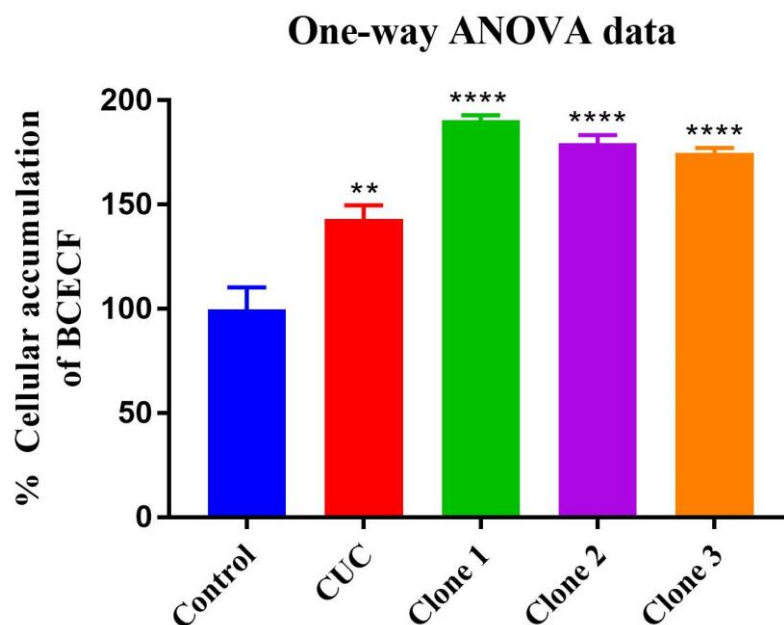


Figure 5-7: BCECF accumulation in control (only Cas9 transfected) and ABCC5 knockout clones of PANC-1 cells. CUC (10 μ M) was used as a positive control as an MRP5 inhibitor in wild-type PANC-1 cells. Data are presented as the mean and SEM from three independent experiments; $n=3$. Multiple comparisons between control and different treatment groups were analysed using one-way ANOVA with Dunnett's post-hoc. ** $P = 0.0016$ and **** $P < 0.000$.

Figure 5-7 shows ~1.8-fold increase of BCECF accumulation in PANC-1 cells derived from single-cell ABCC5-knockout clones compared with control (only Cas9 transfected). Significantly higher BCECF accumulation indicates low MRP5 activity and thus successful knockout of the ABCC5 gene in the isolated single cell clones. Mean percentage of BCECF accumulation for CUC, Clone 1, 2 and 3 (from sgRNA-2) are – 143.13 ± 5.76 , 190.36 ± 2.24 , 179.59 ± 3.29 and 174.92 ± 1.95 respectively.

5.2.5 Cleavage Detection Assay

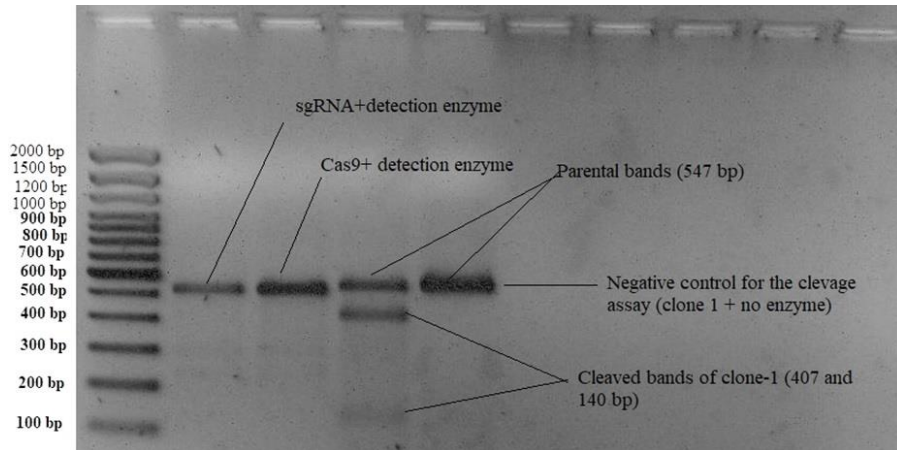


Figure 5-8 Cleavage detection assay for single cell clone 1 of the sgRNA-2 transfected cell population. Cleavage detection assay for Clone-1 of the sgRNA-2 transfected population shows two distinct cleavage bands for clone-1 confirming gene editing. Cas-9 (no guide RNA) and sgRNA-2 no Cas-9 protein) were used as the negative control for CRISPR-Cas9 transfection assay and Clone-1 without cleavage detection enzyme was used as the negative control for the assay.

5.2.6 MTT Assay

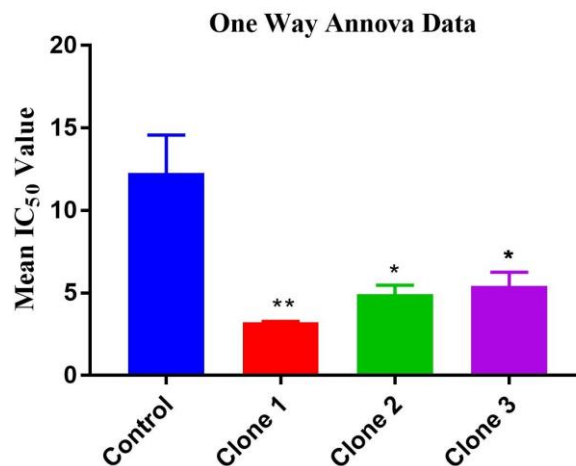


Figure 5-9: Comparison of mean gemcitabine IC₅₀ values for ABCC5 knockout PANC-1 clones. Data are presented as the mean and SEM from three independent experiments; n=3. Multiple comparisons between control and different treatment groups were analysed using one-way ANOVA with Dunnett's post-hoc. * $P < 0.05$, ** $P < 0.005$

Gemcitabine sensitivity in ABCC5 knockout clones was significantly increased as compared to the control (only Cas9 transfected). The IC₅₀ values for the control, Clone 1, 2 and 3 (from sgRNA-2) are: $12.25 \pm 2.32 \mu\text{M}$, $3.20 \pm 0.059 \mu\text{M}$, $4.92 \pm 0.55 \mu\text{M}$ and $5.43 \pm 0.82 \mu\text{M}$ respectively.

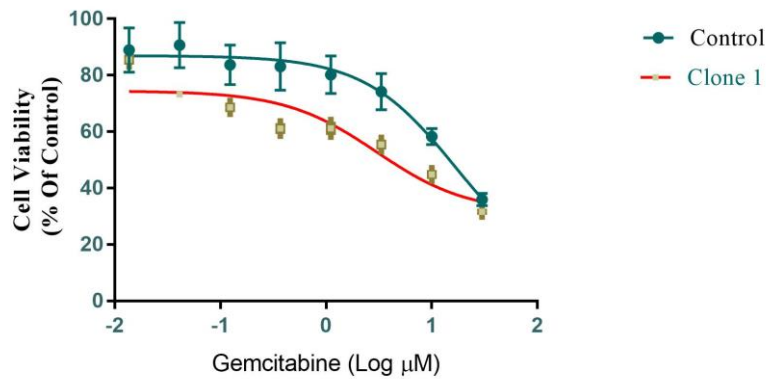


Figure 5-10: Comparison of gemcitabine cytotoxicity in ABCC5 knockout clone-1 and control in PANC-1 cells. Data are presented as the mean and SEM from three independent experiments; n=3.

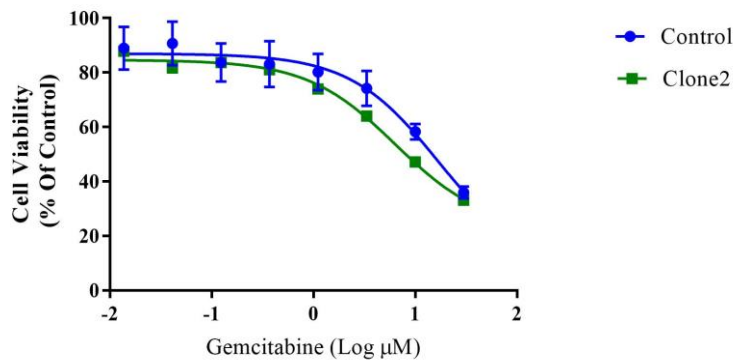


Figure 5-11: Comparison of gemcitabine cytotoxicity in ABCC5 knockout clone -2 and control in PANC-1 cells. Data are presented as the mean and SEM from three independent experiments; n=3.

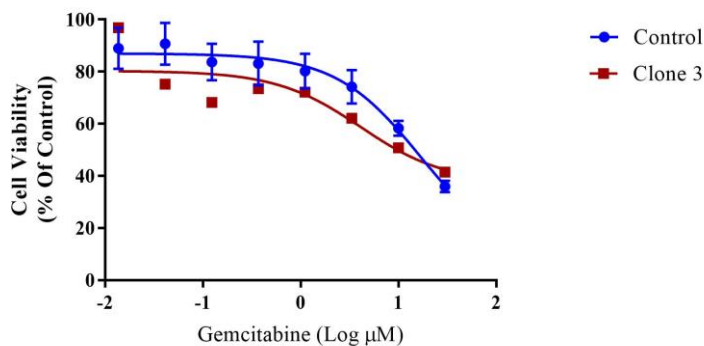


Figure 5-12: Comparison of gemcitabine cytotoxicity in ABCC5 knockout clone-3 and control in PANC-1 cells. Data are presented as the mean and SEM from three independent experiments; n=3.

Figures: 5-9, 5-10 and 5-11 are typical graphs of gemcitabine's cytotoxicity effects for ABCC5 knockout clones in PANC-1. A significant decrease in the IC_{50} values

represents a crucial role of MRP5 in drug resistance. Above results follow the similar pattern and are in accordance with our previous data of gemcitabine's sensitivity as described in chapter 4, i.e. reduction in MRP5 levels increased gemcitabine sensitivity in the knock-out clones as compared to the control (only Cas9 transfected).

5.3 Discussion

As we know, the CRISPR-Cas9 system is absent in eukaryotes, and that's why its use has significant advantages over RNAi for a variety of applications which involves the use of endogenous pathways[327]. For example, RNAi is dependent on the components like – Dicer, Argonaute etc. which are present in a limited amount in the cell and thus targeting multiple genes simultaneously becomes difficult and competitive [327]. CRISPR-Cas9 system is independent of such mechanisms and therefore has ease of use and higher efficiency over RNAi. CRISPR-Cas9 system can make a permanent change in the genome and could up or down-regulate a gene expression at the transcriptional and post-transcriptional level [327]. Whereas, RNAi is mostly limited to the knockdown of gene activity. Another significant advantage of the CRISPR-Cas9 system is minimum off-target effects.

Genome editing using CRISPR-Cas9 system involves three basic strategies – first is the use of a plasmid-based CRISPR-Cas9 system i.e. incorporating the Cas9 gene and sgRNA in the same vector to avoid multiple transfections for each component [322, 324]. The second strategy involves the delivery of a mixture of Cas9 mRNA and the sgRNA [328]. The third strategy involves the delivery of a mixture of Cas9 protein with the sgRNA [329]. The plasmid-based delivery system is quite straightforward and has ease of use by avoiding multiple transfections of each component, and it has shown good stability than the second strategy which involves the delivery of Cas9 mRNA with sgRNA [324]. Many delivery systems involving the use of plasmids are available commercially, e.g. pX260 and pX330 systems where Cas9 protein and sgRNA are expressed from the same plasmid [322]. Restriction enzyme in the cells digests the plasmid which is then ligated with an annealed oligonucleotide designed to target a specific site [324, 330]. Though, the plasmid-based system is easy to use it has some major challenges. For gene editing plasmid must be delivered to the nucleus of the cell which is relatively difficult to achieve and thus creates efficiency issues with the gene editing [324, 330]. Another issue associated with the plasmid-based system is the time of gene editing. As the plasmid inside the cells needs to be translated into Cas9 mRNA, the process of gene editing is elongated [330, 331]. One of the major problems

associated with using a plasmid-based delivery system is more off-target effects. It was seen in the past that plasmid transfection causes small and large insertions apart from the target sites in the genome resulting in off-target effects [330, 331].

The second strategy which involves the delivery of Cas9 mRNA and sgRNA into target cells edits genome once the Cas9 protein is expressed into the cells forming a sgRNA-Cas9 complex [332, 333]. The major advantage of using this system is the transient expression of Cas9 protein which limits the duration of gene editing. This system has lower off-target effects than the plasmid-based system [334]. Another advantage is that mRNA only needs to be delivered in the cytoplasm of the cells to exert its effects. This system has reported a lower cytotoxicity than the plasmid-based system [324, 334]. But due to stability issues of mRNA, this system is not very popular to use for gene editing [324].

For our experiments, we used the third strategy, i.e. delivery of Cas9 protein and sgRNA mixture via liposome into the cells for gene knockout. One of the advantages of using this approach is that Cas9 protein binds efficiently to the sgRNA and form a ribonucleoprotein complex (RNPs) [324, 335]. Direct delivery of RNPs has many advantages, e.g. high efficiency of gene editing, less time for gene editing, promoter selection and codon optimisation are not necessary, less off-target effects and low toxicity and immune responses [324, 335]. Use of RNPs is very efficient for gene editing, studies have reported up to 80% efficiency when using RNPs [324].

Apart from the type of method of transfection the delivery vehicle used for the transfection is also very important. Various delivery methods are available for transfection of the CRISPR-Cas9 complex into the cells, e.g. use of lentivirus and adeno-associated viruses, electroporation, lipid nanoparticles, microinjections, cell-penetrating peptides and electroporation [329, 336, 337]. For our experiments, we used liposomes (lipid-based delivery vehicle) for the transfection. It is one of the widely used methods for delivering RNPs into the cells in vitro and in-vivo, and some of them have also entered in the clinical stages for RNAi therapy [338, 339]. Lipid particles which are positively charged efficiently encapsulate negatively charged nucleic acids via electrostatic interactions [324]. Lipid particles not only protect the nucleic acid/ Cas9 RNPs from nucleases/proteinase but also facilitate their swift entry into the cells via endocytosis or macropinocytosis [324]. Many lipid formulations are available commercially, e.g. Lipofectamine 2000, Lipofectamine 3000, RNAiMAX for the

transfection. Studies have reported more than 70% efficiency for lipid particle-based delivery system [340].

Study of off-target effects is also very significant when it comes to genome editing, and some off-target effects have been reported and are associated with the CRISPR-Cas9 system. Off-target effects occur when CRISPR/sgRNA complex binds to the site other than the target site away from the PAM region [324]. As the sgRNA target only 20 base-pairs in the DNA sequence, to find the off-target effects in the complete human genome is very difficult, tedious and expensive [324]. We were not able to incorporate off-target studies related to the CRISPR-Cas9 system due to time constraints. Strategies like the design of sgRNA, selection of a proper target site, use of paired Cas9 nickase are recommended to minimise the off-target effects [324, 341]. As mentioned before the choice of delivery system could also have a significant impact on the off-target effects. In general, use of a non-viral delivery system has less off-target effects [341]. Some recent studies [342] have shown less off-target effects with the use of the lipid-based delivery system.

Use of limited dilution method is straightforward and simple for the isolation of single cell CRISPR-Cas9 knockout clones of the cell, but the technique does not provide any strategy to isolate the homogenous knockouts from the population. Surface staining data not only showed a significantly lower MRP5 expression (88.14 ± 4.87 % lower as compared to the control, $p < 0.0001$). Cellular accumulation of BCECF in ABCC5-knock out clones increased by $90.36 \pm 2.24\%$ ($p < 0.0001$) compared with those in wild-type confirming low MRP5 activity in the knockout clones. Our qRT-PCR data showed reduced mRNA expression in the isolated knockout clones re-confirming the heterozygous nature of the selected clones. Our MTT data showed a significant increase in the drug sensitivity in ABCC5 knockout clones re-confirming our hypothesis that MRP5 plays a crucial role in gemcitabine sensitivity. The exact nature of IC_{50} value could be more precisely predicted with the selection of homozygous ABCC5 knockout clones. From our data, we can conclude that the CRISPR-Cas9 system and its delivery using lipofectamine is efficient for gene knockout in PANC1 cells and knock-out of ABCC5 significantly increased gemcitabine sensitivity in PANC-1 cells.

Chapter 6 General Discussion

6.1 Restatement of the aims

ABC transporters are over-expressed in many cancer types and are involved directly or indirectly in MDR. In-depth screening of all ABC transporters for their roles in different cancer types could open new gates for the drug resistance related research in cancer and may help in the development of drugs or the drug delivery strategies to increase the survival rate in cancer patients. The main aim of this thesis was to evaluate the role of MRP5 in gemcitabine resistance in two human pancreatic cancer cells. ABCC5 gene silencing was achieved by using siRNA transient knockdown, and a robust qRT-PCR method was developed and validated for the evaluation of gemcitabine-related transporters and enzymes mRNA expression levels. To achieve the genome editing, CRISPR-Cas9 system was delivered by using liposome-mediated transfection.

ABC transporters are over-expressed in many cancer types and are involved directly or indirectly in MDR. In-depth screening of all ABC transporters for their roles in different cancer types could open new gates for the drug resistance related research in cancer and may help in the development of drugs or the drug delivery strategies to increase the survival rate in cancer patients.

6.2 Summary of results

In this study, we used two different approaches to modulate the gene activity in pancreatic cancer cell lines. We used siRNA and CRISPR-Cas9 mediated gene silencing methods for ABCC5 and compared the effects of gene modulation on gemcitabine cytotoxicity. To confirm the gene knockdown and knockout effects on the protein level flow-cytometer based approach was used followed by MTT assay for determination of gemcitabine IC₅₀ value in control and gene modulated cell population. Both approaches followed a similar pattern, i.e. the ABCC5 knockdown/knockout cells were more sensitive to gemcitabine.

Initially, when we started with the siRNA mediated knockdown of ABCC5 gene optimisation of few factors like housekeeping/reference gene, siRNA concentration and time of transfection were required. First to optimise the transfection time we started with 24 and 48 hours of time course and found that 48 hours of transfection time yielded more than 80% of ABCC5 gene knockdown. After optimisation of transfection time two housekeeping genes GAPDH and RPL13A were tested in both cell lines. In

our experiments, GAPDH activity was stable before and after transfection for both cell lines as compared to RPL13A, and GAPDH also had less Cp values indicating abundant expression. Thus, GAPDH was selected as the reference gene in all relative gene quantitation experiments. To find the minimum optimal concentration for ABCC5 knockdown we started with 20 and 10 pmols of ABCC5-siRNAs. Using the qRT-PCR and relative gene quantitation method ($2^{-\Delta\Delta C_t}$) we found that the minimum optimal gene knockdown concentration was 10 pmols. A maximum of 85.18 ± 1.50 % and 80.94 ± 3.26 % of ABCC5 mRNA knockdown (10 pmol) was achieved, respectively, in MiaPaca-2 and PANC-1 cells transfected with ABCC5 siRNAs. For off-target effects, we included genes related to the gemcitabine metabolism and seven other ABC transporters which could play a part in the drug resistance. The off-target effects related to siRNA mediated gene silencing were significant in both cell lines, i.e. MIA PaCa2 and PANC-1. In general, a similar trend was seen in the off-target effects, i.e. after the ABCC5 knockdown, most of the ABC transporters were seen to be upregulated while a variation was seen with the enzymes related to gemcitabine metabolism. The reason behind such upregulation in the activity of other ABC transporter genes remains un-conclusive. Initially, we started with the transfection of 3 different siRNA sequences for ABCC5, but we had to stop the use of the third siRNA due to its high off-target effects even after concentration and time optimisation.

For the MRP5 functional assay, we carried BCECF accumulation studies for MIA PaCa-2 and PANC-1 cell lines. In the initial optimisation step, we used 2 different time courses 5 and 15 minutes; the steady state was achieved in the 5 minutes time course. That's why only one-time point was used for all MRP5 functional experiments in both cell lines. Our group has previously reported concentration-dependant inhibitory effects of curcumin (CUC) on MRP5 in human pancreatic cancer cells. Thus, CUC was used as the positive control in our experiments. The cellular BCECF accumulation in ABCC5 transfected MIA PaCa-2 and PANC-1 cell lines were increased by 2 folds as compared to the control, suggesting successful gene knockdown on the protein level. To further confirm the gene knock-down on the protein level we carried cell surface staining of MRP5. The MRP5 surface immunostaining was significantly lower for the ABCC5 siRNA transfected cells as compared to the control, confirming knockdown at the protein level. More than 3 folds decrease in surface MRP5 levels was seen in the PANC-1 cells after ABCC5 silencing.

In our experiments, we also tested gemcitabine for any apoptotic effects and compared the apoptosis before and after the ABCC5 knockdown. For the apoptosis assay, three gemcitabine concentrations (800, 400 and 200 nM) were used in both cell lines. While the control and ABCC5 siRNAs have no apparent effects on cell apoptosis in both pancreatic cancer cell lines tested, more than 3 fold increase in the apoptotic population was seen for the ABCC5 knockdown cells treated with gemcitabine compared with the control. Another interesting observation made in the data was variation in apoptosis percentage with the drug concentration. It was seen that 800 nM concentration yielded a slightly low apoptosis percentage as compared to the 400 and 200 nM concentrations in MIA PaCa-2 cells. This observation indicates that pancreatic cancer cells start to build or become more resistant after a certain concentration of gemcitabine. Reason for such resistance either could be presence/development of an alternate mechanism to skip the apoptosis process.

To compare the gemcitabine cytotoxicity MTT assay was carried out for ABCC5 knock-down and control cells. From the results, we can see that gemcitabine sensitivity for the knockdown cells was increased by almost 2 fold for MIA PaCa-2 and more than 4 fold for PANC-1 cells. This signifies the role of MRP-5 in the gemcitabine resistance and proves our hypothesis that overexpression of MRP5 is one of the major reasons for gemcitabine resistance in the pancreatic cancer cells. One of the major problems with the use of siRNA was its off-target effects. It is evident from the previous results that ABCC5 knockdown sensitises pancreatic cancer cell lines MIA PaCa-2 and PANC-1, therefore, we decided to opt a method yielding permanent gene knockout with less off-target effects. This led us to switch to the CRISPR-Cas9 system which is reported to have less off-target effects and high gene editing efficiency.

For CRISPR-Cas9 transfection lipofectamineTM based transfection technique was used, as it reported to have higher efficiency and less off-target effects. Two different sgRNA sequences targeting the ABCC5 gene were used in combination with Cas9 protein. We used recommended 72 hours of transfection time to achieve higher gene knockout percentage in the transfected population. Our preliminary data of BCECF accumulation post-transfection in PANC-1 cells show significantly higher BCECF percentage. For CRISPR-Cas9 transfected cells, more than 70% increase in the BCECF accumulation indicates the high efficiency of transfection. We used limiting dilution method for isolation of single cell ABCC5 knockout PANC-1 cells. Though this method is quite straightforward, it doesn't provide any strategy to isolate a homozygous clone from the

pool of transfected cells. We carried out qRT-PCR to check the mRNA levels of isolated PANC-1 clones. The mRNA levels were significantly low for the ABCC5 knockout clones, but the presence of mRNA expression represents the heterozygous nature of the clones. MRP5 protein levels were further tested using the surface staining technique. More than 70% reduction in the MRP5 level was observed for the knockout clones as compared to the control. To assess gemcitabine's cytotoxicity MTT assay was used and a significant increase in the drug sensitivity was observed for the knockout clones as compared to the control (up to 4 fold decrease in the IC₅₀ value). For the knockout clones,

6.3 RNAi

As we already know that RNAi (siRNA) uses cell machinery to exert its effects, but still there are some barriers to the delivery of siRNA *in vivo*. After injecting the siRNA complex, it goes through the navigation system of the body and must avoid aggregation, filtration via kidneys, degradation by various enzymes and phagocytosis. One of the major problems with the delivery of the siRNA complex is its degradation by 3' exonucleases in the plasma and tissues [343-345]. The half-life of un-modified siRNA is supposed to be around a few minutes to one hour which again is an issue with the efficacy of siRNA [346]. Previous bio-distribution studies of siRNA in animals have reported high absorption into the kidneys leading to the renal clearance. Renal endothelial system (RES) up to some extent is also responsible for siRNA uptake [347]. RES is composed of phagocytic cells like macrophages and monocytes which again are involved in the clearance of siRNA from the body [348]. One of the major reasons for coating siRNA in lipids or any delivery vehicle is its negative charge. The hydrophilicity and negative charge of siRNA make its movement difficult across the biological membranes [349]. Factor like cell doubling time also has an impact on the efficacy of the transfected siRNA. It was seen in the studies that cells with low cell-doubling time have shorter silencing effects as compared to the non-dividing cells or cells with high doubling time [350]. The dilution effect in the fast-dividing cells is the rate-limiting step.

Another factor which we mentioned before is the off-target effect associated with siRNAs. Genes which share common homology with the target gene have a high probability of getting silenced by the siRNA leading and thus could create problems with the normal metabolism of the organism [344]. miRNA like silencing effects of the siRNA could lead to the silencing of a huge number of transcripts which partial

similarity is causing unpredictable cellular consequences which could be toxic to phenotype[351, 352]. Large doses to compensate short half-life could lead to the activation of immune response into the subject's body leading to very low efficacy [344]. Few of the reasons for activation of the immune response are – inflammatory cytokines, protein kinase R, dsRNA sensor and interferons[353-355]. Thus, the use of proper delivery vehicles like lipids or micelles is recommended for the delivery of siRNA in vivo. Few other practices which are in use for the safe and efficient delivery of siRNA are- chemical modification of siRNA, efficient encapsulation of siRNA to avoid degradation by cellular enzymes, use of inorganic nanoparticles like – carbon nanotubes, gold nanoparticles and quantum dots[344]. These practices increase the serum stability of the siRNA in vivo, low toxicity, vascular permeability and less renal clearance[344]. As we know that siRNA deals with various cellular components and therefore all siRNA modifications should be very carefully done, e.g., modifications may lead to a higher positive charge on the surface of Nano-particles used, causing aggregation[344]. Chemically modified siRNAs are shown to more potent, some of the common modifications involve – replacement of the phosphodiester group (PO₄) by phosphorothioate (PS) at the 3' end[356]. These modifications give stability to siRNA by avoiding degradation by the exonucleases. To increase the half-life of the siRNA a fluoro (2-F) group or 2-methoxyethyl (2'-O-MOE) is introduced in the siRNA [357]. Even though these modifications have some advantages, they can be toxic after the degradation of the siRNA into the cells. Thus, the use of the non-toxic, degradable delivery vehicle is the most popular method to increase the half-life and the efficacy of the un-modified siRNA [344]. The lipid-based delivery system of siRNA is the most popular practice in use. This system includes various lipid particles, emulsions, micelles and nanoparticles[349]. Many lipids formulations or liposomes are commercially available for the delivery of siRNAs, e.g. Lipofectamine 2000 and 3000. Cellular localisation of siRNA and concomitant siRNA activity are strongly associated with each other Chiu and colleagues [358] demonstrated that siRNAs transfected with lipofectamine were primarily localised to perinuclear regions while those delivered with a high concentration of the Nano-lipid particles were localised around nucleus and nucleolus[344]. Such change in the sub-cellular localisation was found to be associated with the efficacy. This also signifies the type and size of the delivery vehicle used for siRNAs[344]. Though cationic lipid formulations can enhance biodistribution and pharmacokinetics of the siRNA, they could also enhance the immune-stimulatory activity of siRNAs by delivering the siRNA to the endosome where immune sensors

such as TLRs are located [359]. Cationic lipid combinations have also been reported to have their own non-specific toxic effects which could also affect the gene expression [360-363]. But overall picture associated with the use of cationic lipids as the delivery vehicle is favourable for siRNA. Use of lipids gives us a major advantage by reducing the dose of siRNA and thus reduces the dose-related toxicities and off-target effects [364].

Another major problem associated with the use of siRNA is the saturation of RNAi machinery in the cells. Use of synthetic siRNAs was proposed to overcome the saturation problem because synthetic siRNAs enter the RNAi pathway at a later stage and do not require processing or export from the nucleus [365, 366]. But still simultaneous multiple targeting is an issue with the use of siRNAs, reduction in the efficacy was observed for siRNAs when transfected simultaneously. This lower efficiency suggests that the use of multiple siRNAs can saturate some components of RNAi pathways [364]. Thus, we can say that cells have limited resources to assemble RISC complex on exogenous siRNAs that could affect expression levels and siRNA function[364].

In our experiments apart from the intended downregulation of the ABCC5 gene, some off-targets were seen which included upregulation of almost all ABC transporter genes. Such off-target effect associated with the siRNA use is not new, and some studies have reported up-regulation of other transcripts apart from the targeted knockdown of the gene. Apart from the up-regulation of transcripts co-silencing of other transcripts was also seen in our experiments similar to the previously published studies[364]. This co-silencing indicates that- 1) transcripts have similar seed sites as that transfected siRNA and 2) there is a high possibility of the competition of transfected siRNA with the endogenous micro RNAs [364]. For highly expressed endogenous. Some authors have also suggested that up-regulation of other transcripts during the transfection of siRNA follow the same kinetics and dose-response as silencing of the target and off-target effects [364]. Though, off-target effects have also been associated with the concentration of the siRNA used but could not be completely eradicated even after the dose optimisation. Similarly, up-regulation of the other transcripts is dose independent of the siRNA used for silencing [364].

6.4 Liposomes & siRNA

Delivery of siRNA, particularly to the target cells or tissues, is a significant obstacle because siRNA should be delivered to the RNAi machinery for the functional gene silencing, which is present in the cell cytoplasm. siRNA delivery into the cell cytoplasm is blocked by the rapid degradation by nucleases in the serum unless they are some way or another shielded from this nuclease digestion [367]. For overcoming the issue of siRNA delivery, various systems have been proposed, for example, hydrodynamic infusion [368, 369], viral genomes [370], electroporation, liposomal and polymeric nanoparticles [371, 372]. Among distinctive delivery strategies, liposomal delivery has long been favoured because of its safety, non-immunogenicity, and also a varied range of morphologies, different sizes, tissue targeting and controlled release characteristics. Liposome more than 400 nm of size will enter cells easily and will stay there. Nanosome will act as passive targets and siRNA will act as an active target. It will be like a guided missile to the target [367].

6.5 CRISPR-Cas9

The “GeneArt™ Platinum™ Cas9 Nuclease” was purchased from Invitrogen and is *Streptococcus pyogenes* Cas9 nuclease protein containing a nuclear localization signal (NLS) for targeting to the nucleus. As mentioned before the family of Cas9 proteins have characteristic RuvC and HNH nuclease domains [373]. While HNH is a single nuclease domain RuvC is further sub-divided into three domains – RuvC I close to the N-terminal of Cas9 protein and RuvC II and III flanking the HNH domain [373].

The structural details of the RNA guided Cas9 (*Streptococcus pyogenes*) cleavage show a huge structural rearrangement between unbound apo-Cas9 and Cas9 in the complex with CrRNA and tracrRNA creating a centralised channel of RNA-DNA heteroduplex [374]. Another structural study of Cas9-sgRNA complex with the complementary target DNA strand proposed a new domain organisation where α -helical recognition (REC) lobe and nuclease lobe (NUC) consisting HNH domain have shown to assemble RuvC subdomains and PAM-interacting (PI) c-terminal region [375]. Thus, these two studies propose the idea that Cas9 protein not integrated with the target DNA sequence or the sgRNA show an autoinhibited conformation where the RuvC domain blocks the active HNH domain site and is placed away from the REC lobe [374]. Thus, apo-Cas9 is unable to perform any DNA cleavage due to the steric hindrance [375]. The structure

of *Streptococcus pyogenes* Cas9 protein provides a scaffolding for the execution of sgRNA-Cas9 complex. Domain recombination or truncation is one of the proposed approaches for minimising the size of Cas9 protein because REC2 domain in the Cas9 protein of *Streptococcus pyogenes* is poorly conserved in shorter orthologs [375]. In the studies, it was found that Cas9 mutants of *Streptococcus pyogenes* lacking REC2 domain have approximately 50% of cleavage activity as compared to the wild-type Cas9 [373, 375]. Thus, re-combinations of ortholog domains, peptides and truncation could help in the production of Cas9 protein variant which could be optimised for different parameters in the sgRNA-Cas9 complex like – DNA cleavage and binding or overall protein [373].

The specificity of *Streptococcus pyogenes* Cas9 is well characterised, but some previous studies [330, 376-378] have shown the tolerance of Cas9 protein to mismatches. Such tolerance throughout the guide sequence is very sensitive to the number, position and distribution of mismatches. Though PAM sequences are responsible for the specificity, overall sequence match plays a very crucial part in the specificity [373]. Thus, off-target sites followed by the PAM sequence could also lead to the cleavage and may cause serious problems [373]. For CRISPR-Cas9 to exert its effect homology of sgRNA with target DNA is necessary; Cas9 semi transiently binds with an only short stretch of complementary sequence. This indicates that Cas9 may have a few off-target sites to bind but cleaves very small fraction of that [379]. Thus, off-target effects could widely vary depending on the Cas9 protein used and sgRNA and PAM sequence [373]. Another factor which could lead to a higher off-target effect percentage is the concentration of the Cas9 protein [330]. Thus, concentration optimisation to a “low effector dose” may result in low off-target effects. Apart from the concentration, the time of Cas9 expression is also one of the major factors which could result in off-target effects, i.e. higher time of expression leads to a higher probability of off-target effects [373].

PAM is one of the most crucial features of CRISPR-Cas9 target specific cleavage activity. PAM is present in the 3' end of the DNA and helps Cas9 protein in target search mechanism [373]. Some of the studies [374, 375, 380] have also suggested that apart from the target specificity PAM is also involved in the transition of initiating the Cas9 binding to the target and the cleavage confirmations. After recognition of the PAM site and integration of the sgRNA-Cas9 protein complex to the target site unwinding of the DNA occurs. The complete mechanism behind the unwinding of the

DNA is still not completely understood [380]. After unwinding of the DNA Cas9 creates a double-stranded break by HNH and RuvC domains [380]. The target sequence length of the Cas9 protein is also dependent on the complexity of PAM sequence, e.g. 5'NGG of *Streptococcus pyogenes* Cas9 protein allows it to target ~8 bp within the human genome [381]. The PAM sequence is very specific to each ortholog of Cas9 protein even though they are from same species, e.g. 5'-NNAGAAW for *Streptococcus thermophilus* CRISPR1 [382] and 5'-NGGNG for *Streptococcus thermophilus* CRISPR3 [383].

Cas9 protein could either be coupled with crRNA or tracrRNA or with a chimera of both known as sgRNA [374, 377, 381]. As we now know that the sgRNA ~20 bp long sequence and matches the target site. While human genome editing, in case of *Streptococcus pyogenes* Cas9 an early discrepancy of higher levels of NHEJ indels in the same target site was observed [381]. This observation was prominent with the use of the engineered dual guide RNA system and very low with the use of engineered sgRNA (+48) scaffold, which only contained up to the 48th base of tracrRNA [374]. It was also observed that even though the sgRNA(+48) is sufficient enough for in vitro editing and yielded good results an extension of the 3' tracrRNA sequence preserved several hairpin structures (sgRNA(+72) and sgRNA(+84)) were more efficient in editing in vivo [374, 376, 377]. This additional stem loops provide the structural stability to the sgRNA [376] and helps in the formation of more stable sgRNA-Cas9 protein complex [375]. Thus, the sgRNA design is very crucial for efficient genome editing by the CRISPR-Cas9 system.

6.6 Future Directions

Another approach which could increase the efficacy is co-delivery of siRNA and drug in a nanocarrier. This will increase the in vivo tumour accumulation of the mixture via both passive and active tumour-targeting abilities and thus, the efficacy of the drug. Hence, the multifactorial approach of the nanomedicine could help in overcoming the drawbacks of the current regimen. By using short guide RNAs in the CRISPR-Cas9 system, multiplexed targeting can be achieved at an unprecedented scale. Ease of Cas9 use, its high efficacy and specificity and the possibility of multiplexed modifications have opened a vast range of its biological applications [373]. Such customisable DNA domains have many advantages which go beyond genome editing. A combination of such customisable domains with modular, sequence-agnostic functional effector domains allows flexible selection of perturbations at will [373]. This could include the

substitution of modular enzymatic component leading to increase in the arsenal of the gene-editing tools. Furthermore, a fusion of inducible proteins with the genome and epigenome-modifying enzymes could give us an edge on the control of this random process [373].

Metagenomic analysis and bioinformatics studies of archaea and bacteria containing CRISPR loci may lead us to the discovery of new Cas9 proteins with different PAMs to increase target range [384]. Thus, transfection of multiple Cas9 proteins with different PAMs could lead to orthogonal genome engineering. Such approach could allow us to make simultaneous changes at the multiple sites in the same genome at the same time, e.g. *Streptococcus pyogenes* Cas9 protein, and NmCas9 could be used simultaneously for independent nuclease activity [373, 384]. Specificity due to the PAM sequence could also be modified, e.g. orthologous replacement of the PAM-interacting domain in *Streptococcus thermophilus* CRISPR3 Cas9 with the corresponding domain of *Streptococcus pyogenes* Cas9 resulted in the change of PAM sequence from 5'-NGGNG to 5'-NGG [375]. Thus, PAM sites can be re-engineered to meet the needs, and short Cas9 orthologs could be created with a customisable PAM domain [373].

As we know that Cas9 nuclease creates a blunt-ended dsDNA break, *Streptococcus pyogenes* Cas9 could be altered to create a single-stranded DNA break by catalytically inactivating the RuvC or HNH domains [374, 385]. As these single-stranded breaks are repaired by the high-fidelity base excision repair pathway, Cas9 nickases could be exploited for more specific NHEJ as well as HDR [386]. To increase the efficiency and specificity on-target double-stranded break a double nicking strategy similar to ZFNs and TALENs could be used [377]. Truncated sgRNAs with 2-3 nucleotides could also increase the efficacy and specificity. More structural and functional studies of Cas9 via protein engineering could lead us to a more specific and efficient Cas9 protein [373]. CRISPR-Cas9 system is the most popular gene editing tool in the present time, and various efforts are being made to improve its efficiency and specificity. But apart from its on-target effects one of the most important pitfall to be considered while using this method is its off-target effects. Up until now studies related to the Cas9 off-target effects are dependent on in silico computational prediction or in vitro selection [373]. Thus, the activity of Cas9 which is unpredictable by sequence homology to the sgRNA remains unaccountable. Therefore, unbiased profiling methods are needed to increase our understanding of the off-target effects related to Cas9 activity. Development of the techniques for detection of the double-stranded break in DNA could help us in

achieving a wide-ranging map of Cas9-induced off-target indels. Techniques like Cas9-based chromatin immunoprecipitation sequencing (CHIP-seq) analysis at various target sites could help us to better understand all the binding related discrepancies [379]. As the CRISPR-Cas9 method deals directly with gene editing, a better understanding of Cas9 cleavage and binding in terms of epigenetic states and chromatin accessibility could lead us to design more specific sgRNA. A better understanding of the Cas9 cleavage and its binding is required in the cells with different chromatin states, especially in the post-mitotic cells where genomic architecture is quite stable [373]. Thus, a better understanding of the above-mentioned points will help us to improve our knowledge with the CRISPR-Cas9 method and could lead to protein engineering and metagenomic mining efforts to improve the efficacy of this approach.

In a recent study, it was found apart from the on-target indels which are usually 20 bp in length some indels measuring up to a few hundred base pairs were also seen. Although the frequency of such indels is very low still their presence and association with CRISPR-Cas system are of concern [387]. Some of the studies related to paired gRNAs have reported more complex genotypes, e.g. exogenous and endogenous insertions, inversions and a few but unexpected deletions. Single sgRNAs have also reported deletions up to 600 bp in mouse zygotes and up to 1.5 kb in haploid cancer cell lines [387]. Furthermore, the analysis of alleles generated due to such unexpected mutations is assessed by amplification of very short regions (<1 kb) [387]. Such short regions are with either around the specific target site or are assessed at the potential off-target site(s) predicted using bioinformatics approach; such an approach limits the scope of assessment [387]. We now know about the abnormal nature of the cancer genome and its DNA repair mechanism and study of such cancer cell lines for Cas9 based lesions makes extrapolation to normal tissues and cells very difficult [387].

Currently one of the most popular methods for the delivery of the CRISPR-Cas9 system in vivo is the use of viral-based delivery vehicles, e.g. adeno associated viruses (AAV) or lentivirus. A major reason for using such a delivery vehicle is their low immunogenicity in the host, reduced oncogenic risk and serotype specificity [373, 388]. Albeit all these advantages their payload capacity is still not very impressive when it comes to the delivery of fragment length >4.5 kb, e.g. Cas9 nuclease-encoding gene from *Streptococcus pyogenes* [388]. Therefore, more efficient delivery vehicles need to be developed for the delivery of the CRISPR-Cas9 system in vivo. Use of non-viral approaches currently includes liposomes, molecular trojan horse and the cell penetrating

peptides [388]. On the contrary, efforts are also being made on designing of smaller Cas9 orthologs. But currently one of the major problems associated with shorter Cas9 orthologs is their long PAM sequences e.g. SpCas9 (5'-NNAGAAW from *Streptococcus thermophilus* CRISPR1 or 5'-NNNNGATT from *Neisseria meningitidis*) [389, 390], whereas some longer orthologs have more relaxed PAMs (5'-NG from *Francisella novicida*) [391]. Even though the CRISPR-Cas9 system is independent of any cellular machinery, it still depends on the cellular DNA repair mechanism for NHEJ and HDR [373]. In many cases, the frequency of HDR is very low yielding to the low efficacy. Such low efficacy is not very significant for in vitro experiments because the cells with HDR can be enriched using FACS approach. But its practicality reduces in the case in vivo experiments [373]. Homologous recombination proteins are very low in the cells which have already passed the G2 phase of the cell cycle making HDR based gene editing quite difficult [373]. Thus, the development of methods to increase the HDR rate or effective gene insertions are urgently needed.

Furthermore, most of the CRISPR-based approaches are Cas9 based, i.e. they are from the type II CRISPR system. Thus, still there is a wide scope of developing and accessing the other types of CAS protein approaches which could open new research horizons, e.g. Cas RAMP module (Cmr) proteins identified in *Pyrococcus furiosus* and *Sulfolobus solfataricus* [392] constitute an RNA-targeting CRISPR immune system, forming a complex guided by small CRISPR RNAs that target and cleave complementary RNA instead of DNA

6.6.1 Multi-targeting for gemcitabine related genes

CRISPR-Cas9 system comes with the advantage of simultaneous targeting of multiple genes. Gemcitabine and its combination are the most popular treatment regimens in the present and pharmacokinetics of gemcitabine are well characterised. Our data (Refer to chapter 4 and 5) in the thesis also show that MRP5 targeting helps in increasing the gemcitabine sensitivity. Thus, to increase the drug efficacy CRISPR-Cas9 system could be used to target the other genes involved in the gemcitabine metabolism, e.g. dCK, CDA and RR enzymes. This could also help in the evaluation of roles of various factors involved in the drug metabolism and could increase pharmacogenomics related drug information. Though a lipid formulation of CRISPR for in vivo purposes is still in its initial stages, it is a very potent tool for multiple targeting. A combination of different sgRNAs for different genes with Cas9 protein could be coated with nanoliposome for simultaneous transfection followed by gemcitabine treatment.

Another approach which could be used is the co-delivery of a combination of the CRISPR-Cas9 system with gemcitabine in a Nano-liposome. The later suggested approach could also increase the gemcitabine efficacy and could be more effective if the combination of different sgRNAs acting on different molecular targets (e.g. gemcitabine metabolism-related genes or factors involved in apoptosis) are used. Such an approach of CRISPR-Cas9/gemcitabine co-transfection with multiple gene targeting could not only increase the efficacy but could also lead to personalised therapy in cancer patients.

6.6.2 Limitations of gemcitabine Therapy:

Gemcitabine; a weak base with pKa 3.6, is a strong anticancer drug usually utilized for the treatment of pancreatic disease and other solid tumours, for example, lung growth, bladder malignancy and metastatic bosom growth [393-395]. Besides, gemcitabine is a prodrug that must be taken up by the cell and phosphorylated inside of the cell to form the active moiety, gemcitabine triphosphate, which restrains the combination of DNA [394, 396]. Nevertheless, after systemic organization, gemcitabine is quickly changed over into the dormant metabolite by cytidine deaminase and discharged through the pee with a half-life running from 9 to 22 min, which confines its anti-cancer effects [397-400]. Moreover, multidrug resistance (MDR) has been accounted for decreasing the clinical efficiency of gemcitabine [396, 401].

Past first-line therapy, alternatives for metastatic pancreatic malignancy turn out to be less clear, as patients frequently show fast clinical degeneration and are no more suitable contender for extra treatment past best steady care. One cooperative group trial reported that just 45% of patients with advanced pancreatic cancer (APC) went ahead to get extra treatment taking after movement on cutting-edge study treatment [402]. Various little imminent single-arm studies have assessed both cytotoxic and/or focused on specialists in the setting of gemcitabine-refractory disease, for the most part exhibiting low reaction rates and progression-free survival of a couple of months [403-409]. Results from a randomized German trial for the second-line treatment of APC (CONKO-003) recommended a week by week regimen called OFF (oxaliplatin, 5-FU given as a 24-hour mixture, and folinic acid) may enhance persistent results in patients refractory to gemcitabine [409, 410]. At present, there is no recognized standard of care in this setting.

Due to the un-favourable diagnosis, there is an urgent need to develop the diagnostic biomarker for early detection. Biomarkers like - CA19-9, Macrophage inhibitory

cytokine 1 and PAM4, Genetic and epigenetic markers (KRAS) are in research pipeline [411]. Development of treatment predictive biomarkers is also necessary to predict the outcome of chemotherapy e.g. low hENT, CNT and dCK expression results in less gemcitabine efficacy [411]. Thus, a more personalised approach for treatment in pancreatic cancer is needed which should involve screening for various markers and genes to increase drug efficacy and thus the overall patient survival.

6.6.3 Liposomes

Liposomes are nontoxic vesicular drug bearers with an aqueous centre encased in one or more phospholipid bilayers with the ability to accommodate both water solvent and lipid soluble drugs. It has been all around reported that the cytotoxicity of many anti-cancer drugs can be augmented both in vitro and in vivo by utilizing liposomes as transporters [412-414]. Furthermore, cell culture studies have shown that liposomes are taken into cells by means of endocytosis that may build the effectiveness of drug conveyance for mixes, for example, gemcitabine that requires active transport into the cell [394]. PEGylated liposomes, for instance, Doxil® have been utilized as bearers for various drugs to get a more extended flowing time in vivo [396, 415-417].

Remedial Alternative

Remedial alternatives for patients with advanced pancreatic growth range from gemcitabine monotherapy to numerous drug regimens, contingent upon age, performance status, comorbid conditions, and patient and doctor penchant [409]. One of the rate-limiting steps in the gemcitabine mechanism is its uptake by the transporter (especially hENT1). Thus, less uptake of the drug results in decreased cytotoxicity resulting in tumour growth. Therefore, gemcitabine delivery to the tumour cells is a crucial aspect of gemcitabine treatment/chemotherapy. Liposomes are one of the safest and efficient drug delivery vehicles [409].

Nanosomes

Nanosomes are nano-sized liposomes, and conjugated agents [418], usually 30-100 nm in size. Nanosomes are further subdivided into stabilized and non-stabilized or conventional nanosomes. Nanospheres and dendrimers are subclasses of nanoparticles. Conjugated agents comprise polymer-linked and PEGylated agents [419]. One of the most important characteristics of the bi-layer-forming molecules is their designated polar and nonpolar regions. Such an arrangement allows the hydrophobic drug to get easily encapsulated in the lipid bilayer when the molecule is hydrophilic [420, 421].

Nanoliposomes are being widely used in biochemistry, cosmetics, medicine and biology [420]. Nanoliposomes have the capability of increasing the bioavailability of the drug *in vivo* by preventing interactions of the transported drug and provide more stability [420]. Nanoliposomes have also been found to be associated with low toxic side effects [422]. Apart from low toxicity use nanoliposomes has few advantages like customisable size and surface of the particle (for biocompatibility) and biodegradability [423]. Few techniques can be used to avoid the degradation of nanoliposomes by macrophages e.g. PEGylation that is coating the particle surface with polymers like polyethylene glycol. PEGylation also helps in increasing the stability and circulation half-time [420, 424]. Efforts are being made to increase the target specificity of the nanoliposomes. Coating the surface of nanoliposomes with ligands capable of recognizing and binding to a particular cell group are in process [420]. Herceptin/trastuzumab antibody which targets the Her-2 antigen expressed by certain breast cancer cells, folate to target folate receptors which are overexpressed in a subset of ovarian cancer cells to target integrins that are upregulated by proliferating endothelial cells of the tumour vasculature [425, 426]. Up to 15 liposomal-drug formulations for different conditions are in clinical use [420]. The process by which these agents preferentially accumulate in a tumour and tissues is called the enhanced permeation and retention effect [427]. There are more than 100 nanosomal, nanoparticle, and conjugated anticancer agents that are in preclinical and clinical improvement. A new generation of carrier-mediated agents is still in preclinical and clinical development [419]. These new generation carrier-mediated agents can accommodate containing two anticancer agents within a single nanosome and antibody-targeted nanosomes or nanoparticles that may improve selective cytotoxicity [419, 428-431].

DaunoXome (liposomal daunorubicin) for blood tumours, Doxil and Lipid-dox (PEGylated liposomal doxorubicin) for ovarian and breast cancers, and for Kaposi's sarcoma patients are some of the liposomal formulations for cancer treatment [420, 432]. For pre-treated metastatic breast cancer patients US Food and Drug Administration (FDA) has approved Nab-paclitaxel (Abraxane) to overcome the solvent-related problems of paclitaxel [433]. Few of the liposomal formulations have also reached the stage of clinical trials e.g. nanoliposomal CPT-11, a Phase I study, is used for patients with recurrent high-grade gliomas [420]. CPT-11 is a multi-component liposomal formulation containing a camptothecin derivate and a topoisomerase-I inhibitor [420, 434]. Other liposomal drug formulations include, SPI-077 (liposomal

cisplatin for solid tumours), CPX-351 (cytarabine: daunorubicin for acute myeloid leukemia), Lipoplatin (cisplatin for non-small cell lung cancer), ThermoDox (a thermosensitive doxorubicin for hepatocellular carcinoma, and other advanced cancers), and Stimulax (an anti-MUC1 cancer vaccine for non-small cell lung cancer) [420].

Pancreatic cancer has complex biology, thus, targeting one gene or pathway may not be enough [435]. There is an immediate need to develop a multi-gene target treatment strategy that recognises various proteins and inhibit several pathways [435]. Nanosomal delivery of siRNA targeting various genes of different pathways followed by chemotherapy could yield better results and may increase the overall survival of the patient.

6.6.4 Specific targeting of Cancer cells

Formulation of siRNA or CRISPR-Cas9 with lipids or lipophilic conjugates such as cholesterol could increase their cellular uptake and could be used for more specific tissue/cell targeting. One of the major drawbacks related to present chemotherapy approach is its toxic side effects leading to the death of normal or non-cancerous cells. Use of lipid-based delivery vehicle may help in targeting more specifically. Lipids can be coated with either antibodies or ligands and can be customised to target a specific tissue or group of cells. Up-till now targeted delivery is not successfully optimised for many cell types and tissues. One of the major reasons for the underdevelopment of such targeting method is the lack of knowledge of associated effects, e.g. development of immunogenicity or other adverse effects related to such an approach. Furthermore, these methods are primarily tested in mouse first, and there are significant differences in the mouse and human innate immune responses which need to be scanned for the safety. The pancreatic tumour microenvironment plays a very important role in the drug therapy response. One of the major barriers to chemotherapy of pancreatic cancer is its dense stroma which consists of various cell types e.g. cancer-associated fibroblasts, inflammatory cells and nerve cells. The stroma also contains extracellular matrix components like collagen, fibronectin and laminin. Thus, penetrating this complex stroma could enhance the drug response rate.

Immunotherapy

Another suggested approach for pancreatic cancer treatment is the use of immune therapy. One of the main reasons for the survival of cancer cells is escape from the immune response. This property of cancer cells has been defined as one of the

hallmarks of cancer [436]. Inhibition of T-cell checked point proteins and programmed cell death have shown some good response in many cancer types [436]. However, to this date pancreatic cancer has not shown much response to this approach [436]. Probably because of the immunosuppressive nature of the pancreatic cancer tumour microenvironment. More studies are needed in this area to increase the response rate of immunotherapy in pancreatic cancer.

6.7 Concluding Remarks

The main aim of this study was to determine the effect of MRP5 expression on the gemcitabine cytotoxicity and to compare the effects of cytotoxicity before and after the modulation of ABCC5 activity. In our study, we found that MRP5 plays a very significant role in MDR and can influence the gemcitabine cytotoxicity. Compared with the control cells, siRNA/CRISPR-Cas9 treated pancreatic cancer cells showed significantly low IC₅₀ values for gemcitabine. One of the major problems encountered with the use of siRNAs is the off-target effects. The off-target effects were assessed for a few the genes involved in gemcitabine uptake, efflux and metabolism. Our results showed upregulation of seven ABC transporters incorporated in the study while some parallel knockdown effects were seen for CDA and dCK involved in gemcitabine metabolism. Such off-target effects made it complicated to predict the exact nature of IC₅₀ changes after ABCC5 modulation. Though, siRNA knockdown of ABCC5 confirmed our hypothesis that MRP5 plays a crucial role in MDR. So, we considered creating an ABCC5 knock-out cell line with the CRISPR-Cas9 system. CRISPR-Cas9 system is reported to have low off-target effects and edits the genome permanently. The comparison of drug cytotoxicity of the knock-out clones with the control followed a similar trend of reduction in the IC₅₀ values; re-confirming the hypothesis. Screening tumour MRP5 expression levels to select patients for treatment with gemcitabine-based regimen alone or in combination with MRP5 modulation, could improve outcomes of pancreatic cancer treatment.

References

1. Adamska, A., A. Domenichini, and M. Falasca, *Pancreatic Ductal Adenocarcinoma: Current and Evolving Therapies*. Int J Mol Sci, 2017. **18**(7).
2. Von Hoff, D.D., et al., *Increased survival in pancreatic cancer with nab-paclitaxel plus gemcitabine*. N Engl J Med, 2013. **369**(18): p. 1691-703.
3. Vaccaro, V., I. Sperduti, and M. Milella, *FOLFIRINOX versus gemcitabine for metastatic pancreatic cancer*. N Engl J Med, 2011. **365**(8): p. 768-9; author reply 769.
4. Gnanamony, M. and C.S. Gondi, *Chemoresistance in pancreatic cancer: Emerging concepts*. Oncol Lett, 2017. **13**(4): p. 2507-2513.
5. Maisonneuve, P. and A. Lowenfels, *Epidemiology and Prospects for Prevention of Pancreatic Cancer 2nd ed*. Pancreatic Cancer, 2017: p. 1-16.
6. Siegel, R.L., K.D. Miller, and A. Jemal, *Cancer statistics, 2016*. CA: a cancer journal for clinicians, 2016. **66**(1): p. 7-30.
7. Weir, H.K., et al., *The past, present, and future of cancer incidence in the United States: 1975 through 2020*. Cancer, 2015. **121**(11): p. 1827-1837.
8. Schulte, A., et al., *Association between Helicobacter pylori and pancreatic cancer risk: a meta-analysis*. Cancer Causes & Control, 2015. **26**(7): p. 1027-1035.
9. Xu, J.-H., et al., *Hepatitis B or C viral infection and risk of pancreatic cancer: a meta-analysis of observational studies*. World journal of gastroenterology: WJG, 2013. **19**(26): p. 4234.
10. Wolfgang, C.L., et al., *Recent progress in pancreatic cancer*. CA Cancer J Clin, 2013. **63**(5): p. 318-48.
11. Chari, S.T., et al., *Probability of pancreatic cancer following diabetes: a population-based study*. Gastroenterology, 2005. **129**(2): p. 504-511.
12. Schellenberg, D., et al., *¹⁸Fluorodeoxyglucose PET is prognostic of progression-free and overall survival in locally advanced pancreas cancer treated with stereotactic radiotherapy*. International Journal of Radiation Oncology• Biology• Physics, 2010. **77**(5): p. 1420-1425.
13. Tamm, E.P., et al., *Imaging of pancreatic adenocarcinoma: update on staging/resectability*. Radiologic Clinics, 2012. **50**(3): p. 407-428.
14. Vauthey, J.-N. and E. Dixon, *AHPBA/SSO/SSAT Consensus Conference on Resectable and Borderline Resectable Pancreatic Cancer: rationale and overview of the conference*. Annals of surgical oncology, 2009. **16**(7): p. 1725-1726.
15. Bailey, P., et al., *Genomic analyses identify molecular subtypes of pancreatic cancer*. Nature, 2016. **531**(7592): p. 47.
16. Xu, Z., et al., *Pancreatic cancer and its stroma: a conspiracy theory*. World journal of gastroenterology: WJG, 2014. **20**(32): p. 11216.
17. Garrido-Laguna, I. and M. Hidalgo, *Pancreatic cancer: from state-of-the-art treatments to promising novel therapies*. Nature reviews Clinical oncology, 2015. **12**(6): p. 319.
18. Liu, Q., Q. Liao, and Y. Zhao, *Chemotherapy and tumor microenvironment of pancreatic cancer*. Cancer Cell Int, 2017. **17**: p. 68.
19. Neoptolemos, J., et al., *Adjuvant chemoradiotherapy and chemotherapy in resectable pancreatic cancer: a randomised controlled trial*. The Lancet, 2001. **358**(9293): p. 1576-1585.

20. Neoptolemos, J.P., et al., *Adjuvant chemotherapy with fluorouracil plus folinic acid vs gemcitabine following pancreatic cancer resection: a randomized controlled trial*. *Jama*, 2010. **304**(10): p. 1073-1081.
21. Oettle, H., et al., *Adjuvant chemotherapy with gemcitabine vs observation in patients undergoing curative-intent resection of pancreatic cancer: a randomized controlled trial*. *Jama*, 2007. **297**(3): p. 267-277.
22. Uesaka, K., et al., *Adjuvant chemotherapy of S-1 versus gemcitabine for resected pancreatic cancer: a phase 3, open-label, randomised, non-inferiority trial (JASPAC 01)*. *The Lancet*, 2016. **388**(10041): p. 248-257.
23. Neoptolemos, J.P., et al., *Comparison of adjuvant gemcitabine and capecitabine with gemcitabine monotherapy in patients with resected pancreatic cancer (ESPAC-4): a multicentre, open-label, randomised, phase 3 trial*. *The Lancet*, 2017. **389**(10073): p. 1011-1024.
24. Conroy, T., et al., *FOLFIRINOX versus gemcitabine for metastatic pancreatic cancer*. *New England Journal of Medicine*, 2011. **364**(19): p. 1817-1825.
25. Wang-Gillam, A., et al., *Nanoliposomal irinotecan with fluorouracil and folinic acid in metastatic pancreatic cancer after previous gemcitabine-based therapy (NAPOLI-1): a global, randomised, open-label, phase 3 trial*. *The Lancet*, 2016. **387**(10018): p. 545-557.
26. Gillen, S., et al., *Preoperative/neoadjuvant therapy in pancreatic cancer: a systematic review and meta-analysis of response and resection percentages*. *PLoS medicine*, 2010. **7**(4): p. e1000267.
27. Ferrone, C.R., et al., *Radiological and surgical implications of neoadjuvant treatment with FOLFIRINOX for locally advanced and borderline resectable pancreatic cancer*. *Annals of surgery*, 2015. **261**(1): p. 12.
28. Hammel, P., et al., *Effect of chemoradiotherapy vs chemotherapy on survival in patients with locally advanced pancreatic cancer controlled after 4 months of gemcitabine with or without erlotinib: the LAP07 randomized clinical trial*. *Jama*, 2016. **315**(17): p. 1844-1853.
29. Adamska, A., A. Domenichini, and M. Falasca, *Pancreatic ductal adenocarcinoma: current and evolving therapies*. *International journal of molecular sciences*, 2017. **18**(7): p. 1338.
30. Rothenberg, M., et al., *A phase II trial of gemcitabine in patients with 5-FU-refractory pancreas cancer*. *Annals of Oncology*, 1996. **7**(4): p. 347-353.
31. Di Costanzo, F., et al., *Gemcitabine with or without continuous infusion 5-FU in advanced pancreatic cancer: a randomised phase II trial of the Italian oncology group for clinical research (GOIRC)*. *British journal of cancer*, 2005. **93**(2): p. 185.
32. Min, Y.J., et al., *Gemcitabine therapy in patients with advanced pancreatic cancer*. *The Korean journal of internal medicine*, 2002. **17**(4): p. 259.
33. Poplin, E., et al., *Randomized, multicenter, phase II study of CO-101 versus gemcitabine in patients with metastatic pancreatic ductal adenocarcinoma: including a prospective evaluation of the role of hENT1 in gemcitabine or CO-101 sensitivity*. *Journal of Clinical Oncology*, 2013. **31**(35): p. 4453-4461.
34. Young, J.D., et al., *The human concentrative and equilibrative nucleoside transporter families, SLC28 and SLC29*. *Mol Aspects Med*, 2013. **34**(2-3): p. 529-47.
35. Long, J., et al., *Overcoming drug resistance in pancreatic cancer*. *Expert Opin Ther Targets*, 2011. **15**(7): p. 817-28.
36. Trédan, O., et al., *Drug resistance and the solid tumor microenvironment*. *Journal of the National Cancer Institute*, 2007. **99**(19): p. 1441-1454.

37. Bisht, S., et al., *In vivo characterization of a polymeric nanoparticle platform with potential oral drug delivery capabilities*. *Molecular cancer therapeutics*, 2008. **7**(12): p. 3878-3888.
38. Tempero, M.A., et al., *Pancreatic Adenocarcinoma: Clinical Practice Guidelines in Oncology*. *Journal of the National Comprehensive Cancer Network*, 2010. **9**(8): p. 972–1017.
39. Bergman, A.M., H.M. Pinedo, and G.J. Peters, *Determinants of resistance to 2', 2'-difluorodeoxycytidine (gemcitabine)*. *Drug Resistance Updates*, 2002. **5**(1): p. 19-33.
40. Mini, E., et al., *Cellular pharmacology of gemcitabine*. *Ann Oncol*, 2006. **17 Suppl 5**: p. v7-12.
41. Griffith, D.A. and S.M. Jarvis, *Nucleoside and nucleobase transport systems of mammalian cells*. *Biochimica et Biophysica Acta (BBA)-Reviews on Biomembranes*, 1996. **1286**(3): p. 153-181.
42. Hammond, J.R., S. Lee, and P.J. Ferguson, *[3H] gemcitabine uptake by nucleoside transporters in a human head and neck squamous carcinoma cell line*. *Journal of Pharmacology and Experimental Therapeutics*, 1999. **288**(3): p. 1185-1191.
43. Fang, X., et al., *Functional characterization of a recombinant sodium-dependent nucleoside transporter with selectivity for pyrimidine nucleosides (cNT1rat) by transient expression in cultured mammalian cells*. *Biochem. J*, 1996. **317**: p. 457-465.
44. Burke, T., et al., *Interaction of 2', 2'-difluorodeoxycytidine (gemcitabine) and formycin B with the Na⁺-dependent and-independent nucleoside transporters of Ehrlich ascites tumor cells*. *Journal of Pharmacology and Experimental Therapeutics*, 1998. **286**(3): p. 1333-1340.
45. Ueno, H., K. Kiyosawa, and N. Kaniwa, *Pharmacogenomics of gemcitabine: can genetic studies lead to tailor-made therapy?* *British journal of cancer*, 2007. **97**(2): p. 145-151.
46. Mini, E., et al., *Cellular pharmacology of gemcitabine*. *Annals of Oncology*, 2006. **17**(suppl 5): p. v7-v12.
47. Spratlin, J., et al., *The absence of human equilibrative nucleoside transporter 1 is associated with reduced survival in patients with gemcitabine-treated pancreas adenocarcinoma*. *Clinical Cancer Research*, 2004. **10**(20): p. 6956-6961.
48. Bouffard, D.Y., J. Laliberté, and R.L. Momparler, *Kinetic studies on 2', 2'-difluorodeoxycytidine (Gemcitabine) with purified human deoxycytidine kinase and cytidine deaminase*. *Biochemical pharmacology*, 1993. **45**(9): p. 1857-1861.
49. Heinemann, V., et al., *Comparison of the cellular pharmacokinetics and toxicity of 2', 2'-difluorodeoxycytidine and 1-β-d-arabinofuranosylcytosine*. *Cancer research*, 1988. **48**(14): p. 4024-4031.
50. Wang, L., et al., *Human thymidine kinase 2: molecular cloning and characterisation of the enzyme activity with antiviral and cytostatic nucleoside substrates*. *FEBS letters*, 1999. **443**(2): p. 170-174.
51. Bergman, A.M., et al., *Decreased resistance to gemcitabine (2', 2'-difluorodeoxycytidine) of cytosine arabinoside-resistant myeloblastic murine and rat leukemia cell lines: role of altered activity and substrate specificity of deoxycytidine kinase*. *Biochemical pharmacology*, 1999. **57**(4): p. 397-406.
52. Ueno, H., K. Kiyosawa, and N. Kaniwa, *Pharmacogenomics of gemcitabine: can genetic studies lead to tailor-made therapy?* *Br J Cancer*, 2007. **97**(2): p. 145-51.

53. Mackey, J.R., et al., *Gemcitabine transport in xenopus oocytes expressing recombinant plasma membrane mammalian nucleoside transporters*. Journal of the National Cancer Institute, 1999. **91**(21): p. 1876-1881.
54. Mackey, J.R., et al., *Functional nucleoside transporters are required for gemcitabine influx and manifestation of toxicity in cancer cell lines*. Cancer research, 1998. **58**(19): p. 4349-4357.
55. Mackey, J.R., et al., *Functional nucleoside transporters are required for gemcitabine influx and manifestation of toxicity in cancer cell lines*. Cancer Res, 1998. **58**(19): p. 4349-57.
56. Hung, S.W., H.R. Mody, and R. Govindarajan, *Overcoming nucleoside analog chemoresistance of pancreatic cancer: a therapeutic challenge*. Cancer letters, 2012. **320**(2): p. 138-149.
57. Robins, M.J., et al., *Improved syntheses of 5'-S-(2-aminoethyl)-6-N-(4-nitrobenzyl)-5'-thioadenosine (SAENTA), analogues, and fluorescent probe conjugates: analysis of cell-surface human equilibrative nucleoside transporter 1 (hENT1) levels for prediction of the antitumor efficacy of gemcitabine*. Journal of medicinal chemistry, 2010. **53**(16): p. 6040-6053.
58. Bird, N.T., et al., *Immunohistochemical hENT1 expression as a prognostic biomarker in patients with resected pancreatic ductal adenocarcinoma undergoing adjuvant gemcitabine-based chemotherapy*. Br J Surg, 2017. **104**(4): p. 328-336.
59. OHHASHI, S., et al., *Down-regulation of deoxycytidine kinase enhances acquired resistance to gemcitabine in pancreatic cancer*. Anticancer research, 2008. **28**(4B): p. 2205-2212.
60. Williams, T.K., et al., *pp32 (ANP32A) expression inhibits pancreatic cancer cell growth and induces gemcitabine resistance by disrupting HuR binding to mRNAs*. PloS one, 2010. **5**(11): p. e15455.
61. Funamizu, N., et al., *Is the resistance of gemcitabine for pancreatic cancer settled only by overexpression of deoxycytidine kinase?* Oncology reports, 2010. **23**(2): p. 471-475.
62. Farrell, J., et al., *Cytidine deaminase single-nucleotide polymorphism is predictive of toxicity from gemcitabine in patients with pancreatic cancer: RTOG 9704*. The pharmacogenomics journal, 2012. **12**(5): p. 395.
63. Nakahira, S., et al., *Involvement of ribonucleotide reductase M1 subunit overexpression in gemcitabine resistance of human pancreatic cancer*. International journal of cancer, 2007. **120**(6): p. 1355-1363.
64. Akita, H., et al., *Significance of RRM1 and ERCC1 expression in resectable pancreatic adenocarcinoma*. Oncogene, 2009. **28**(32): p. 2903.
65. Kim, R., et al., *Prognostic roles of human equilibrative transporter 1 (hENT - 1) and ribonucleoside reductase subunit M1 (RRM1) in resected pancreatic cancer*. Cancer, 2011. **117**(14): p. 3126-3134.
66. Fujita, H., et al., *Gene expression levels as predictive markers of outcome in pancreatic cancer after gemcitabine-based adjuvant chemotherapy*. Neoplasia, 2010. **12**(10): p. 807-817.
67. Konig, J., et al., *Expression and localization of human multidrug resistance protein (ABCC) family members in pancreatic carcinoma*. Int J Cancer, 2005. **115**(3): p. 359-67.
68. Wolfgang Haggmann , R.J.a.J.M.L., *Interdependence of Gemcitabine Treatment, Transporter Expression, and Resistance in Human Pancreatic Carcinoma Cells1*

69. Kim, M.P. and G.E. Gallick, *Gemcitabine resistance in pancreatic cancer: picking the key players*. Clin Cancer Res, 2008. **14**(5): p. 1284-5.
70. Jedlitschky G, B.B., Keppler D. , *The multidrug resistance protein 5 functions as an ATP-dependent export pump for cyclic nucleotides*. J Biol Chem;275:30069-74, 2000: p.
71. Reid, G., et al., *Characterization of the transport of nucleoside analog drugs by the human multidrug resistance proteins MRP4 and MRP5*. Molecular pharmacology, 2003. **63**(5): p. 1094-1103.
72. Wielinga, P.R., et al., *Characterization of the MRP4- and MRP5-mediated transport of cyclic nucleotides from intact cells*. J Biol Chem, 2003. **278**(20): p. 17664-71.
73. Wijnholds, J., et al., *Multidrug-resistance protein 5 is a multispecific organic anion transporter able to transport nucleotide analogs*. Proc Natl Acad Sci U S A, 2000. **97**(13): p. 7476-81.
74. König, J., et al., *Expression and localization of human multidrug resistance protein (ABCC) family members in pancreatic carcinoma*. International journal of cancer, 2005. **115**(3): p. 359-367.
75. Kohan, H.G. and M. Boroujerdi, *Time and concentration dependency of P-gp, MRP1 and MRP5 induction in response to gemcitabine uptake in Capan-2 pancreatic cancer cells*. Xenobiotica, 2015: p. 1-11.
76. Hagmann, W., R. Jesnowski, and J.M. Löhr, *Interdependence of gemcitabine treatment, transporter expression, and resistance in human pancreatic carcinoma cells*. Neoplasia, 2010. **12**(9): p. 740-747.
77. Chen, Z.-S., K. Lee, and G.D. Kruh, *Transport of cyclic nucleotides and estradiol 17- β -D-glucuronide by multidrug resistance protein 4 resistance to 6-mercaptopurine and 6-thioguanine*. Journal of Biological Chemistry, 2001. **276**(36): p. 33747-33754.
78. Jedlitschky, G., B. Burchell, and D. Keppler, *The multidrug resistance protein 5 functions as an ATP-dependent export pump for cyclic nucleotides*. Journal of Biological Chemistry, 2000. **275**(39): p. 30069-30074.
79. van Aubel, R.A., et al., *The MRP4/ABCC4 gene encodes a novel apical organic anion transporter in human kidney proximal tubules: putative efflux pump for urinary cAMP and cGMP*. Journal of the American Society of Nephrology, 2002. **13**(3): p. 595-603.
80. Wielinga, P.R., et al., *Characterization of the MRP4-and MRP5-mediated transport of cyclic nucleotides from intact cells*. Journal of Biological Chemistry, 2003. **278**(20): p. 17664-17671.
81. Borst, P., et al., *The multidrug resistance protein family*. Biochimica et Biophysica Acta (BBA)-Biomembranes, 1999. **1461**(2): p. 347-357.
82. Keppler, D., I. Leier, and G. Jedlitschky, *Transport of glutathione conjugates and glucuronides by the multidrug resistance proteins MRP1 and MRP2*. Biological chemistry, 1997. **378**(8): p. 787-791.
83. Schuetz, J.D., et al., *MRP4: a previously unidentified factor in resistance to nucleoside-based antiviral drugs*. Nature medicine, 1999. **5**(9): p. 1048-1051.
84. Wielinga, P., et al., *Thiopurine metabolism and identification of the thiopurine metabolites transported by MRP4 and MRP5 overexpressed in human embryonic kidney cells*. Molecular Pharmacology, 2002. **62**(6): p. 1321-1331.
85. Wijnholds, J., et al., *Multidrug-resistance protein 5 is a multispecific organic anion transporter able to transport nucleotide analogs*. Proceedings of the National Academy of Sciences, 2000. **97**(13): p. 7476-7481.

86. Kiuchi, Y., et al., *cDNA cloning and inducible expression of human multidrug resistance associated protein 3 (MRP3)*. FEBS letters, 1998. **433**(1-2): p. 149-152.
87. Kool, M., et al., *MRP3, an organic anion transporter able to transport anti-cancer drugs*. Proceedings of the National Academy of Sciences, 1999. **96**(12): p. 6914-6919.
88. Lu, Z., et al., *Expression of the multidrug-resistance 1 (MDR1) gene and prognosis in human pancreatic cancer*. Pancreas, 2000. **21**(3): p. 240-247.
89. Sandusky, G., et al., *Expression of multidrug resistance - associated protein 2 (MRP2) in normal human tissues and carcinomas using tissue microarrays*. Histopathology, 2002. **41**(1): p. 65-74.
90. Schaarschmidt, T., et al., *Expression of multidrug resistance proteins in rat and human chronic pancreatitis*. Pancreas, 2004. **28**(1): p. 45-52.
91. Scheffer, G.L., et al., *Tissue distribution and induction of human multidrug resistant protein 3*. Laboratory investigation, 2002. **82**(2): p. 193-201.
92. Suwa, H., et al., *Immunohistochemical Localization of P - Glycoprotein and Expression of the Multidrug Resistance - 1 Gene in Human Pancreatic Cancer: Relevance to Indicator of Better Prognosis*. Cancer Science, 1996. **87**(6): p. 641-649.
93. Tanaka, M., et al., *Association of multi-drug resistance gene polymorphisms with pancreatic cancer outcome*. Cancer, 2011. **117**(4): p. 744-51.
94. Wolfgang Haggmann , R.J.a.J.M.L., *Interdependence of Gemcitabine Treatment, Transporter Expression, and Resistance in Human Pancreatic Carcinoma Cells*. Neoplasia, 2010. **12**(9): p. 740-747.
95. Borst, P., C. de Wolf, and K. van de Wetering, *Multidrug resistance-associated proteins 3, 4, and 5*. Pflügers Archiv-European Journal of Physiology, 2007. **453**(5): p. 661-673.
96. König, J., et al., *Characterization of the human multidrug resistance protein isoform MRP3 localized to the basolateral hepatocyte membrane*. Hepatology, 1999. **29**(4): p. 1156-1163.
97. Slitt, A.L., et al., *Induction of genes for metabolism and transport by trans-stilbene oxide in livers of Sprague-Dawley and Wistar-Kyoto rats*. Drug metabolism and disposition, 2006. **34**(7): p. 1190-1197.
98. Huang, P., et al., *Action of 2' , 2' -difluorodeoxycytidine on DNA synthesis*. Cancer research, 1991. **51**(22): p. 6110-6117.
99. Obata, T., et al., *The molecular targets of antitumor 2'-deoxycytidine analogues*. Current drug targets, 2003. **4**(4): p. 305-313.
100. Weckbecker, G., *Biochemical pharmacology and analysis of fluoropyrimidines alone and in combination with modulators*. Pharmacology & therapeutics, 1991. **50**(3): p. 367-424.
101. Lai, L. and T. TAN, *Role of glutathione in the multidrug resistance protein 4 (MRP4/ABCC4)-mediated efflux of cAMP and resistance to purine analogues*. Biochem. J, 2002. **361**: p. 497-503.
102. Reid, G., et al., *The human multidrug resistance protein MRP4 functions as a prostaglandin efflux transporter and is inhibited by nonsteroidal antiinflammatory drugs*. Proceedings of the National Academy of Sciences, 2003. **100**(16): p. 9244-9249.
103. Tanaka, M., et al., *Association of multi - drug resistance gene polymorphisms with pancreatic cancer outcome*. Cancer, 2011. **117**(4): p. 744-751.
104. Volm, M. and J. Mattern, *Resistance mechanisms and their regulation in lung cancer*. Critical Reviews™ in Oncogenesis, 1996. **7**(3-4).

105. Dietel, M., *What's new in cytostatic drug resistance and pathology*. Pathology-Research and Practice, 1991. **187**(7): p. 892-905.
106. Beck, W.T., *Mechanisms of multidrug resistance in human tumor cells. The roles of P-glycoprotein, DNA topoisomerase II, and other factors*. Cancer treatment reviews, 1990. **17**: p. 11-20.
107. Morrow, C. and K. Cowan, *Glutathione S-transferases and drug resistance*. Cancer cells (Cold Spring Harbor, NY: 1989), 1990. **2**(1): p. 15-22.
108. Hammond, J.R., R.M. Johnstone, and P. Gros, *Enhanced efflux of [3H] vinblastine from Chinese hamster ovary cells transfected with a full-length complementary DNA clone for the *mdr1* gene*. Cancer research, 1989. **49**(14): p. 3867-3871.
109. Liu, Y.-y., et al., *Ceramide glycosylation potentiates cellular multidrug resistance*. The FASEB Journal, 2001. **15**(3): p. 719-730.
110. Bosch, I. and J. Croop, *P-glycoprotein multidrug resistance and cancer*. Biochimica et Biophysica Acta (BBA)-Reviews on Cancer, 1996. **1288**(2): p. F37-F54.
111. Hrycyna, C.A. and M.M. Gottesman, *Multidrug ABC transporters from bacteria to man: an emerging hypothesis for the universality of molecular mechanism and function*. Drug Resistance Updates, 1998. **1**(2): p. 81-83.
112. Mitscher, L.A., et al., *Multiple drug resistance*. Medicinal research reviews, 1999. **19**(6): p. 477-496.
113. Van Veen, H.W. and W.N. Konings, *The ABC family of multidrug transporters in microorganisms*. Biochimica et Biophysica Acta (BBA)-Bioenergetics, 1998. **1365**(1): p. 31-36.
114. Vasiliou, V., K. Vasiliou, and D.W. Nebert, *Human ATP-binding cassette (ABC) transporter family*. Human genomics, 2009. **3**(3): p. 281.
115. Bugde, P., et al., *The therapeutic potential of targeting ABC transporters to combat multi-drug resistance*. Expert Opinion on Therapeutic Targets, 2017. **21**(5): p. 511-530.
116. Jiang, Z.-S., et al., *Epithelial-mesenchymal transition: potential regulator of ABC transporters in tumor progression*. Journal of Cancer, 2017. **8**(12): p. 2319.
117. Robey, R.W., et al., *Revisiting the role of ABC transporters in multidrug-resistant cancer*. Nat Rev Cancer, 2018. **18**(7): p. 452-464.
118. Hong, M., *Biochemical studies on the structure-function relationship of major drug transporters in the ATP-binding cassette family and solute carrier family*. Advanced drug delivery reviews, 2017. **116**: p. 3-20.
119. George, A.M., *ABC Transporters--40 Years on*. 2016: Springer.
120. ter Beek, J., A. Guskov, and D.J. Slotboom, *Structural diversity of ABC transporters*. The Journal of general physiology, 2014. **143**(4): p. 419-435.
121. Nobuyoshi, K., et al., *Membrane topology of ABC - type macrolide antibiotic exporter MacB in Escherichia coli*. FEBS Letters, 2003. **546**(2-3): p. 241-246.
122. Jones, P.M. and A.M. George, *Subunit interactions in ABC transporters: towards a functional architecture*. FEMS Microbiology Letters, 1999. **179**(2): p. 187-202.
123. Rich, D., et al., *Effect of deleting the R domain on CFTR-generated chloride channels*. Science, 1991. **253**(5016): p. 205-207.
124. Seeger, M.A., E. Bordignon, and M. Hohl, *ABC Exporters from a Structural Perspective*, in *ABC Transporters-40 Years on*. 2016, Springer. p. 65-84.
125. Xu, Y., et al., *Crystal Structure of the Periplasmic Region of MacB, a Noncanonical ABC Transporter*. Biochemistry, 2009. **48**(23): p. 5218-5225.

126. Chen, Z., et al., *Mammalian drug efflux transporters of the ATP binding cassette (ABC) family in multidrug resistance: a review of the past decade*. Cancer letters, 2016. **370**(1): p. 153-164.
127. Choudhuri, S. and C.D. Klaassen, *Structure, function, expression, genomic organization, and single nucleotide polymorphisms of human ABCB1 (MDR1), ABCC (MRP), and ABCG2 (BCRP) efflux transporters*. International journal of toxicology, 2006. **25**(4): p. 231-259.
128. Fletcher, J.I., et al., *ABC transporters in cancer: more than just drug efflux pumps*. Nature Reviews Cancer, 2010. **10**(2): p. 147-156.
129. Kim, R.B., *Drugs as P-glycoprotein substrates, inhibitors, and inducers*. Drug metabolism reviews, 2002. **34**(1-2): p. 47-54.
130. Borst, P., et al., *A family of drug transporters: the multidrug resistance-associated proteins*. J Natl Cancer Inst, 2000. **92**(16): p. 1295-302.
131. Slot, A.J., S.V. Molinski, and S.P. Cole, *Mammalian multidrug-resistance proteins (MRPs)*. Essays in biochemistry, 2011. **50**: p. 179-207.
132. Jedlitschky, G., U. Hoffmann, and H.K. Kroemer, *Structure and function of the MRP2 (ABCC2) protein and its role in drug disposition*. Expert Opin Drug Metab Toxicol, 2006. **2**(3): p. 351-66.
133. Nies, A.T. and D. Keppler, *The apical conjugate efflux pump ABCC2 (MRP2)*. Pflugers Arch, 2007. **453**(5): p. 643-59.
134. Nies, A.T., M. Schwab, and D. Keppler, *Interplay of conjugating enzymes with OATP uptake transporters and ABCC/MRP efflux pumps in the elimination of drugs*. Expert Opin Drug Metab Toxicol, 2008. **4**(5): p. 545-68.
135. Schinkel, A.H. and J.W. Jonker, *Mammalian drug efflux transporters of the ATP binding cassette (ABC) family: an overview*. Advanced drug delivery reviews, 2003. **55**(1): p. 3-29.
136. Zhou, S.F., et al., *Substrates and inhibitors of human multidrug resistance associated proteins and the implications in drug development*. Curr Med Chem, 2008. **15**(20): p. 1981-2039.
137. Chen, J., et al., *A tweezers-like motion of the ATP-binding cassette dimer in an ABC transport cycle*. Molecular cell, 2003. **12**(3): p. 651-661.
138. Davidson, A.L., H.A. Shuman, and H. Nikaido, *Mechanism of maltose transport in Escherichia coli: transmembrane signaling by periplasmic binding proteins*. Proceedings of the National Academy of Sciences, 1992. **89**(6): p. 2360-2364.
139. Gradia, S., et al., *hMSH2-hMSH6 forms a hydrolysis-independent sliding clamp on mismatched DNA*. Molecular cell, 1999. **3**(2): p. 255-261.
140. Kreimer, D.I., K.P. Chai, and G. Ferro-Luzzi Ames, *Nonequivalence of the nucleotide-binding subunits of an ABC transporter, the histidine permease, and conformational changes in the membrane complex*. Biochemistry, 2000. **39**(46): p. 14183-14195.
141. Lamers, M.H., H.H. Winterwerp, and T.K. Sixma, *The alternating ATPase domains of MutS control DNA mismatch repair*. The EMBO journal, 2003. **22**(3): p. 746-756.
142. Ramachandra, M., et al., *Human P-glycoprotein exhibits reduced affinity for substrates during a catalytic transition state*. Biochemistry, 1998. **37**(14): p. 5010-5019.
143. Linton, K.J., *Structure and function of ABC transporters*. Physiology, 2007. **22**(2): p. 122-130.
144. Aleksandrov, A.A., et al., *The non-hydrolytic pathway of cystic fibrosis transmembrane conductance regulator ion channel gating*. The Journal of physiology, 2000. **528**(2): p. 259-265.

145. Hrycyna, C.A., et al., *Both ATP sites of human P-glycoprotein are essential but not symmetric*. *Biochemistry*, 1999. **38**(42): p. 13887-13899.
146. Urbatsch, I.L., et al., *P-glycoprotein Catalytic Mechanism STUDIES OF THE ADP-VANADATE INHIBITED STATE*. *Journal of Biological Chemistry*, 2003. **278**(25): p. 23171-23179.
147. Martin, C., et al., *Communication between multiple drug binding sites on P-glycoprotein*. *Molecular pharmacology*, 2000. **58**(3): p. 624-632.
148. Hrycyna, C.A., et al., *Mechanism of Action of Human P-glycoprotein ATPase Activity PHOTOCHEMICAL CLEAVAGE DURING A CATALYTIC TRANSITION STATE USING ORTHOVANADATE REVEALS CROSS-TALK BETWEEN THE TWO ATP SITES*. *Journal of Biological Chemistry*, 1998. **273**(27): p. 16631-16634.
149. Higgins, C.F., et al., *A family of related ATP-binding subunits coupled to many distinct biological processes in bacteria*. 1986.
150. Kerr, K.M., Z.E. Sauna, and S.V. Ambudkar, *Correlation between Steady-state ATP Hydrolysis and Vanadate-induced ADP Trapping in Human P-glycoprotein EVIDENCE FOR ADP RELEASE AS THE RATE-LIMITING STEP IN THE CATALYTIC CYCLE AND ITS MODULATION BY SUBSTRATES*. *Journal of Biological Chemistry*, 2001. **276**(12): p. 8657-8664.
151. Reyes, C.L. and G. Chang, *Structure of the ABC transporter MsbA in complex with ADP· vanadate and lipopolysaccharide*. *Science*, 2005. **308**(5724): p. 1028-1031.
152. Stenham, D.R., et al., *An atomic detail model for the human ATP binding cassette transporter P-glycoprotein derived from disulfide cross-linking and homology modeling*. *The FASEB journal*, 2003. **17**(15): p. 2287-2289.
153. Zaitseva, J., et al., *H662 is the linchpin of ATP hydrolysis in the nucleotide - binding domain of the ABC transporter HlyB*. *The EMBO journal*, 2005. **24**(11): p. 1901-1910.
154. Davidson, A.L. and S. Sharma, *Mutation of a single MalK subunit severely impairs maltose transport activity in Escherichia coli*. *Journal of bacteriology*, 1997. **179**(17): p. 5458-5464.
155. Higgins, C.F. and K.J. Linton, *The ATP switch model for ABC transporters*. *Nature structural & molecular biology*, 2004. **11**(10): p. 918-926.
156. Qu, Q., P.L. Russell, and F.J. Sharom, *Stoichiometry and affinity of nucleotide binding to P-glycoprotein during the catalytic cycle*. *Biochemistry*, 2003. **42**(4): p. 1170-1177.
157. Sonveaux, N., et al., *Secondary and Tertiary Structure Changes of Reconstituted P-glycoprotein A FOURIER TRANSFORM ATTENUATED TOTAL REFLECTION INFRARED SPECTROSCOPY ANALYSIS*. *Journal of Biological Chemistry*, 1996. **271**(40): p. 24617-24624.
158. Vergani, P., et al., *CFTR channel opening by ATP-driven tight dimerization of its nucleotide-binding domains*. *Nature*, 2005. **433**(7028): p. 876-880.
159. Schmitt, L., et al., *Crystal structure of the nucleotide-binding domain of the ABC-transporter haemolysin B: identification of a variable region within ABC helical domains*. *Journal of molecular biology*, 2003. **330**(2): p. 333-342.
160. Lamers, M.H., et al., *ATP increases the affinity between MutS ATPase domains Implications for ATP hydrolysis and conformational changes*. *Journal of Biological Chemistry*, 2004. **279**(42): p. 43879-43885.
161. Ambudkar, S.V., et al., *P-glycoprotein: from genomics to mechanism*. *Oncogene*, 2003. **22**(47): p. 7468-7485.

162. Borst, P., et al., *A family of drug transporters: the multidrug resistance-associated proteins*. Journal of the National Cancer Institute, 2000. **92**(16): p. 1295-1302.
163. König, J., et al., *Conjugate export pumps of the multidrug resistance protein (MRP) family: localization, substrate specificity, and MRP2-mediated drug resistance*. Biochimica et Biophysica Acta (BBA)-Biomembranes, 1999. **1461**(2): p. 377-394.
164. Kruh, G.D. and M.G. Belinsky, *The MRP family of drug efflux pumps*. Oncogene, 2003. **22**(47): p. 7537-7552.
165. Adachi, M., G. Reid, and J.D. Schuetz, *Therapeutic and biological importance of getting nucleotides out of cells: a case for the ABC transporters, MRP4 and 5*. Advanced drug delivery reviews, 2002. **54**(10): p. 1333-1342.
166. Haimeur, A., et al., *The MRP-related and BCRP/ABCG2 multidrug resistance proteins: biology, substrate specificity and regulation*. Current drug metabolism, 2004. **5**(1): p. 21-53.
167. Zelcer, N., et al., *Steroid and bile acid conjugates are substrates of human multidrug-resistance protein (MRP) 4 (ATP-binding cassette C4)*. Biochem. J, 2003. **371**: p. 361-367.
168. Oguri, T., et al., *The determinants of sensitivity and acquired resistance to gemcitabine differ in non-small cell lung cancer: a role of ABCC5 in gemcitabine sensitivity*. Molecular cancer therapeutics, 2006. **5**(7): p. 1800-1806.
169. Keppler, D., *Multidrug resistance proteins (MRPs, ABCCs): importance for pathophysiology and drug therapy*, in *Drug Transporters*. 2011, Springer. p. 299-323.
170. Jedlitschky, G., B. Burchell, and D. Keppler, *The multidrug resistance protein 5 functions as an ATP-dependent export pump for cyclic nucleotides*. J Biol Chem, 2000. **275**(39): p. 30069-74.
171. Fromm, M.F. and R.B. Kim, *Drug transporters*. Vol. 201. 2010: Springer Science & Business Media.
172. Norman, B.H., et al., *Tricyclic isoxazoles are novel inhibitors of the multidrug resistance protein (MRP1)*. Bioorganic & medicinal chemistry letters, 2002. **12**(6): p. 883-886.
173. Norman, B.H., et al., *Cyclohexyl-linked tricyclic isoxazoles are potent and selective modulators of the multidrug resistance protein (MRP1)*. Bioorganic & medicinal chemistry letters, 2005. **15**(24): p. 5526-5530.
174. Rius, M., J. Hummel-Eisenbeiss, and D. Keppler, *ATP-dependent transport of leukotrienes B4 and C4 by the multidrug resistance protein ABCC4 (MRP4)*. Journal of Pharmacology and Experimental Therapeutics, 2008. **324**(1): p. 86-94.
175. Pratt, S., et al., *The multidrug resistance protein 5 (ABCC5) confers resistance to 5-fluorouracil and transports its monophosphorylated metabolites*. Molecular cancer therapeutics, 2005. **4**(5): p. 855-863.
176. Hopper-Borge, E., et al., *Human multidrug resistance protein 7 (ABCC10) is a resistance factor for nucleoside analogues and epothilone B*. Cancer research, 2009. **69**(1): p. 178-184.
177. Zhang, Y.K., et al., *Multidrug Resistance Proteins (MRPs) and Cancer Therapy*. AAPS J, 2015. **17**(4): p. 802-12.
178. van Zanden, J.J., et al., *Quantitative structure activity relationship studies on the flavonoid mediated inhibition of multidrug resistance proteins 1 and 2*. Biochem Pharmacol, 2005. **69**(4): p. 699-708.

179. Belinsky, M.G., et al., *Characterization of MOAT-C and MOAT-D, new members of the MRP/cMOAT subfamily of transporter proteins*. Journal of the National Cancer Institute, 1998. **90**(22): p. 1735-1741.
180. Kool, M., et al., *Analysis of expression of cMOAT (MRP2), MRP3, MRP4, and MRP5, homologues of the multidrug resistance-associated protein gene (MRP1), in human cancer cell lines*. Cancer research, 1997. **57**(16): p. 3537-3547.
181. McAleer, M.A., et al., *pABC11 (also known as MOAT-C and MRP5), a member of the ABC family of proteins, has anion transporter activity but does not confer multidrug resistance when overexpressed in human embryonic kidney 293 cells*. Journal of Biological Chemistry, 1999. **274**(33): p. 23541-23548.
182. Dazert, P., et al., *Expression and localization of the multidrug resistance protein 5 (MRP5/ABCC5), a cellular export pump for cyclic nucleotides, in human heart*. The American journal of pathology, 2003. **163**(4): p. 1567-1577.
183. Nies, A., et al., *Expression and immunolocalization of the multidrug resistance proteins, MRP1–MRP6 (ABCC1–ABCC6), in human brain*. Neuroscience, 2004. **129**(2): p. 349-360.
184. zu Schwabedissen, H.E.M., et al., *Expression, localization, and function of MRP5 (ABCC5), a transporter for cyclic nucleotides, in human placenta and cultured human trophoblasts: effects of gestational age and cellular differentiation*. The American journal of pathology, 2005. **166**(1): p. 39-48.
185. Boadu, E. and G. Sager, *Reconstitution of ATP-dependent cGMP transport into proteoliposomes by membrane proteins from human erythrocytes*. Scandinavian journal of clinical and laboratory investigation, 2003. **64**(1): p. 41-48.
186. Boadu, E., et al., *Inhibition by guanosine cyclic monophosphate (cGMP) analogues of uptake of [³H] 3', 5'-cGMP without stimulation of ATPase activity in human erythrocyte inside-out vesicles*. Biochemical pharmacology, 2001. **62**(4): p. 425-429.
187. Ravna, A.W., I. Sylte, and G. Sager, *A molecular model of a putative substrate releasing conformation of multidrug resistance protein 5 (MRP5)*. European journal of medicinal chemistry, 2008. **43**(11): p. 2557-2567.
188. Dawson, R.J. and K.P. Locher, *Structure of a bacterial multidrug ABC transporter*. Nature, 2006. **443**(7108): p. 180.
189. Ravna, A.W., I. Sylte, and G. Sager, *Theoretical Biology and Medical Modelling*. Theoretical Biology and Medical Modelling, 2007. **4**: p. 33.
190. Zolnerciks, J.K., C. Wooding, and K.J. Linton, *Evidence for a Sav1866-like architecture for the human multidrug transporter P-glycoprotein*. The FASEB Journal, 2007. **21**(14): p. 3937-3948.
191. Saier, M.H., *A functional-phylogenetic classification system for transmembrane solute transporters*. Microbiology and Molecular Biology Reviews, 2000. **64**(2): p. 354-411.
192. Bouige, P., et al., *Phylogenetic and functional classification of ATP-binding cassette (ABC) systems*. Current Protein and Peptide Science, 2002. **3**(5): p. 541-559.
193. Igarashi, Y., et al., *The evolutionary repertoires of the eukaryotic-type ABC transporters in terms of the phylogeny of ATP-binding domains in eukaryotes and prokaryotes*. Molecular biology and evolution, 2004. **21**(11): p. 2149-2160.
194. Carthew, R.W. and E.J. Sontheimer, *Origins and Mechanisms of miRNAs and siRNAs*. Cell, 2009. **136**(4): p. 642-55.
195. Cheema, S.K., et al., *Regulation and guidance of cell behavior for tissue regeneration via the siRNA mechanism*. Wound Repair Regen, 2007. **15**(3): p. 286-95.

196. Meister, G. and T. Tuschl, *Mechanisms of gene silencing by double-stranded RNA*. Nature, 2004. **431**(7006): p. 343-9.
197. Tomari, Y. and P.D. Zamore, *Perspective: machines for RNAi*. Genes Dev, 2005. **19**(5): p. 517-29.
198. Zhang, H., et al., *Single processing center models for human Dicer and bacterial RNase III*. Cell, 2004. **118**(1): p. 57-68.
199. Macrae, I.J., et al., *Structural basis for double-stranded RNA processing by Dicer*. Science, 2006. **311**(5758): p. 195-8.
200. Yigit, E., et al., *Analysis of the C. elegans Argonaute family reveals that distinct Argonautes act sequentially during RNAi*. Cell, 2006. **127**(4): p. 747-57.
201. Landthaler, M., et al., *Molecular characterization of human Argonaute-containing ribonucleoprotein complexes and their bound target mRNAs*. Rna, 2008. **14**(12): p. 2580-96.
202. Parker, J.S., S.M. Roe, and D. Barford, *Crystal structure of a PIWI protein suggests mechanisms for siRNA recognition and slicer activity*. Embo j, 2004. **23**(24): p. 4727-37.
203. Song, J.J., et al., *Crystal structure of Argonaute and its implications for RISC slicer activity*. Science, 2004. **305**(5689): p. 1434-7.
204. Gregory, R.I., et al., *Human RISC couples microRNA biogenesis and posttranscriptional gene silencing*. Cell, 2005. **123**(4): p. 631-40.
205. Maniataki, E. and Z. Mourelatos, *A human, ATP-independent, RISC assembly machine fueled by pre-miRNA*. Genes Dev, 2005. **19**(24): p. 2979-90.
206. MacRae, I.J., et al., *In vitro reconstitution of the human RISC-loading complex*. Proc Natl Acad Sci U S A, 2008. **105**(2): p. 512-7.
207. Hock, J., et al., *Proteomic and functional analysis of Argonaute-containing mRNA-protein complexes in human cells*. EMBO Rep, 2007. **8**(11): p. 1052-60.
208. Meister, G., et al., *Identification of novel argonaute-associated proteins*. Curr Biol, 2005. **15**(23): p. 2149-55.
209. Agrawal, N., et al., *RNA interference: biology, mechanism, and applications*. Microbiol Mol Biol Rev, 2003. **67**(4): p. 657-85.
210. Orban, T.I. and E. Izaurralde, *Decay of mRNAs targeted by RISC requires XRNI, the Ski complex, and the exosome*. Rna, 2005. **11**(4): p. 459-69.
211. Shen, B. and H.M. Goodman, *Uridine addition after microRNA-directed cleavage*. Science, 2004. **306**(5698): p. 997.
212. Forstemann, K., et al., *Drosophila microRNAs are sorted into functionally distinct argonaute complexes after production by dicer-1*. Cell, 2007. **130**(2): p. 287-97.
213. Rivas, F.V., et al., *Purified Argonaute2 and an siRNA form recombinant human RISC*. Nat Struct Mol Biol, 2005. **12**(4): p. 340-9.
214. Chi, J.T., et al., *Genomewide view of gene silencing by small interfering RNAs*. Proc Natl Acad Sci U S A, 2003. **100**(11): p. 6343-6.
215. Qiu, S., C.M. Adema, and T. Lane, *A computational study of off-target effects of RNA interference*. Nucleic Acids Res, 2005. **33**(6): p. 1834-47.
216. Liu, J., et al., *MicroRNA-dependent localization of targeted mRNAs to mammalian P-bodies*. Nat Cell Biol, 2005. **7**(7): p. 719-23.
217. Chu, C.Y. and T.M. Rana, *Translation repression in human cells by microRNA-induced gene silencing requires RCK/p54*. PLoS Biol, 2006. **4**(7): p. e210.
218. Robb, G.B., et al., *Specific and potent RNAi in the nucleus of human cells*. Nat Struct Mol Biol, 2005. **12**(2): p. 133-7.
219. Kim, V.N., *RNA interference in functional genomics and medicine*. J Korean Med Sci, 2003. **18**(3): p. 309-18.

220. McManus, M.T. and P.A. Sharp, *Gene silencing in mammals by small interfering RNAs*. Nature reviews genetics, 2002. **3**(10): p. 737-747.
221. Kim, V.N., *RNA interference in functional genomics and medicine*. Journal of Korean medical science, 2003. **18**(3): p. 309.
222. Rao, D.D., et al., *siRNA vs. shRNA: similarities and differences*. Advanced drug delivery reviews, 2009. **61**(9): p. 746-759.
223. Aigner, A., *Nonviral in vivo delivery of therapeutic small interfering RNAs*. Current opinion in molecular therapeutics, 2007. **9**(4): p. 345-352.
224. Luten, J., et al., *Biodegradable polymers as non-viral carriers for plasmid DNA delivery*. Journal of Controlled Release, 2008. **126**(2): p. 97-110.
225. Zhang, S., et al., *Cationic lipids and polymers mediated vectors for delivery of siRNA*. Journal of Controlled Release, 2007. **123**(1): p. 1-10.
226. Heidel, J.D., et al., *Potent siRNA inhibitors of ribonucleotide reductase subunit RRM2 reduce cell proliferation in vitro and in vivo*. Clinical Cancer Research, 2007. **13**(7): p. 2207-2215.
227. Heidel, J.D., *Linear cyclodextrin-containing polymers and their use as delivery agents*. 2006.
228. van Engeland, M., et al., *Annexin V-affinity assay: a review on an apoptosis detection system based on phosphatidylserine exposure*. Cytometry, 1998. **31**(1): p. 1-9.
229. Kerr, J.F., A.H. Wyllie, and A.R. Currie, *Apoptosis: a basic biological phenomenon with wide-ranging implications in tissue kinetics*. Br J Cancer, 1972. **26**(4): p. 239-57.
230. Horvitz, H.R., *Genetic control of programmed cell death in the nematode Caenorhabditis elegans*. Cancer Res, 1999. **59**(7 Suppl): p. 1701s-1706s.
231. Elmore, S., *Apoptosis: a review of programmed cell death*. Toxicol Pathol, 2007. **35**(4): p. 495-516.
232. Ouyang, L., et al., *Programmed cell death pathways in cancer: a review of apoptosis, autophagy and programmed necrosis*. Cell Prolif, 2012. **45**(6): p. 487-98.
233. Reutelingsperger, C.P., G. Hornstra, and H.C. Hemker, *Isolation and partial purification of a novel anticoagulant from arteries of human umbilical cord*. Eur J Biochem, 1985. **151**(3): p. 625-9.
234. Nagata, S., *Apoptosis by death factor*. Cell, 1997. **88**(3): p. 355-65.
235. Vermes, I., et al., *A novel assay for apoptosis. Flow cytometric detection of phosphatidylserine expression on early apoptotic cells using fluorescein labelled Annexin V*. J Immunol Methods, 1995. **184**(1): p. 39-51.
236. Connor, J., et al., *Bidirectional transbilayer movement of phospholipid analogs in human red blood cells. Evidence for an ATP-dependent and protein-mediated process*. J Biol Chem, 1992. **267**(27): p. 19412-7.
237. Tang, X., et al., *A subfamily of P-type ATPases with aminophospholipid transporting activity*. Science, 1996. **272**(5267): p. 1495-7.
238. Gottesman, M.M. and I. Pastan, *Biochemistry of multidrug resistance mediated by the multidrug transporter*. Annu Rev Biochem, 1993. **62**: p. 385-427.
239. Fadok, V.A., et al., *Particle digestibility is required for induction of the phosphatidylserine recognition mechanism used by murine macrophages to phagocytose apoptotic cells*. J Immunol, 1993. **151**(8): p. 4274-85.
240. Fadok, V.A., et al., *Exposure of phosphatidylserine on the surface of apoptotic lymphocytes triggers specific recognition and removal by macrophages*. J Immunol, 1992. **148**(7): p. 2207-16.

241. Inaba, N., et al., *The immunocytochemical location of two membrane-associated placental tissue proteins in human and cynomolgus monkey placentae*. *Tumour Biol*, 1984. **5**(2): p. 75-85.
242. Castedo, M., et al., *Sequential acquisition of mitochondrial and plasma membrane alterations during early lymphocyte apoptosis*. *J Immunol*, 1996. **157**(2): p. 512-21.
243. Susin, S.A., et al., *Bcl-2 inhibits the mitochondrial release of an apoptogenic protease*. *J Exp Med*, 1996. **184**(4): p. 1331-41.
244. Zeiss, C.J., *The apoptosis-necrosis continuum: insights from genetically altered mice*. *Vet Pathol*, 2003. **40**(5): p. 481-95.
245. Igney, F.H. and P.H. Krammer, *Death and anti-death: tumour resistance to apoptosis*. *Nat Rev Cancer*, 2002. **2**(4): p. 277-88.
246. Ashkenazi, A. and V.M. Dixit, *Death receptors: signaling and modulation*. *Science*, 1998. **281**(5381): p. 1305-8.
247. Trapani, J.A. and M.J. Smyth, *Functional significance of the perforin/granzyme cell death pathway*. *Nat Rev Immunol*, 2002. **2**(10): p. 735-47.
248. Russell, J.H. and T.J. Ley, *Lymphocyte-mediated cytotoxicity*. *Annu Rev Immunol*, 2002. **20**: p. 323-70.
249. Barry, M. and R.C. Bleackley, *Cytotoxic T lymphocytes: all roads lead to death*. *Nat Rev Immunol*, 2002. **2**(6): p. 401-9.
250. Fan, Z., et al., *Tumor suppressor NM23-H1 is a granzyme A-activated DNase during CTL-mediated apoptosis, and the nucleosome assembly protein SET is its inhibitor*. *Cell*, 2003. **112**(5): p. 659-72.
251. Hill, M.M., et al., *Analysis of the composition, assembly kinetics and activity of native Apaf-1 apoptosomes*. *Embo j*, 2004. **23**(10): p. 2134-45.
252. Joza, N., et al., *Essential role of the mitochondrial apoptosis-inducing factor in programmed cell death*. *Nature*, 2001. **410**(6828): p. 549-54.
253. Li, L.Y., X. Luo, and X. Wang, *Endonuclease G is an apoptotic DNase when released from mitochondria*. *Nature*, 2001. **412**(6842): p. 95-9.
254. Ferraro-Peyret, C., et al., *Caspase-independent phosphatidylserine exposure during apoptosis of primary T lymphocytes*. *J Immunol*, 2002. **169**(9): p. 4805-10.
255. Mandal, D., et al., *Fas-, caspase 8-, and caspase 3-dependent signaling regulates the activity of the aminophospholipid translocase and phosphatidylserine externalization in human erythrocytes*. *J Biol Chem*, 2005. **280**(47): p. 39460-7.
256. Ghobrial, I.M., T.E. Witzig, and A.A. Adjei, *Targeting apoptosis pathways in cancer therapy*. *CA Cancer J Clin*, 2005. **55**(3): p. 178-94.
257. Li, L., et al., *Liposomal curcumin with and without oxaliplatin: effects on cell growth, apoptosis, and angiogenesis in colorectal cancer*. *Molecular cancer therapeutics*, 2007. **6**(4): p. 1276-1282.
258. Wu, C.-P., A.M. Calcagno, and S.V. Ambudkar, *Reversal of ABC drug transporter-mediated multidrug resistance in cancer cells: evaluation of current strategies*. *Current molecular pharmacology*, 2008. **1**(2): p. 93.
259. Long, J., et al., *Overcoming drug resistance in pancreatic cancer*. *Expert opinion on therapeutic targets*, 2011. **15**(7): p. 817-828.
260. Dean, M., *ABC transporters, drug resistance, and cancer stem cells*. *Journal of mammary gland biology and neoplasia*, 2009. **14**(1): p. 3-9.
261. Ozben, T., *Mechanisms and strategies to overcome multiple drug resistance in cancer*. *FEBS letters*, 2006. **580**(12): p. 2903-2909.
262. Dean, M. and M. Dean, *The human ATP-binding cassette (ABC) transporter superfamily*. 2002.

263. Fukuda, Y. and J.D. Schuetz, *ABC transporters and their role in nucleoside and nucleotide drug resistance*. *Biochemical pharmacology*, 2012. **83**(8): p. 1073-1083.
264. Sittampalam, G.S., et al., *Cell Viability Assays*. 2013.
265. Li, Y., et al., *Modulatory effects of curcumin on multi-drug resistance-associated protein 5 in pancreatic cancer cells*. *Cancer Chemother Pharmacol*, 2011. **68**(3): p. 603-10.
266. McAleer, M.A., et al., *pABC11 (also known as MOAT-C and MRP5), a member of the ABC family of proteins, has anion transporter activity but does not confer multidrug resistance when overexpressed in human embryonic kidney 293 cells*. *J Biol Chem*, 1999. **274**(33): p. 23541-8.
267. Wong, M.L. and J.F. Medrano, *Real-time PCR for mRNA quantitation*. *BioTechniques*, 2005. **39**(1): p. 75-85.
268. Tichopad, A., et al., *Standardized determination of real-time PCR efficiency from a single reaction set-up*. *Nucleic Acids Res*, 2003. **31**(20): p. e122.
269. Heid, C.A., et al., *Real time quantitative PCR*. *Genome Res*, 1996. **6**(10): p. 986-94.
270. Roche, *Roche Applied Science Technical Note No. Lc 13/ Pdf. (n.d.)*.
271. Souaze, F., et al., *Quantitative RT-PCR: limits and accuracy*. *Biotechniques*, 1996. **21**(2): p. 280-5.
272. Muller, P.Y., et al., *Processing of gene expression data generated by quantitative real-time RT-PCR*. *Biotechniques*, 2002. **32**(6): p. 1372-4, 1376, 1378-9.
273. Pfaffl, M.W., et al., *Determination of stable housekeeping genes, differentially regulated target genes and sample integrity: BestKeeper--Excel-based tool using pair-wise correlations*. *Biotechnol Lett*, 2004. **26**(6): p. 509-15.
274. Giulietti, A., et al., *An overview of real-time quantitative PCR: applications to quantify cytokine gene expression*. *Methods*, 2001. **25**(4): p. 386-401.
275. Livak, K.J. and T.D. Schmittgen, *Analysis of relative gene expression data using real-time quantitative PCR and the 2(-Delta Delta C(T)) Method*. *Methods*, 2001. **25**(4): p. 402-8.
276. Liu, W. and D.A. Saint, *A new quantitative method of real time reverse transcription polymerase chain reaction assay based on simulation of polymerase chain reaction kinetics*. *Anal Biochem*, 2002. **302**(1): p. 52-9.
277. Marino, J.H., P. Cook, and K.S. Miller, *Accurate and statistically verified quantification of relative mRNA abundances using SYBR Green I and real-time RT-PCR*. *J Immunol Methods*, 2003. **283**(1-2): p. 291-306.
278. Peirson, S.N., J.N. Butler, and R.G. Foster, *Experimental validation of novel and conventional approaches to quantitative real-time PCR data analysis*. *Nucleic Acids Res*, 2003. **31**(14): p. e73.
279. Bustin, S.A., *Quantification of mRNA using real-time reverse transcription PCR (RT-PCR): trends and problems*. *J Mol Endocrinol*, 2002. **29**(1): p. 23-39.
280. Vandesompele, J., et al., *Accurate normalization of real-time quantitative RT-PCR data by geometric averaging of multiple internal control genes*. *Genome Biol*, 2002. **3**(7): p. Research0034.
281. Schmittgen, T.D. and B.A. Zakrajsek, *Effect of experimental treatment on housekeeping gene expression: validation by real-time, quantitative RT-PCR*. *J Biochem Biophys Methods*, 2000. **46**(1-2): p. 69-81.

282. Bustin, S.A., *Absolute quantification of mRNA using real-time reverse transcription polymerase chain reaction assays*. J Mol Endocrinol, 2000. **25**(2): p. 169-93.
283. Shakeel, M., et al., *Gene expression studies of reference genes for quantitative real-time PCR: an overview in insects*. Biotechnol Lett, 2018. **40**(2): p. 227-236.
284. Pritchard, C.C., H.H. Cheng, and M. Tewari, *MicroRNA profiling: approaches and considerations*. Nature reviews. Genetics, 2012. **13**(5): p. 358-369.
285. Ginzinger, D.G., *Gene quantification using real-time quantitative PCR: an emerging technology hits the mainstream*. Exp Hematol, 2002. **30**(6): p. 503-12.
286. www.thermofisher.com/id/en/home/life-science/pcr/real-time-pcr/real-time-pcr-applications/genetic-variation-analysis-using-real-time.html.
287. Nagy, B., *Application of real-time polymerase chain reaction in the clinical genetic practice*. J Pediatr Genet, 2013. **2**(1): p. 1-8.
288. Battaglia, M., et al., *Epithelial tumour cell detection and the unsolved problems of nested RT-PCR: a new sensitive one step method without false positive results*. Bone Marrow Transplant, 1998. **22**(7): p. 693-8.
289. Mannhalter, C., D. Koizar, and G. Mitterbauer, *Evaluation of RNA isolation methods and reference genes for RT-PCR analyses of rare target RNA*. Clin Chem Lab Med, 2000. **38**(2): p. 171-7.
290. Vandesompele, J., A. De Paepe, and F. Speleman, *Elimination of primer-dimer artifacts and genomic coamplification using a two-step SYBR green I real-time RT-PCR*. Anal Biochem, 2002. **303**(1): p. 95-8.
291. Vernel-Pauillac, F. and F. Merien, *Proinflammatory and immunomodulatory cytokine mRNA time course profiles in hamsters infected with a virulent variant of Leptospira interrogans*. Infection and immunity, 2006. **74**(7): p. 4172-4179.
292. Calcagno, A.M. and S.V. Ambudkar, *Analysis of expression of drug resistance-linked ABC transporters in cancer cells by quantitative RT-PCR*. Methods Mol Biol, 2010. **637**: p. 121-32.
293. Galmarini, C.M., et al., *Expression of a non-functional p53 affects the sensitivity of cancer cells to gemcitabine*. Int J Cancer, 2002. **97**(4): p. 439-45.
294. Candelaria, M., et al., *DNA methylation-independent reversion of gemcitabine resistance by hydralazine in cervical cancer cells*. PLoS One, 2012. **7**(3): p. e29181.
295. Jesnowski, R., et al., *Immortalization of pancreatic stellate cells as an in vitro model of pancreatic fibrosis: deactivation is induced by matrigel and N-acetylcysteine*. Lab Invest, 2005. **85**(10): p. 1276-91.
296. Li, C., et al., *Knockdown of ribosomal protein L39 by RNA interference inhibits the growth of human pancreatic cancer cells in vitro and in vivo*. Biotechnol J, 2014. **9**(5): p. 652-63.
297. Tichopad, A., A. Didier, and M.W. Pfaffl, *Inhibition of real-time RT-PCR quantification due to tissue-specific contaminants*. Mol Cell Probes, 2004. **18**(1): p. 45-50.
298. Liss, B., *Improved quantitative real-time RT-PCR for expression profiling of individual cells*. Nucleic Acids Res, 2002. **30**(17): p. e89.
299. Lekanne Deprez, R.H., et al., *Sensitivity and accuracy of quantitative real-time polymerase chain reaction using SYBR green I depends on cDNA synthesis conditions*. Anal Biochem, 2002. **307**(1): p. 63-9.
300. Gibson, U.E., C.A. Heid, and P.M. Williams, *A novel method for real time quantitative RT-PCR*. Genome Res, 1996. **6**(10): p. 995-1001.
301. Shimomaye, E. and M. Salvato, *Use of avian myeloblastosis virus reverse transcriptase at high temperature for sequence analysis of highly structured RNA*. Gene Anal Tech, 1989. **6**(2): p. 25-8.

302. Krishan, A. and R.M. Hamelik, *Flow cytometric monitoring of fluorescent drug retention and efflux*. *Methods Mol Med*, 2005. **111**: p. 149-66.
303. Shapiro, H.M., *Learning Flow Cytometry*. In *Practical Flow Cytometry*. John Wiley & Sons, Inc., (2005a): p. 61–72.
304. Nabekura, T., S. Kamiyama, and S. Kitagawa, *Effects of dietary chemopreventive phytochemicals on P-glycoprotein function*. *Biochem Biophys Res Commun*, 2005. **327**(3): p. 866-70.
305. Szakacs, G., et al., *The role of ABC transporters in drug absorption, distribution, metabolism, excretion and toxicity (ADME-Tox)*. *Drug Discov Today*, 2008. **13**(9-10): p. 379-93.
306. Wang, E.J., et al., *In vitro flow cytometry method to quantitatively assess inhibitors of P-glycoprotein*. *Drug Metab Dispos*, 2000. **28**(5): p. 522-8.
307. Mosmann, T., *Rapid colorimetric assay for cellular growth and survival: application to proliferation and cytotoxicity assays*. *J Immunol Methods*, 1983. **65**(1-2): p. 55-63.
308. van Meerloo, J., G.J. Kaspers, and J. Cloos, *Cell sensitivity assays: the MTT assay*. *Methods Mol Biol*, 2011. **731**: p. 237-45.
309. Boncler, M., et al., *Comparison of PrestoBlue and MTT assays of cellular viability in the assessment of anti-proliferative effects of plant extracts on human endothelial cells*. *J Pharmacol Toxicol Methods*, 2014. **69**(1): p. 9-16.
310. Cree, I.A., *Cancer Cell Culture*. Springer, 2011. **731**.
311. Li, Y., et al., *Modulatory effects of curcumin on multi-drug resistance-associated protein 5 in pancreatic cancer cells*. *Cancer chemotherapy and pharmacology*, 2011. **68**(3): p. 603-610.
312. Catalanotto, C., et al., *Gene silencing in worms and fungi*. *Nature*, 2000. **404**(6775): p. 245.
313. Ullu, E., C. Tschudi, and T. Chakraborty, *RNA interference in protozoan parasites*. *Cell Microbiol*, 2004. **6**(6): p. 509-19.
314. Elbashir, S.M., et al., *Duplexes of 21-nucleotide RNAs mediate RNA interference in cultured mammalian cells*. *Nature*, 2001. **411**(6836): p. 494-8.
315. Semizarov, D., et al., *Specificity of short interfering RNA determined through gene expression signatures*. *Proc Natl Acad Sci U S A*, 2003. **100**(11): p. 6347-52.
316. Tuschl, T., et al., *Targeted mRNA degradation by double-stranded RNA in vitro*. *Genes Dev*, 1999. **13**(24): p. 3191-7.
317. Elbashir, S.M., et al., *Functional anatomy of siRNAs for mediating efficient RNAi in Drosophila melanogaster embryo lysate*. *Embo j*, 2001. **20**(23): p. 6877-88.
318. Caffrey, D.R., et al., *siRNA off-target effects can be reduced at concentrations that match their individual potency*. *PLoS One*, 2011. **6**(7): p. e21503.
319. Reynolds, A., et al., *Rational siRNA design for RNA interference*. *Nat Biotechnol*, 2004. **22**(3): p. 326-30.
320. Awasthi, N., et al., *Comparative benefits of Nab-paclitaxel over gemcitabine or polysorbate-based docetaxel in experimental pancreatic cancer*. *Carcinogenesis*, 2013. **34**(10): p. 2361-9.
321. Hanahan, D. and R.A. Weinberg, *Hallmarks of cancer: the next generation*. *Cell*, 2011. **144**(5): p. 646-74.
322. Ran, F.A., et al., *Genome engineering using the CRISPR-Cas9 system*. *Nat Protoc*, 2013. **8**(11): p. 2281-2308.
323. Oude Blenke, E., et al., *CRISPR-Cas9 gene editing: Delivery aspects and therapeutic potential*. *J Control Release*, 2016. **244**(Pt B): p. 139-148.

324. Liu, C., et al., *Delivery strategies of the CRISPR-Cas9 gene-editing system for therapeutic applications*. J Control Release, 2017. **266**: p. 17-26.
325. Yi, L. and J. Li, *CRISPR-Cas9 therapeutics in cancer: promising strategies and present challenges*. Biochim Biophys Acta, 2016. **1866**(2): p. 197-207.
326. Kim, H. and J.S. Kim, *A guide to genome engineering with programmable nucleases*. Nat Rev Genet, 2014. **15**(5): p. 321-34.
327. Doudna, J.A. and E. Charpentier, *Genome editing. The new frontier of genome engineering with CRISPR-Cas9*. Science, 2014. **346**(6213): p. 1258096.
328. Niu, Y., et al., *Generation of gene-modified cynomolgus monkey via Cas9/RNA-mediated gene targeting in one-cell embryos*. Cell, 2014. **156**(4): p. 836-43.
329. Zuris, J.A., et al., *Cationic lipid-mediated delivery of proteins enables efficient protein-based genome editing in vitro and in vivo*. Nat Biotechnol, 2015. **33**(1): p. 73-80.
330. Fu, Y., et al., *High-frequency off-target mutagenesis induced by CRISPR-Cas nucleases in human cells*. Nat Biotechnol, 2013. **31**(9): p. 822-6.
331. Cradick, T.J., et al., *CRISPR/Cas9 systems targeting beta-globin and CCR5 genes have substantial off-target activity*. Nucleic Acids Res, 2013. **41**(20): p. 9584-92.
332. Shen, B., et al., *Generation of gene-modified mice via Cas9/RNA-mediated gene targeting*. Cell Res, 2013. **23**(5): p. 720-3.
333. Shen, B., et al., *Efficient genome modification by CRISPR-Cas9 nickase with minimal off-target effects*. Nat Methods, 2014. **11**(4): p. 399-402.
334. Li, L., et al., *CGMP-compliant, clinical scale, non-viral platform for efficient gene editing using CRISPR/Cas9*. Cytotherapy, 2014. **16**(4): p. S37.
335. Kim, S., et al., *Highly efficient RNA-guided genome editing in human cells via delivery of purified Cas9 ribonucleoproteins*. Genome Res, 2014. **24**(6): p. 1012-9.
336. Gori, J.L., et al., *Delivery and Specificity of CRISPR-Cas9 Genome Editing Technologies for Human Gene Therapy*. Hum Gene Ther, 2015. **26**(7): p. 443-51.
337. Qin, W., et al., *Efficient CRISPR/Cas9-Mediated Genome Editing in Mice by Zygote Electroporation of Nuclease*. Genetics, 2015.
338. Coelho, T., et al., *Safety and efficacy of RNAi therapy for transthyretin amyloidosis*. N Engl J Med, 2013. **369**(9): p. 819-29.
339. Fitzgerald, K., et al., *Effect of an RNA interference drug on the synthesis of proprotein convertase subtilisin/kexin type 9 (PCSK9) and the concentration of serum LDL cholesterol in healthy volunteers: a randomised, single-blind, placebo-controlled, phase I trial*. Lancet, 2014. **383**(9911): p. 60-68.
340. Wang, M., et al., *Efficient delivery of genome-editing proteins using bioreducible lipid nanoparticles*. Proc Natl Acad Sci U S A, 2016. **113**(11): p. 2868-73.
341. Mout, R., et al., *In Vivo Delivery of CRISPR/Cas9 for Therapeutic Gene Editing: Progress and Challenges*. Bioconjug Chem, 2017. **28**(4): p. 880-884.
342. Yin, H., et al., *Therapeutic genome editing by combined viral and non-viral delivery of CRISPR system components in vivo*. Nat Biotechnol, 2016. **34**(3): p. 328-33.
343. Pecot, C.V., et al., *RNA interference in the clinic: challenges and future directions*. Nat Rev Cancer, 2011. **11**(1): p. 59-67.
344. Singh, A., P. Trivedi, and N.K. Jain, *Advances in siRNA delivery in cancer therapy*. Artif Cells Nanomed Biotechnol, 2018. **46**(2): p. 274-283.
345. Alexis, F., et al., *Factors affecting the clearance and biodistribution of polymeric nanoparticles*. Mol Pharm, 2008. **5**(4): p. 505-15.

346. Layzer, J.M., et al., *In vivo activity of nuclease-resistant siRNAs*. *Rna*, 2004. **10**(5): p. 766-71.
347. Mosser, D.M. and J.P. Edwards, *Exploring the full spectrum of macrophage activation*. *Nat Rev Immunol*, 2008. **8**(12): p. 958-69.
348. Jackson, A.L., et al., *Expression profiling reveals off-target gene regulation by RNAi*. *Nat Biotechnol*, 2003. **21**(6): p. 635-7.
349. Whitehead, K.A., R. Langer, and D.G. Anderson, *Knocking down barriers: advances in siRNA delivery*. *Nat Rev Drug Discov*, 2009. **8**(2): p. 129-38.
350. Singh, S., A.S. Narang, and R.I. Mahato, *Subcellular fate and off-target effects of siRNA, shRNA, and miRNA*. *Pharm Res*, 2011. **28**(12): p. 2996-3015.
351. Jackson, A.L., et al., *Widespread siRNA "off-target" transcript silencing mediated by seed region sequence complementarity*. *Rna*, 2006. **12**(7): p. 1179-87.
352. Hornung, V., et al., *Sequence-specific potent induction of IFN- α by short interfering RNA in plasmacytoid dendritic cells through TLR7*. *Nature Medicine*, 2005. **11**: p. 263.
353. Marques, J.T. and B.R. Williams, *Activation of the mammalian immune system by siRNAs*. *Nat Biotechnol*, 2005. **23**(11): p. 1399-405.
354. Kariko, K., et al., *Small interfering RNAs mediate sequence-independent gene suppression and induce immune activation by signaling through toll-like receptor 3*. *J Immunol*, 2004. **172**(11): p. 6545-9.
355. Harborth, J., et al., *Sequence, chemical, and structural variation of small interfering RNAs and short hairpin RNAs and the effect on mammalian gene silencing*. *Antisense Nucleic Acid Drug Dev*, 2003. **13**(2): p. 83-105.
356. Czauderna, F., et al., *Structural variations and stabilising modifications of synthetic siRNAs in mammalian cells*. *Nucleic Acids Research*, 2003. **31**(11): p. 2705-2716.
357. Liao, H. and J.H. Wang, *Biomembrane-permeable and Ribonuclease-resistant siRNA with enhanced activity*. *Oligonucleotides*, 2005. **15**(3): p. 196-205.
358. Chiu, Y.L., et al., *Visualizing a correlation between siRNA localization, cellular uptake, and RNAi in living cells*. *Chem Biol*, 2004. **11**(8): p. 1165-75.
359. Judge, A.D., et al., *Sequence-dependent stimulation of the mammalian innate immune response by synthetic siRNA*. *Nat Biotechnol*, 2005. **23**(4): p. 457-62.
360. Akhtar, S. and I. Benter, *Toxicogenomics of non-viral drug delivery systems for RNAi: potential impact on siRNA-mediated gene silencing activity and specificity*. *Adv Drug Deliv Rev*, 2007. **59**(2-3): p. 164-82.
361. Hollins, A.J., et al., *Toxicogenomics of drug delivery systems: Exploiting delivery system-induced changes in target gene expression to enhance siRNA activity*. *J Drug Target*, 2007. **15**(1): p. 83-8.
362. Omid, Y., et al., *Toxicogenomics of non-viral vectors for gene therapy: a microarray study of lipofectin- and oligofectamine-induced gene expression changes in human epithelial cells*. *J Drug Target*, 2003. **11**(6): p. 311-23.
363. Omid, Y., et al., *Polypropylenimine dendrimer-induced gene expression changes: the effect of complexation with DNA, dendrimer generation and cell type*. *J Drug Target*, 2005. **13**(7): p. 431-43.
364. Jackson, A.L. and P.S. Linsley, *Recognizing and avoiding siRNA off-target effects for target identification and therapeutic application*. *Nat Rev Drug Discov*, 2010. **9**(1): p. 57-67.
365. Bitko, V., et al., *Inhibition of respiratory viruses by nasally administered siRNA*. *Nat Med*, 2005. **11**(1): p. 50-5.
366. Hutvagner, G., et al., *Sequence-specific inhibition of small RNA function*. *PLoS Biol*, 2004. **2**(4): p. E98.

367. Kundu, A.K., et al., *Development and optimization of nanosomal formulations for siRNA delivery to the liver*. European Journal of Pharmaceutics and Biopharmaceutics, 2012. **80**(2): p. 257-267.
368. McCaffrey, A.P., et al., *Gene expression: RNA interference in adult mice*. Nature, 2002. **418**(6893): p. 38-39.
369. Lewis, D.L., et al., *Efficient delivery of siRNA for inhibition of gene expression in postnatal mice*. Nature genetics, 2002. **32**(1): p. 107-108.
370. McCaffrey, A.P., et al., *Inhibition of hepatitis B virus in mice by RNA interference*. Nature biotechnology, 2003. **21**(6): p. 639-644.
371. Yano, J., et al., *Antitumor activity of small interfering RNA/cationic liposome complex in mouse models of cancer*. Clinical Cancer Research, 2004. **10**(22): p. 7721-7726.
372. Andersen, M.Ø., et al., *Delivery of siRNA from lyophilized polymeric surfaces*. Biomaterials, 2008. **29**(4): p. 506-512.
373. Hsu, P.D., E.S. Lander, and F. Zhang, *Development and applications of CRISPR-Cas9 for genome engineering*. Cell, 2014. **157**(6): p. 1262-78.
374. Jinek, M., et al., *Structures of Cas9 endonucleases reveal RNA-mediated conformational activation*. Science, 2014. **343**(6176): p. 1247997.
375. Nishimasu, H., et al., *Crystal structure of Cas9 in complex with guide RNA and target DNA*. Cell, 2014. **156**(5): p. 935-49.
376. Hsu, P.D., et al., *DNA targeting specificity of RNA-guided Cas9 nucleases*. Nat Biotechnol, 2013. **31**(9): p. 827-32.
377. Mali, P., et al., *CAS9 transcriptional activators for target specificity screening and paired nickases for cooperative genome engineering*. Nat Biotechnol, 2013. **31**(9): p. 833-8.
378. Pattanayak, V., et al., *High-throughput profiling of off-target DNA cleavage reveals RNA-programmed Cas9 nuclease specificity*. Nat Biotechnol, 2013. **31**(9): p. 839-43.
379. Wu, X., et al., *Genome-wide binding of the CRISPR endonuclease Cas9 in mammalian cells*. Nat Biotechnol, 2014. **32**(7): p. 670-6.
380. Sternberg, S.H., et al., *DNA interrogation by the CRISPR RNA-guided endonuclease Cas9*. Nature, 2014. **507**(7490): p. 62-7.
381. Cong, L., et al., *Multiplex genome engineering using CRISPR/Cas systems*. Science, 2013. **339**(6121): p. 819-23.
382. Deveau, H., et al., *Phage response to CRISPR-encoded resistance in Streptococcus thermophilus*. J Bacteriol, 2008. **190**(4): p. 1390-400.
383. Horvath, P., et al., *Diversity, activity, and evolution of CRISPR loci in Streptococcus thermophilus*. J Bacteriol, 2008. **190**(4): p. 1401-12.
384. Esvelt, K.M., et al., *Orthogonal Cas9 proteins for RNA-guided gene regulation and editing*. Nat Methods, 2013. **10**(11): p. 1116-21.
385. Gasiunas, G., et al., *Cas9-crRNA ribonucleoprotein complex mediates specific DNA cleavage for adaptive immunity in bacteria*. Proc Natl Acad Sci U S A, 2012. **109**(39): p. E2579-86.
386. Dianov, G.L. and U. Hubscher, *Mammalian base excision repair: the forgotten archangel*. Nucleic Acids Res, 2013. **41**(6): p. 3483-90.
387. Kosicki, M., K. Tomberg, and A. Bradley, *Repair of double-strand breaks induced by CRISPR-Cas9 leads to large deletions and complex rearrangements*. Nat Biotechnol, 2018. **36**(8): p. 765-771.
388. Niewoehner, J., et al., *Increased brain penetration and potency of a therapeutic antibody using a monovalent molecular shuttle*. Neuron, 2014. **81**(1): p. 49-60.
389. Zhang, Y., et al., *Processing-independent CRISPR RNAs limit natural transformation in Neisseria meningitidis*. Mol Cell, 2013. **50**(4): p. 488-503.

390. Garneau, J.E., et al., *The CRISPR/Cas bacterial immune system cleaves bacteriophage and plasmid DNA*. *Nature*, 2010. **468**(7320): p. 67-71.
391. Fonfara, I., et al., *Phylogeny of Cas9 determines functional exchangeability of dual-RNA and Cas9 among orthologous type II CRISPR-Cas systems*. *Nucleic Acids Res*, 2014. **42**(4): p. 2577-90.
392. Hale, C.R., et al., *Essential features and rational design of CRISPR RNAs that function with the Cas RAMP module complex to cleave RNAs*. *Mol Cell*, 2012. **45**(3): p. 292-302.
393. Toschi, L., et al., *Role of gemcitabine in cancer therapy*. 2005.
394. Hilbig, A. and H. Oettle, *Gemcitabine in the treatment of metastatic pancreatic cancer*. 2008.
395. Mylonakis, N., et al., *Phase II study of liposomal cisplatin (Lipoplatin™) plus gemcitabine versus cisplatin plus gemcitabine as first line treatment in inoperable (stage IIIB/IV) non-small cell lung cancer*. *Lung Cancer*, 2010. **68**(2): p. 240-247.
396. Xu, H., et al., *Development of high-content gemcitabine PEGylated liposomes and their cytotoxicity on drug-resistant pancreatic tumour cells*. *Pharmaceutical research*, 2014. **31**(10): p. 2583-2592.
397. Abbruzzese, J.L., et al., *A phase I clinical, plasma, and cellular pharmacology study of gemcitabine*. *Journal of Clinical Oncology*, 1991. **9**(3): p. 491-498.
398. Storniolo, A.M., S. Allerheiligen, and H.L. Pearce. *Preclinical, pharmacologic, and phase I studies of gemcitabine*. in *Seminars in oncology*. 1997.
399. Kiani, A., et al., *Pharmacokinetics of gemcitabine in a patient with end-stage renal disease: effective clearance of its main metabolite by standard hemodialysis treatment*. *Cancer chemotherapy and pharmacology*, 2003. **51**(3): p. 266-270.
400. Kuenen, B.C., et al., *Dose-finding and pharmacokinetic study of cisplatin, gemcitabine, and SU5416 in patients with solid tumors*. *Journal of Clinical Oncology*, 2002. **20**(6): p. 1657-1667.
401. Ali, S., et al., *Gemcitabine sensitivity can be induced in pancreatic cancer cells through modulation of miR-200 and miR-21 expression by curcumin or its analogue CDF*. *Cancer research*, 2010. **70**(9): p. 3606-3617.
402. Schrag, D., et al. *A patterns-of-care study of post-progression treatment (Rx) among patients (pts) with advanced pancreas cancer (APC) after gemcitabine therapy on Cancer and Leukemia Group B (CALGB) study# 80303*. in *ASCO Annual Meeting Proceedings*. 2007.
403. Burris, H.A., et al., *Phase II trial of oral rubitecan in previously treated pancreatic cancer patients*. *The Oncologist*, 2005. **10**(3): p. 183-190.
404. Boeck, S., et al., *Second-line chemotherapy with pemetrexed after gemcitabine failure in patients with advanced pancreatic cancer: a multicenter phase II trial*. *Annals of oncology*, 2007.
405. Kulke, M.H., et al., *Capecitabine plus erlotinib in gemcitabine-refractory advanced pancreatic cancer*. *Journal of Clinical Oncology*, 2007. **25**(30): p. 4787-4792.
406. Ko, A.H., et al., *Excess toxicity associated with docetaxel and irinotecan in patients with metastatic, gemcitabine-refractory pancreatic cancer: results of a phase II study*. *Cancer investigation*, 2008. **26**(1): p. 47-52.
407. Oh, S.Y., et al., *Pilot study of irinotecan/oxaliplatin (IROX) combination chemotherapy for patients with gemcitabine-and 5-fluorouracil-refractory pancreatic cancer*. *Investigational new drugs*, 2010. **28**(3): p. 343-349.

408. O'Reilly, E.M., et al., *A Cancer and Leukemia Group B phase II study of sunitinib malate in patients with previously treated metastatic pancreatic adenocarcinoma (CALGB 80603)*. *The oncologist*, 2010. **15**(12): p. 1310-1319.
409. Ko, A., et al., *A multinational phase 2 study of nanoliposomal irinotecan sucrosfate (PEP02, MM-398) for patients with gemcitabine-refractory metastatic pancreatic cancer*. *British journal of cancer*, 2013. **109**(4): p. 920-925.
410. Pelzer, U., et al., *Best supportive care (BSC) versus oxaliplatin, folinic acid and 5-fluorouracil (OFF) plus BSC in patients for second-line advanced pancreatic cancer: a phase III-study from the German CONKO-study group*. *European Journal of Cancer*, 2011. **47**(11): p. 1676-1681.
411. Loosen, S.H., et al., *Current and future biomarkers for pancreatic adenocarcinoma*. *Tumour Biol*, 2017. **39**(6): p. 1010428317692231.
412. Celia, C., et al., *Improved in vitro anti-tumoral activity, intracellular uptake and apoptotic induction of gemcitabine-loaded pegylated unilamellar liposomes*. *Journal of nanoscience and nanotechnology*, 2008. **8**(4): p. 2102-2113.
413. Kim, I.-Y., et al., *Antitumor activity of EGFR targeted pH-sensitive immunoliposomes encapsulating gemcitabine in A549 xenograft nude mice*. *Journal of Controlled Release*, 2009. **140**(1): p. 55-60.
414. Federico, C., et al., *Gemcitabine-loaded liposomes: rationale, potentialities and future perspectives*. *International journal of nanomedicine*, 2012. **7**: p. 5423.
415. Suzuki, R., et al., *Effective anti-tumor activity of oxaliplatin encapsulated in transferrin-PEG-liposome*. *International journal of pharmaceutics*, 2008. **346**(1): p. 143-150.
416. Barenholz, Y., *Liposome application: problems and prospects*. *Current opinion in colloid & interface science*, 2001. **6**(1): p. 66-77.
417. Shepushkin, V., et al., *Sterically stabilized pH-sensitive liposomes*. *J. Biol. Chem*, 1997. **272**: p. 2382-2388.
418. D'Emanuele, A. and D. Attwood, *Dendrimer-drug interactions*. *Advanced drug delivery reviews*, 2005. **57**(15): p. 2147-2162.
419. Zamboni, W.C., *Concept and clinical evaluation of carrier-mediated anticancer agents*. *The oncologist*, 2008. **13**(3): p. 248-260.
420. Diaz, M.R. and P.E. Vivas-Mejia, *Nanoparticles as Drug Delivery Systems in Cancer Medicine: Emphasis on RNAi-Containing Nanoliposomes*. *Pharmaceuticals (Basel)*, 2013. **6**(11): p. 1361-80.
421. Mozafari, M.R., et al., *Nanoliposomes and their applications in food nanotechnology*. *J Liposome Res*, 2008. **18**(4): p. 309-27.
422. Abreu, A.S., et al., *Nanoliposomes for encapsulation and delivery of the potential antitumoral methyl 6-methoxy-3-(4-methoxyphenyl)-1H-indole-2-carboxylate*. *Nanoscale Res Lett*, 2011. **6**(1): p. 482.
423. Doll, T.A., et al., *Nanoscale assemblies and their biomedical applications*. *J R Soc Interface*, 2013. **10**(80): p. 20120740.
424. Torchilin, V.P., *Recent advances with liposomes as pharmaceutical carriers*. *Nat Rev Drug Discov*, 2005. **4**(2): p. 145-60.
425. Colbern, G.T., et al., *Antitumor activity of Herceptin in combination with STEALTH liposomal cisplatin or nonliposomal cisplatin in a HER2 positive human breast cancer model*. *J Inorg Biochem*, 1999. **77**(1-2): p. 117-20.
426. Lee, R.J. and P.S. Low, *Delivery of liposomes into cultured KB cells via folate receptor-mediated endocytosis*. *J Biol Chem*, 1994. **269**(5): p. 3198-204.
427. Maeda, H., et al., *Tumor vascular permeability and the EPR effect in macromolecular therapeutics: a review*. *Journal of controlled release*, 2000. **65**(1): p. 271-284.

428. Abraham, S.A., et al., *In vitro and in vivo characterization of doxorubicin and vincristine coencapsulated within liposomes through use of transition metal ion complexation and pH gradient loading*. Clinical cancer research, 2004. **10**(2): p. 728-738.
429. Laginha, K., D. Mumbengegwi, and T. Allen, *Liposomes targeted via two different antibodies: assay, B-cell binding and cytotoxicity*. Biochimica et Biophysica Acta (BBA)-Biomembranes, 2005. **1711**(1): p. 25-32.
430. Park, J.W., C.C. Benz, and F.J. Martin. *Future directions of liposome- and immunoliposome-based cancer therapeutics*. in *Seminars in oncology*. 2004. Elsevier.
431. Zamboni, W.C., *Liposomal, nanoparticle, and conjugated formulations of anticancer agents*. Clinical cancer research, 2005. **11**(23): p. 8230-8234.
432. Wang, A.Z., R. Langer, and O.C. Farokhzad, *Nanoparticle delivery of cancer drugs*. Annu Rev Med, 2012. **63**: p. 185-98.
433. Miele, E., et al., *Albumin-bound formulation of paclitaxel (Abraxane ABI-007) in the treatment of breast cancer*. Int J Nanomedicine, 2009. **4**: p. 99-105.
434. Drummond, D.C., et al., *Development of a highly active nanoliposomal irinotecan using a novel intraliposomal stabilization strategy*. Cancer Res, 2006. **66**(6): p. 3271-7.
435. Stathis, A. and M.J. Moore, *Advanced pancreatic carcinoma: current treatment and future challenges*. Nat Rev Clin Oncol, 2010. **7**(3): p. 163-72.
436. Neoptolemos, J.P., et al., *Therapeutic developments in pancreatic cancer: current and future perspectives*. Nat Rev Gastroenterol Hepatol, 2018. **15**(6): p. 333-348.

Appendix A: Supplementary data for siRNA 3

1.1 Appendix: MTT

1.1.1 MIA PaCa-2 Control Vs ABCC5-siRNA-3

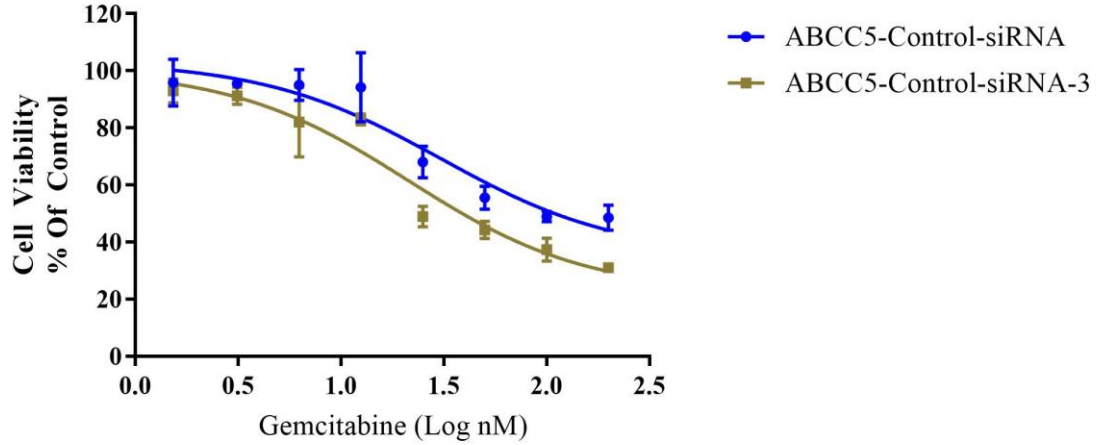


Figure 0-1: Comparison of gemcitabine induced cytotoxicity in ABCC5-siRNA-3 transfected MIA PaCa-2 cells and control

1.1.2 PANC-1 Control Vs ABCC5-siRNA-3

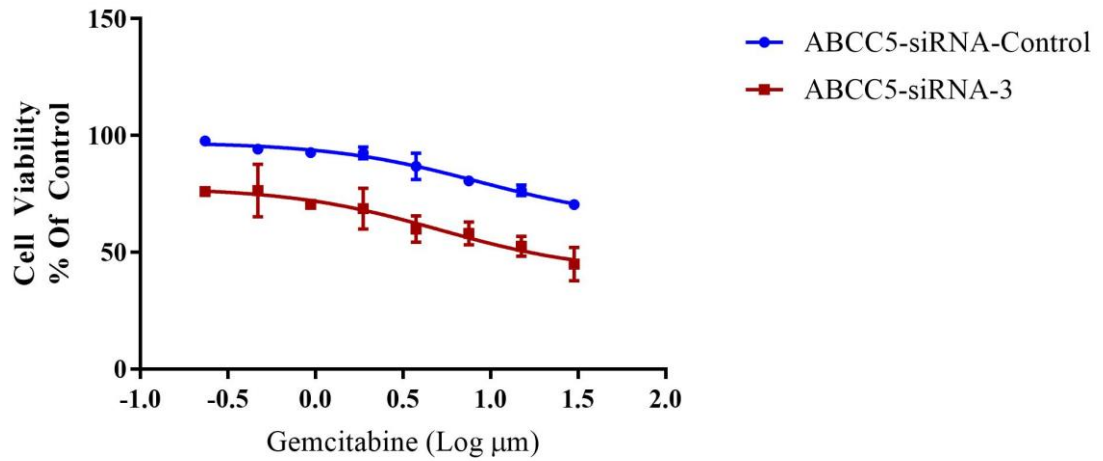


Figure 0-2: Comparison of gemcitabine induced cytotoxicity in ABCC5-siRNA-3 transfected PANC-1 cells and control

Appendix B: qRT-PCR supplementary data

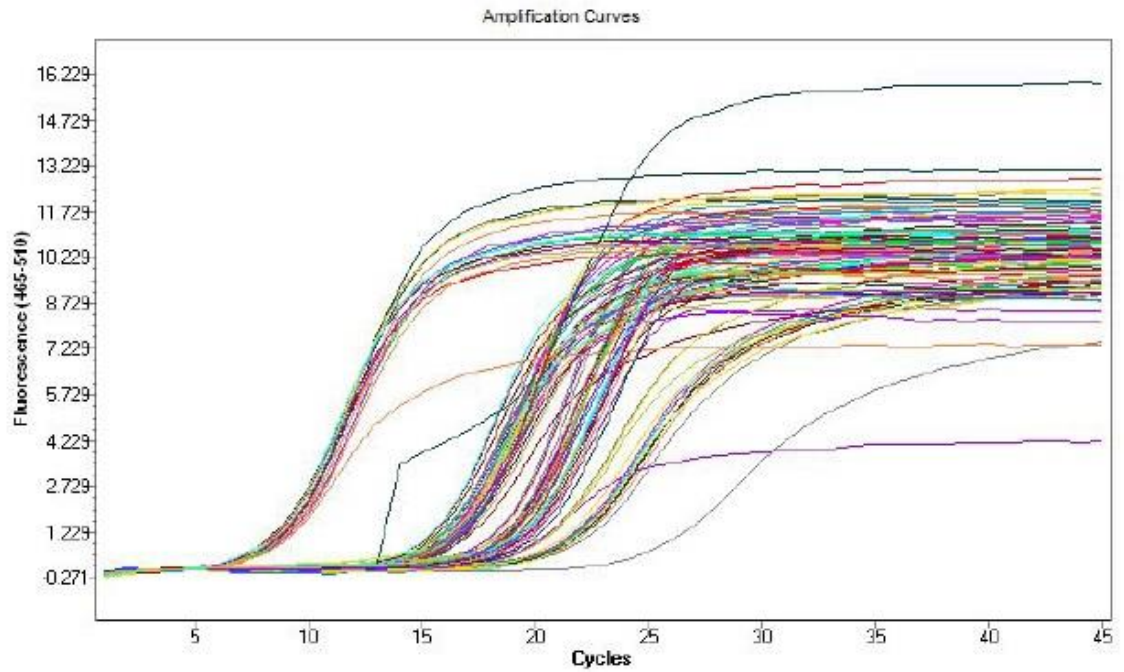


Figure 0-1: Off-target effects - amplification curves of 7 ABC transporters, dCK, CDA, hENT1 and GAPDH in MIA PaCa-2 cells. Refer to the table: 3-5 for details on primer sequences and target genes.

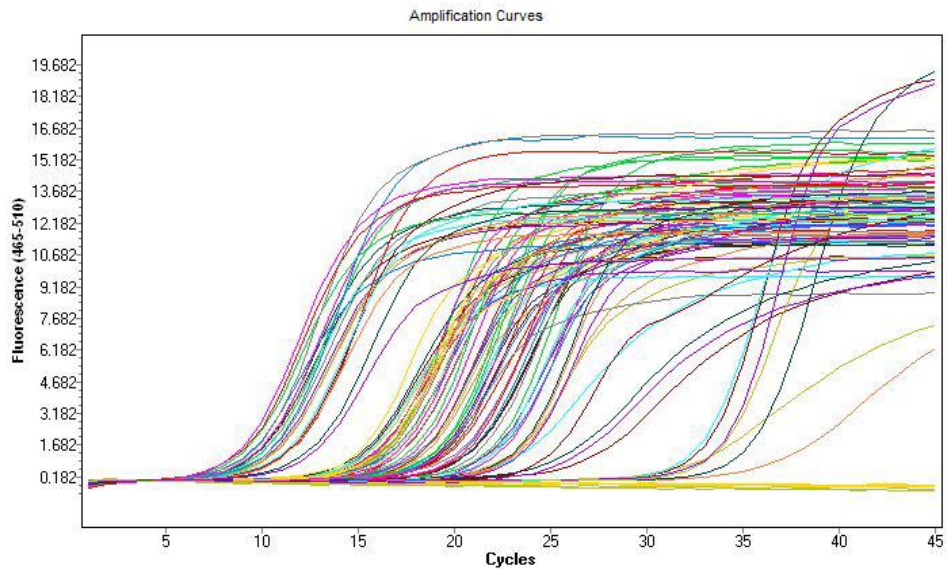


Figure 0-2: Off-target effects – amplification curves of 7 ABC transporters, dCK, CDA, hENT1 and GAPDH in PANC-1.

Refer to the table: 3-5 for details on the target genes and primer sequences used